

# **INCORPORATION OF PLATINUM ONTO ZEOLITE KL FOR AROMATISATION REACTIONS**

**By**

*Chamu Mark M'kombe BSc (Chem. Eng. Honours)*

Submitted to the University Of Cape Town in fulfilment of the  
requirements for the degree of

**MASTER OF SCIENCE IN ENGINEERING**

Department Of Chemical Engineering  
University Of Cape Town  
P.Bag Rondebosch 7700  
Cape Town  
South Africa

December 1994



The copyright of this thesis vests in the author. No quotation from it or information derived from it is to be published without full acknowledgement of the source. The thesis is to be used for private study or non-commercial research purposes only.

Published by the University of Cape Town (UCT) in terms of the non-exclusive license granted to UCT by the author.

## ACKNOWLEDGEMENTS

I would like to thank my supervisor professor Mark Dry for his help and guidance without which this work would not have been accomplished. I would also like to thank Dr Jack Fletcher for initially supervising this work as well as Professor Cyril O'Connor for his input into this work.

I would like to thank Johnson Matthey Materials Technology (U.K) for their generous provision of the platinum salt  $\text{Pt}(\text{NH}_3)_4\text{Cl}_2$  used in this work. Special thanks also goes to CSIR for their donation of zeolite KL and to Engelhard for their donation of zeolite U.S. H/Y.

Many thanks also go to Leslie who helped with the TEM and EDX analysis as well as by making her calcination rigs available. To Pam, I would like to express my appreciation for all her hard work in ordering the needed equipment.

I would like to thank Klauss and Eric for their valuable input as well as their willingness to solve problems related to the equipment used. Many thanks also go the staff in charge of the computer network as well as to the workshop staff.

I would like to thank Michael, my laboratory partner for his encouragement and friendship. Thank you Gillian, Peter and the other catalysis group members for your friendship. Thanks to Sarah, Rein and Rob for making your rigs available when needed.

I would also like to thank my friends Steve, Carien, Jane, Scott, Janine, Tony (T.C.), Warren, Keith, Tania, Gary and Timmy for keeping me sane when the research was taking its toll on me.

Lastly I would like to thank my family for their inspiration, love and support. I do not know what I would do without you guys.

To my parents Harry and Tracey who taught me that the real meaning of life  
and joy can only be found through Jesus Christ who  
came, saw, conquered and is alive.

It is the glory of God to conceal a matter;  
to search out a matter is the glory of the wise - Proverbs 25:2

## SYNOPSIS

The incorporation of platinum onto zeolite KL involves three stages namely platinum loading, calcination and reduction. The platinum salt commonly used for the loading step is  $\text{Pt}(\text{NH}_3)_4\text{Cl}_2$ . The calcination stage involves heating the catalyst in order to decompose the ammonia ligands as well as to drive off the water molecules trapped in the zeolite KL pores. In the reduction step, the  $\text{Pt}^{2+}$  left after calcination would be reduced to the neutral metallic form thus rendering them active for catalytic purposes.

The main objectives of the work presented in this thesis were two fold - i) to determine the effect of varying various parameters on the platinum dispersion and ii) to determine the conditions that would yield the highest platinum dispersion on the zeolite KL. Loading of platinum onto the zeolite KL was mainly via liquid state ion exchange. Loading via impregnation and solid state ion exchange were also briefly investigated in order to compare these techniques with liquid ion exchange. After loading the platinum onto the zeolite KL the Pt/KL samples obtained were then calcined under different conditions in order to see the effect of calcination temperature, calcination medium, and calcination time on the dispersion of the platinum. After obtaining the optimum calcination conditions, a set of samples were then prepared under these calcination conditions and used to investigate the different reduction parameters. It was important to observe the effect of varying the different reduction parameters on the dispersion of the platinum. The parameters investigated during reduction were the reduction medium, the reduction temperature and the reduction time.

The extent of platinum dispersion in the Pt/KL samples was determined using carbon monoxide chemisorption. Transmission electron microscopy (TEM), energy dispersive x-ray (EDX) analysis together with hydrogenation and aromatisation reactions were used to verify the results obtained using carbon monoxide chemisorption. Using temperature programmed desorption (TPD) of ammonia, the acidity of the Pt/KL catalysts were monitored at different stages of the incorporation process. The reduction temperatures of the platinum species were determined using temperature programmed reduction (TPR).

It was established that for the 1.55 % Pt/KL catalyst, the liquid state ion exchange parameters did not affect the final dispersion of the platinum on the zeolite KL. However, the calcination conditions greatly influenced the dispersion of the platinum. Oxygen was found to be the best calcination medium. This could have been due to the fact that during calcination in oxygen, the ammonia ligands would decompose to yield nitrogen and water to leave the  $\text{Pt}^{2+}$  ions. During calcination in nitrogen or hydrogen however, sintering would occur as a result of either the formation of labile hydrides or the premature reduction of platinum ions by the coordinating ammonia ligands. A calcination temperature of 350 °C was found to yield a better platinum dispersion compared to a calcination temperature of 600 °C. The platinum dispersion was found to be independent of the calcination time in oxygen.

It was found that reduction in hydrogen would result in a better platinum dispersion compared to reduction in carbon monoxide. It was possible that during reduction in carbon monoxide, large platinum carbonyl clusters formed resulting in a low dispersion. TEM results showed that a Pt/KL sample reduced in carbon monoxide had larger platinum clusters compared to a Pt/KL sample reduced in hydrogen. It is also possible that during reduction in carbon monoxide, the Boudouard reaction could have taken place resulting in the deposition of carbon either on the zeolite pore mouth or on the surface of the platinum particles. This could have contributed to the low dispersion values obtained. The dispersion of the platinum was independent of the period of reduction.

Comparison of the platinum dispersion of the samples prepared via liquid state ion exchange, solid state ion exchange and impregnation indicated that the solid state ion exchange technique yielded the highest platinum dispersion. However, at the solid state ion exchange conditions studied, only 0.75 wt % platinum was loaded onto the zeolite KL while in liquid state ion exchange and impregnation, 1.55 wt % platinum was loaded.

The TEM and EDX results indicated that Pt/KL catalysts with high platinum dispersion would have small platinum clusters, the majority of which would not be detected using TEM at a magnification of 200 000 times. On the other hand, Pt/KL catalysts with low dispersion would have large platinum clusters. These clusters would be easily detected using TEM at a

magnification of 200 000 times. The hydrogenation reactions together with the aromatisation of n-hexane indicated that Pt/KL catalysts with high platinum dispersion would exhibit higher activities compared to catalysts with low platinum dispersion.

The zeolite KL used in this study exhibited an ammonia desorption peak in the temperature range 240 °C to 290 °C as well as a second one in the temperature range 520 °C to 600 °C when analysed using temperature programmed desorption of ammonia. The peak in the lower temperature range was attributed to the desorption of weakly adsorbed ammonia while the peak in the higher temperature range was attributed to the desorption of ammonia from strong acid sites. The acidity of the platinum loaded zeolite KL was found to increase after the calcination step. This indicated that either i) reduction of the  $\text{Pt}^{2+}$  ions by the co-ordinating ammonia ligands was occurring resulting in the formation of  $\text{H}^+$  ions or ii)  $\text{Pt}^{2+}$  ions were reacting with the water produced during calcination in oxygen to yield  $\text{H}^+$  ions. It was also established that the carbon monoxide reduction of the Pt/KL sample calcined in oxygen did not increase the acidity of the sample. Treatment of Pt/KL samples at temperatures close to 600 °C was found to result in the removal of Bronsted acidity via de-hydroxylation.

The results of this study highlighted the crucial importance of carefully selecting the calcination and reduction conditions in order to get high platinum dispersion when incorporating platinum onto zeolite KL. This would be important in the industrial manufacture of Pt/KL catalysts because the activity obtained for a catalyst with a high platinum dispersion would be higher than the activity obtained for a catalyst with low dispersion. The former catalyst could thus make an industrial process more efficient and cost effective due to its longer lifetime. Since solid state ion exchange yielded the highest platinum dispersion, it was recommended that further studies should be done using this platinum loading technique. The studies should establish the treatment conditions which would enable most of the platinum to be loaded onto the zeolite KL.

## TABLE OF CONTENTS

ACKNOWLEDGEMENTS .....	i
SYNOPSIS .....	iii
TABLE OF CONTENTS .....	vi
LIST OF FIGURES .....	xiv
LIST OF TABLES .....	xvii
EXPLANATION OF SYMBOLS AND ABBREVIATIONS USED .....	xix
INTRODUCTION .....	xxi
1 REVIEW OF PUBLISHED INFORMATION .....	1
1.1 Platinum As A Catalyst .....	1
2.1.1 Physical Adsorption .....	1
1.1.2 Chemisorption .....	2
1.2 Zeolites As Catalysts .....	2
1.2.1 Structure .....	2
1.2.2 Acidity .....	3
1.2.3 Shape Selectivity .....	4
1.2.3.1 Primary shape selectivity .....	4
1.2.3.2 Secondary shape selectivity .....	5
1.2.4 Zeolite L as A Catalyst .....	6
2.2.4.1 Structure of zeolite-L .....	6
1.2.4.2 Activity of zeolite L in the aromatisation of n-hexane ..	8
1.2.5 Zeolite Y As A Catalyst .....	11
1.2.5.1 Structure of zeolite Y .....	11
1.2.5.2 Acidity And Stability .....	12



1.3 Supported Metal Catalysts . . . . .	12
1.3.1 Bi-functional Catalysts . . . . .	12
1.3.2 Mono-functional Catalysts . . . . .	13
1.3.3 Metal Support Interactions . . . . .	13
1.3.4 Metal Loading Methods . . . . .	13
1.3.4.1 Liquid ion exchange . . . . .	14
1.3.4.2 Solid state ion exchange . . . . .	15
1.3.4.3 Impregnation . . . . .	18
1.3.4.4 Crystallisation . . . . .	19
1.3.5 Activation Of Prepared Catalysts . . . . .	20
1.3.5.1 Calcination parameters affecting final metal distribution . . . . .	20
1.3.6 Reduction Of Metals . . . . .	24
1.3.6.1 Reducibility . . . . .	24
1.3.6.2 Proposed mechanism of reduction . . . . .	26
1.3.7 Distribution Of Metal On Supports . . . . .	28
1.3.7.1 Effect of activation conditions . . . . .	28
1.3.7.2 Size and location of metal clusters . . . . .	28
1.3.7.3 Chemical anchoring . . . . .	29
1.3.7.4 Metal re-dispersion . . . . .	30
1.4 Characterisation Techniques . . . . .	32
1.4.1 Atomic Absorption Spectroscopy (A.A.S) . . . . .	32
1.4.2 Transmission Electron Microscopy (TEM) . . . . .	33
1.4.3 Infrared Spectroscopy (IR) . . . . .	33
1.4.4 X-Ray Methods . . . . .	34
1.4.5 Temperature Programmed Reduction (TPR) . . . . .	36
1.4.6 Temperature Programmed Desorption (TPD) . . . . .	38
1.4.7 Chemisorption . . . . .	39
1.4.9 Chemical Reactions . . . . .	43
OBJECTIVES . . . . .	44

2 EXPERIMENTAL PROCEDURE . . . . .	46
2.1 Catalyst Preparation And Reduction . . . . .	46
2.1.1 Liquid State Ion Exchange . . . . .	46
2.1.1.1 Factorial Design . . . . .	47
2.1.2 Calcination . . . . .	49
2.1.4 Solid State Ion Exchange . . . . .	52
2.1.4 Incipient Wetness Impregnation . . . . .	53
2.2 Analytical Procedure . . . . .	53
2.2.1 X-Ray Diffraction . . . . .	53
2.2.2 Elemental Analysis . . . . .	54
2.2.2.1 Atomic absorption spectroscopy . . . . .	54
2.2.2.2 Electron beam micro-analysis . . . . .	55
2.2.3 Chemisorption . . . . .	56
2.2.3.1 Chemisorption procedure for all the samples . . . . .	57
2.2.3.2 Hydrogen chemisorption . . . . .	58
2.2.4 Temperature Programmed Reduction (TPR) . . . . .	61
2.2.4.1 Calibration of H <sub>2</sub> concentration in the H <sub>2</sub> /N <sub>2</sub> stream . . . . .	61
2.2.4.2 TPR procedure for all the samples . . . . .	62
2.2.5 Temperature Programmed Desorption (TPD). . . . .	64
2.2.6 Transmission Electron Microscopy (TEM) . . . . .	66
2.2.7 Energy Dispersive X-ray (EDX) Analysis . . . . .	67
2.2.7 Reactions . . . . .	68
2.2.7.1 Hydrogenation reactions . . . . .	68
2.2.7.2 Aromatisation Reactions . . . . .	69
3 RESULTS . . . . .	71
3.1 X-Ray Diffraction Patterns . . . . .	71
3.2 Elemental Analysis . . . . .	73
3.2.1 Atomic Absorption Analysis . . . . .	73
3.2.2 Electron Beam Micro-analysis Results . . . . .	75
3.3 Calcination And Reduction . . . . .	77
3.3.1 Minimum Calcination Temperature . . . . .	77

3.3.2 Temperature Programmed Reduction (TPR) Results . . . . .	78
3.3.3.1 Calibration of the hydrogen concentration in the H <sub>2</sub> /N <sub>2</sub> stream . . . . .	78
3.3.2.2 TPR profiles of 1.55 wt % Pt/KL and 1.43 wt % Pt/HY samples . . . . .	79
3.4 Results Of Temperature Programmed Desorption (TPD) Of Ammonia . .	84
3.5 Chemisorption Results . . . . .	93
3.5.1 Carbon Monoxide Chemisorption . . . . .	93
3.5.1.1 Reproducibility of catalyst preparation procedure and chemisorption technique. . . . .	93
3.5.1.2 Effect of ion exchange temperature on dispersion. . . .	94
3.5.1.3 Effect of ion exchange time on dispersion. . . . .	95
3.5.1.3 Chemisorption results of Factorial Design for calcination . . . . .	96
3.5.1.4 Additional studies of the effect of calcination time in oxygen on dispersion. . . . .	97
3.5.1.5 Effect of rate of temperature increase from 25 °C to 350 °C during calcination. . . . .	98
3.5.1.6 Effect of oxygen flowrate during calcination on dispersion. . . . .	99
3.5.1.7 Effect of not reducing the catalyst after calcination in oxygen. . . . .	99
3.5.1.8 Chemisorption results of Factorial Design for reduction . . . . .	100
3.5.1.9 Effect of rate of temperature increase from 25 °C to 350 °C during reduction. . . . .	101
3.5.1.10 Comparison between different platinum loading methods employed. . . . .	102
3.5.1.11 Effect of different calcination media on platinum dispersion. . . . .	104
3.5.1.12 Chemisorption results on 1.43 wt % Pt/HY. . . . .	105
3.5.2 Hydrogen Chemisorption . . . . .	105

3.5.2.1 Hydrogen chemisorption test cycles on 0.5 %	
Pt/Al <sub>2</sub> O <sub>3</sub> . . . . .	105
3.5.2.2 Hydrogen chemisorption test cycles on 0.78 %	
Pt/KL . . . . .	106
3.6 Transmission Electron Microscopy (TEM) . . . . .	109
3.7 Energy Dispersive X-Ray (EDX) Analysis . . . . .	112
3.8 Chemical Reactions . . . . .	113
3.8.1 Hydrogenation Results . . . . .	113
3.8.1.1 Hydrogenation of cyclohexene . . . . .	113
3.8.1.2 Hydrogenation of cyclododecene . . . . .	114
3.8.1 Aromatisation Of n-hexane Results . . . . .	114
4 DISCUSSION . . . . .	117
4.1 XRD And Elemental Analysis . . . . .	117
4.2. Ion Exchange . . . . .	117
4.2.1. Ion Exchange Temperature . . . . .	117
4.2.2. Ion Exchange Solution Concentration . . . . .	118
4.2.3. Ion Exchange Time . . . . .	118
4.3. Calcination . . . . .	119
4.3.1. Calcination Medium . . . . .	119
4.3.2 Effect Of Oxygen Flowrate During Calcination . . . . .	120
4.3.3 Calcination Temperature . . . . .	121
4.3.4 Rate of Temperature Increase . . . . .	123
4.3.5 Effect of Calcination Time in Oxygen At 350 °C . . . . .	123
4.4. Reduction . . . . .	124
4.4.1 Temperature Programmed Reduction . . . . .	124
4.4.1.1 TPR of 1.55 Pt/KL samples . . . . .	124
4.4.1.2 TPR of 1.43 % Pt/HY samples . . . . .	126
4.4.2. Reduction Temperature . . . . .	128
4.4.2.1. Rate of temperature increase from 25°C to 350°C	
during reduction . . . . .	129
4.4.3 Reduction Medium . . . . .	129

4.4.3.1 Formation of platinum carbonyls . . . . .	129
4.4.3.2 Bouduard reaction . . . . .	131
4.4.3.2 Strong adsorption of carbon monoxide during reduction . . . . .	133
4.4.4. Reduction Time . . . . .	134
4.5. Comparison Between Liquid Ion Exchange, Impregnation And Solid State Ion Exchange As Methods of Incorporating The Platinum Onto Zeolite KL. . . . .	134
4.5.1 Treatment In Oxygen, At 350°C . . . . .	134
4.5.2 Treatment At 600 °C In Nitrogen . . . . .	136
4.6 Hydrogen Chemisorption . . . . .	137
4.7 Acidity . . . . .	139
4.7.1 Acidity Of Zeolite KL Without Any Platinum . . . . .	139
4.7.2 Acidity Of Calcined 1.55 wt % Pt/KL samples . . . . .	140
4.7.2.1 1.55% Pt/KL calcined at 350 °C in O <sub>2</sub> for 6.33 hours without subsequent reduction . . . . .	140
4.7.2.2 1.55% Pt/KL calcined at 350 °C in N <sub>2</sub> for 6.33 hours without subsequent reduction . . . . .	141
4.7.2.3 1.55% Pt/KL calcined at 600 °C in O <sub>2</sub> for 6.33 hours without subsequent reduction . . . . .	141
4.7.3 Acidity Of Calcined And Reduced 1.55 wt % Pt/KL samples . .	142
4.7.3.1 1.55% Pt/KL calcined at 350 °C in O <sub>2</sub> for 6.33 hours and reduced in H <sub>2</sub> at 350 °C for 4.5 hours . . . . .	142
4.7.3.2 1.55% Pt/KL calcined at 350 °C in O <sub>2</sub> for 6.33 hours and reduced in CO at 350 °C for 4.5 hours . . . . .	143
4.7.4 Acidity Of Calcined, Reduced And Back Exchanged 1.55 wt % Pt/KL samples . . . . .	144
4.8 TEM And EDX Analysis . . . . .	146
4.9 Reactions . . . . .	147
4.9.1 Hydrogenation Reactions . . . . .	147

4.9.1.1 Hydrogenation of cyclohexene . . . . .	147
4.9.1.2 Hydrogenation of cyclododecene . . . . .	147
4.9.2 Conversion Of N-hexane . . . . .	148
 5 CONCLUDING REMARKS AND RECOMMENDATION . . . . .	 149
5.1 Platinum Loading Procedure . . . . .	149
5.2 Catalyst Activation . . . . .	149
5.2.1 Calcination Medium. . . . .	149
5.2.2 Calcination Temperature . . . . .	150
5.2.3 Calcination Time in Oxygen. . . . .	150
5.3 Catalyst Reduction . . . . .	151
5.3.1 Temperature Programme Reduction (TPR) Studies . . . . .	151
5.3.2. Reduction Temperatures . . . . .	151
5.3.3 Reduction Medium . . . . .	151
5.3.4 Reduction Time . . . . .	152
5.4 Comparison Between The Pt/ KL And Pt/ HY Catalysts . . . . .	152
5.5 Hydrogen Spillover. . . . .	152
5.6 Acidity . . . . .	153
5.7 Chemical Reactions . . . . .	154
5.7.1. Hydrogenation Reactions . . . . .	154
5.7.1. Aromatisation of n-hexane . . . . .	155
 LIST OF REFERENCES . . . . .	 156
 APPENDIX A : ELEMENTAL ANALYSIS DURING LIQUID STATE ION EXCHANGE . . . . .	  164
APPENDIX B : CHEMISORPTION . . . . .	172
APPENDIX C : REACTIONS . . . . .	175

## LIST OF FIGURES

Figure 1.1 showing the formation of Lewis acidity from Bronsted acidity . . . . .	3
Figure 1.2 showing the formation of 'True' Lewis acid sites . . . . .	4
Figure 1.3 showing primary shape selectivity . . . . .	5
Figure 1.4 showing the $\epsilon$ -cage and the D6R units . . . . .	6
Figure 1.5 showing part of the three-dimensional structure of zeolite L as well as the projection view of the zeolite L framework . . . . .	7
Figure 1.6 showing the structure of zeolite Y . . . . .	11
Figure 1.7 showing how the degree of solid state ion exchange on (MnCl <sub>2</sub> /H-ZSM-5) is affected by temperature and time . . . . .	16
Figure 1.8 showing a TPR profile of Pt/KL . . . . .	37
Figure 1.9 showing typical chemisorption results . . . . .	40
Figure 2.1 showing the liquid state ion exchange apparatus. . . . .	46
Figure 2.2 Showing The Calcination Rig . . . . .	49
Figure 2.3 showing the flow diagram of the equipment used for chemisorption studies. . . . .	56
Figure 2.4 showing the schematic representation of the H <sub>2</sub> chemisorption test cycle employed to investigate the effect of varying the evacuation time while reducing the temperature from 350 °C to 35 °C. . . . .	59
Figure 2.5 showing the schematic representation of the chemisorption procedure employed to investigate the effect of varying the evacuation time at 350 °C. . . . .	60
Figure 2.6 Showing The Rig For Temperature Programmed Reduction (TPR) . . . . .	61
Figure 2.7 Showing The TPD Rig. . . . .	64
Figure 2.8 showing the aromatisation rig . . . . .	70
Figure 3.1 showing the simulated XRD pattern of zeolite L (Na <sub>3</sub> K <sub>6</sub> Si <sub>27</sub> O <sub>72</sub> .21H <sub>2</sub> O) . . . . .	71
Figure 3.2 showing the experimentally determined XRD pattern of the zeolite KL used in this study . . . . .	72
Figure 3.3 showing the time taken to load 1.55% Pt onto zeolite KL at 15° C . . . . .	73
Figure 3.4 showing the time taken to load 1.55% Pt onto zeolite KL at 100°C . . . . .	74
Figure 3.5 showing the time taken to load 1.55% Pt onto zeolite KL via multiple exchange cycles at 40°C . . . . .	74

Figure 3.6 showing the temperature at which the ammonia ligands disintegrate. . . . .	77
Figure 3.7 showing the TPR profiles of the oxides used to calibrate the TPR rig. . .	78
Figure 3.8 showing the TPR profile of 1.55 wt % Pt/KL calcined at 350 °C in O <sub>2</sub> for 6.33 hours. . . . .	80
Figure 3.9 showing the TPR profile of 1.55 wt % Pt/KL calcined at 350 °C in N <sub>2</sub> for 6.33 hours . . . . .	80
Figure 3.10 showing the TPR profile of 1.55 wt % Pt/KL calcined at 600 °C in O <sub>2</sub> for 6.33 hours . . . . .	81
Figure 3.11 showing the TPR profile of 1.43 wt % Pt/HY calcined at 350 °C in O <sub>2</sub> for 6.33 hours . . . . .	81
Figure 3.12 showing the TPR profile of 1.43 wt % Pt/HY calcined at 600 °C in O <sub>2</sub> for 6.33 hours . . . . .	82
Figure 3.13 showing the TPR profile of 1.43 wt % Pt/HY calcined at 600 °C in N <sub>2</sub> for 6.33 hours . . . . .	82
Figure 3.14 showing the TPD profile of 1.55% Pt/SiO <sub>2</sub> Calcined : 350°C, He, 6.33hr. No reduction. . . . .	84
Figure 3.15 showing the TPD profile of pure silica Calcined : 350°C, He, 6.33hr. No reduction. . . . .	85
Figure 3.16 showing the TPD profile of untreated zeolite KL . . . . .	86
Figure 3.17 showing the TPD profile of zeolite KL calcined : 350°C, O <sub>2</sub> , 1.5 hr. No reduction . . . . .	86
Figure 3.18 showing the TPD profile of 1.55% Pt/KL. Calcined : 350°C, O <sub>2</sub> , 6.33hr. No reduction . . . . .	87
Figure 3.19 showing the TPD profile of 1.55% Pt/KL. Calcined : 350°C, N <sub>2</sub> , 1.5 hr. No reduction. . . . .	88
Figure 3.20 showing the TPD profile of 1.55% Pt/KL Calcined : 600°C, O <sub>2</sub> , 6.33hr. No reduction. . . . .	88
Figure 3.21 showing the TPD profile of 1.55% Pt/KL. Calcined : 350°C, O <sub>2</sub> , 6.33hr. Reduced : 350°C, H <sub>2</sub> , 4.5hr. . . . .	89
Figure 3.22 showing the TPD profile of 1.55% Pt/KL Calcined : 350°C, O <sub>2</sub> , 6.33hr. Reduced : 350°C, CO, 4.5hr. . . . .	89
Figure 3.23 showing the TPD profile of 1.55% Pt/KL. Back exchanged with K <sup>+</sup>	



using KCl in O <sub>2</sub> at 350 °C. Prior to back exchange, sample had been calcined in O <sub>2</sub> and reduced in H <sub>2</sub> . . . . .	90
Figure 3.24 showing a repeat of the TPD profile of 1.55 % Pt/KL. Back exchanged K <sup>+</sup> using KCl in O <sub>2</sub> at 350 °C. . . . .	91
Figure 3.25 showing the effect of ion exchange temperature on dispersion . . . . .	95
Figure 3.26 showing the effect of calcination time on dispersion . . . . .	98
Figure 3.27 showing the effect of oxygen flowrate during calcination on dispersion . . . . .	99
Figure 3.28 showing the apparent dispersion vs evacuation time for hydrogen chemisorption on 0.5 % Pt/Al <sub>2</sub> O <sub>3</sub> . . . . .	106
Figure 3.29 showing the apparent dispersion vs evacuation time for hydrogen chemisorption on 0.78 % Pt/KL. Evacuation time at 350 °C was varied. . . . .	107
Figure 3.30 showing the apparent dispersion vs evacuation time for hydrogen chemisorption on 0.78 % Pt/KL. Evacuation time was varied while cooling from 350 °C to 25 °C. . . . .	108
Figure 3.31 showing the apparent dispersion vs evacuation time for carbon monoxide chemisorption on 0.78 % Pt/KL. Evacuation time was varied while cooling from 350 °C to 25 °C. . . . .	108
Figure 3.40 showing the results of batchwise hydrogenation of cyclohexene to cyclohexane . . . . .	113
Figure 3.41 showing the results of batchwise hydrogenation of cyclohexene to cyclododecene . . . . .	114
Figure 3.42 comparing the activities of the catalysts used in the conversion of n-hexane. . . . .	115
Figure 4.1 showing the structure of [Pt <sub>3</sub> (CO) <sub>6</sub> ] <sup>2-</sup> <sub>n</sub> ions with n =2,3 and 5 . . . . .	130
Figure 4.2 showing two views of the [Pt <sub>19</sub> (CO) <sub>22</sub> ] <sup>4-</sup> ion structure . . . . .	131
Figure 4.3 showing the ΔG vs T relationship for the Boudouard reaction. . . . .	132

## LIST OF TABLES

Table 1.1 showing cation positions in zeolite L . . . . .	8
Table 2.1 showing an example of a full factorial design . . . . .	48
Table 2.2 showing the factorial design sequence for calcination . . . . .	51
Table 2.3 showing the factorial design sequence for reduction . . . . .	52
Table 2.4 showing XRD parameters used. . . . .	54
Table 3.2 showing a summary of the TPR results. . . . .	83
Table 3.3 showing a summary of the TPD results . . . . .	92
Table 3.4 showing the reproducibility of the catalyst preparation procedure. . . . .	94
Table 3.5 showing the effect of ion exchange time on dispersion . . . . .	96
Table 3.6 showing the chemisorption results of Factorial Design for calcination of 1.55% Pt/KL . . . . .	96
Table 3.7 showing a summary of the chemisorption results for Factorial Design for calcination . . . . .	97
Table 3.8 showing the effect of rate of temperature increase during calcination on dispersion . . . . .	98
Table 3.9 showing the effect of not reducing the 1.55% Pt/KL sample after calcination in oxygen. . . . .	100
Table 3.10 showing the chemisorption results of Factorial Design for reduction . . .	100
Table 3.11 showing a summary of the chemisorption results for Factorial Design for reduction . . . . .	101
Table 3.12 showing the effect of rate of temperature increase during reduction in hydrogen . . . . .	102
Table 3.13 showing the comparison between different platinum loading methods for samples calcined in oxygen at 350 °C. . . . .	103
Table 3.14 showing the comparison between different platinum loading methods for samples calcined in nitrogen at 600 °C. . . . .	104
Table 3.15 showing the effect of different calcination media on dispersion. . . . .	104
Table 3.16 showing the comparison between dispersion of 1.43% Pt/HY and 1.55% Pt/KL samples treated at similar conditions. . . . .	105
Table 3.17 showing the results of EDX analysis on areas with visible platinum	

clusters for a sample with a platinum dispersion of 44%. . . . .	112
Table 3.18 showing the results of EDX analysis on areas without visible platinum clusters for a sample with a platinum dispersion of 111%. . . . .	112
Table 3.19 showing the product selectivities for the conversion of n-hexane over 1.55% Pt/KL catalysts.....	116

## LIST OF PLATES

Plate 3.1 showing the TEM image of untreated zeolite KL . . . . .	109
Plate 3.2 showing the TEM image of 1.55% Pt/KL calcined in O <sub>2</sub> , at 350 °C for 6.33 hours and reduced in H <sub>2</sub> at 350 °C for 4.5 hours . . . . .	109
Plate 3.3 showing the TEM image of 1.55% Pt/KL calcined in N <sub>2</sub> , at 600 °C for 6.33 hours and reduced in H <sub>2</sub> at 350 °C for 4.5 hours . . . . .	110
Plate 3.4 showing the TEM image of 1.55% Pt/KL calcined in O <sub>2</sub> , at 350 °C for 1.5 hours and reduced in CO at 350 °C for 1.5 hours . . . . .	110
Plate 3.5 showing the TEM image of 0.75% Pt/KL solid state ion exchanged in O <sub>2</sub> , at 350 °C for 6.5 hours and reduced in H <sub>2</sub> at 350 °C for 4.5 hours . . . . .	110
Plate 3.6 showing the TEM image of 0.75 % Pt/KL solid state ion exchanged in N <sub>2</sub> , at 600 °C for 6.5 hours and reduced in H <sub>2</sub> at 350 °C for 4.5 hours . . . . .	111

## EXPLANATION OF ABBREVIATIONS, SYMBOLS AND COMMON UNITS USED

### Abbreviations

AAS	atomic absorption spectroscopy
B	benzene
C1	methane
C2	ethane
c-2-C6	cis-2-cyclohexene
C3	propane
DME	di-methyl-ether
EDX	energy dispersive x-ray analysis
MCP	methyl cyclopentane
nC4	n-butane
nC5	n-heptane
STEM	scanning transmission electron microscopy
TCD	thermal conductivity detector
TEM	transmission electron microscopy
TPD	temperature programmed desorption
TPR	temperature programmed reduction
t-2-C6	trans-2-cyclohexene
XRD	x-ray diffraction
2m-C5	2 methyl pentane
2m-1-C5	2 methyl cyclopent-1-ene
2m-2-C5	2 methyl cyclopent-2-ene
3m-C5	3 methyl pentane

### Symbols

B	breadth of a diffraction line observed under given experimental conditions
$E_a$	activation energy
$I_0$	intensity of light from lamp
$I_t$	intensity of light after passing through a filament in atomic absorption spectroscopy

xx

N	Avogadro's number
R	universal gas constant
x	effective capillary length of pores
$\beta$	x-ray diffraction broadening
$\theta$	Bragg angle used in x-ray line broadening
$\lambda$	radiation wavelength in x-ray line broadening
$\mu$	dynamic viscosity of liquid
$\rho$	density of a substance
$\sigma$	surface tension of a solution

### Common units used

Å	unit of length measurement ( $10^{-10}$ meters)
°C	unit of temperature measurement
hr	unit of time measurement (hours)
kPa	unit of pressure measurement
kV	unit of voltage measurement
mA	unit of current measurement
nm	unit of length measurement ( $10^{-9}$ meters)
pm	unit of length measurement ( $10^{-12}$ meters)
s	unit of time measurement (seconds)
$\mu\text{m}$	unit of length measurement ( $10^{-6}$ meters)

## INTRODUCTION

In South Africa there is a limited production of aromatics for the chemical industry. The producers of synthetic fuels (Sasol and Moss gas), on the other hand, have large amounts of linear paraffins available which could be converted to aromatics. In the early 1970s platinum supported on zeolite L was found to have a high activity for the aromatisation of n-hexane and other paraffins such as heptane. However, until a few years ago, little was published on this subject. It is desirable to understand the chemical processes occurring during the incorporation of platinum onto microporous supports. It was thus decided to study the loading of platinum onto zeolite L with the purpose of utilising the produced catalyst in aromatisation reactions.

At present, most of the literature regarding the incorporation of metals onto zeolites involves zeolite Y. It was therefore also important for comparison purposes to study the incorporation of platinum onto zeolite Y. Ion exchange methods, namely liquid ion-exchange and solid state ion exchange were studied.

Due to the high cost of catalytic material, such as platinum, there is a strong economic incentive to minimise the amount of metal used. It is thus imperative to prepare catalysts with well dispersed platinum to ensure that as much surface area of the platinum as possible is exposed to the reactants. The preparation of metal-supported catalysts involves three stages, namely: loading, activation and reduction. Various parameters in these preparation stages affect the size and location of the metal supported on microporous supports. For the Pt/KL system, it is important to establish the effect that these parameters have on the dispersion and location of the metal. The optimum conditions yielding the most dispersed metal on KL need to be determined. At each stage of the incorporation process, the modified catalysts should be characterised.

## **CHAPTER 1**



## 1 REVIEW OF PUBLISHED INFORMATION

### 1.1 Platinum As A Catalyst

In a microscopic sense, almost all solid surfaces are irregular with valleys and peaks alternating over the surface area. The regions of irregularity are susceptible to residual force fields causing the solid to attract other atoms in the surrounding gas or liquid phase. Atoms on a perfectly smooth surface could also attract molecules from a surrounding fluid. However, the amount of fluid attracted would be minimal compared to that on an irregular surface. Like other transition metals, platinum can be used as a catalyst in various reactions such as hydrogenation, isomerisation and oxidation of hydrocarbons. The specific catalytic properties of solid surfaces such as platinum have their origin in the ability of each surface to interact with at least one of the reactants or at least one of the products. This interaction is called adsorption. There are two types of adsorption namely physical adsorption and chemisorption.

#### 2.1.1 Physical Adsorption

Physical adsorption occurs when forces similar to van der Waal's forces attract the molecules to the surface atoms of the catalyst. Equilibrium between the solid surface and the gas molecules is usually rapidly attained and easily reversible due to the small energy requirements of the process. Physical adsorption is independent of the irregularities in the nature of the surface and is directly proportional to the surface area. Furthermore, the extent of adsorption is not limited to a monomolecular layer on the solid surface.

Reactions of atoms and free radicals at surfaces sometimes involve small activation energies. These reactions could be facilitated by physical adsorption. Catalytic activity of solids for reactions involving stable molecules could not occur via physical adsorption. This is because the activation energy of the reaction would not be sufficiently reduced.

The amount of physical adsorption decreases with an increase in temperature to become

negligible above the critical temperature of the adsorbed substance. In the dehydrogenation of n-hexane using Pt/(K/L), physical adsorption is expected to play a very small part.

### 1.1.2 Chemisorption

Chemisorption occurs when chemical bonds are formed between reactants and/or products with the metal surface. This is because the surface atoms of the metal have incompletely filled dsp-hybrid orbitals which have a tendency to become saturated. Two kinds of chemisorption are encountered, namely: *Activated Chemisorption* and *Non-Activated Chemisorption*. In activated chemisorption, the rate varies with temperature according to a finite activation energy in the Arrhenius equation. In non-activated chemisorption, the chemisorption occurs rapidly. In some systems, the initial chemisorption is non-activated becoming activated in later stages.

Due to the high heat of adsorption, the energy possessed by the chemisorbed molecules is usually different from unattached molecules. This explains why the activation energy of reactions associated with chemisorption can be lower than normal. The extent of chemisorption will not exceed that corresponding to a monomolecular layer. This is because the valence forces holding the molecules on the surface rapidly diminish with distance, becoming too small to form the adsorption compound when the distance from the surface is greater than usual bond distances.

## 1.2 Zeolites As Catalysts

### 1.2.1 Structure

Zeolites are crystalline aluminosilicates with three-dimensional structures arising from a framework of  $[\text{SiO}_4]^{4-}$  and  $[\text{AlO}_4]^{5-}$  tetrahedra. These units are linked via the oxygen atoms to generate an open framework containing channels and cavities.

The channel structure of the zeolites enables molecules of certain sizes to enter these

channels. The molecules then react within the cavities and the products which are formed move out of the channel structures. Ideally, pore sizes of zeolites should be slightly larger than the diameters of the reactants and products. The pore sizes of the zeolites create both product and shape selectivity via molecular sieving. Compared to the conventional catalysts, polymerisation of products and reactants in the zeolite pores would be greatly reduced due to the spatial constraints. Thus, zeolites have more practical advantages over the more traditional catalysts.

### 1.2.2 Acidity

The reactivity and selectivity of some zeolites is determined by active sites provided by an imbalance in charge between the silicon and aluminium ions in the framework. Each aluminium atom in the zeolite induces a potential active acid site. Bronsted and Lewis acidity are used to describe the acidity in zeotype materials.

Bronsted acidity is proton donor acidity and occurs in zeolites when the charge stabilising cations are protons. Lewis acidity is electron acceptor acidity arising from the presence of tri-coordinated aluminium and silicon sites within the zeolite framework. The sites can then accept electron pairs. [Szostak, 1989] Bronsted acidity can be obtained if a zeolite containing a metal (e.g Na) as a charge stabilising cation is ion exchanged with an ammonium salt and subsequently calcined to release ammonia and leave protons. Lewis acidity can be obtained by heating the zeolite which contains Bronsted acidity to release water as shown in figure 1. The tri-coordinated Al (shown as Al\*) in figure 1.1 acts as a weak acid.

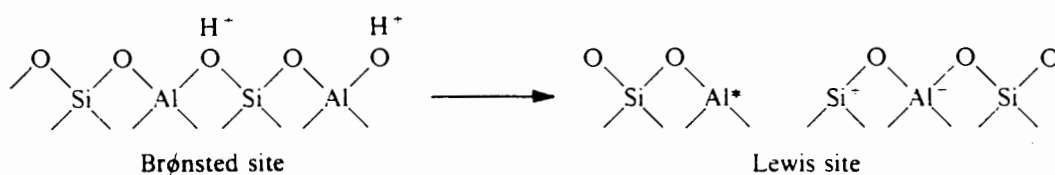


Figure 1.1 showing the formation of Lewis acidity from Bronsted acidity [from Dyer, 1988]

Lewis acid sites are unstable, particularly in the continued presence of water vapour, because this leads to the formation of 'True' Lewis sites by ejecting Al species from the framework as shown in figure 1.2. The 'True' Lewis sites are the  $(\text{AlO})^+$  species which are strong acid sites. The  $\text{Al}^+$  species act as weak acid sites.

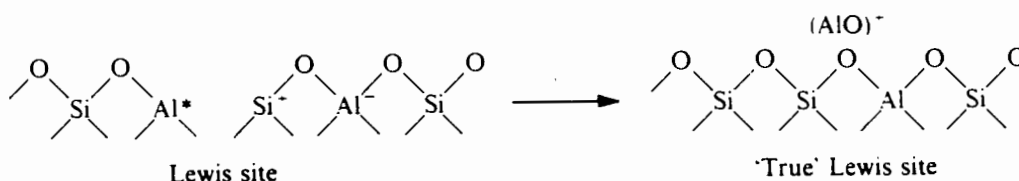


Figure 1.2 showing the formation of 'True' Lewis acid sites [from Dyer, 1988]

Reactions such as the aromatisation of n-hexane to benzene over platinum supported on zeolite L do not require acidity for them to occur. [Derouane and Vanderverken, 1988]

### 1.2.3 Shape Selectivity

#### 1.2.3.1 Primary shape selectivity

Primary shape selectivity involves reactant, transition state and product selectivity. In reactant selectivity, the molecules that are too large or highly branched do not have access into the zeolite pores. Product shape selectivity occurs when reaction products of different sizes are formed within the interior of the zeolite crystals and some of the products are too bulky to diffuse out. The products which cannot diffuse out may undergo secondary reactions to smaller molecules or they may deactivate the catalyst by blocking the pores. Transition state selectivity means that the transition state intermediates which are too large to form in the pores of the zeolites are prohibited from forming. However, neither the reactants nor the products are restricted from diffusing through the zeolite pores. Primary shape selectivity is represented in figure 1.3.

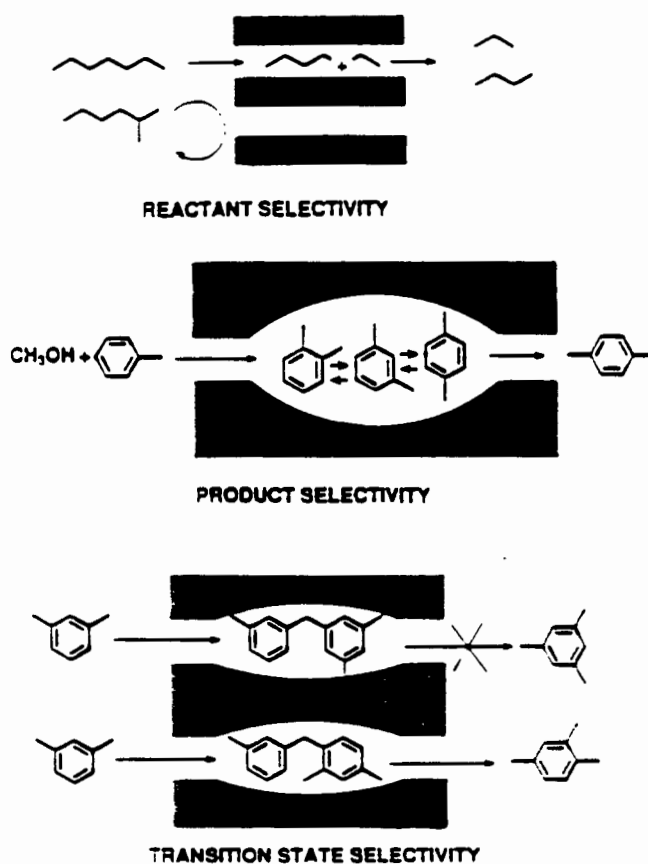


Figure 1.3 showing primary shape selectivity [from Davies and Suib, 1993]

### 1.2.3.2 Secondary shape selectivity

Secondary shape selectivity (or co-reactant induced modification) occurs when the shape selectivity behaviour of zeolites is altered due to the presence of other molecules in addition to the reactants. This phenomenon, which only occurs in restricted environments, is attributed to steric hindrances of the reactant caused by the non reactant. [Khouw and Davies, 1993]

## 1.2.4 Zeolite L as A Catalyst

### 1.2.4.1 Structure of zeolite-L

The structure of zeolite L was determined in 1969 based on powder X-ray diffraction data obtained from a hydrated Na,K - form of the zeolite. It is a unidimensional microporous zeolite whose pores are 12 membered rings with an average pore size of 7.1 Å. Its crystal structure is based on the 18 tetrahedra unit ( $\epsilon$ -cage). These are symmetrically placed across D6R units to give a framework structure which is hexagonal. The space group is P6/mmm with  $a = 18.4$  Å and  $c = 7.5$  Å. Normally, the charge stabilising elements in zeolite L are alkali metals such as potassium. The  $\epsilon$ -cages and the D6R units are presented in figure 1.4.

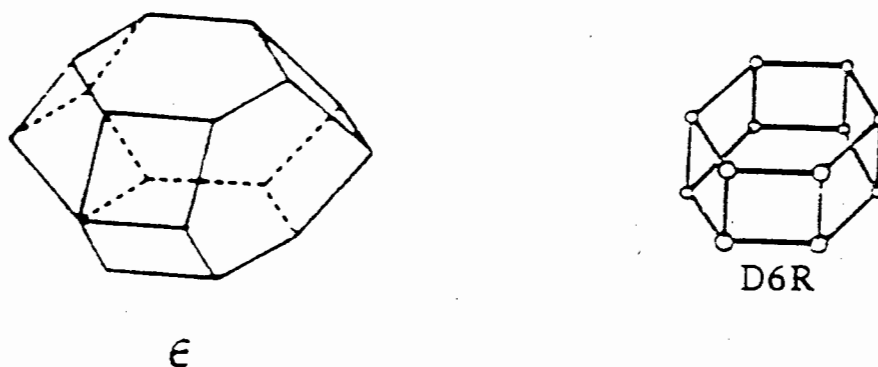


**Figure 1.4** showing the  $\epsilon$ -cage and the D6R units [from Breck, 1974]

Part of the three-dimensional structure of zeolite L as well as the projection view of the zeolite L framework are shown in figure 1.5.

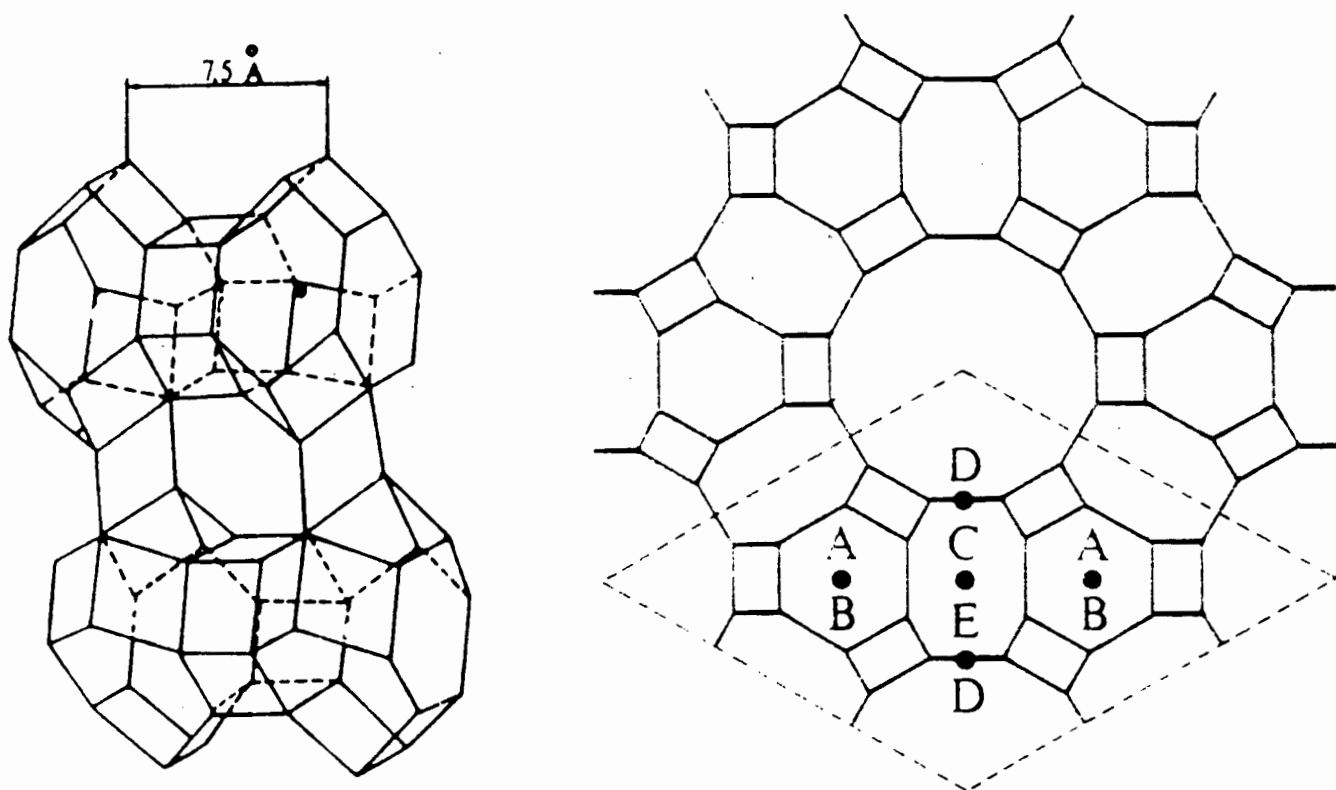


**Figure 1.5** showing part of the three-dimensional structure of zeolite L as well as the projection view of the zeolite L framework [from Breck, 1974 and Delafosse, 1986]

When fully hydrated, zeolite L has four cation positions labelled A to D in the projected view above. Table 1.1 gives a description of the cation positions.

Site	Location	No. sites / unit cell	Occupancy Observed
A	Center of D6R	2	1.4
B	Center of $\epsilon$ -cage	2	2.0
C	Between adjacent $\epsilon$ -cage	3	2.7
D	Wall of main channel	6	3.6
Total		13	9.7 *

\* 9.7 is a calculated value based on partial occupancy of site A by Na<sup>+</sup>

**Table 1.1** showing cation positions in zeolite L [from Breck, 1974]

During dehydration, cations from site D withdraw from the channel walls to a fifth site E located between the A sites. During calcination at high temperatures of about 593 °C, metal ions in the channels can migrate to inaccessible sites such as site E leaving the zeolite pores free of cations that could hinder molecular diffusion. [Derouane and Vanderveken, 1988] In site D, the cations are coordinated with two water molecules in the channels. Cations in the D site are readily ion exchanged. [Breck, 1974] It has been observed that in barium exchanged zeolite L, the barium can be transferred from the C and D sites to the A and B sites by calcining the sample in the temperature range 590 °C - 650 °C. [Hughes *et al*, 1986]

#### 1.2.4.2 Activity of zeolite L in the aromatisation of n-hexane

When loaded with platinum metal, potassium exchanged zeolite L (K/L) has an activity for the aromatisation of n-hexane to benzene. [Larsen and Haller, 1993] Tauster and Steger [1990] suggest that the high selectivity to aromatisation of the platinum K/L zeolite is due to the confining undulating parallel structures of the zeolite L. According to this explanation,



the zeolite L channels might pre-orientate the n-hexane molecule so as to make 1,6 adsorption more probable. Tauster and Steger also made a comparison between Pt/SiO<sub>2</sub> and Pt/(KL). They postulated that Pt/SiO<sub>2</sub>, which has bigger pore diameters, would behave like Pt/(KL) zeolite with the metal situated on the surface. The small pores of zeolite K/L prevent bimolecular coke formation. This reduces the rate of deactivation of the platinum sites within the unidimensional pores of the zeolite L. In Pt/SiO<sub>2</sub>, bimolecular coke formation could easily occur causing the catalyst to deactivate faster.

Another proposal for the aromatisation selectivity of Pt/KL was that the interaction of the Pt particle with the basic L - zeolite walls caused the particles to be electron rich, thus enabling them to catalyse the aromatisation reactions. [Besoukharoun *et al.*, 1980] Another proposal states that the Pt/(KL) catalyses aromatisation reactions because the zeolite L structure, like other non-acidic microporous supports, can stabilise the extremely small platinum clusters. However it is inferred in this proposal that the stability is based on an electronic or bonding nature and not on the zeolite geometry. [Mielczarski *et al.*, 1992] The presence of alkali cations could generate specific platinum crystallite configurations and concentrate adsorbed hydrocarbons. [Derouane and Vanderveken, 1988] This is in agreement with the postulate stating that the platinum zeolite interactions would be enhanced when the acidity of the zeolite is reduced.

Derouane and Vanderveken propose that the aromatisation reaction occurs as a result of structural recognition and pre-organisation as follows:

In step 1, the n-hexane molecule diffuses through the open zeolite channel which should be free of bulky cations and acidic sites. The molecule then meets head-on with a platinum particle and interacts with it by a terminal methyl group. In step 2, the n-hexane molecule then curves itself along the groove of the zeolite cage to optimise its interaction with the zeolite framework. This motion is sterically hindered resulting in the methyl group in the 6 position coming into close proximity with the platinum metal. In step 3, a metallocycle involving the terminal carbons is formed on the platinum particle. This species is the precursor to the cyclohexane, cyclohexene, and eventually benzene. This sequence occurs according to acceptable chemistry principles. The fourth and final step then involves the

desorption of the formed benzene. [Derouane and Vanderveken, 1988]

The high aromatisation selectivities observed over Pt/(KL) were also observed on other microporous supports such as faujasite that had been rendered non-acidic. Mielczarski *et al* then concurred that 1,6 ring closure was an intrinsic property of very small platinum particles and could be achieved on other supports besides zeolite L provided that the acidity of the supports had been decreased and the pore sizes were comparable with those of zeolite-L. This suggests that a high Bronsted acidity of the support would reduce the electron density of the platinum particles thus reducing the aromatisation activity of the platinum particles.

Sugimoto *et al.* found that the zeolite L prepared by impregnation techniques had a higher selectivity to aromatics when compared to zeolite L prepared according to the ion exchange method. This could have been due to the fact that ion exchanged catalysts are more acidic than the impregnated catalysts. [Larsen and Haller, 1993] Catalyst acidity is known to impede the selectivity to aromatisation.

When zeolite Y, mordenite and zeolite L were exchanged with the same alkaline cations, zeolite L was found to have weaker acidic sites. Furthermore, when these supports were loaded with platinum and treated with halocarbons, the acidic strength of the zeolite Y and mordenite were enhanced, resulting in an increased electron deficiency of the platinum particles. [Sugimoto *et al.*, (vol 96) 1993] The acidity of zeolite KL that had been treated with halocarbons was not adversely affected. Sugimoto *et al.* also found that treating zeolite L with halocarbons enhanced its activity towards aromatisation. This was because the halocarbons enhanced the electron density of the platinum particles by reducing the effect of the interaction of the particles with oxygen [Sugimoto *et al.*, (vol 95) 1993].

Under the conditions of the aromatisation reaction, the platinum particles tend to agglomerate and form large clusters. These can be re-dispersed using halocarbons. Forger and Jaeger suggest that re-dispersion of platinum particles on used catalysts was due to a partial rupture of Si-O-Al linkages and a subsequent bonding of a platinum (IV) halide species to the aluminium in the zeolite [Forger and Jaeger, 1989]. They proposed that only strongly bound Pt (IV) species led to a catalyst of high dispersion.

Platinum loaded zeolite L is extremely sensitive to sulphur poisoning causing its activity for dehydrogenation to be greatly reduced in the presence of sulphur. [Hughes *et al.*, 1986]

### 1.2.5 Zeolite Y As A Catalyst

#### 1.2.5.1 Structure of zeolite Y

Zeolite Y is a synthetic type of faujasite the structure of which is shown below. The unit cell of zeolite Y is cubic with a large cell dimension of about 25 Å and it contains 192 (Si, Al)O<sub>4</sub> tetrahedra. The unit is stable and contains the largest void space of any known zeolite amounting to about 50 vol % of the dehydrated crystal. [Breck, 1974]

The chemical composition of zeolite Y can be represented as Na<sub>56</sub>[(AlO<sub>2</sub>)<sub>56</sub>(SiO<sub>2</sub>)<sub>136</sub>].250H<sub>2</sub>O. [Breck, 1974] In HY the sodium is replaced by hydrogen. The aluminosilicate framework consists of a diamond-like array of linked octahedra which are joined tetrahedrally through 6 rings. The linkage between adjoining truncated octahedra is a double 6-ring or hexagonal prism containing 12(S,Al)O<sub>4</sub> tetrahedra. [Breck, 1974] The arrangement of octahedra and hexagonal prisms give rise to a structure shown in figure 1.6.

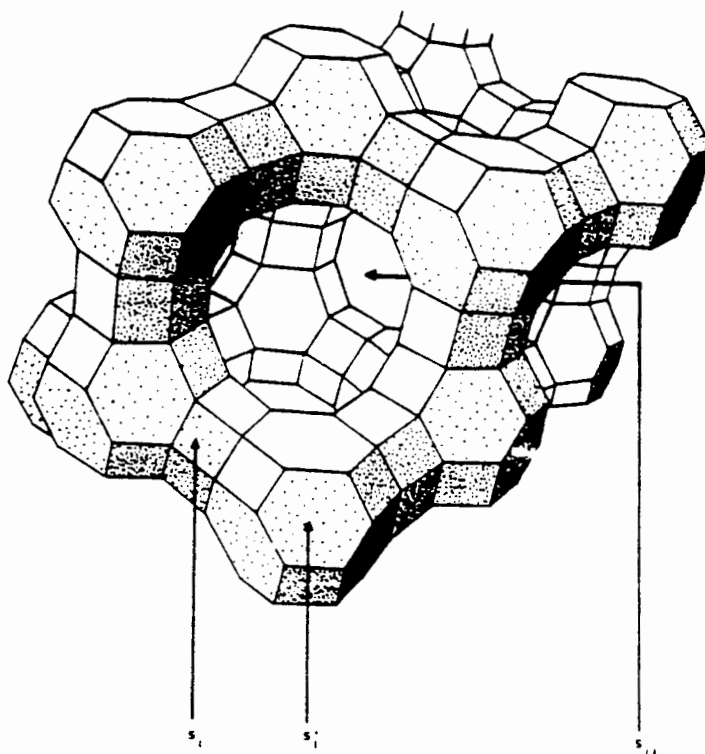
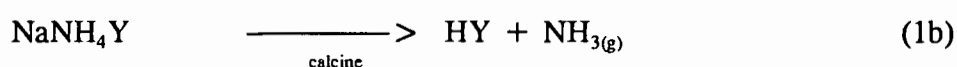


Figure 1.6 showing the structure of zeolite Y [from Delafosse, 1986]

### 1.2.5.2 Acidity And Stability

The protonated form of zeolite Y is normally prepared by loading ammonium ions onto the zeolite and then applying heat to release ammonia and leave protons attached to the lattice oxygen. These protons are the Bronsted acid sites. The process can be represented by the following:



Zeolite Y can be made ultra-stable by treating it with steam at high temperatures (500 °C) to remove aluminium from the framework [Kerr, 1973]. The ultra-stable zeolite can withstand temperatures of up to 1000 °C. [Dyer, 1988]

## 1.3 Supported Metal Catalysts

### 1.3.1 Bi-functional Catalysts

Bi functional catalysis describes situations in which two types of active sites intervene in succession during a chemical reaction. For metals supported on zeotype catalysts the two active sites are the metal atoms and the acid sites on the support. [Jacobs, 1977]

Most bi-functional mechanisms assume efficient mass transport of the reacting molecules and products to and from the metal and acidic functions of the catalyst. There is a required intimacy of the two functions in order to get maximum catalyst activity.

Zeolites containing ion - exchanged transition metals can be used for a wide range of reactions some of which are dehydrogenation, oxidation, cracking and cyclisation. The metal on the zeolite is normally in its neutral solid state. This state is obtained after the reduction of the metal ions. The dispersion of the metal and the particle sizes are dependent on the calcination and reduction conditions.

### 1.3.2 Mono-functional Catalysts

Some catalysts such as platinum on non acidic zeolite-L in aromatisation reactions do not utilise the bi-functionality described above. The platinum catalyses the reaction. The non-acidic zeolite KL does not play any direct chemical role. However, due to its pore structure, it acts as a shape selective support.

### 1.3.3 Metal Support Interactions

The electronic properties of very small metal crystallites are different from those of larger crystallites. Studies have shown that the smaller the crystallite size, the larger the effect of the support on the electronic properties. The electron transfer from the metal atom to the support results in an increase of the metal's hydrogenation activity. The charge transfer can increase with the support acidity. [Alvarez *et al*, 1988] The more acidic the support, the more electrons are transferred from the metal to the support Bronsted acid sites. This leaves the metal in a more electrophilic state.

In non acidic zeolite Pt/KL, the platinum metal particles are stabilised by the electronic interactions between the basic metals already ion exchanged in the zeolite. [Hicks *et al*, 1993] In zeolite Y, charged platinum ions favour the sodalite cages and the hexagonal prisms of the zeolite supports. The negative charge density in hexagonal prisms is higher than at any other sites of the zeolite. The charge on cations would thus be effectively stabilised in these hexagonal prisms. [Tzou *et al*, 1988]

### 1.3.4 Metal Loading Methods

Due to the high cost of noble metals, they must be well dispersed and have an even distribution over the available zeolite surface. Loading should be low in percentage and the exposed metal surface area should be as high as possible.

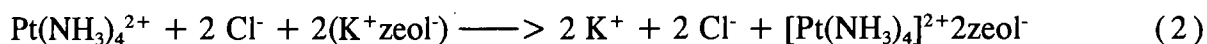
### 1.3.4.1 Liquid ion exchange

In an ideal ion exchange process, incoming metal ions exchange with charge stabilising cations on the zeolite such as sodium and potassium. In practice, the metals to be loaded are ion exchanged as complexes. Since zeolites show a basic reaction in water, care should be taken to ensure that no hydrolysis of the metal occurs during ion-exchange. The extent of cation hydrolysis is affected by three parameters : ionic strength of the exchange solution, liquid to solid ratio and the exchange temperature [Jacobs, 1977]. A high concentration of ions increases the electric field of the cations which in turn increases the dissociation of water. This would then cause cation hydrolysis [Schoonheydt *et al*, 1976]. To avoid hydrolysis of the metal ions, ion exchange is normally carried out in dilute solutions, at high liquid to solid ratios and at low temperatures. [Jacobs, 1977]

Hydrolysis of the cation can also be avoided by using stable cation complexes such as amine complexes. [Jacobs, 1977] In loading platinum in microporous supports, the square planar tetra-ammine complex ions of platinum have easy access into the pores compared to larger octahedral and hexa co-ordinated complexes such as those of cobalt and rhodium. [Dessau, 1984] The platinum compound commonly used in impregnation is  $\text{H}_2\text{PtCl}_6$ . Unlike the tetra-ammine complex, this would dissolve in water to give  $\text{PtCl}_6^{2-}$  which are large, octahedral and negatively charged. These ions would then be unsuitable for ion exchange.

In ion-exchange, the amount of metal loaded onto the support can be controlled by either varying the amount of metal in the liquid phase or, subsequently back exchanging with ions such as those of sodium and cesium. [Dessau, 1984] Kampers *et al* predict that ion exchange would produce atomic dispersion of the metal because one tetra-ammine complex can be associated with an aluminium site [1990]. These complexes are charged and are Coulomb bound to the support matrix thus hindering their mobility during calcination. This helps to prevent sintering of the metal atoms.

Using  $\text{Pt}(\text{NH}_3)_4\text{Cl}_2$  to ion-exchange a zeolite containing potassium as a charge stabilising atom can be seen as occurring via reaction 2:



The  $\text{K}^+$  and the  $\text{Cl}^-$  ions are removed by filtration and subsequent washing. [Ostgard, 1992]

Due to strong interaction between the metal complex and the zeolite, Kouwenhoven *et al* suggest that the metal complex would be deposited near the surface of the zeolite particle [1991]. This effect would be reduced by the addition of a competing ion such as  $\text{NH}_4^+$  and  $\text{K}^+$ .

Sometimes zeolites in which ion-exchange is performed contain less metal than theoretically possible. This might be due to one or more of the following factors:

- i. Ion sieving, in which the cations are excluded from the pores as a result of the shape selectivity of the zeolites.
- ii. Volume exclusion, in which cations whose size is similar to pore size block the zeolite pores. This would prevent other ions from entering the pores and exchanging with other sites along the pores.
- iii. Different exchange sites may have different energies of interaction. This would cause difficulty in removing cations from certain sites.

#### 1.3.4.2 Solid state ion exchange

In solid state ion exchange, a finely dispersed powder of the compound of the in-going ion is intimately mixed with a finely dispersed powder of the starting zeolite. The mixture is then heat treated in various media such as in air, inert gas or in a vacuum.

#### Effect of temperature

The temperature required for achieving a certain degree of exchange frequently depends on the nature of the cations and anions involved. In the solid state ion exchange of metal chlorides (eg  $\text{NaCl}$ ) onto  $\text{NH}_4/\text{ZSM-5}$ , the reaction is accompanied by the evolution of  $\text{HCl}_{(\text{g})}$ . The solid state ion exchange of alkali chlorides with low lattice energy occurs at low temperatures while that of salts with high lattice energy occurs at high temperatures. The low

temperature reaction is often associated with the evolution of the water of hydration in the crystals of the metal compounds. [Karge, 1991]

Some results of the  $\text{MnCl}_2$  / H-ZSM-5 system studied by Beran *et al* are presented in figure 1.7. According to this system, high temperatures favour high degrees of exchange. [Beran *et al*, 1990] At a particular temperature, the solid state ion exchange reaction occurs very quickly to a certain degree and then it continues very slowly. However, the effect of temperature and time on OH groups may depend on cations that are already incorporated into the zeolite. [Beran *et al*, 1990] For the system  $\text{NaCl}/\text{NH}_4$  zeolite at temperatures as low as 25 °C, some degree of solid state reaction occurs as evidenced by the release of  $\text{HCl}_{(g)}$  and  $\text{NH}_{3(g)}$ . [Beyer and Karge, 1988]

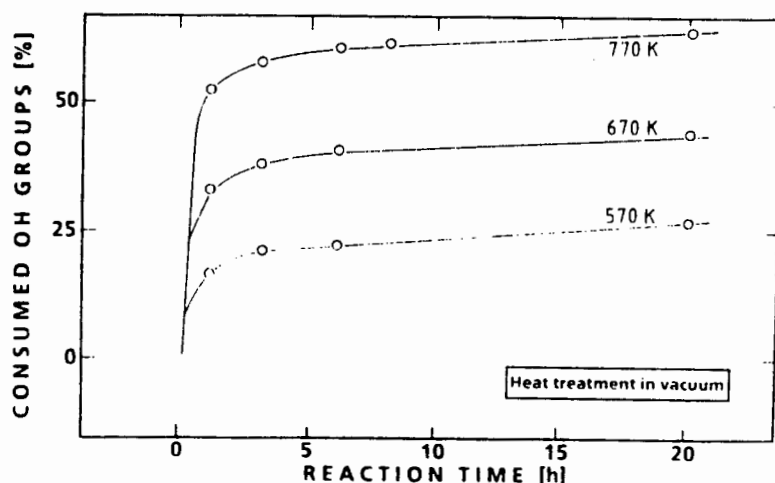


Figure 1.7 showing how the degree of solid state ion exchange on ( $\text{MnCl}_2$ /H-ZSM-5) is affected by temperature and time [from Karge, 1991]

Although the degree of solid state ion exchange is affected by temperature, it is not apparent which step is controlled by temperature. At present, little is known about the mechanisms of solid state ion exchange. For the reaction occurring between a hydrogen form of a zeolite and a metal chloride, the following two mechanisms have been proposed [Beyer and Karge, 1988]:



- 1) Protons may migrate to the outer surface of the zeolite crystals and may react there with the crystalline alkali metal chloride while the metal ions migrate to cationic sites in the zeolite.
- 2) Interaction between the outer zeolite surface and the crystalline metal chloride may reduce the bonding energy of the latter. This would enable chloride molecules to migrate into the zeolite cavities where they would then react with protons to give gaseous HCl.

For the high temperature reactions, the second mechanism would seem more probable.

### **Effect of stoichiometry**

Normally, solid state ion exchange is carried out in stoichiometric mixtures of the metal compounds and zeolites. The stoichiometry is related to the aluminium content of the zeolites. However, mixtures containing an excess of in-going cations may be used and the excess metal cation removed by washing with water.

### **Effect of cations and anions**

For highly siliceous zeolites, the exchange of bi or trivalent cations into zeolite by solid state ion exchange is considerably more difficult compared to monovalent cations. [Karge, 1992] Chlorides and oxides of most metals can successfully take part in solid state ion exchange reactions. However, carbonates, sulphates, acetates, bromides, fluorides and nitrates are unfavourable for solid state ion exchange because they decompose quite easily.

### **Role of water**

In a mixture of metal chloride and H-ZSM-5, and at low temperatures (100 °C), the evolution of  $\text{HCl}_{(g)}$  during solid state ion exchange occurs simultaneously with the removal of the water of crystallisation associated with the metal compound. This led some researchers to think that solid state ion exchange could only occur in the presence of water. However, it has been shown that solid state ion exchange can occur in ultra high vacuum and in the absence of water. [Karge, 1991]

When the hydrogen form of mordenite is used in solid state ion exchange with  $\text{CaCl}_2$ , the acidic sites were replaced by the metal ions. Subsequent treatment of the zeolite with water was found to restore up to 91 % of the OH groups. This could have been due to the generation of the Bronsted acidic sites via dissociating water molecules in the electrostatic field of the cations. The  $\text{OH}^-$  ions then attach themselves to the zeolite wall. [Karge, 1991]

#### 1.3.4.3 Impregnation

In impregnation, the support is wetted with just enough of the impregnating solution to fill the pores, followed by drying and calcination. In co-impregnation, one or more chemical species are added to the solution to modify the deposition characteristics of the active ingredient in order to achieve a desired distribution effect within the catalyst support particle.

The solution is transported into the pores by capillary action. For porous supports such as silica and alumina, the characteristic time governing the capillary suction in a cylindrical pore may be characterised by

$$t = 2\eta x^2 / \sigma r \quad (3)$$

where  $t$  is the impregnation time in seconds

$\eta$  is the dynamic viscosity of the liquid,

$x$  is the effective capillary length,

$\sigma$  is the surface tension of the solution,

$r$  is the mean pore radius.

The flow of the solution into the pores is accompanied by the adsorption of the active ingredients onto the pore walls. The rate of adsorption and desorption of the active species and their relative amounts determines the distribution of the metal on the support. [Becker and Nuttall, 1978]

Unlike ion-exchange, the adsorption process in impregnation results in a random distribution of the metal. The adsorbed species are neutral without any Coulombic interactions with the support matrix. This makes them mobile and thus encourages sintering of the metal during calcination. Unlike liquid state ion exchange, the anions are not washed out during impregnation. If chloride anions are present as is the case in  $\text{Pt}(\text{NH}_3)_4\text{Cl}_2$ , then these might enhance the dispersion of the metal.

In impregnating metal complexes onto alumina, Heise and Schwarz [1987] propose that ingredients added to the impregnating solution can be classified according to their effect on interfacial phenomena.

- i. Inorganic electrolytes such as  $\text{NaNO}_3$ ,  $\text{NaCl}$  which affect the electrostatics of the solution-surface interface. This in turn affects the accessibility of the metal to available surface sites. The electrolytes electrically screen the active sites uniformly along the support pore. This causes the metal coating to be thinner and to extend deeper into the pore.
- ii. Inorganic acids and bases such as  $\text{HCl}$  and  $\text{HNO}_3$  which alter the chemistry of the surface by changing the surface potential. This affects the number of available surface sites.
- iii. Compounds that compete with the metal ion for possible adsorption sites and affect the metal adsorption in a chromatographic manner. The most effective of these compounds contain hydroxyl and carboxyl groups.

#### 1.3.4.4 Crystallisation

In this method, the metal on a support is added as a seed to a gel in order to provide nucleation centres for the synthesis of a zeolite. An example of this is the addition of ruthenium on alumina to a gel from which ZSM-34 eventually crystallises. It is difficult to determine whether the product is just an intimate physical mixture of the metal on support with the zeolite or whether the metal becomes occluded in the zeolite.

### 1.3.5 Activation Of Prepared Catalysts

When the catalysts have either been ion-exchanged or impregnated, they are heated at high temperatures in order to decompose the metal complex and give off the ligands. At these temperatures, water in the zeolite pores is also removed. This process is called calcination.

The distribution of the metal in the catalyst is affected by the processes occurring during calcination. It is thus important to calcine the catalysts under specific controlled conditions so as to obtain the required metal distribution.

Park *et al* [1986] proposed the following mechanism for the calcination process in oxygen of zeolite Y exchanged with platinum II tetra-ammonium complex ( $\text{Pt}(\text{NH}_3)_4\text{Cl}_2$ ):

- 1 Decomposition of the  $\text{NH}_3$  ligands to form  $\text{Pt}^{2+}$  ions.
- 2 Auto-reduction of some  $\text{Pt}^{2+}$  ions by the decomposing  $\text{NH}_3$ .
- 3 Migration of some  $\text{Pt}^{2+}$  ions from the supercages to the sodalite cages and hexagonal prisms.
- 4 Reaction of  $\text{Pt}^{2+}$  with water to form  $\text{PtO}$  particles and protons. The water is formed during the decomposition of the  $\text{NH}_3$  ligands.

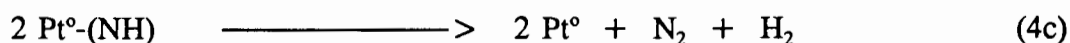
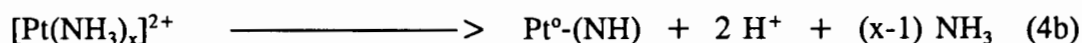
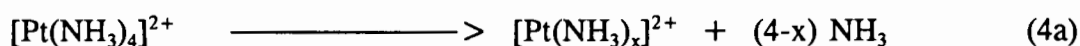
Each of these steps is observed at a certain temperature. In the case of reduction, the first step is very important because the ammonia ligands protect the platinum ions from attack by hydrogen. Therefore, if removed, the reduction would occur easily at a low temperature.

#### 1.3.5.1 Calcination parameters affecting final metal distribution

##### Calcination atmosphere

Reagan *et al* reported that air was an inert medium in the decomposition of the platinum ammonium complex during calcination. However ammonia given off in the calcination could be catalysed in an oxidation reaction by the platinum on the support. The desired decomposition of the tetra-ammine complex would yield  $\text{Pt}^{2+}$  attached to the zeolite matrix.

If calcination is performed in oxygen, platinum could be oxidised to yield PtO which would in turn interact with the zeolite matrix. The  $\text{Pt}^{2+}$  is referred to as a bare metal ion. In an inert atmosphere, auto-reduction of the tetra-ammine complex could occur. This process occurs via electron transfer between the metal ions and the ammonia ligands. [Reagan *et al*, 1981]



If bare metal ions were formed as a result of the decomposition of  $\text{NH}_3$  ligands during calcination, they could also be reduced to the neutral form. This is because the  $\text{NH}_3$  ligands removed may decompose to give nitrogen and hydrogen. The hydrogen formed could then reduce some of these metal ions. The  $\text{H}^+$  ions produced would then attach themselves to the zeolite matrix to yield Bronsted acid sites. The maximum rate of auto-reduction was observed to occur at the same temperature at which maximum metal distribution occurred if calcination was carried out in oxygen. [Reagan *et al*, 1981] If partially decomposed complexes are present, then hydrides (e.g  $\text{Pt}(\text{NH}_3)_2\text{H}_2$ ) could be formed.

To avoid sintering of the metal particles during calcination, oxygen should be used. Oxygen prevents the formation of neutral hydride molecules which easily cause sintering. The oxygen oxidises the  $\text{NH}_3$  to form water and nitrogen. A high gas rate would then be needed to remove the water and the nitrogen from the vicinity of the metal. [Engelen *et al*, 1986] However small amounts of the hydrides have also been observed in an oxygen atmosphere. [Reagan *et al*, 1981]

Reagan *et al* contradict most workers by claiming that the thermal decomposition of the platinum tetra-ammine complex always results in the formation of platinum metal and not ions. [Reagan *et al*, 1981] On the other hand, Chmelka *et al* claim that the decomposition of the tetra-ammine complex in oxygen at 400 °C results in the formation of PtO attached to the zeolite wall. The PtO may then lose the oxygen atom at 500 °C to give  $\text{Pt}^{2+}$  cations. [Chmelka *et al*, 1988] It has also been claimed that thermodynamically, supported oxides species are easier to reduce than metal ions. [Jacobs, 1977] It could thus be advantageous to

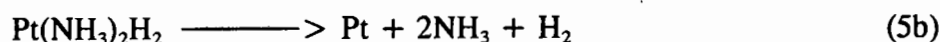
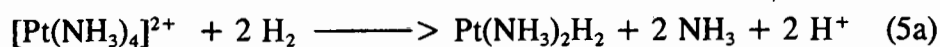
first form the metal oxide before reducing the catalyst .

### Temperature

The temperature at which the catalysts are calcined determines the location of the metal ions prior to reduction. Shpiro *et al* report that a 0.5 weight % Pt/H-ZSM-5 catalyst calcined at 447 °C resulted in smaller particles (8 Å) compared to the particles obtained after calcination at 527 °C (15 Å) [Shpiro *et al.*, 1991].

Alvarez *et al* [1988] as well as Park *et al* [1986] reported a maximum platinum distribution in PtH mordenite at a calcination temperature of 300 °C. This temperature was found to give optimum dispersion in other supports such as ZSM-5 as well. The maximum value of the dispersion would be obtained at the minimum temperature necessary to attain complete decomposition of the complex. Below this temperature, some of the complex ions are not decomposed and some are partly decomposed. If a small amount of platinum metal is formed during calcination, the ammonia given off could be catalytically converted on the platinum metal to nitrogen and hydrogen. The hydrogen could then attack the metal ammine complex, which is partly decomposed, leading to the formation of hydrides which are mobile in the zeolite structure. The mobile hydride species lead to platinum sintering [Alvarez *et al*, 1988]. Hydrides could also be formed during the reduction of the undecomposed complex ions by hydrogen.

Hydride formation and subsequent metal formation are shown in equation 5.



At high calcination temperatures in air, decomposition of the complex is almost instantaneous. If the dry air flow can not immediately remove the ammonia, nitrogen and hydrogen produced, mobile hydride species leading to metal agglomeration could be produced. This could occur via the reversal of equation 5b.

According to Tzou *et al* [1988], the distribution of the metal ions between the sodalite cages and the supercages of zeolite Y is determined by the calcination temperature. At a calcination temperature of 633 K the majority of  $\text{Pt}^{2+}$  ions would be in the supercages. At a higher temperature of 723 K, some of the  $\text{Pt}^{2+}$  ions migrate to the sodalite cages and these require high temperatures for reduction. In subsequent reduction treatments, the ions in the supercages are reduced to neutral particles which then act as nucleation sites for the  $\text{Pt}^0$  leaving the sodalite cages. In zeolite L, high calcination temperatures would cause the cations to migrate to inaccessible exchange sites located in the cancrinite cavities. [Besoukhanova *et al*, 1981]

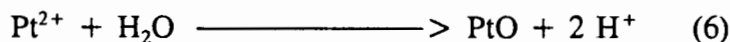
In zeolite Y, the migration of the ions to the sodalite cages and hexagonal prisms as well as the subsequent reduction require high temperatures. At these high temperatures vibrations of the sodalite structures and hexagonal prisms would stretch the openings thus allowing passage of atomic size material such as the reducing gas. [Chmelka *et al*, 1991] The metal ions are more stable in the sodalite cages where the negative charge density is higher. After reduction, the  $\text{Pt}^0$  formed migrate to the supercage in zeolite Y. If they encounter a neutral metal atom there they would nucleate around it otherwise they would migrate to the external surface of the zeolite where they form large particles. The metal particles formed after reduction might exit the hexagonal prisms because of various reasons such as the sudden increase in radius in going from the ion to the neutral atom. The atom would be much bigger than the hexagonal prism and would break out of the prism. Other factors such as the reduced electrostatic interaction between the support and the metal, as well as the fact that metal atoms are more stable in clusters than when they are dispersed, might also encourage the metal atoms to leave the hexagonal prisms and sodalite cages.

The optimum calcination temperature was found to be related to the nature of the compensating cations. [Jacobs, 1977] The optimum calcination temperature for PtNaY was found to be 573 K while that for PtHY was found to be higher than this. The reason for this phenomenon is not yet fully understood. Calcination at excessively high temperatures can result in thermal damage of the zeolite catalysts.

The time taken to calcine a catalyst is also important [Jacobs, 1986]. This means that the rate at which the temperature is ramped should be determined carefully. In large catalyst batches, the sample amount and bed geometry affect the temperature and time of calcination. For large amounts of catalysts, reproducibility of calcination results is very difficult. This might be due to a non uniform temperature across the large catalyst bed.

### Water content

Park *et al* note that the decomposition of  $\text{NH}_3$  ligands in the presence of oxygen, results in the formation of water which then reacts with  $\text{Pt}^{2+}$  as follows:



These workers also suggest that the agglomeration of platinum atoms to particles does not only occur after reduction of the  $\text{Pt}^{2+}$  ions but also takes place during calcination when  $(\text{PtO})_n$  particles are formed by interaction of water vapour with  $\text{Pt}^{2+}$  ions. [Park *et al*, 1986]

### Treatment with halocarbons

The treatment of some zeolites especially zeolite-L with halocarbons before loading them with the metal has been found to improve their activity and selectivity for n-hexane aromatisation. [Sugimoto *et al*, (vol 96) 1993] The halogen contents of the KL zeolites were found to depend on the halogen species. The catalyst treated with  $\text{CFCl}_3$  at 500 °C had the lowest aromatisation selectivity while that treated with  $\text{CF}_3\text{Cl}$  at 500 °C had the highest. This difference could be attributed to the different carbon-halogen bond cleavages.

## 1.3.6 Reduction Of Metals

### 1.3.6.1 Reducibility

Reducibility can be quantified as i) the initial rate of reduction at a given temperature and ii) the degree of reduction at a given temperature and after a given reduction time. [Jacobs, 1986] Parameters influencing the reducibility of the metal cations are the calcination



conditions, the nature of the compensating ions, the presence of anchoring ions and the nature of the zeolite. [Jacobs, 1977] If NiX catalyst is dehydrated at high temperatures during calcination, then the reducibility of the nickel ions is decreased. This is probably due to the fact that the metal ions migrate to the hexagonal prisms under these conditions. It has been found that 99 % of the hexagonal prisms contain two or more aluminium atoms for Y zeolites with a Si/Al ratio of 2.49. The high Coulombic interaction and the steric difficulty of admitting dihydrogen molecules through O<sub>6</sub> rings of the hexagonal prisms, contribute towards the low reducibility of the cations in these positions. [Tzou *et al*, 1988]

The addition of other cations with a preference for sodalite cages and hexagonal prisms such as cerium would increase the reducibility of the nickel ions. [Jacobs, 1977] Though it has been found that the nature of the zeolite determines to a certain extent the reducibility of nickel ions and therefore the degree of dispersion, [Jacobs, 1977] no definite explanation has yet been found for this behaviour. It may be rationalised in terms of the different electrostatic forces existing between the metal cations and the zeolite matrix.

Provided that the reduction is not kinetically controlled, the reducibilities of transition metal ions in a zeolite will be enhanced for thermodynamic reasons if atomic, rather than molecular hydrogen, is used as the reducing agent. [Jacobs, 1986] *In situ* generation of H atoms would be necessary for this. In NaY zeolite, Ni reduction using atomic hydrogen can be performed at a low temperature of 273 K. [Delafosse, 1980] This makes cations situated in the sodalite cages accessible to hydrogen resulting in complete cation reduction to the neutral form. At this low temperature, the mobility of the cations and the metals would be restricted resulting in less agglomeration of the metal particles.

There appears to be a critical value for the lattice hydroxyl groups above which certain cations such as Ni<sup>2+</sup> become almost irreducible. [Jacobs, 1986] It has been inferred that these hydroxyl groups decrease the reduction rate of the metal cations. [Jacobs, 1986] Zeolites exchanged to a high degree with transition metal ions do not easily undergo complete reduction. In this case, the reduction could be considered as an equilibrium reaction [Jacobs, 1986].

### 1.3.6.2 Proposed mechanism of reduction

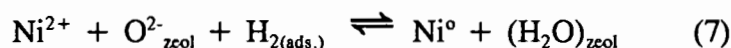
Many materials such as sodium metal vapour, hydroxylamine, carbon monoxide and hydrogen are used to reduce the metal precursors. Hydrogen is the most frequently used medium. The mechanism for hydrogen reduction of platinum on zeolite L is expected to be similar to that obtained for platinum supported on NaY. Homeyer and Sachtler suggest the following mechanism for the reduction of platinum ions in the supercages in NaY zeolite ;

- 1 Formation of a neutral nucleus  $Pt_n$  ( $n = 1, 2, \dots$ );
- 2 Migration of the complexed or bare ions to a supercage containing a nucleus;
- 3 Adsorption of the cation on the nucleus;
- 4 Release of the ligands;
- 5 Dissociative adsorption of dihydrogen;
- 6 Release of two protons for each Pt ion reduced which become attached to oxide ions of the cage wall;
- 7 Migration of the primary particles and their coalescence to larger particles.

Step 2 is the growth limiting step whose rate depends on the degree of complexation. A high growth rate implies that the nuclei mop up all the available material and metal dispersion will be low. A low growth rate combined with a moderate rate of nucleation will result in the formation of numerous small particles which would in turn lead to high dispersion. Steps 3 to 6 are fast. The particle growth stage, (7) would then be limited by the size of the supercage. [Homeyer and Sachtler, 1991]

Various other mechanisms have been proposed for the reduction of different metals. Generally, for all metals, the initial hydrogen uptake is fast and is followed by a slower rate. In NiX zeolites, it was found that the slower process was independent of the  $Ni^{2+}$  content and was poisoned by traces of water. [Jacobs, 1977] This suggested the following mechanism for the reduction of the Nickel

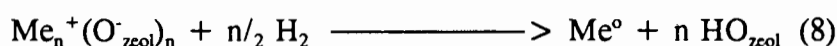
- 1 Chemisorption of hydrogen on supercage  $\text{Ni}^{2+}$  ions.
- 2 Reduction of the  $\text{Ni}^{2+}$  ions and a simultaneous back reaction :



- 3 Migration and aggregation of the nickel atoms.

The produced protons are then attached to the oxide ions of the supercage wall to form Bronsted acid sites. This is undesirable for aromatization catalysts such as zeolite L. Acid sites can be minimised by back exchanging the protons with the original metal ions [Larsen and Haller, 1993] or by reduction with a substance that does not contain hydrogen such as sodium vapour [Gallezot, 1975] or carbon monoxide.

For platinum and nickel it has been noticed that the reduction process:

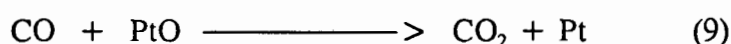


can be reversed for ions in sodalite cages. At high temperature and in an inert atmosphere, the metal atoms are re-oxidised by the protons and hydrogen is released.

De-hydroxylation of some of the produced lattice hydroxyl groups would then occur to produce water. If metal oxides are formed during calcination, these are reduced to neutral form with the formation of water. [Park *et al*, 1986]

Roland *et al* have shown that reduction of Pt/HY in hydrogen can result in a higher hydrogen uptake than required to reduce all the platinum ions present. This has been attributed to the adsorption of the hydrogen onto the zeolite support via a process called spillover. In spillover, the hydrogen molecule is split into two atoms by the neutral platinum particles. The hydrogen atoms formed then diffuse onto the support. [Roland *et al*, 1994]

If carbon monoxide is used then, the zeolite should first be calcined in oxygen to produce a metal oxide which on reduction with CO would yield  $\text{CO}_2$  as shown in equation 9.



However, at temperatures higher than 300 °C, CO undergoes disproportionation to yield CO<sub>2</sub> and carbon (C). The carbon would then be deposited on the zeolite resulting in coking. Thus reduction temperatures in CO should be monitored closely to prevent this from happening.

### **1.3.7 Distribution Of Metal On Supports**

#### **1.3.7.1 Effect of activation conditions**

As discussed above, the calcination procedure is crucial for the determination of the distribution of the metal ions between the supercages and the sodalite cages in zeolite Y. This distribution then governs the size and location of the metal. The best distribution of a metal in a molecular sieve is achieved when water is completely removed from the zeolite during calcination at high temperatures. This is because partial dehydration results in less active and less stable products with poor metal dispersion. A calcination temperature of 573 K enables maximum metal distribution in ion-exchanged zeolites. [Alvarez, 1988] Reduction conditions also influence metal location.

#### **1.3.7.2 Size and location of metal clusters**

Studies have shown that reduction of platinum in zeolite KL at high temperatures ( > 500 °C) results in large metal particles. [Vaarkamp *et al*, 1993] At high temperatures, platinum particles have much energy and they migrate easily and meet with other particles to form larger clusters. In the presence of hydrogen (as is the case when NH<sub>3</sub> ligands disintegrate and form the tetra-ammine complex), platinum hydrides could easily be formed at high temperatures. These would also migrate to form large clusters.

Reduction of the platinum at 300 °C would result in the formation of small metal particles of about 6 atoms as determined by Extended X Ray Absorption Fine Spectrum (EXAFS). The platinum atoms would be supported by oxygen atoms from the support at a distance which suggest the presence of interfacial hydrogen between the platinum and the oxide support. Reduction at high temperatures of 610 °C would result in the loss of interfacial hydrogen which in turn would cause the Pt-O distance to be reduced thus enhancing the electron interaction between the platinum and the support. Vaarkamp *et al* also found that

the catalytic activity of the Pt/KL was increased with an increase in reduction temperature. This was attributed to the changes in the electronic structure of platinum induced by the zeolites and not to the particle size which increased with reduction temperature. [Vaarkamp *et al*, 1993]

Knowledge of the size of the metal particles allows speculation about their location in a zeolite matrix. Studies to determine the size of particles in zeolite channels have suggested that metal particles resulting from low temperature calcination are situated at channel intersections of three-dimensional supports. Metal agglomerates larger than the channel sizes could be accommodated in the zeolite pores by distorting the zeolite framework. Cylindrically shaped particles could also be found in the zeolite channels. Encapsulation of the zeolite matrix by the metal could also occur. [Shapiro *et al*, 1991] The performance of some metal supported catalysts depends more on the metal particle size than on the electron transfer between the metal and the support. [Jacobs, 1986]

It is possible to prepare Pt/(K/L) catalysts containing large metal particles on the external surface of the zeolite. [Hughes *et al*, 1986] In this case the metal loading and the calcination temperature were quite high - 5 wt % and 480°C respectively.

#### 1.3.7.3 Chemical anchoring

Chemical anchoring involves loading secondary polyvalent metals onto the support in order to prevent sintering of the desired metal species. The anchoring agents prevent sintering in two ways. Firstly these agents which are difficult to reduce occupy the sodalite cages and the hexagonal prisms of zeolite Y thus preventing migration of the desired metal to these cages during calcination. [Jacobs, 1977] These ions are held at their positions by Coulombic interactions with cage walls. [Tzou *et al*, 1987] Secondly, they increase the interaction between the zeolite matrix and the desired metal species. [Tzou *et al*, 1986] The anchoring agents are electrostatically bound to the zeolite matrix and they interact chemically with the platinum particles thus increasing the interaction between the platinum and the zeolite. This stops the platinum from sintering easily. Care must be exercised in choosing anchoring agents since they can also catalyse certain reactions.

In zeolite Y, anchoring agents increase the reducibility of platinum by forcing the platinum ions to remain in the supercages during calcination. The migration of the platinum to the sodalite cages normally results in the formation of large external platinum particles after reduction of the platinum ions. Use of the anchoring agents would ensure that these large particles are not formed even at high calcination temperatures. Tzou *et al* [1988] found that co-exchanging  $\text{Fe}^{2+}$  into NaY dramatically decreased the size of Platinum particles in the same zeolite. Delafosse also noted that the size of Nickel particles on zeolite Y after hydrogen reduction in the presence of  $\text{Ce}^{3+}$  ions was reduced. [1980]

#### 1.3.7.4 Metal re-dispersion

In re-dispersing used platinum catalysts, it is possible to restore the platinum particles to their original electron density state. [Sugimoto *et al*, vol (95) 1993] Agglomerated platinum on zeolites can be re-dispersed when reacted with halogens. In the case of chlorine, successful re-dispersion always requires the formation of platinum chloride compounds, which are able to migrate over the support until they are trapped at surface sites.

The interaction between the zeolite surface and the platinum halide species has to exceed intermolecular forces between the platinum halide species itself in order to prevent bulk crystal formation. A scheme is proposed which involves partial rupture of Si-O-Al linkages and bonding of a platinum (IV) halide species to the aluminium in the zeolite. Only the strongly bound  $\text{Pt}^{\text{IV}}$  species leads to the catalysts of high dispersion upon reduction. [Forger and Jaeger, 1989]

Sugimoto *et al* also found that treating K/L zeolites with chlorotrifluoromethane ( $\text{CF}_3\text{Cl}$ ) increased the catalytic activity of the catalyst for the aromatisation of hexane. From their treatment of the catalyst with ( $\text{CF}_3\text{Cl}$ ), they inferred the following about the effect of the halogen on the catalyst:

- i They cause high dispersion of the platinum particles due to the depression of sintering and the promotion of dispersion during reduction.
- ii They maintain the platinum metal dispersion during hexane aromatisation.
- iii They reduce the accumulation rate of the carbon deposits as a result of the low hydrogenolysis activity. However, removal of the small amounts of accumulated coke was hampered by the halogens due to their depression of the burning of coke or due to the deposition of incompletely burned halocarbons as coke.

Sugimoto *et al* found that in the treatment of KL with  $\text{CF}_3\text{Cl}$ , increasing the temperature from 573 K to 773 K increased the halogen content of the zeolite. This resulted in a better selectivity to aromatics. [Sugimoto *et al*, (vol 96) 1993]

Only a small amount of aluminum was reported to be removed from the zeolite framework and the terminal OH groups were replaced by the halogens during the halocarbon treatment. Based on their results of infrared spectroscopy of adsorbed CO and X-ray photoelectron spectroscopy, Sugimoto *et al* deduced that platinum particles supported on  $\text{CF}_3\text{Cl}$ -treated KL zeolite became electron-rich. This was due to the fact that the interaction of the platinum particles with framework oxygen on zeolite KL had been reduced. [Sugimoto *et al*, (vol 96) 1993] The Bronsted acidity of the catalysts was not affected by the treatment with the halocarbons. It was found that the specific surface area of zeolite KL treated with halocarbons was less than that of the untreated zeolites. [Sugimoto *et al*, (vol 96) 1993] This could have been due to the formation of  $\text{AlF}_3$  or  $\text{AlCl}_3$  which cause pore blockages.

In contrast to the zeolite KL treatment, zeolite NaY treated with halocarbons had their acidity increased. This could have been due to the fact that their OH groups which were not substituted by the halocarbons had their acidity enhanced by the inductive effect of the halocarbons. [Sugimoto *et al*, (vol 96) 1993]

## 1.4 Characterisation Techniques

At each stage of the incorporation process, the modified catalysts need to be characterised in order to determine the chemical changes occurring at each stage. Most of the characterisation techniques are not conclusive on their own. However, when a number of these techniques are used together, they could give results which may be interpreted reliably.

### 1.4.1 Atomic Absorption Spectroscopy (A.A.S)

Atomic absorption spectroscopy (AAS) is based on absorption of light by atoms or elementary ions. Certain regions of the spectrum yield atomic information. These are the ultraviolet/visible and the X-ray regions. Visible and ultraviolet spectra are obtained by converting the components of a sample into gaseous atoms or elementary ions by suitable heat treatment. The sample should be converted into an atomic vapour by a process called atomisation. Atomisation is the step which determines the accuracy of atomic absorption. The absorption of light by the resulting mixture then enables qualitative and quantitative determination of one or more of the elements present in the sample.

The solution containing the analyte is atomised in the following steps. A nebulizer takes the solution and then turns it into very fine droplets which are subsequently mixed in the spray chamber with both the fuel and support gases. This mixture is then injected into the flame which finally produces the atoms of the element to be analysed.

In AAS an external light source is used to irradiate atoms in the flame. This source consists of a hollow cathode lamp which emits only the wavelengths characteristic of the analyte atom. If the analyte atoms are present in the flame, they would absorb the specific wavelengths. The energy that they absorb would cause them to change to an excited state. The light not absorbed would then pass through to the flame of the monochromator where the analytical wavelength would be isolated.

The intensity of the light emitted by the lamp would be reduced after passing through the



flame. The amount of light absorbed would be directly proportional to the number of analyte atoms present in the flame and therefore to the analyte concentration. Absorption would then be measured as the difference between the light absorbed when the analyte is present in the flame and when absent. If the intensity of the light from the lamp is  $I_0$  and that of the light that has passed through the flame is  $I_t$ , then the absorbance  $A$  is given by Beer's law as

$$A = \log_{10} \frac{I_0}{I_t} \quad (10)$$

Atomic spectral methods such as AAS have been used to determine 70 elements in sensitivities that fall in the parts per million to parts per billion range. [Skouge and Leary, 1992] In the atomic absorption analysis of modified zeolites, the zeolites are firstly dissolved according to prescribed methods and then analysed.

#### **1.4.2 Transmission Electron Microscopy (TEM)**

Transmission electron microscopy (TEM) is advantageous because it enables one to see the platinum particles. Studies can reveal the particle size distribution as well as the average particle sizes. TEM can also help to determine whether the metal particles are in the zeolite pores or on the external surface. It can also determine whether the particles are randomly distributed or whether they are concentrated in clusters. If the particles are large enough, then their shape and crystalline form can be determined. High atomic weight elements such as platinum can be distinguished from the support due to different electron absorption.

#### **1.4.3 Infrared Spectroscopy (IR)**

Infrared spectroscopy is used for both qualitative and quantitative analysis. In order to absorb infrared radiation, a molecule must undergo a net change in dipole moment as a consequence of its vibrational or rotational motion. Only under these circumstances can the alternating electrical field of the radiation interact with the molecule and cause changes in the amplitude of one of its motions. If the frequency of vibration exactly matches a natural vibration

frequency of the molecule, then a net transfer of energy takes place. This would result in a change of the amplitude of the molecular vibration. The radiation would then be absorbed. The rotation of asymmetric molecules around their centers of mass would also result in periodic dipole fluctuation that would interact with radiation.

Instruments for measuring infrared absorption require a source of continuous infrared radiation and a sensitive infrared detector. Changes in the linear vibration and rotational vibration of molecules due to the proximity of other species such as a metal ion would result in changes in the infrared absorption spectra of the molecules. This could help identify the state and form of the species responsible for the spectra change.

There appears to be a correlation between the infra red stretching frequency of NO absorbed onto platinum metal and the metal particle size. It has been shown that the higher the absorption frequency, the smaller the platinum particles. [Gallezot, 1979] However, obtaining quantitative information on the size of the particles using this method is not very accurate.

The I.R. bands of CO adsorbed onto the surface of Pt/KL can be used to give information on the acidity of the zeolite. If the zeolite is acidic, the I.R. band of the OH group would increase after CO adsorption. This is because the  $H^+$  ions in  $(Pt_n-H)^+$  adducts are displaced by the CO and are subsequently attached to the oxygen in the zeolite wall. This in turn increases the intensity of the I.R. spectrum of the OH group. [Kustov *et al*, 1991]

#### **1.4.4 X-Ray Methods**

##### **X-Ray Powder Diffraction**

X-ray powder diffraction is a "fingerprint" of individual zeolite structures. It provides information on the degree of crystallinity as well as phase purity. Unit cell volume calculated from the diffraction data can indicate the degree of incorporation of other framework elements. [Szostak, 1989]

For the measurement of zeolite crystallinity, about 8 peaks from the diffraction pattern are

chosen and the peak heights are summed. The selected peaks should be the ones least affected by the degree of hydration of the sample. The percentage crystallinity is given by the following equation

$$\% \text{ crystallinity} = \frac{\text{Sum of peak heights (unknown)}}{\text{Sum of peak heights (standard)}} \quad (11)$$

where "unknown" stands for the unknown material

"standard" stands for the material which has been designated to be 100 % crystalline

### **X-Ray Line Broadening**

X-ray line broadening can be used to determine the dispersion of metal on zeolite support. The accuracy of information given by this method depends on the amount of metal loaded in the zeolite and on the magnitude of atomic scattering factors.

The mean diameter  $D$  of crystallites composing a powder is related to the pure X-ray diffraction broadening  $\beta$ , by

$$D = k\lambda/(\beta\cos\theta) \quad (12)$$

where  $k$  is a constant approximately equal to unity

$\lambda$  is the radiation wavelength

$\theta$  is the Bragg angle

$\beta$  must be distinguished from the breadth of a diffraction line ( $B$ ) observed under given experimental conditions. [Whyte, 1973]

Line Broadening due to crystalline size effects may be corrected for the effects of instrumental broadening by

$$\beta = (B^2 - b^2)^{1/2} \quad (13)$$

where  $b$  is the breadth of a line produced under similar geometrical conditions by a material with a crystalline size well in excess of 1 000 Å.

$B$  is the breadth of a diffraction line observed under given experimental conditions.

Line broadening can be used to measure crystalline sizes larger than 20 Å but the actual limit of detection depends on the nature and amount of metal present. [Gallezot, 1979] Well dispersed small platinum particles on zeolite KL cannot be detected by X ray line broadening. For this reason, this technique is not employed to determine the platinum dispersion. Application of X-ray line broadening is complicated because the major diffraction lines of the support often coincide with those of the metal. It is also difficult to apply to catalysts with less than 1 % metal loading. [Whyte, 1973]

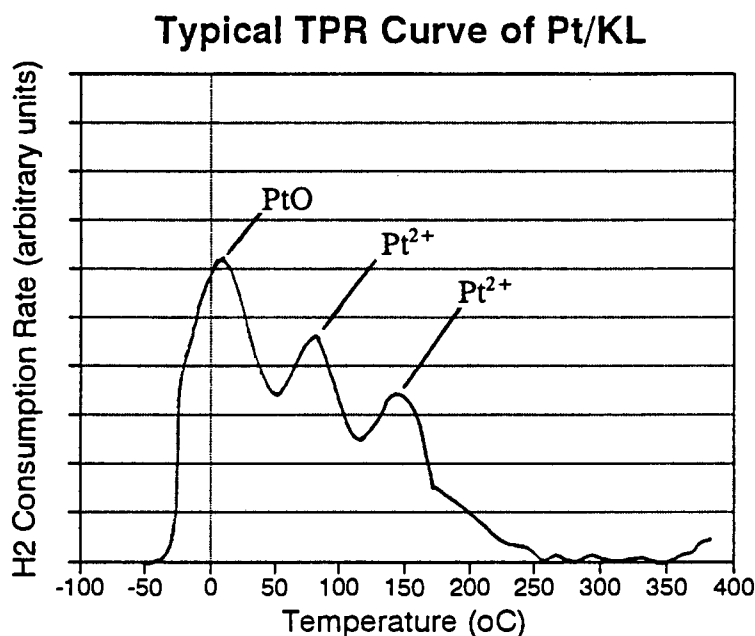
#### 1.4.5 Temperature Programmed Reduction (TPR)

Different reducible components on zeolite surfaces can be analysed by the temperature at which they are reduced. If metal ions are to be reduced then hydrogen gas can be used as the reducing agent. If metal oxides are to be reduced, carbon monoxide can also be used as the reducing agent. The measurement is carried out by increasing the temperature of the catalyst at a slow uniform rate and then observing the temperatures at which reductions occur as well as the rate at which they occur. This gives a series of reduction peaks which correspond to the reduction of different types of species loaded onto the catalyst. If the reduction stoichiometry is known, then the concentration of any component can be calculated. The advantage of TPR is that small changes over a wide temperature range can be measured with high sensitivity.

Monitoring the rate of reduction can be done via several means such as measuring concentration / pressure changes in the gas phase (reactants or products) or measuring the weight changes in the solid. The concentration of hydrogen can be measured in the gas phase by means of a Thermal Conductivity Detector (TCD) system. It is convenient to measure the

uptake of hydrogen by measuring the difference in thermal conductivity of the gas before and after passing through the sample. This is achieved by using low concentrations of hydrogen in nitrogen (about 5 vol %  $H_2$  in  $N_2$ ). In a TPR experiment, the thermal conductivity of the ( $H_2$  in  $N_2$ ) stream exiting the reactor is measured and compared with the thermal conductivity of a pure  $N_2$  stream which acts as a reference stream.

In the temperature programmed reduction of Pt/KL it has been shown that reduction can take place at temperatures below 11 °C if oxides are formed during the calcination step. [Ostgard *et al*, 1992] If metal ions are formed during the calcination step, then reduction of these would occur at higher temperatures as shown in figure 1.8.



Prior to TPR, catalyst was treated in  $O_2$  at 400 °C for 2 hours

Heating Rate : 8 °C/minute. Gas flowrate : 25 ml/ minute

**Figure 1.8** showing a TPR profile of Pt/KL [from Ostgard *et al*, 1992]

Meaningful comparison of the temperatures at which peaks occur in separate TPR curves can only be made if conditions such as gas flow rates and the rate of temperature increase are similar. According to figure 1.8, the  $Pt^{2+}$  species reduced at two different temperatures. This could have been due to the fact that the platinum ions were in different positions in the zeolite.

### 1.4.6 Temperature Programmed Desorption (TPD)

The concentration and strength of acid sites are commonly determined using temperature programmed desorption of ammonia. Quantitative information requires the identification of ammonia via continuous mass spectrometry or infra-red monitoring. The strength of the acid sites can be determined by monitoring the loss of ammonia with increasing temperature. The temperature at which all the ammonia is removed from the material has been related to the acid strength. The desorption peaks are related to the rate at which the sample is heated. The temperature programmed desorption of a base is a kinetic phenomenon and not an equilibrium one. Szostak gives the following equation for the relationship between the maximum peak temperature,  $T_M$  and the heating rate,  $B$ .

$$2\log T_M - \log B = E_a / 2.3 \cdot R \cdot T_M + E_a \cdot a_m / R \cdot k_o \quad (14)$$

where  $a_m$  is the amount adsorbed at saturation

$k_o$  is the exponential factor in the absorption rate

$E_a$  is the activation energy for desorption.

$R$  is the universal gas constant.

From equation 14, it is evident that for a fast heating rate, a high value for the maximum peak temperature would be obtained. This equation assumes that no re-adsorption occurs and that the adsorption sites are far apart such that interaction does not occur [Szostak, 1989]. With some zeolites such as mordenite however, re-adsorption of the ammonia does occur.

From the TPD curves obtained, the quantity and strength of the acid sites can be obtained. The quantity is obtained by integrating the area under the curve. Qualitative information on the strength of the acid sites can be obtained by observing the temperature at which the ammonia desorbs. High desorption temperature corresponds to strong acid sites while low temperature desorption corresponds to weak acid sites. As for TPR curves, comparison between different TPD curves should be made only if the flow rates and the heating rates employed are the same.

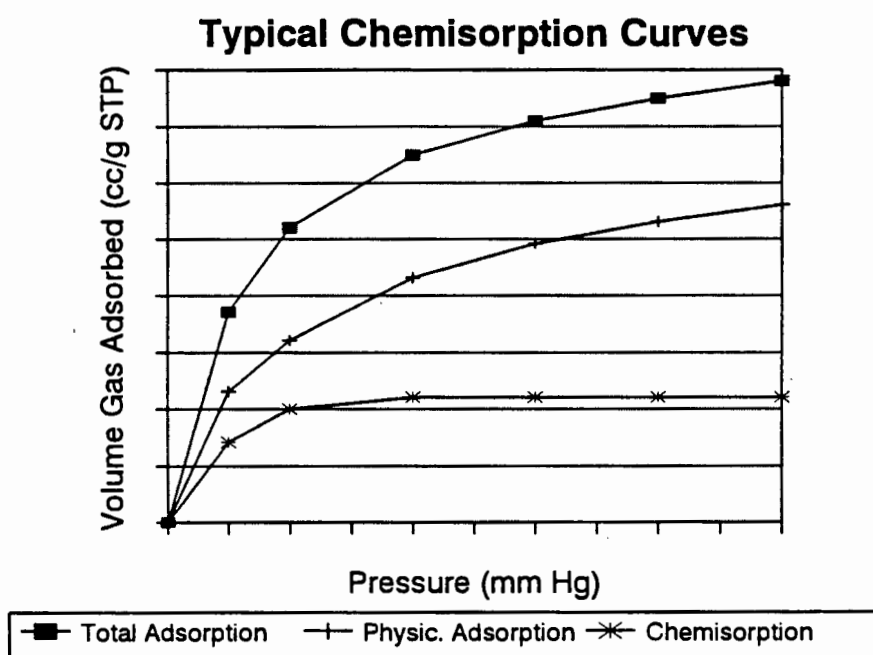
### 1.4.7 Chemisorption

The surface area of supported metal catalysts can be estimated by selective chemisorption of gases such as hydrogen, carbon monoxide and oxygen on completely reduced and neutral metal particles. This technique requires that the adsorbate form a chemisorbed monolayer and that a simple relationship exists between the number of molecules sorbed and the number of surface atoms. By assuming a stoichiometry for the reaction between a surface metal atom and the chemisorbing gas, it is possible to calculate the ratio of the surface to the total metal atoms. In addition, if the metal crystals are assumed to have a certain geometry, then the average particle size can be calculated. [Adler and Kearney, 1960]

This technique allows particles to be detected which have an average size below that measurable by X-ray diffraction. Wilson and Hall showed that H/Pt ratios which indicate high metal dispersion are close to unity. This indicates that each surface platinum atom chemisorbs one hydrogen atom. [p 206] In a certain chemisorption procedure, measurements need to be done at low temperatures (0 to 35 °C) and extrapolation of the isotherms to zero pressure is required. The amount of gas obtained by extrapolating to zero pressure would then correspond to the amount of gas chemisorbed onto the catalyst. At high pressures, the obtained results could indicate a higher hydrogen uptake than normal. This could be due to a change of H/Pt stoichiometry or to activated hydrogen spilled over to the support. Both the chemisorption of hydrogen on Pt and the adsorption on the support increases with pressure. [Gallezot, 1979]

Other researchers such as Zheng *et al* [1994] and Ihee *et al* [1994] have shown that at acceptable pressure and temperature conditions, the H/Pt ratio for well dispersed platinum particles can be as high as 1.5. Sharma *et al* performed some calorimetric measurements of the differential heats of hydrogen adsorption versus adsorbate coverage on zeolite supported platinum catalysts. They found weak adsorption sites on zeolite KL which they attributed to spillover hydrogen originating from stronger adsorption sites on platinum. They also found that hydrogen adsorption spillover did not occur on zeolite KL which did not contain platinum. [Sharma *et al*, 1994]

In another chemisorption process, the sample would firstly be subjected to both chemisorption and physical adsorption of the analysis gas (e.g  $H_2$ ) at 35 °C and a curve of the volume gas adsorbed versus pressure obtained. The sample holder would then be evacuated to low pressures while maintaining the temperature constant. This is meant to remove all the physically adsorbed gas. After this, the sample would be subjected to physical adsorption and a second curve of volume gas adsorbed versus pressure obtained. The difference between the first and second curves would then represent the Langmuir isotherm for chemisorption. Typical chemisorption curves are presented in figure 1.9.



Chemisorption values obtained by subtracting Physical Adsorption values from Total Adsorption values

Figure 1.9 showing typical chemisorption results

Apart from its dependency on the conditions of measurement, chemisorption is also dependent on the size and location of the metal particles. Gallezot *et al* concluded that isolated Pt(0) atoms in sodalite cages of zeolite Y do not chemisorb hydrogen. Four interpretations have been proposed for this : (1) at least 2 Pt atoms are required for the



dissociation of molecular hydrogen, (2) atomically dispersed platinum loses its metallic properties including chemisorption, (3) hydrogen chemisorption is inhibited because a partial electron transfer occurs from Pt atoms to electron acceptor site of the support, and (4) molecular hydrogen cannot enter the sodalite cages of zeolite Y because its kinetic diameter is 2.89 Å compared to the 2.2 Å aperture of six-membered oxygen ring. [Gallezot, 1979]

A chemisorption method was developed by Spenadel and Boudart [Spenadel and Boudart, 1960]. In this method, to be able to convert the H<sub>2</sub> adsorption data into the average size of the supported platinum particles, two assumptions would have to be made. First, on the surface, the low index planes (100 and 110) of the metal are on average equally exposed. The densities of sites on these planes are  $1.31 \times 10^{15}$  and  $0.93 \times 10^{15} \text{ cm}^{-2}$  or  $1.12 \times 10^{15} \text{ cm}^{-2}$  on average. This would correspond to an area of  $8.9 \text{ Å}^2$  per atom of platinum. From this and the number of hydrogen atoms adsorbed, the specific surface area (S) of the platinum particles can be calculated. Second, the platinum crystallites are assumed to be cubes with five exposed faces, the sixth being in contact with the support. If a side of a cube is d, then d would be given by

$$d = 5 / S\rho \quad (15)$$

where  $\rho$  is the density of platinum.

Chemisorption of a large molecule such as oxygen results in low gas uptake on Pt/HY. This could be due to the inability of the oxygen to reach the metal located in the limited space of the sodalite cages as is the case when hydrogen is used. The electronegative oxygen atoms whose bonding energy with the electron deficient clusters is smaller than that of hydrogen would not chemisorb to the metal as much as hydrogen would. [Gallezot, 1979] Wilson and Hall also showed that hydrogen chemisorption is better than oxygen chemisorption in determining the metal surface area [1970]. Carbon monoxide is not commonly used in chemisorption because this molecule can adsorb in two different ways : a linear and a bridged configuration. This then results in considerable difficulty in the interpretation of the results. [Whyte, 1973] This is because the linear form gives a stoichiometry of one while the bridged form gives a stoichiometry of two with the metal atoms. However in cases where hydrogen spillover is likely to occur, carbon monoxide chemisorption can be used as long as all the

conditions are kept constant for all the samples to be analysed. This would allow reliable qualitative comparison of the different samples.

A rapid chemisorption technique to characterise Group VIII metals on a variety of supports has been developed. [Whyte, 1973] This technique involves three stages, namely: i) the reduction of the sample in flowing hydrogen, ii) the equilibration of the reduced sample at 0 °C with a stream of argon containing a low concentration of hydrogen and iii) heating the sample in the same argon -hydrogen stream. The sample is heated to remove the adsorbed hydrogen which can be measured by means of a thermal conductivity detector. However, when examining a new metal supported catalyst using this technique, the conditions (argon-hydrogen composition, equilibration time, and desorption temperatures) must initially be established by means of the more sensitive and accurate static high vacuum equipment in order to obtain meaningful chemisorption values.

For any chemisorption procedure, if  $L$  is the amount of gas consumed (in moles/g catalyst) during the chemisorption process, and if  $z$  is the number of gaseous molecules reacting per surface atom of the metal, then the dispersion is defined as follows. [Lemaitre *et al*, 1984]

$$D = AL/zW * 100 \quad (16)$$

where  $W$  is the weight fraction of the metal in the catalyst

$A$  is the atomic weight of the metal

The metal surface area per gram of catalyst can be obtained from the following equation

$$\text{Surface Area} = z^{-1} LNp \quad \text{m}^2 / \text{g} \quad (17)$$

where  $N$  is Avogadro's number

$p$  is the area occupied by one atom ( $\text{m}^2/\text{atom}$ )

### 1.4.9 Chemical Reactions

One of the reliable methods of characterising catalysts is subjecting them to a test reaction. This gives reliable data because the modified catalyst would be studied under typical reaction conditions. For platinum on zeolites, it is important to determine whether the metal is on the internal or the external surface of the zeolite support. Platinum can be used as a hydrogenation catalyst for alkenes. Hydrogenation of a small molecule such as cyclohexene and a big molecule such as cyclododecene would help to determine the location of the metal.

The pore diameter of zeolite KL is 7.1 Å. Large hydrocarbons such as cyclododecene ( $> 7.4$  Å) might not enter into the pores of zeolite KL. Small molecules such as cyclohexene ( $< 7.1$  Å) would easily enter into the pores of zeolite KL. If the Pt/KL readily hydrogenates cyclododecene then this could suggest that the platinum metal is predominantly on the external surface of the catalyst. However, if the catalyst does not readily hydrogenate cyclododecene but readily hydrogenates cyclohexene then this would suggest that the platinum is predominantly inside the zeolite pores.

## OBJECTIVES

Based on the review of published literature, the objectives of the work were formulated. The main objectives of the work were two fold, namely: i) to establish the effect of specific parameters on the incorporation of platinum onto zeolite KL and ii) to determine the optimum conditions which would yield a high dispersion of platinum.

In the loading of metal via the ion exchange process, it was necessary to establish the following:

- i The effect of temperature on the rate of ion exchange.
- ii The effect of platinum concentration on the amount and location of metal loaded onto the zeolite.

In the activation stage of the incorporation process, the following questions were addressed:

- i Which of the following calcination medium would give the best metal dispersion : O<sub>2</sub>, N<sub>2</sub>, or H<sub>2</sub> ?
- ii How would temperature affect metal precursor distribution ?
- iii What calcination time period would give the best metal precursor distribution?

During the reduction process, work was done to establish the following:

- i The better reduction media between H<sub>2</sub> and CO. The better media which would give a non acidic catalyst with well dispersed platinum.
- ii The temperature at which reduction would occur.
- iii The optimum reduction time.

The amount of platinum loaded onto the zeolite was to be determined using atomic absorption spectroscopy (AAS)

At each stage of the platinum incorporation process, the amount and strength of acidity was

to be measured using temperature programmed desorption (TPD) of ammonia.

The dispersion of the catalyst was to be measured using chemisorption, transmission electron microscopy (TEM), energy dispersive x-ray (EDX) analysis. Chemical reactions such as the hydrogenation of cyclohexene and the aromatisation of n-hexane were to be used to confirm the dispersion results obtained using these three techniques.

## **CHAPTER 2**

## 2 EXPERIMENTAL PROCEDURE

### 2.1 Catalyst Preparation And Reduction

#### 2.1.1 Liquid State Ion Exchange

##### Apparatus

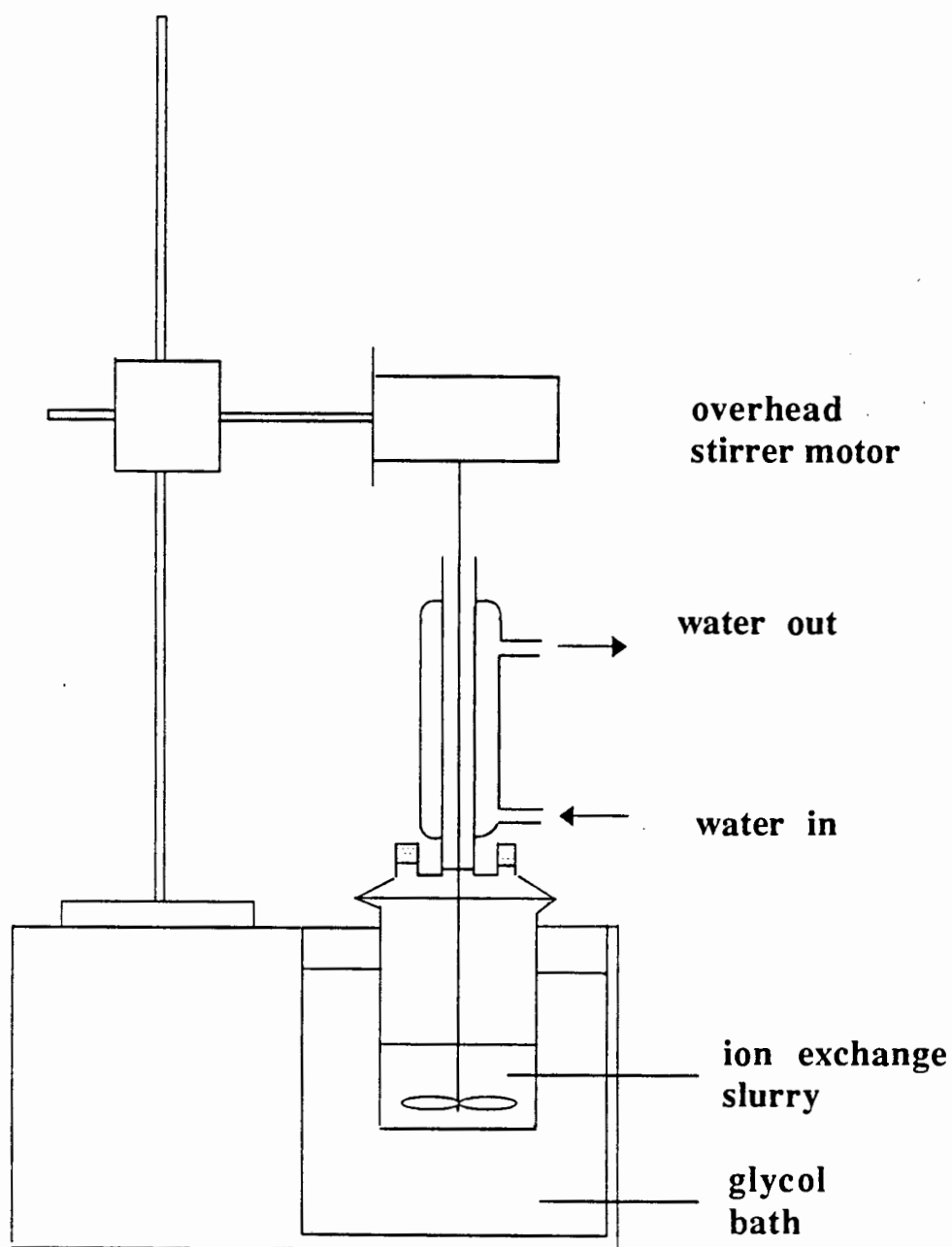


Figure 2.1 showing the liquid state ion exchange apparatus.

The zeolites KL, HY and the platinum tetrammine chloride used had the following specifications:

Zeolite KL : Type ELZ-L, Lot Number 4140-088, supplied by Union Carbide

Zeolite HY : Type EZ-190P USY (commonly known as ultra stable Y powder), supplied by Engelhard

$\text{Pt}(\text{NH}_3)_4\text{Cl}_2 \cdot \text{H}_2\text{O}$  : Batch Number 521511, supplied by Johnson Matthey, Materials Technology, U.K

For the conditions employed, it was important to firstly determine the amount of platinum that would be ion exchanged from solution onto the zeolite. Based on this, the platinum solution was prepared in a flask by dissolving the required amount of  $\text{Pt}(\text{NH}_3)_4\text{Cl}_2 \cdot \text{H}_2\text{O}$  in 450 ml of de-ionised water. The flask was subsequently immersed in the water/glycol bath and brought to the ion exchange temperature. The overhead stirrer was immediately activated. 5 g of the zeolite was then mixed with 50 ml of de-ionised water in a beaker and then brought to the ion exchange temperature (either on a hot plate or in a cooler). The zeolite slurry was then transferred into the flask and the time clock started.

In order to monitor the ion exchange process, 2 ml of slurry was syringed from the flask at certain time intervals for the first four hours and then every hour for the remainder of the process. The syringed slurry was then immediately centrifuged to separate the liquid and the solid. The liquid was then analysed for platinum using the Atomic Absorption Spectroscopy technique.

On completion of the ion exchange process, the slurry left in the flask was then centrifuged in order to separate out the zeolite. The zeolite was then washed three times with 500 ml of deionised water. After each washing, the zeolite was centrifugally separated out. The zeolite was then dried in an oven at 120 °C for 14 hours before it was stored in a desiccator containing zeolite 5A molecular sieves as the drying agent.

#### 2.1.1.1 Factorial Design

In preparing catalysts, there are a number of variables that could contribute to the dispersion of the metal. These could include ion exchange temperature and concentration, calcination



medium and temperature, reduction medium and temperature, as well as the time of treatment. In addition to determining the effect of one variable, it is important to establish whether these variables interact with one another. It is also advantageous to determine the variables that have the most influence on the dispersion of the metal.

The procedure of studying one variable at a time does not always determine the most important variables as well as their interaction with one another within a reasonable time. It is thus beneficial to employ the statistical analysis method of Factorial Design. Due to the patterning present in statistically designed experiments, the interpretation of the results is often straightforward.

In a full factorial design, three variables are studied at two levels assigned as - or + . This gives a total of eight runs (i.e  $2^3$ ). When the variables are quantitative such as temperature, the higher value is assigned + while the lower value is assigned -. If the variables are qualitative such as the treatment medium, then the assignment of the positive and negative signs is arbitrary. The results (eg percent of metal dispersion) are recorded for each run and are known as the responses of the factorial design. A typical full factorial design representation for three variables is given in table 2.1.

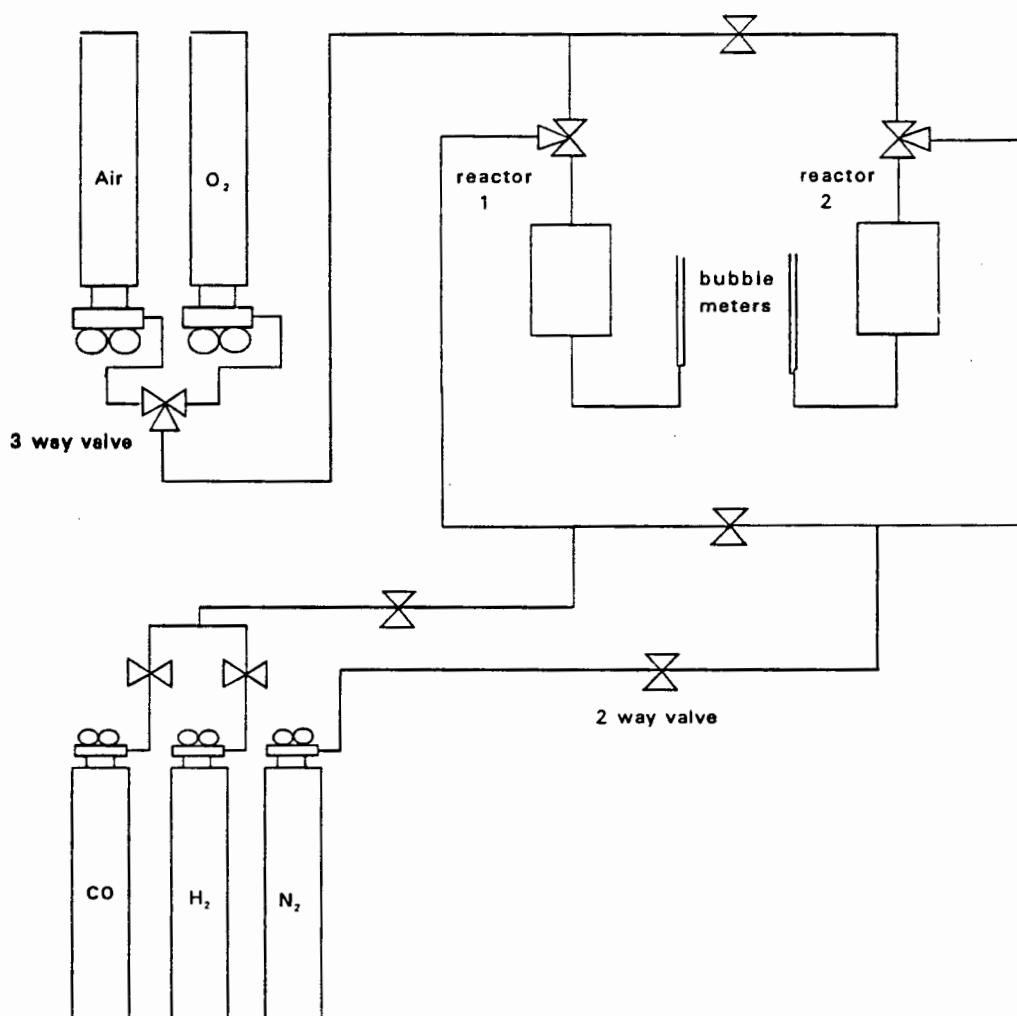
Run No.	Variables			Response 1	Response 2
	A	B	C		
1	-	-	-		
2	+	-	-		
3	-	+	-		
4	+	+	-		
5	-	-	+		
6	+	-	+		
7	-	+	+		
8	+	+	+		

Table 2.1 showing an example of a full factorial design

To enable efficient study of the calcination and reduction parameters, Factorial Design of experiments was employed.

### 2.1.2 Calcination

#### Apparatus



**Figure 2.2** Showing The Calcination Rig

Calcination is used to decompose the ammonia ligands. Therefore the minimum calcination temperature should not be less than the decomposition temperature of the ammonia ligands. The minimum calcination temperature was obtained by heating 0.25 g zeolite KL which had been ion exchanged with  $\text{Pt}(\text{NH}_3)_4\text{Cl}_2$  to give 1.55 wt % platinum. The sample was placed in a temperature programmed desorption apparatus fitted with a mass spectrometer. The temperature was increased from 20 °C to 600 °C at a rate of 5 °C per minute. The

temperature at which  $\text{NH}_3$  ligands and their derivatives were given off signified the temperature at which the platinum ammonium complex decomposed.

After determining the minimum calcination temperature, all the catalysts were calcined in the calcination rig (figure 2.2). In the reactor, the catalyst was supported on glass wool. Typical catalyst loading was 0.65 g and the calcination gas flow rate was 300 ml/minute/g catalyst at 25 °C. The gas flow rate had to be high enough to ensure rapid removal of calcination products such as water and ammonia. During calcination, the temperature was increased manually to the final value in the required time. The temperature was then maintained at the final value for an appropriate period. After each calcination step, the samples were cooled down to room temperature in flowing nitrogen. The gases used in the calcination studies had the following specifications:

Oxygen of purity 99.995 % supplied by Fedgas, South Africa

Nitrogen of purity 99.990 % supplied by Fedgas, South Africa

Hydrogen of purity 99.999 % supplied by Fedgas, South Africa

In order to determine the calcination parameters that greatly affected metal dispersion, Factorial Design of experiments was applied. Chemisorption was used as the main technique to characterise the dispersion of the metal after calcination. However, it was decided to perform chemisorption tests on samples whose platinum was in the reduced neutral state. This meant that after treating the samples according to the sequence for Factorial Design for calcination, they were all reduced in the same way before applying chemisorption. It was decided to reduce the samples in hydrogen while increasing the temperature from 25 °C to 350 °C at a rate of 21.7 °C/10 minutes. The temperature was held at 350 °C for 4.5 hours before cooling down to 25 °C in nitrogen. Table 2.2 shows the Factorial Design schedule of the calcination variables studied.

Medium	Temp. (°C) <sup>a</sup>	Time (hr) <sup>b</sup>
N <sub>2</sub>	25-350; 350	1; 1
O <sub>2</sub>	25-350; 350	1; 1
N <sub>2</sub>	25-600; 600	1; 1
O <sub>2</sub>	25-600; 600	1; 1
N <sub>2</sub>	25-350; 350	4.33; 6.66
O <sub>2</sub>	25-350; 350	4.33; 6.66
N <sub>2</sub>	25-600; 600	4.33; 6.66
O <sub>2</sub>	25-600; 600	4.33; 6.66

- a The temperature column shows that the temperature was increased from 25 °C to the final value and then held at the final temperature.
- b The first number in the time column corresponds to the time taken to increase the temperature to the final value. The second number corresponds to the length of time for which the temperature was maintained at the final temperature.

**Table 2.2** showing the factorial design sequence for calcination

### 2.1.3 Reduction

After performing the Factorial Design experiments for calcination, the calcination conditions which yielded the best metal dispersion were obtained. These conditions were then used to prepare a number of samples for the Factorial Design of reduction experiments. Table 2.3 shows this factorial design sequence.

Reduction in hydrogen resulted in the hydrogen ions produced attaching themselves onto the zeolite wall causing an increase in the Bronsted acidity. The hydrogen reduced samples giving the best metal dispersion had the hydrogen ions back exchanged by potassium ions using solid state ion exchange. The potassium salt used was potassium chloride (KCl). The amount of KCl used was double that required to just remove all the H<sup>+</sup> ions from the zeolite. The solid state ion exchange was performed in oxygen at 350 °C for 7 hours. The back exchanged zeolites were then studied using temperature programmed desorption (TPD) to determine the success of the Bronsted acidity removal.

Medium	Temp (°C) <sup>a</sup>	Time (hr) <sup>b</sup>
H <sub>2</sub>	25-150; 150	1; 1
CO	25-150; 150	1; 1
H <sub>2</sub>	25-350; 350	1; 1
CO	25-350; 350	1; 1
H <sub>2</sub>	25-150; 150	2.5; 4.5
CO	25-150; 150	2.5; 4.5
H <sub>2</sub>	25-350; 350	2.5; 4.5
CO	25-350; 350	2.5; 4.5

- a     The temperature column shows that the temperature was increased from 25 °C to the final value and then held at the final temperature
- b     The first number in the time column corresponds to the time taken to increase the temperature to the final value. The second number corresponds to the length of time for which the temperature was maintained at the final temperature.

Table 2.3 showing the factorial design sequence for reduction

2.1.4 Solid State Ion Exchange

In this technique, the catalyst and the exact amount of a salt of the ion to be exchanged were thoroughly mixed by grinding for 120 seconds in a wobble bug grinder. They were then loaded into the same type of reactor as used in the calcination where they were treated under appropriate conditions.

A sample was treated under the same conditions as those which yielded the best metal dispersion. Another one was treated under the same conditions that yielded the worst metal dispersion. After the solid state ion exchange treatment, the samples were washed four times in de-ionised water to remove any excess platinum ions that might not have ion exchanged onto the zeolite. The amount of metal loaded onto the zeolite by solid state ion exchange was determined by atomic absorption spectroscopy.

After hydrogen reduction on samples prepared via liquid ion exchange, solid state ion exchange was also performed on selected samples in order to back exchange  $K^+$  ions onto the zeolite in place of  $H^+$  ions. This was done using KCl and its purpose was to remove Bronsted acidity from the zeolite as this is undesirable for aromatisation reactions. The solid state ion exchange was performed in oxygen at 350°C for 7 hours.

#### **2.1.4 Incipient Wetness Impregnation**

4.2 grams of zeolite KL (dry mass) were loaded with 1.55 wt % platinum via incipient wetness impregnation. This was done by adding 2.85 ml of solution containing 0.1141 g of  $Pt(NH_3)_4Cl_2 \cdot H_2O$ . The solution was added drop-wise with vigorous shaking of the zeolite/solution mixture. The platinum containing zeolite was then dried in an oven at 120 °C for 14 hours. For comparison purposes, samples from this batch were then taken, prepared and characterised under similar conditions to those of some 1.55 wt% Pt/KL samples prepared via liquid state ion exchange.

### **2.2 Analytical Procedures**

#### **2.2.1 X-Ray Diffraction**

X-ray diffractograms were obtained on a Phillips X-ray diffractometer with Cu-K radiation of wavelength 154 pm. The scan range was  $5^\circ < 2\theta < 50^\circ$ . The X-ray pattern of the untreated zeolite KL was compared with the simulated pattern found in literature [von Ballmoss and Higgins, 1990]. The effect of high temperature treatment on the crystallinity of the zeolite KL was also determined using XRD. The XRD machine parameters used are presented in table 2.4.

Range	: $4 \times 10^3$	Current	: 30 mA
Time Constant	: 1	Divergent Slit	: $1/2^\circ$
Scanning Speed	: 2 ( $2\theta^\circ/\text{min}$ )	Receiving Slit	: $1/2^\circ$
Voltage	: 40 kV	Anti-scatter slit	: $1^\circ$

**Table 2.4** showing XRD parameters used.

## 2.2.2 Elemental Analysis

### 2.2.2.1 Atomic absorption spectroscopy

Atomic absorption spectroscopy was used to determine the amount of metal loaded onto the zeolite. This was performed on a Varian Spectra AA-30 spectrometer attached to a D.S. 15 data station. During the liquid state ion exchange process (see section 2.1.1), 2 ml slurry samples were periodically taken from the flask. These were then separated by means of a centrifuge to yield clear solution samples which were subsequently assayed for platinum and potassium.

Potassium analysis was done in order to monitor whether the theoretical amount expected to be ion exchanged into solution by the platinum would correlate with the obtained results. Extra caution had to be taken when assaying for potassium since solution contamination occurs easily as a result of the high solubility of the potassium.

Analysis of solid samples could only be carried out after they had been dissolved in acid. The recipe followed for the digestion of the zeolites was as follows:

- i) Weigh about 0.3 grams of the zeolite into a teflon par bomb.
- ii) Add 5ml of 40 % hydrofluoric acid into par bomb.
- iii) Close par bomb and insert it and its contents into safety metallic casing and place into an oven maintained at a temperature between  $70^\circ\text{C}$  and  $100^\circ\text{C}$ . Keep in oven for 40 minutes.
- iv) Remove from oven and allow to cool to room temperature ( $25^\circ\text{C}$ ). Open par bomb

and check if all of the zeolite has dissolved.

- v) If some of the zeolite is undissolved then add 5 ml of 40 % hydrochloric acid and repeat steps iii) and iv).
- vi) Add 50 ml of boric acid (55 g boric acid crystals dissolved in 1000 ml of de-ionised water) and transfer par bomb contents into a plastic volumetric flask. Make up the volume to 500 ml.

In order to assay an element, standard solutions with different concentration of the element were prepared. The concentration range for the solutions was chosen in such a way that the expected concentration of the sample would fall in this range. Except for the concentration of the element to be assayed, the concentration of all the other elements in the standard solution was the same as in the sample solutions. Results from the assay of the standard solutions were used to plot calibration curves of element concentration versus absorbance. Based on these curves, the concentration of the sample solutions was then determined.

In order to confirm the results obtained from the ion exchange samples, the ion exchanged zeolite was assayed for platinum. To enable this, the zeolite was digested in hydrofluoric and hydrochloric acids. All assays were carried out according to the prescribed methods in the handbook obtained from Varian Techtron Pty. [Varian, 1979]

#### **2.2.2.2 Electron beam micro-analysis**

Electron beam micro-analysis was used to determine the Si/Al ratios of the zeolite KL. Preparation of the samples for electron beam micro-analysis involved fusing the samples at about 1150 °C in a Balzers high vacuum unit which was evacuated to  $5 \cdot 10^{-2}$  kPa. The samples were mounted onto a Molybdenum strip.

The electron beam micro-analysis was done using a CAMECA electron micro-probe using wavelength dispersion spectrometers. The micro-probe was run at a beam voltage of 15 kV, a beam current of  $15 \cdot 10^{-9}$  Amps and a beam size of 20 microns. Natural minerals were used as standards for analysis of the oxides of silicon and aluminium. Pure platinum metal was used as the standard for platinum analysis. The correction procedure used was Z.A.F.



### 2.2.3 Chemisorption

Chemisorption was used to determine the relative metal dispersion of the catalysts. The instrument used was the ASAP 2000 Chemi System obtained from Micromeritics. Carbon monoxide was used as the adsorbing gas for chemisorption measurements. Before chemisorption could be employed to determine the metal dispersion, it was necessary to show that the chemisorption results were reproducible within an acceptable limit of  $\pm 5\%$ . [Micromeritics, 1993] In order to do this, two samples of 1.55% Pt/KL were calcined separately in oxygen at 350 °C for a total time period of 2 hours. The catalysts were then reduced in hydrogen while increasing the temperature from 25 °C to 350 °C at a rate of 21.6 °C/10 minutes. The temperature was then maintained at 350 °C for 4.5 hours. The dispersion of one of the samples was tested twice using the chemisorption equipment in order to test the reproducibility of the chemisorption procedure. The dispersion of the second sample was determined and the results obtained used to measure the reproducibility of the catalyst preparation procedure.

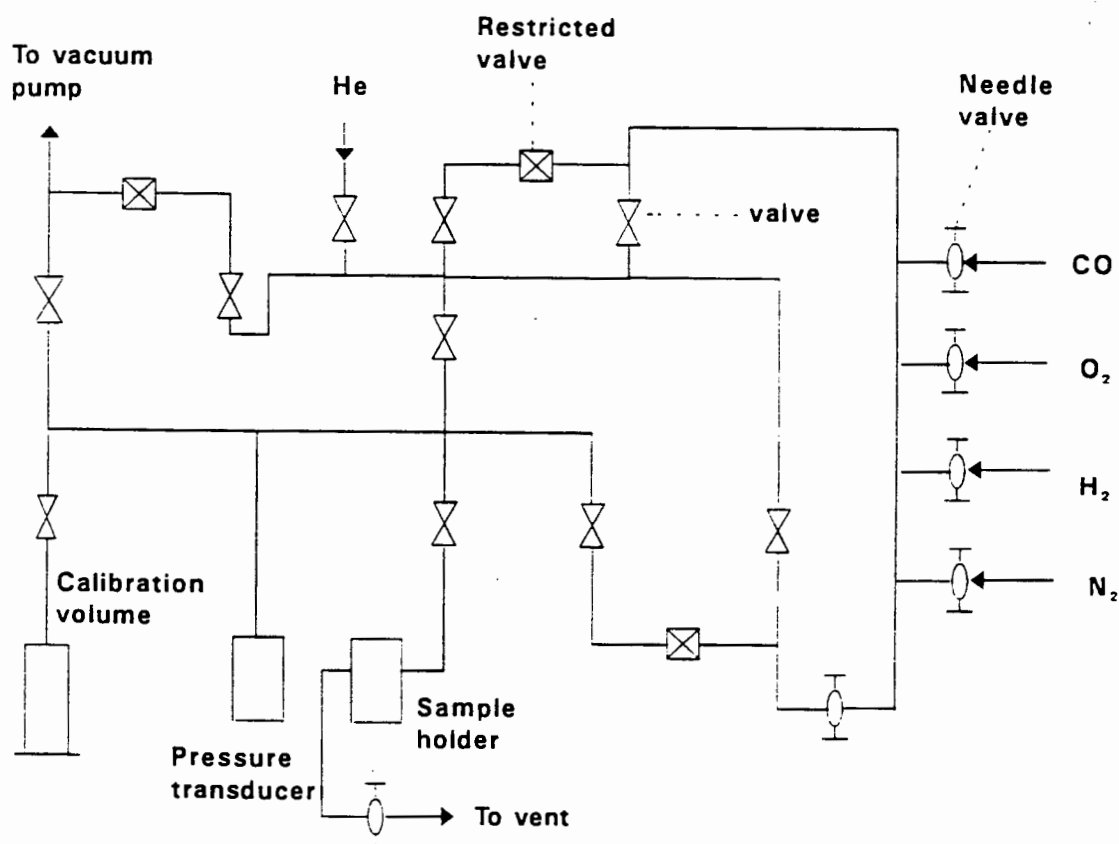


Figure 2.3 showing the flow diagram of the equipment used for chemisorption studies.

### 2.2.3.1 Chemisorption procedure for all the samples

After determining the reproducibility of chemisorption and catalyst preparation procedures, the dispersion of catalyst samples which had been appropriately calcined and reduced were then determined via chemisorption. The reduced catalysts were loaded into the chemisorption equipment where they were re-reduced in the same reduction medium and at the same temperature as that used to yield the neutral metal. This re-reduction step lasted for 2 hours and its purpose was to ensure that any metal that might have been re-oxidised during catalyst handling was reduced.

After re-reduction, the system was evacuated to a pressure of  $5 \cdot 10^{-3}$  mm Hg ( $6.67 \cdot 10^{-4}$  kPa) at the temperature of re-reduction. For re-reduction in carbon monoxide at 150 °C, this pressure was maintained for 6 hours while for re-reduction in carbon monoxide at 350 °C the pressure was maintained for 4 hours. For re-reduction in hydrogen at 150 °C, the pressure of  $6.67 \cdot 10^{-4}$  kPa was maintained for 4 hours while for re-reduction in hydrogen at 350 °C this pressure was maintained for 2 hours. These steps were taken to ensure complete removal of any strongly adsorbed material from the zeolite. Heat was then removed from the sample. The system was subsequently backfilled with 760 mm Hg (101.3 kPa) of helium for half an hour to ensure that the sample temperature reached the desired value of 35 °C. Following this, the system was evacuated for half an hour to remove the helium before applying carbon monoxide chemisorption.

The pressure values employed for chemisorption on platinum were 150, 200, 300, 400 and 500 mm Hg. In the chemisorption, carbon monoxide was adsorbed at each pressure value and a curve of volume adsorbed versus gas pressure was obtained. This curve represented total adsorption. The sample was then evacuated to  $5 \cdot 10^{-3}$  mm Hg in order to remove the physically and weakly adsorbed carbon monoxide. The pressure was maintained at this value for half an hour. The carbon monoxide was then re-adsorbed onto the zeolite. The second curve of volume adsorbed versus gas pressure was then obtained. This curve represented the weakly adsorbed carbon monoxide. The volume difference between the two curves was taken to represent the chemically adsorbed carbon monoxide. This difference was used to determine the metal dispersion. The weight of the catalyst sample used in the calculation of the metal

dispersion was obtained at the end of the chemisorption procedure to ensure that the value represented the dry mass of the catalyst.

### 2.2.3.2 Hydrogen chemisorption

Before applying carbon monoxide chemisorption, attempts had been made to use hydrogen chemisorption because it is recommended for use in determining metal surface area [Scholten, 1978]. However, a number of problems were encountered.

The problems encountered in hydrogen chemisorption were two fold - i) the metal dispersion obtained for any sample was not readily reproducible, ii) the metal dispersion obtained was much higher than 100 %. It was speculated that this could have been a result of two phenomena -i) a leak in the chemisorption apparatus, or ii) hydrogen spillover onto the support as a result of the presence of metal. It was therefore proposed to do the following to investigate these speculations.

- 1 A number of hydrogen chemisorption test cycles were performed on a sample of 0.5 wt % Pt/Al<sub>2</sub>O<sub>3</sub>. This material was the standard supplied by the manufacturers of the chemisorption equipment. Using carbon monoxide as the adsorbing gas, the metal dispersion on this material should be 33 % with an allowable experimental error of +/-5 %. In each chemisorption test cycle, all the parameters were kept constant while varying the time during which the sample was cooled down under vacuum from 350 °C to 35 °C. During this period, the sample was also maintained at 35 °C for a while before backfilling the sample holder with helium. This period is shown as X hours in figure 2.4. If a leak exists then air could possibly enter the apparatus causing oxidation of the platinum. After each chemisorption cycle, the sample was evacuated at  $5 \cdot 10^{-3}$  mm Hg ( $6.67 \cdot 10^{-4}$  kPa) for 1 hour at 35 °C in order to remove all the hydrogen before the following chemisorption cycle.

If a small leak (pressure increase not greater than 0.01 mm Hg/minute) existed in the chemisorption apparatus, the pump used to evacuate the apparatus was strong enough to still reduce the pressure to  $5 \cdot 10^{-3}$  mm Hg. Air would enter the apparatus resulting in the oxidation

of neutral platinum metal. The amount of hydrogen adsorbed would then be a sum of the hydrogen required to reduce the oxidised platinum and the hydrogen chemisorbed onto neutral platinum.

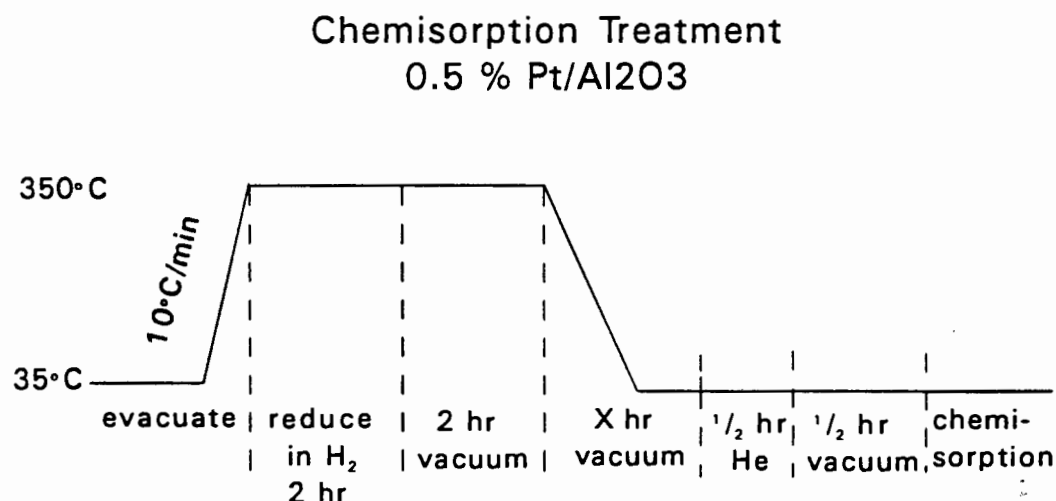


**Figure 2.4** showing the schematic representation of the H<sub>2</sub> chemisorption test cycle employed to investigate the effect of varying the evacuation time while reducing the temperature from 350 °C to 35 °C.

- 2 A number of hydrogen chemisorption test cycles were performed on a sample of 0.78 wt % Pt/KL. This sample had been calcined in nitrogen at 350 °C for 1.5 hours and reduced in hydrogen at 350 °C for 7 hours. Unlike in step 1, the evacuation time at 350 °C was varied. This time is shown as Y in figure 2.5. This was to determine whether the proposed evacuation time of 2 hours at 350 °C was insufficient to remove all the chemisorbed hydrogen from the previous chemisorption step. Varying the evacuation time at 350 °C would also investigate the presence of a leak in the apparatus. After each chemisorption cycle, the sample was evacuated at  $5 \cdot 10^{-3}$  mm Hg ( $6.67 \cdot 10^{-4}$  kPa) for 1 hour in order to remove all the hydrogen before the following chemisorption cycle.

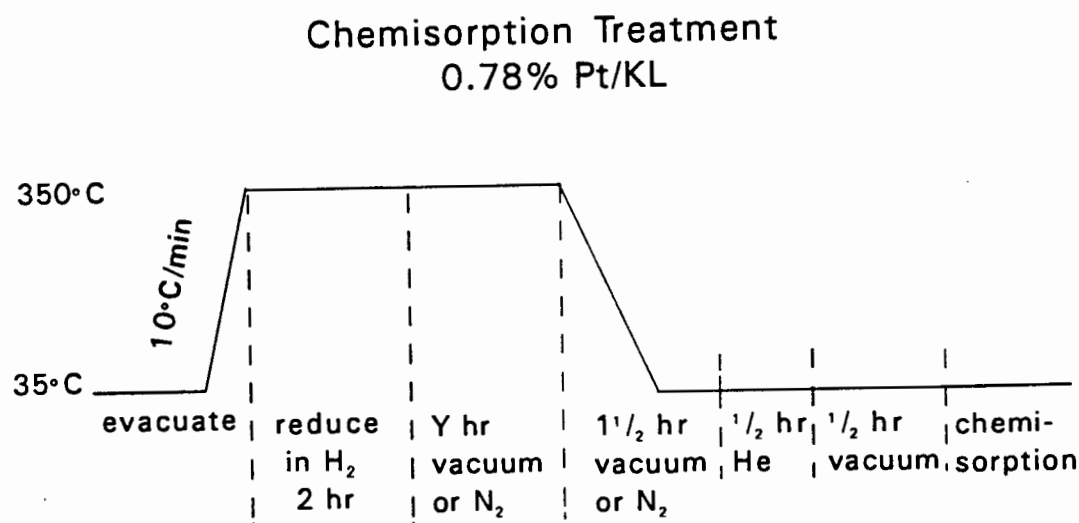


**Figure 2.5** showing the schematic representation of the chemisorption procedure employed to investigate the effect of varying the evacuation time at 350 °C.

- 3 To further investigate the presence of a leak, it was decided to replace the vacuum with 800 mm Hg (106.7 kPa) of nitrogen flow. This would prevent any possible oxidising substance from entering the apparatus during the chemisorption.
- 4 Step 2 was repeated using CO as the chemisorption gas.

The apparatus was leak tested during each cycle. This was done by stopping the evacuation pump just before the chemisorption step and then measuring the pressure in the system after 10 minutes. In each case the leak was found to be less than a tenth of the acceptable value of 0.01 mm Hg/minute.

## 2.2.4 Temperature Programmed Reduction (TPR)

### Apparatus

Diagram of TPR rig

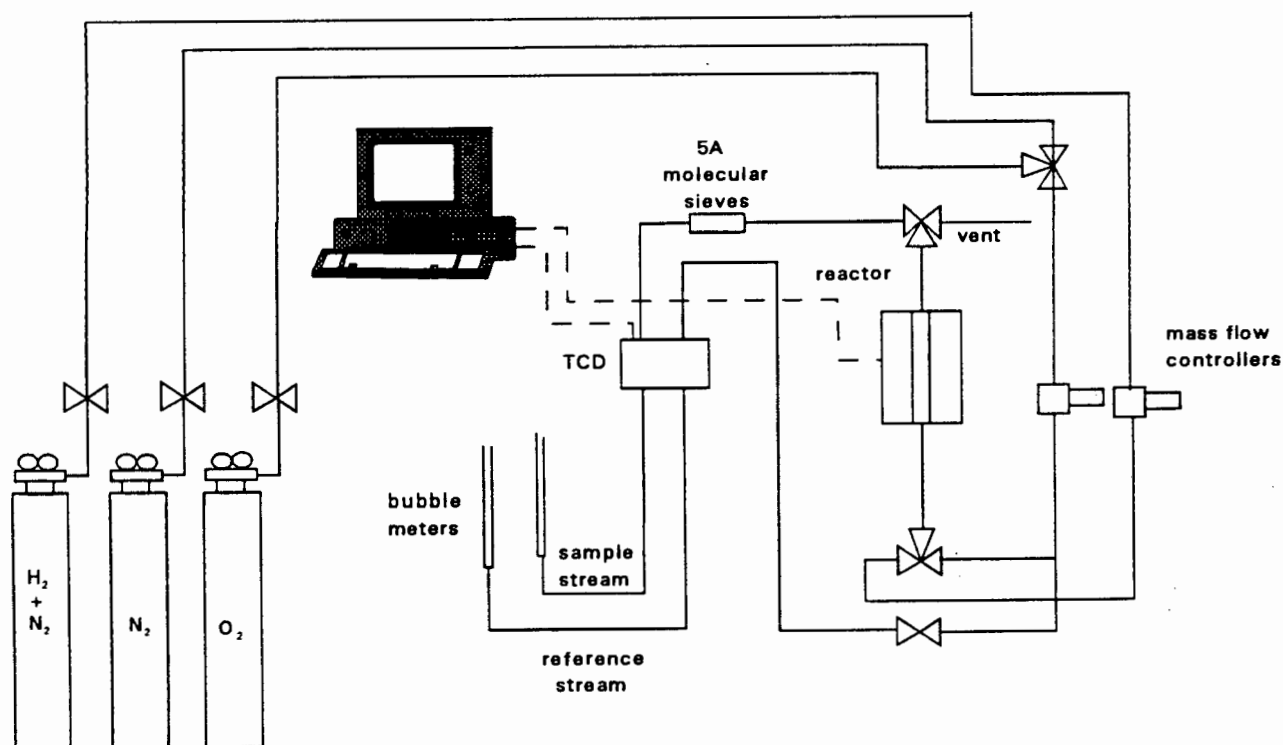


Figure 2.6 Showing The Rig For Temperature Programmed Reduction (TPR)

### 2.2.4.1 Calibration of $\text{H}_2$ concentration in the $\text{H}_2/\text{N}_2$ stream

Temperature programmed reduction was used to determine the temperatures at which reduction of the platinum species occurred. Before work could be carried out on the TPR equipment, the concentration of the hydrogen in the  $\text{H}_2/\text{N}_2$  stream was checked. This was achieved by applying TPR on metal oxides of known quantity and using the hydrogen concentration provided by the gas suppliers (5 %  $\text{H}_2$  in  $\text{N}_2$ ) as a first assumption.

There were no high purity oxides of known metal content available. Therefore the calibration samples were prepared by thermally decomposing metal nitrate salts.  $\text{Cu}(\text{NO}_3)_2 \cdot 3\text{H}_2\text{O}$  (Riedel-de Haen),  $\text{Ni}(\text{NO}_3)_2 \cdot 6\text{H}_2\text{O}$  (GPR), and  $\text{Co}(\text{NO}_3)_2 \cdot 6\text{H}_2\text{O}$  (Merck) were heated in a

muffle oven at a heating rate of 20°C / minute up to 500°C and then held at this temperature for 2 hours. The nitrate compounds decomposed at temperatures between 250°C and 400 °C to form NO<sub>x</sub> and the oxides CuO, NiO, and Co<sub>3</sub>O<sub>4</sub>. Co<sub>3</sub>O<sub>4</sub> was formed as a result of further oxidation of CoO by NO<sub>x</sub>.

A known mass of the oxide was then placed into the TPR reactor (diameter 12 mm) which was subsequently heated up to 100 °C in a nitrogen flow (60 ml/min STP). The temperature was then held at this value for 4 hours in order to stabilise the Thermal Conductivity Detector (TCD). The nitrogen-hydrogen stream was then allowed to flow through the reactor at a rate of 60 ml/min (STP) for 10 minutes while recording the baseline. Using a heating rate of 10 °C / minute the temperature was then increased to 1 000 °C and held at this value for 20 minutes. After the sample had cooled, it was weighed again. The molar ratio of the hydrogen consumed to the metal was then determined and used to quantify the content of hydrogen in the nitrogen stream. In the calibration, it was established that the percentage of hydrogen in the N<sub>2</sub>/H<sub>2</sub> mixture was 4.33 %.

#### 2.2.4.2 TPR procedure for all the samples

About 0.5 g of the catalyst which had been calcined under appropriate conditions was loaded into the TPR reactor. Nitrogen gas was then allowed to flow at a rate of 60 ml/minute through both the sample and reference streams of the thermal conductivity detector (TCD). The TCD was then activated and left for 4 hours to stabilise. When the TCD reading was stable, the base line for a pure nitrogen stream was recorded on a computer diskette for 10 minutes. A nitrogen stream containing 4.33 volume % hydrogen was then allowed to flow through the sample in the reactor while maintaining the nitrogen flow through the reference stream. All flows were maintained at 60 ml/minute. Molecular sieves of diameter 5 Å were used to trap any water leaving the TPR reactor. After each TPR, these were regenerated by heating to 200°C in nitrogen for 2 hours.

The apparatus used to determine the TPR curves had a lagged furnace into which the reactor containing the sample was immersed. The only cooling mechanism available was convection of heat from the furnace to the environment. If PtO is present after calcination, it would

reduce in hydrogen at temperatures below 11°C [Ostgard *et al*,1992]. However due to the lagging of the furnace as well as to the lack of a cooler, the temperature in the furnace could not be cooled down below 40 °C within a reasonable time (16 hours). Therefore when introducing the hydrogen-nitrogen mixture at this temperature, any PtO present would be immediately reduced. In order to record the full peak representing the reduction of PtO at low temperatures, the baseline for the H<sub>2</sub>/N<sub>2</sub> flow should be recorded at a temperature below which the PtO would reduce. However, since it was not possible to cool the TPR equipment to temperatures below 30 °C within 24 hours, this could not be achieved.

After stabilising the TCD, the temperature of the furnace was then increased from 40 °C to 600 °C at a rate of 1 °C/minute. As the hydrogen was consumed by the metal ions undergoing reduction, the thermal conductivity of the stream containing hydrogen decreased. To obtain information on possible baseline drifts during the TPR, the above procedure was repeated for an empty reactor and it was found that there was no baseline drift.

At the end of a TPR run, the information stored on the computer diskette was then analysed using software packages. The information was used to plot curves of the amount of hydrogen consumed/ g catalyst/ °C vs the temperature. The area under the curve represented the amount of hydrogen consumed per gram of catalyst.

Temperature programmed reduction was performed on selected catalysts in order to investigate the temperature at which platinum species would reduce. The catalysts chosen for TPR studies were:

- i 1.55 wt % Pt/KL calcined at 350 °C in O<sub>2</sub> for 6.33 hours,
- ii 1.55 wt % Pt/KL calcined at 600 °C in O<sub>2</sub> for 6.33 hours,
- iii 1.55 wt % Pt/KL calcined at 350 °C in N<sub>2</sub> for 6.33 hours,
- iv 1.43 wt % Pt/HY calcined at 350 °C in O<sub>2</sub> for 6.33 hours,
- v 1.43 wt % Pt/HY calcined at 600 °C in O<sub>2</sub> for 6.33 hours,
- vi 1.43 wt % Pt/HY calcined at 600 °C in N<sub>2</sub> for 6.33 hours.



### 2.2.5 Temperature Programmed Desorption (TPD).

#### Apparatus

Diagram of TPD rig

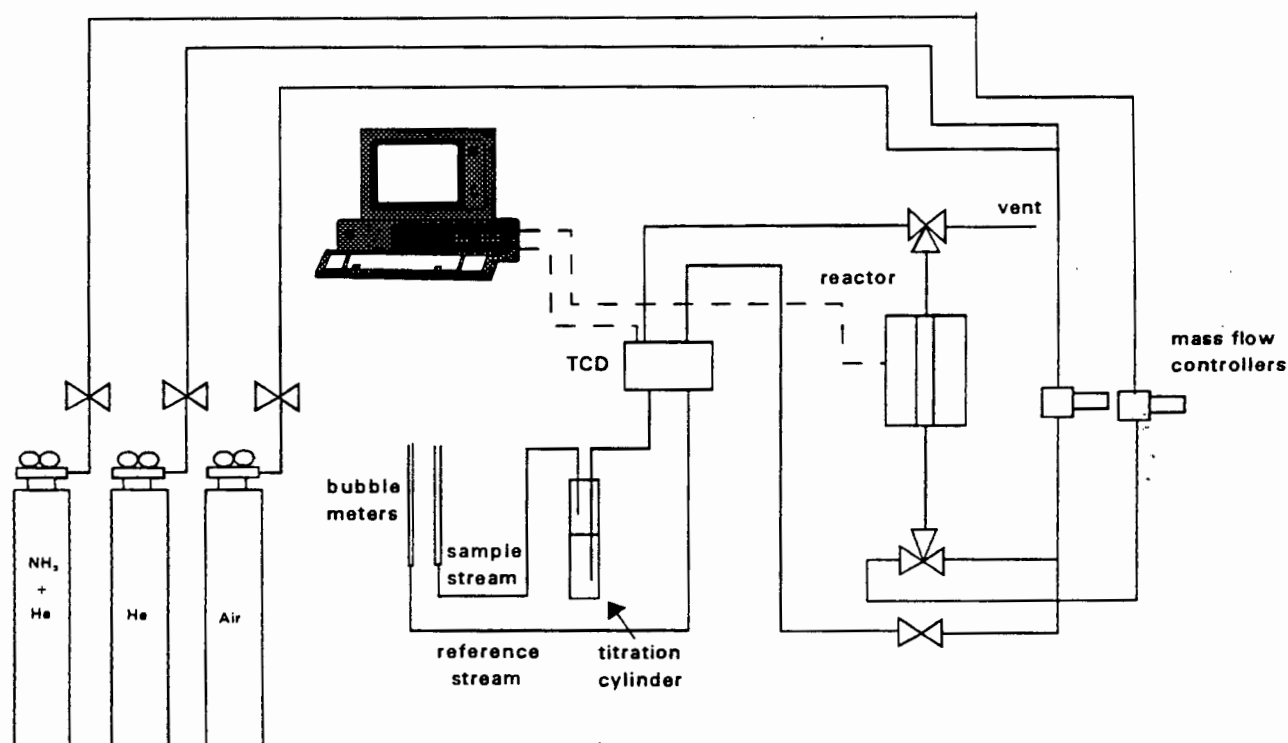


Figure 2.7 Showing The TPD Rig.

Temperature programmed desorption was used to determine the Bronsted and Lewis acidity on the catalyst samples after different preparation stages. About 0.25 grams of sample were loaded into the reactor and then heated in helium from 40 °C to 350 °C at a rate of 30°C/minute. The temperature was then maintained at 350 °C for 2.5 hours. This step was taken to dry the sample. All gas flowrates were kept constant at 60 ml/minute. After cooling the temperature to 100 °C, the Thermal Conductivity Detector (TCD) was then activated and allowed to stabilise over 5 hours. A stream of 5 volume % ammonia in helium was then passed through the catalyst bed for one hour. The system was then left to stand for 24 hours with helium flowing through the catalyst to enable the removal of any physisorbed ammonia.

After removing the physically adsorbed ammonia, the temperature of the system was then increased from 100 °C to 600 °C at a rate of 5 °C/ minute and then held at 600 °C for one hour. The ammonia given off was passed through the TCD cell before it was reacted with 20 ml of 0.1 Normal  $\text{H}_2\text{SO}_4$  diluted in 500 ml of deionised water. At the end of the TPD run, the unreacted  $\text{H}_2\text{SO}_4$  was titrated with 0.1 Normal NaOH and the amount of  $\text{NH}_3$  desorbed thus calculated.

The information obtained from the TPD run was processed using computer software and curves showing the  $\text{NH}_3$  concentration in the reactor exit stream vs temperature were plotted. The area under the curve represented the total amount of  $\text{NH}_3$  physisorbed as well as chemisorbed to the acid sites on the zeolite. In the analysis of the results, a comparison could be made between the amount of chemisorbed  $\text{NH}_3$  determined by the TCD, and that determined by titration.

The samples chosen for TPD studies were:

- i 1.55 % Pt/ $\text{SiO}_2$  Calcined: He, 350°C, 6.33hr. No reduction,
- ii Pure Silica Calcined : He, 350°C, 6.33hr. No reduction.
- iii Untreated zeolite KL,
- iv Zeolite KL Calcined :  $\text{O}_2$ , 350°C, 1.5 hr. No reduction,
- v 1.55 % Pt/KL Calcined :  $\text{O}_2$ , 350°C, 6.33 hr. No reduction,
- vi 1.55 % Pt/KL Calcined :  $\text{N}_2$ , 350°C, 1.5 hr. No reduction,
- vii 1.55 % Pt/KL Calcined :  $\text{O}_2$ , 600°C, 6.33 hr. No reduction,
- viii 1.55 % Pt/KL Calcined :  $\text{O}_2$ , 350°C, 6.33 hr. Reduced : 350°C,  $\text{H}_2$ , 4.5hr,
- ix 1.55 % Pt/KL Calcined :  $\text{O}_2$ , 350°C, 6.33 hr. Reduced : 350°C, CO, 4.5hr,
- x 1.55 % Pt/KL Calcined :  $\text{O}_2$ , 350°C, 1.5 hr. Reduced : 350°C,  $\text{H}_2$ , 4.5hr. Back exchanged : KCl, 350°C,  $\text{O}_2$ ,
- xi Repeat of sample x after cooling it down to 25 °C in helium flow,

All the samples studied using TPD were prepared in similar rigs to the ones used for TPD analysis. After calcination and reduction treatment, they were then stored in a dessicator until needed for TPD analysis. The dessicator was loaded with 5A molecular sieves which acted

as a drying agent.

The TPD spectrum of the 1.55 % Pt/SiO<sub>2</sub> as well as the TPD spectrum of pure silica gel were obtained in an attempt to determine whether ammonia used in the TPD would adsorb onto platinum metal. Platinum was loaded onto the silica gel via impregnation and drying at 120 °C for 14 hours. The impregnated sample was then calcined in helium at 350 °C for 6.33 hours. Calcination in an inert medium would result in the reduction of platinum ions by the ammonia ligands to yield neutral platinum metal. [Reagan *et al*, 1981] It was believed that the silica gel would have neither Bronsted nor Lewis acidity.

In order to determine whether weak chemisorption as well as de-hydroxylation occurred on the zeolite samples, sample x was analysed using TPD, cooled down to room temperature in the TPD rig under helium flow . A second TPD analysis of the sample was then immediately performed (sample xi).

### 2.2.6 Transmission Electron Microscopy (TEM)

Based on the platinum dispersion values obtained using carbon monoxide chemisorption, a few samples were selected and the size of their platinum clusters analysed using TEM. For TEM analysis, the samples had to be embedded in Spurr's resin. Since Spurr's resin is hydrophobic, it was important to remove as much water as possible from the zeolite using methanol. Methanol and the Spurr's resin are immiscible. This required an intermediate washing procedure of the samples with propylene oxide which is miscible with both methanol and Spurr's resin.

About 0.1g of sample was used for TEM analysis. All the samples were ultrasonicated in 10 ml methanol for 20 minutes after which the methanol/(Pt/KL) slurry was centrifuged to separate the methanol from the zeolite. The ultrasonic treatment was meant to separate the zeolite crystallites. Propylene oxide was then added to the samples and the slurry which was formed sonicated for a further 20 minutes.

A 1:1 volume ratio mixture of propylene oxide and Spurr's resin [Spurr, 1969] was then added to the sample and the subsequent slurry obtained left on a rotating table for 16 hours to ensure thorough mixing of the sample with the propylene oxide/Spurr's resin mixture. The slurry was then centrifuged in order to remove the mixture. A 1:3 volume ratio mixture of propylene oxide and Spurr's resin was then added to the sample and the slurry obtained left on the rotating table for 1 hour. This mixture was then separated from the zeolite, replaced with a solution of 100 % Spurr's resin and the obtained slurry mixed on a rotating table for 5 hours. The resin was then removed and replaced with more 100 % Spurr's resin. This was then put in Been capsules in which the zeolite was allowed to sediment to the bottom of the capsules. The capsules were then put in the oven at 60°C for 16 hours during which the resin solidified.

Ultra thin sections (80 - 90 nm) were then cut from the sample using a Reichert Ultracut S Ultramicrotome. The sections were collected on carbon coated copper grids. These were viewed and photographed at 200 kV in a Jeol 200CX microscope.

### 2.2.7 Energy Dispersive X-ray (EDX) Analysis

EDX in combination with Transmission Electron Microscopy (TEM) and Scanning Transmission Electron Microscopy (STEM) was used to analyse the elemental composition of selected areas presented in the TEM photographs. The aim of this exercise was to verify that the large particles detected by TEM were actually platinum clusters and not due to contamination of the samples. It was equally desirable to verify that well dispersed platinum existed in the samples whose platinum particles were well dispersed and too small to be detected by TEM.

The assayed samples were as follows:

- 1.55 % Pt/KL calcined in oxygen while the temperature was increased from 25°C to 350 °C at a rate 12.5°C/10 minutes. It was subsequently held at 350 °C for 6.33 hours. After calcination and subsequent cooling in nitrogen, the sample was then reduced in hydrogen while the temperature was increased from 25 °C to 350 °C at a

rate of 21.7 °C/10 minutes. The temperature was then held at 350 °C for 4.5 hours. The platinum dispersion on this sample was 111 %.

- 1.55 % Pt/KL calcined in nitrogen while increasing the temperature from 25°C to 600°C at a rate of 22.1 °C/10 minutes. It was then held at 600 °C for 6.33 hours. After cooling in nitrogen, the sample was then reduced in hydrogen while the temperature was increased from 25 °C to 350 °C at a rate of 21.7 °C/10 minutes. The temperature was then held at 350 °C for 4.5 hours. The platinum dispersion on this sample was 44 %.

The image of the sample obtained on the TEM instrument (magnification of 175 000 times) was projected onto the screen of the STEM instrument. Areas with or without visible platinum clusters were then selected on the STEM screen and these were assayed for platinum using the EDX facility. The minimum acquisition time of each spectrum obtained on the EDX instrument was 100 seconds. In order to verify the elemental analysis of zeolite KL, assays were also done for silicon, aluminium and potassium.

The beam diameter used in the STEM was 10 nm. It was observed that if left focused on a certain area for a long period, the beam attracted organic compounds in the instrument's column which then built up on the surface of the sample causing the beam diameter to increase even further. In order to minimise this, it was decided that for each spectrum, five areas of similar appearance would be assayed with each area being assayed for a maximum of 20 seconds. The spectra obtained for the five areas were then added to yield one spectrum acquired after 100 seconds.

## **2.2.7 Reactions**

### **2.2.7.1 Hydrogenation reactions**

In an attempt to determine whether the loaded platinum in the zeolite KL was on the external surface or in the pores, hydrogenation reactions were carried out. Cyclododecene and cyclohexene were hydrogenated to cyclododecane and cyclohexane respectively on selected

catalysts. The 1.55 % Pt/KL catalyst with the highest platinum dispersion (calcined at 350 °C in oxygen and reduced in hydrogen at 350 °C) as well as the one with the lowest platinum dispersion (calcined in nitrogen at 600 °C and reduced in hydrogen at 350 °C) were used for the reactions. Hydrogenation of both compounds were carried out at 1 000 kPa hydrogen pressure in batch mode in an autoclave containing a teflon cup.

It had been speculated that cyclododecene would be larger than the zeolite KL pores and would thus not enter into the pores. The platinum particles in the pores would thus be inaccessible to the cyclododecene. Cyclohexene on the other hand had been expected to enter into the pores of the zeolites due to its small diameter.

Hydrogenation of cyclohexene was carried out at 92 °C while that of cyclododecene was carried out at 105 °C. The reaction temperature was maintained for four hours. N-hexane was the internal standard used for the hydrogenation of cyclohexene while n-heptane was used as the internal standard for the hydrogenation of cyclododecene. In both hydrogenation reactions, 0.1g of the catalyst was used. In the hydrogenation of cyclododecene, 2 g of reactant and 2 g of internal standard were added to the autoclave while for the hydrogenation of cyclohexene, 4 g of reactant and 2 g of internal standard were added to the autoclave. In the autoclave the compounds were kept well mixed by a magnetic stirrer. The reaction products were analysed using Gas Chromatography.

#### **2.2.7.2 Aromatisation Reactions**

The performance of a 1.55 % Pt/KL catalyst with high platinum dispersion (111 %) and one with low platinum dispersion (44 %) in the aromatisation of n-hexane to benzene was tested. A representation of the rig used in the aromatisation reactions is given in figure 2.8.

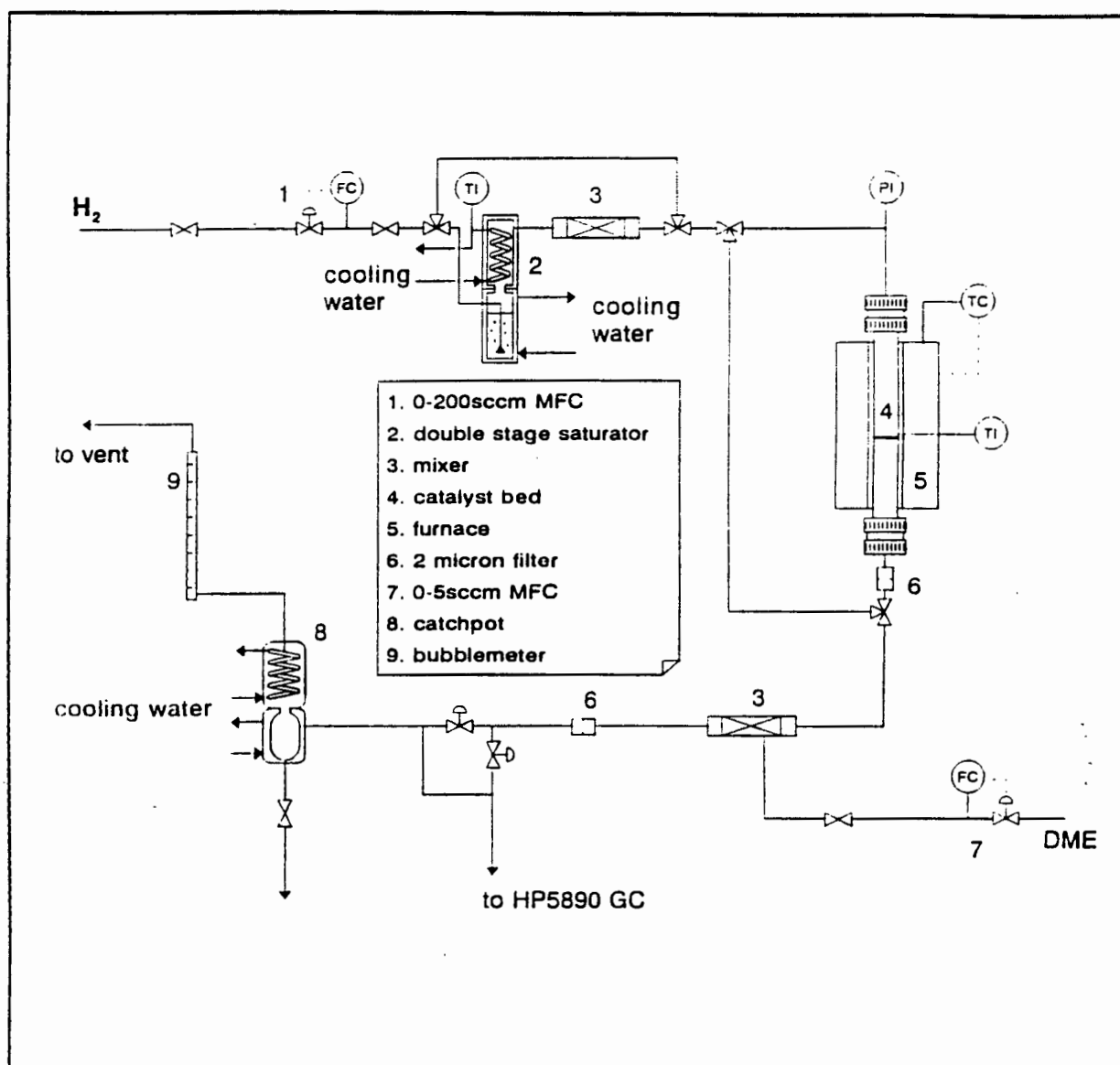


Figure 2.8 showing the aromatisation rig

0.1g of catalyst was put into the reactor and re-reduced in hydrogen at 400 °C for two hours. Hydrogen was used as the carrier gas for the n-hexane in the saturator. The space hourly velocity (WHSV) of the n-hexane was 27.8 hr<sup>-1</sup> and the H<sub>2</sub>/n-hexane mole ratio was 3.0. Di-methyl ether (DME) was used as the internal standard. The bottom section of the saturator was kept at 30 °C while the top section was kept at 0 °C. The reactor was maintained at 400 °C. The conversion of the n-hexane over the two catalyst samples was then monitored.

## **CHAPTER 3**



### 3 RESULTS

#### 3.1 X-Ray Diffraction Patterns

The simulated X-ray diffraction pattern of zeolite KL as well as the experimentally obtained pattern are shown in figures 3.1 and 3.2. Most of the peaks shown in the simulated pattern were present in the experimentally obtained pattern. In the experimentally determined pattern, the peaks at low theta values were not as prominent as in the simulated pattern. This could have been due the instrument limitations in acquiring data at low theta values.

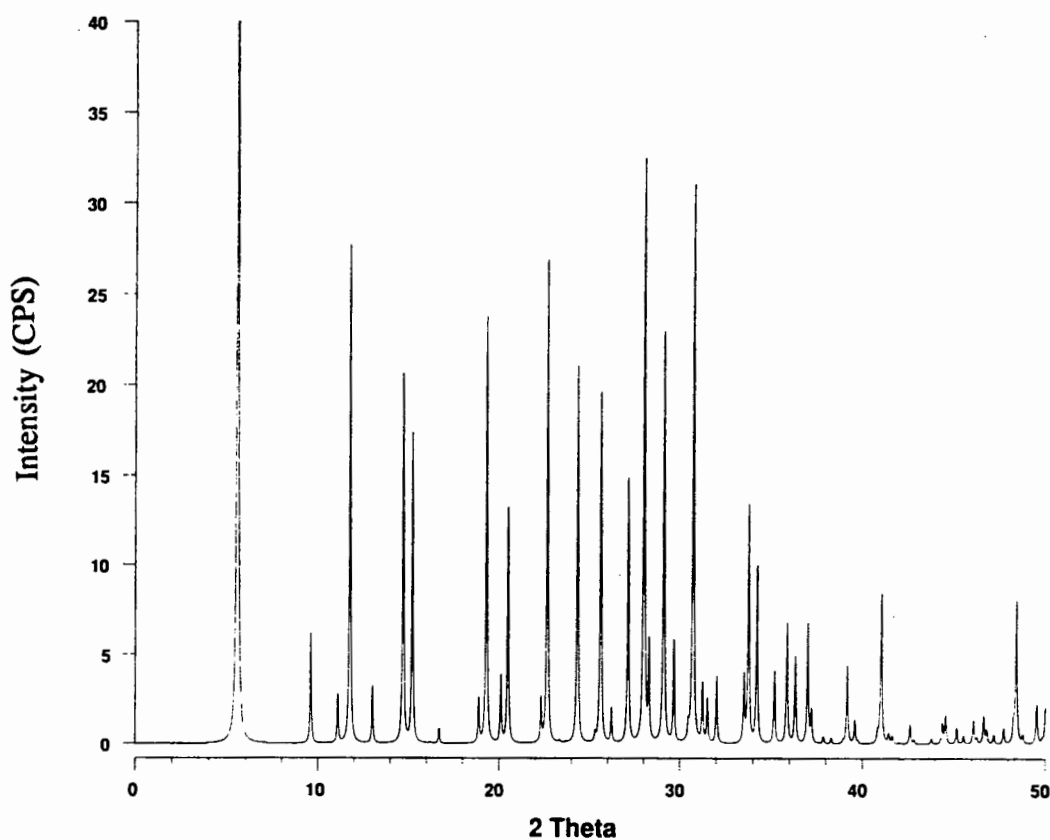
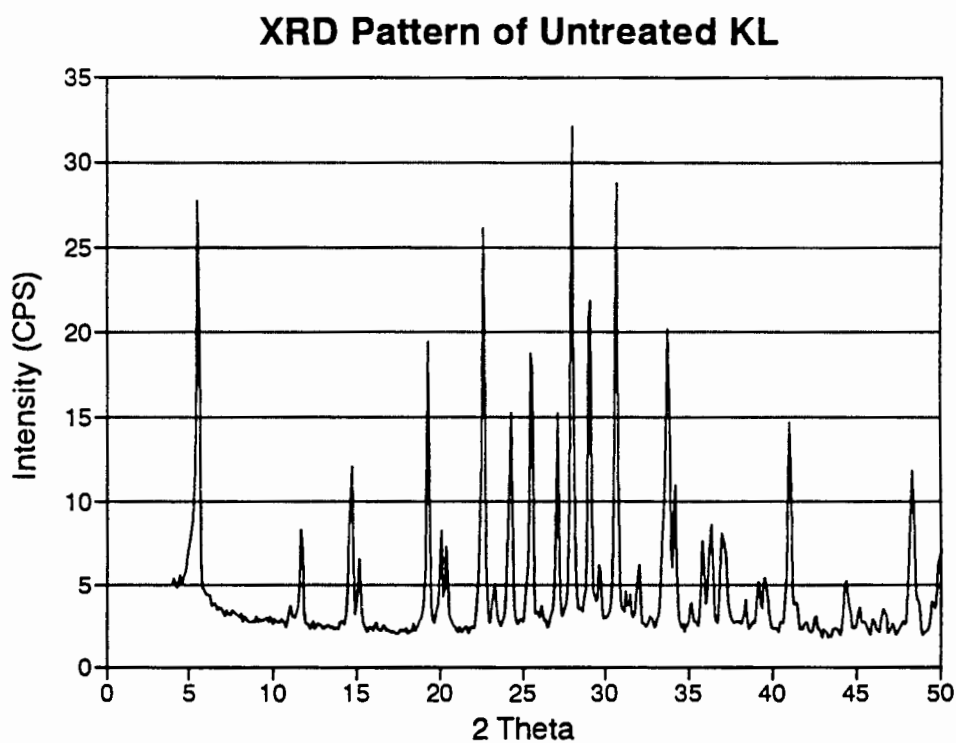


Figure 3.1 showing the simulated XRD pattern of zeolite L ( $\text{Na}_3\text{K}_6\text{Si}_{27}\text{O}_{72} \cdot 21\text{H}_2\text{O}$ ) [from von Ballmou and Higgins, 1990]



**Figure 3.2** showing the experimentally determined XRD pattern of the zeolite KL used in this study

It was found that the XRD pattern of the zeolite KL did not change significantly as a result of either the incorporation of platinum or thermal treatment up to 700 °C of the platinum loaded zeolite.

## 3.2 Elemental Analysis

### 3.2.1 Atomic Absorption Analysis

The time taken for the platinum to be loaded onto the zeolite at different ion exchange temperatures was monitored. The platinum content was determined using atomic absorption spectroscopy. As shown in figures 3.3 to 3.5 the time taken for the platinum in solution to be loaded onto the zeolite was less than 40 minutes.

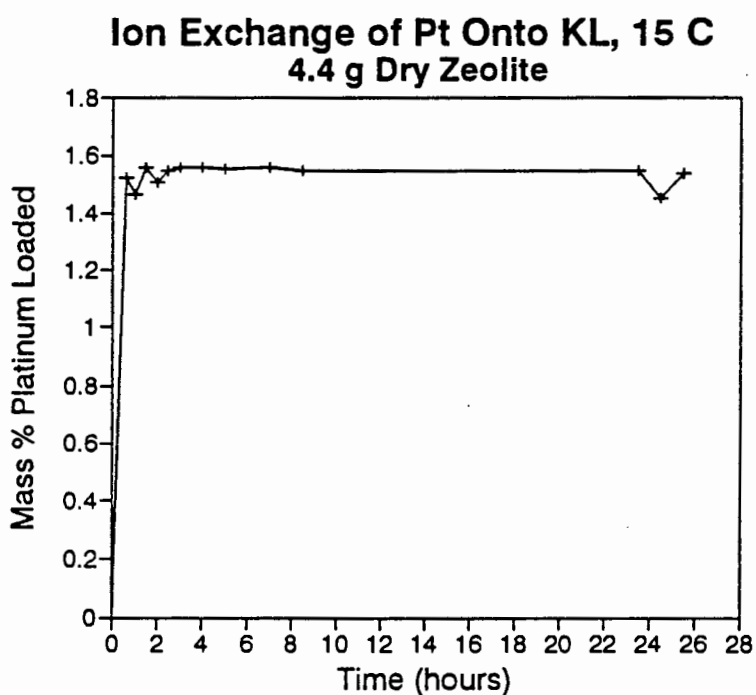


**Figure 3.3** showing the time taken to load 1.55% Pt onto zeolite KL at 15° C

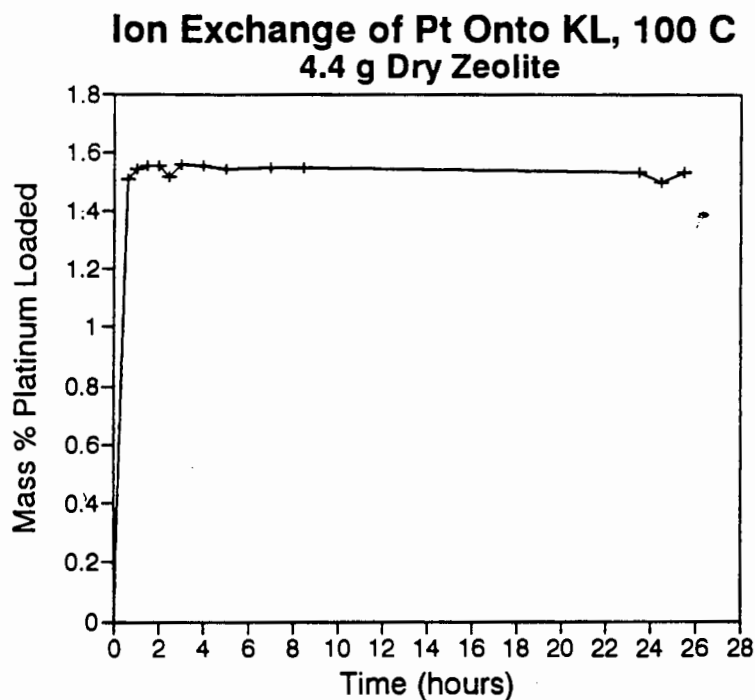


Figure 3.4 showing the time taken to load 1.55% Pt onto zeolite KL at 100°C

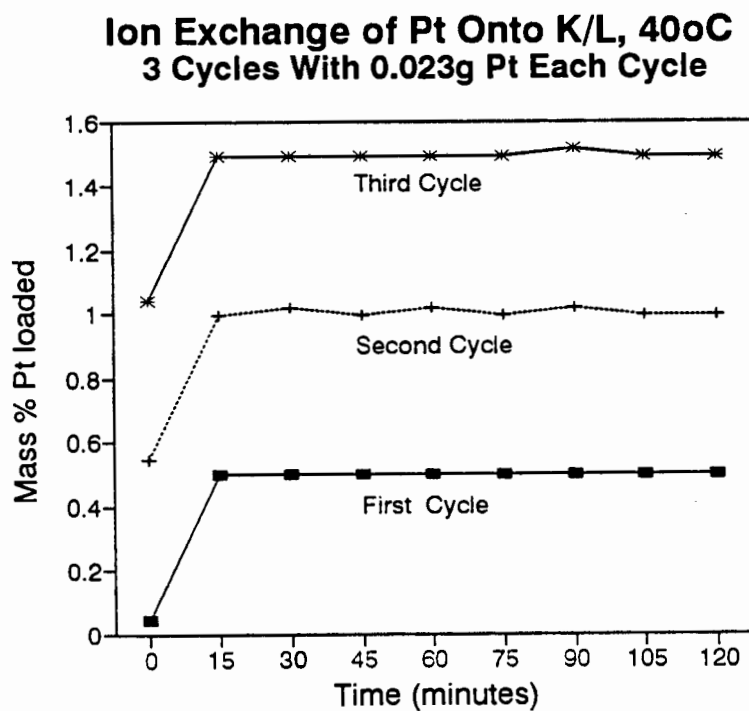


Figure 3.5 showing the time taken to load 1.55% Pt onto zeolite KL via multiple exchange cycles at 40°C

Solid state ion exchange of platinum onto zeolite KL was performed at calcination and reduction conditions which yielded the best platinum distribution in samples whose platinum had been loaded via liquid ion exchange. The calcination conditions were 350 °C in oxygen for 1.5 hours while the reduction conditions were 350°C in hydrogen for 1.5 hours. This was done in order to compare the dispersion of the platinum in the samples whose platinum had been loaded using different methods. After solid state ion exchange, the sample was washed four times with de-ionised water to remove any platinum that had not been ion exchanged onto the zeolite. Using atomic absorption spectroscopy, the amount of platinum loaded onto zeolite KL via the solid state ion exchange method was found to be 0.75 wt %.

The amount of platinum loaded via incipient wetness impregnation was found to be 1.55 wt % using atomic absorption spectroscopy.

Analysis of potassium ion exchanged from the zeolite KL into solution as well as that remaining on the zeolite was done using atomic absorption spectroscopy. The obtained results correlated with the amount expected to be ion exchanged by the platinum. Elemental analysis of silicon and aluminium using atomic absorption spectroscopy could not be carried out reliably. This was because the absorption of these elements was severely depressed in the presence of potassium, hydrofluoric and boric acids [Varian, 1979]. Zeolite KL contained potassium and the digestion of the zeolite for atomic absorption analysis required the use of hydrofluoric and boric acids (section 2.2.2.1).

### **3.2.2 Electron Beam Micro-analysis Results**

The silicon and aluminium analysis of zeolite KL was determined using electron beam micro-analysis. Preparation of samples for the electron beam micro-analysis involved fusing the zeolite samples into homogenous amorphous beads at temperatures greater than 1150 °C.

A Si/Al atom ratio of 3 for zeolite KL was obtained. This agreed well with the theoretical value of 3. Attempts were also made to confirm the results of the platinum content of the

zeolite obtained using atomic absorption analysis. However accurate analysis of the platinum content using the electron beam micro-analysis could not be made. This was because during the fusing process, the platinum agglomerated into large particles thus rendering the sample non homogenous with respect to platinum.

### 3.3 Calcination And Reduction

#### 3.3.1 Minimum Calcination Temperature

The temperature at which the ammonia ligands would decompose was determined by heating the 0.25 g of zeolite KL which had been ion exchanged with  $\text{Pt}(\text{NH}_3)_4\text{Cl}_2$  to give 1.55 wt % platinum. The sample was placed in a temperature programmed desorption apparatus fitted with a mass spectrometer. The temperature was increased from 20 °C to 600 °C at a rate of 5 °C per minute using helium as the carrier gas. The obtained profile is shown in figure 3.6. The decomposition of the ammonia complex was characterised by the evolution of ammonia and its derivatives. The temperature at which the decomposition started was found to be 320 °C. The baselines for nitrogen and water were higher than those of other compounds. This was because the helium carrier gas used contained traces of nitrogen and water.

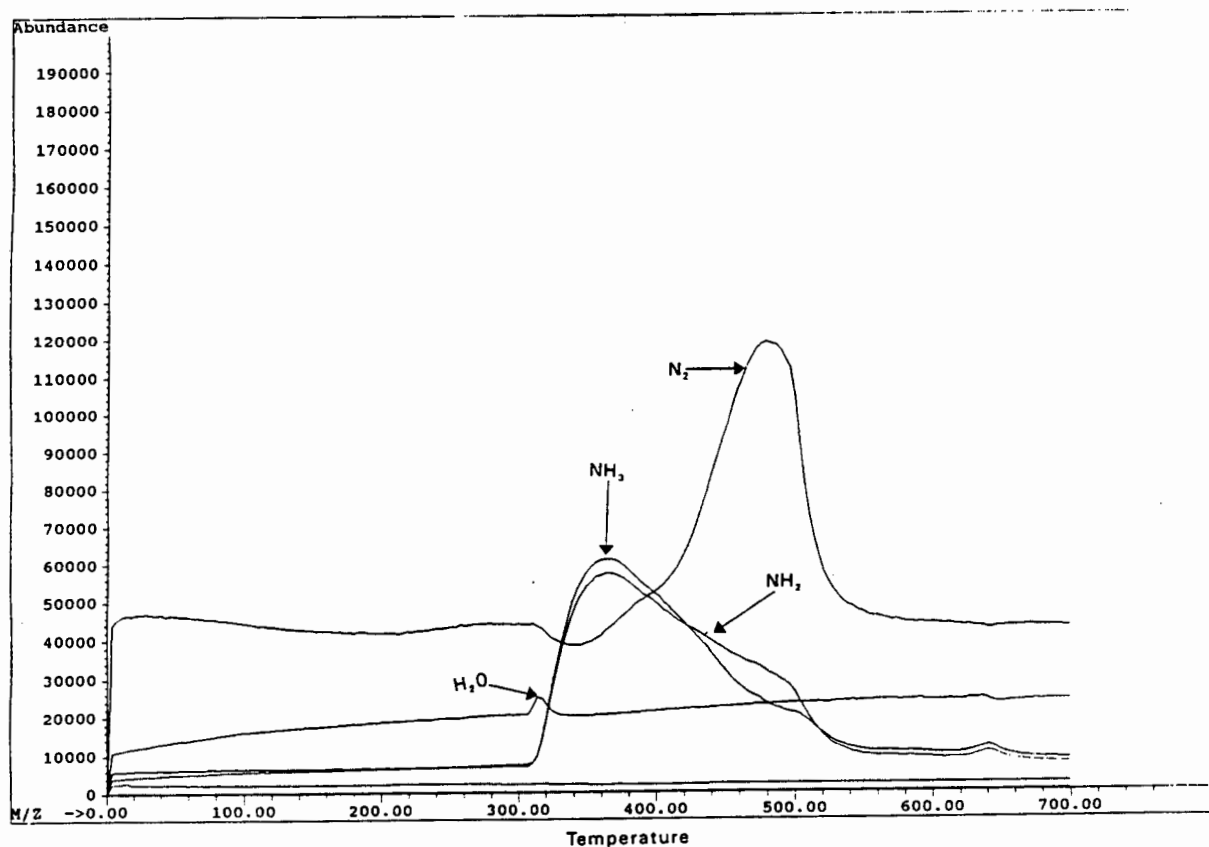


Figure 3.6 showing the temperature at which the ammonia ligands disintegrate.

### 3.3.2 Temperature Programmed Reduction (TPR) Results

#### 3.3.3.1 Calibration of the hydrogen concentration in the $H_2/N_2$ stream

Known quantities of  $Co_3O_4$ ,  $NiO$  and  $CuO$  were reduced in the TPR rig and the results obtained used to calibrate the hydrogen concentration in the  $H_2/N_2$  stream. As an initial estimate, the hydrogen concentration given by the gas suppliers (5%  $H_2$  in  $N_2$ ) was used. The results are shown in figure 3.7 and table 3.1.

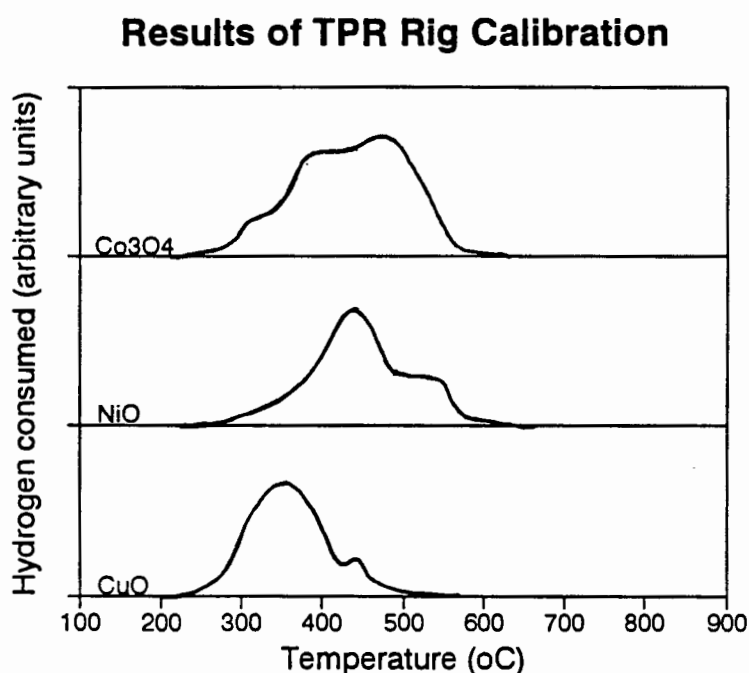


Figure 3.7 showing the TPR profiles of the oxides used to calibrate the TPR rig.

Sample	CuO	NiO	$Co_3O_4$
Mass after reduction (g)	0.0646	0.0663	0.0622
$N_2/H_2$ - flow ml/minute (20 °C)	63.9	63.4	63.0
$H_2$ consumed, mmol *	1.1770	1.3002	1.0272
$H_2$ consumed per metal, mol/mol	1.1576	1.1513	1.5420

\* This is based on a value of 5 % hydrogen in nitrogen given by the gas suppliers

Table 3.1 showing the results of the TPR rig calibration



Using the average value of the mol of  $H_2$  consumed per mol of metal as well as the reported 5 %  $H_2$  in  $N_2$  supplied by the gas manufacturers, the actual concentration of hydrogen in the nitrogen stream was calculated to be 4.33 %.

### 3.3.2.2 TPR profiles of 1.55 wt % Pt/KL and 1.43 wt % Pt/HY samples

In order to determine the temperatures at which different Pt species would reduce in hydrogen, temperature programmed reduction (TPR) was applied to Pt/KL and Pt/HY samples that had been prepared under various conditions. Using TPR, the moles of hydrogen consumed per unit mole of platinum in the sample (i.e. the Pt/ $H_2$  mole ratio) was determined. PtO is reduced by hydrogen at temperatures lower than 11 °C. The technique used in acquiring the TPR data (section 2.2.4) could not record the initial hydrogen uptake as a full peak as is normally obtained in TPR profiles. The 1.55 % Pt/KL sample calcined at 600 °C showed a higher  $H_2$ /Pt ratio compared to those calcined at 350 °C (table 3.2). The 1.43 % Pt/HY samples showed  $H_2$ /Pt ratios which were much higher than the theoretically expected values (table 3.2).

The TPR profiles for the various samples are presented in figures 3.8 to 3.13 and the results are summarised in table 3.2

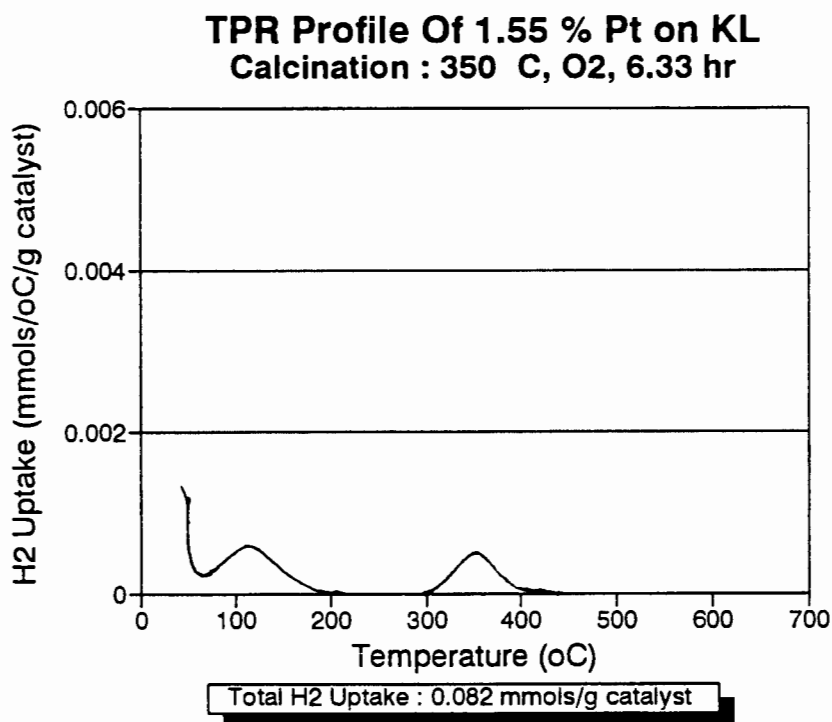


Figure 3.8 showing the TPR profile of 1.55 wt % Pt/KL calcined at 350 °C in O<sub>2</sub> for 6.33 hours.

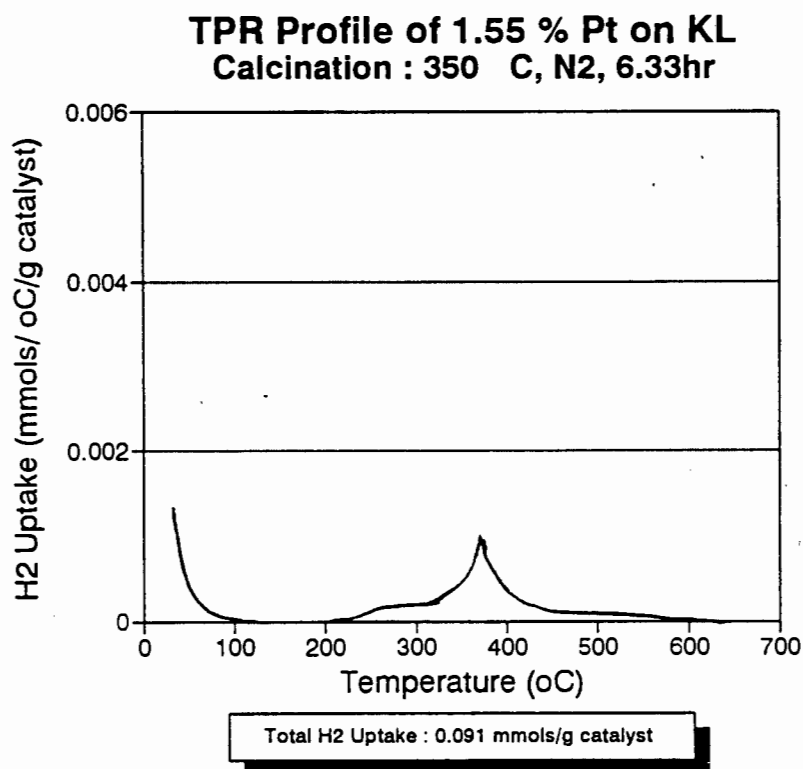


Figure 3.9 showing the TPR profile of 1.55 wt % Pt/KL calcined at 350 °C in N<sub>2</sub> for 6.33 hours

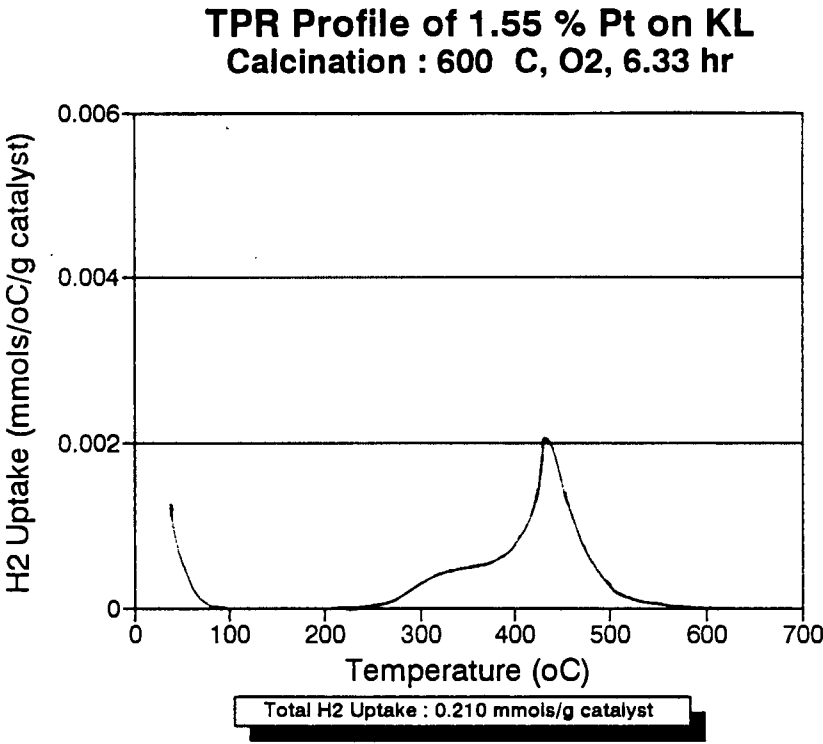


Figure 3.10 showing the TPR profile of 1.55 wt % Pt/KL calcined at 600 °C in O<sub>2</sub> for 6.33 hours

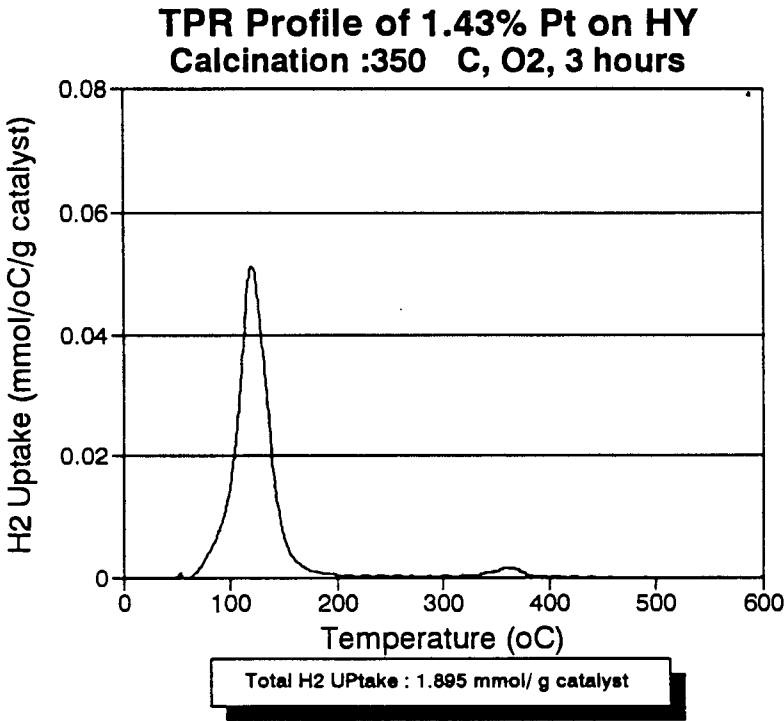


Figure 3.11 showing the TPR profile of 1.43 wt % Pt/HY calcined at 350 °C in O<sub>2</sub> for 6.33 hours

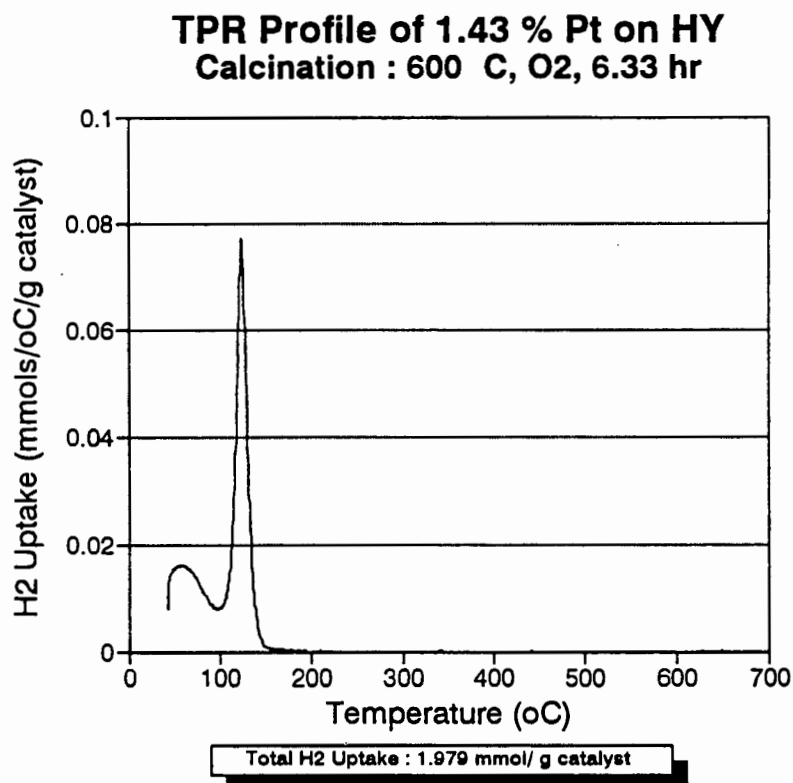


Figure 3.12 showing the TPR profile of 1.43 wt % Pt/HY calcined at 600 °C in O<sub>2</sub> for 6.33 hours

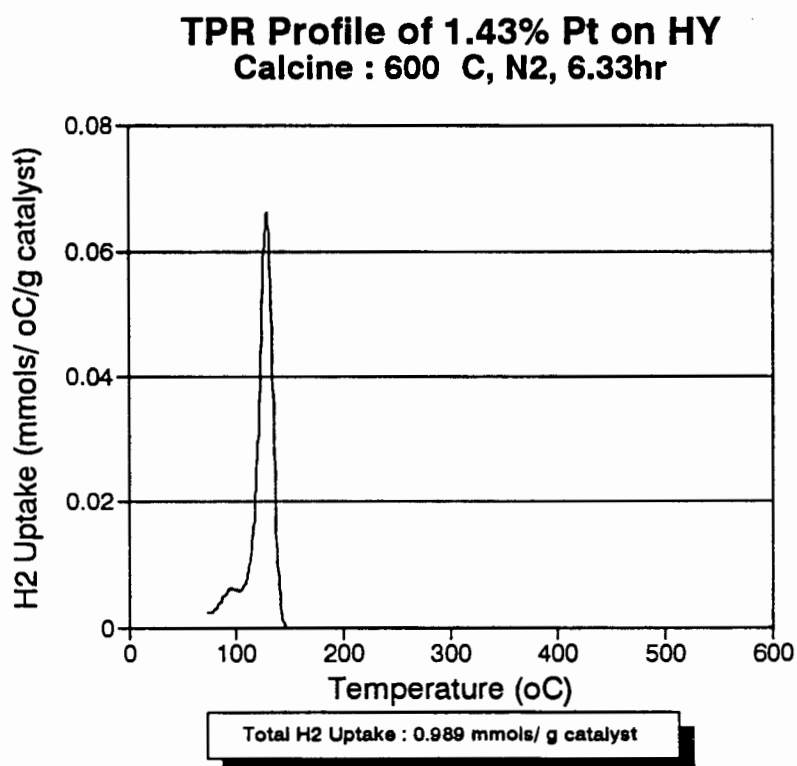


Figure 3.13 showing the TPR profile of 1.43 wt % Pt/HY calcined at 600 °C in N<sub>2</sub> for 6.33 hours

Sample	Mass % Pt	Calcination Medium	Calcination Temp. (oC)	Uptake mmols H <sub>2</sub> /g catalyst	H <sub>2</sub> /Pt mol ratio	Peak of TPR Temp. (°C)
Pt/KL	1.55	O <sub>2</sub>	350	0.082	1.03	42, 115, 350
Pt/KL	1.55	N <sub>2</sub>	350	0.091	1.14	42, 370
Pt/KL	1.55	O <sub>2</sub>	600	0.210	2.64	42, 430
Pt/HY	1.43	O <sub>2</sub>	350	1.895	23.77	120,350
Pt/HY	1.43	O <sub>2</sub>	600	1.979	24.90	60, 120
Pt/HY	1.43	N <sub>2</sub>	600	0.989	13.49	90, 120

**Table 3.2** showing a summary of the TPR results.

### 3.4 Results Of Temperature Programmed Desorption (TPD) Of Ammonia

In the TPD results of KL and Pt/KL samples, the peaks obtained appeared at three sets of temperature ranges. These temperature ranges were 240 °C - 290 °C (peak A); 340 °C - 350 °C (peak B) and 520 °C - 600 °C (peak C). For the Pt/SiO<sub>2</sub> the peaks obtained were at about 470 °C. The TPD profiles obtained for different samples are shown from figure 3.14 to figure 3.24 and the summary of the results are presented in table 3.3. For most of the TPD analysis, the amount of desorbed ammonia determined by titration was within 10 % of the amount determined using the TCD and the computer software. Considering the inevitable human error involved in the titration technique used, this error was acceptable.

In order to determine whether the ammonia used in the TPD analysis would adsorb onto platinum, Pt/SiO<sub>2</sub> was characterised using TPD. It was believed that the silica gel would not have any acid sites. The results obtained are presented in figures 3.14 and 3.15.

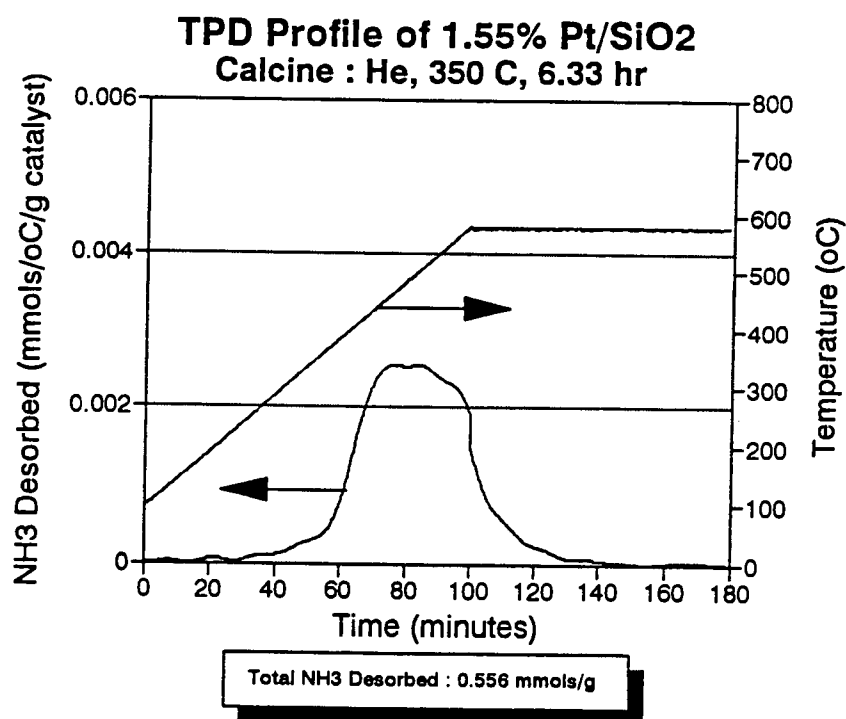


**Figure 3.14** showing the TPD profile of 1.55 % Pt/SiO<sub>2</sub> Calcined : 350°C, He, 6.33hr. No reduction.

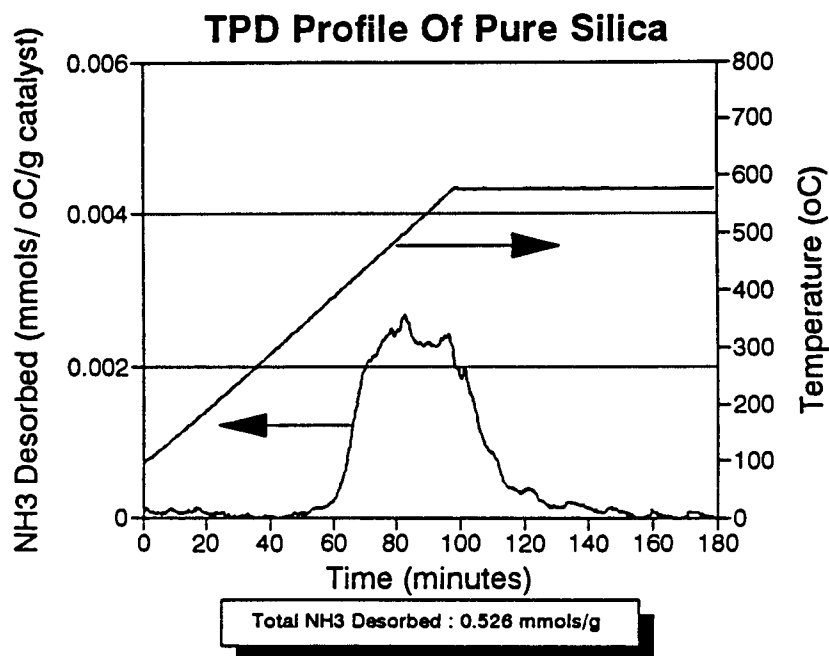


Figure 3.15 showing the TPD profile of pure silica Calcined : 350°C, He, 6.33hr. No reduction.

Evidently from figures 3.14 and 3.15, the silica gel contained some acidity. None the less, the difference in the amount of desorbed ammonia between the two samples indicated that platinum metal did not adsorb ammonia to any significant degree..

Figures 3.16 and 3.17 show the TPD profiles of untreated fresh zeolite KL and zeolite KL that has been calcined in oxygen. As expected, these TPD profiles are similar.

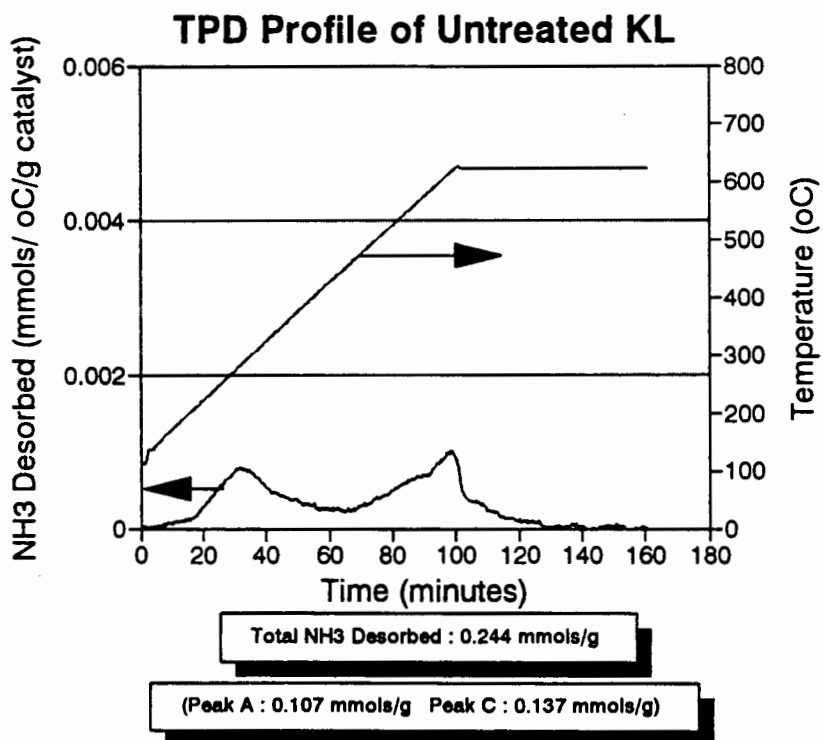


Figure 3.16 showing the TPD profile of untreated zeolite KL

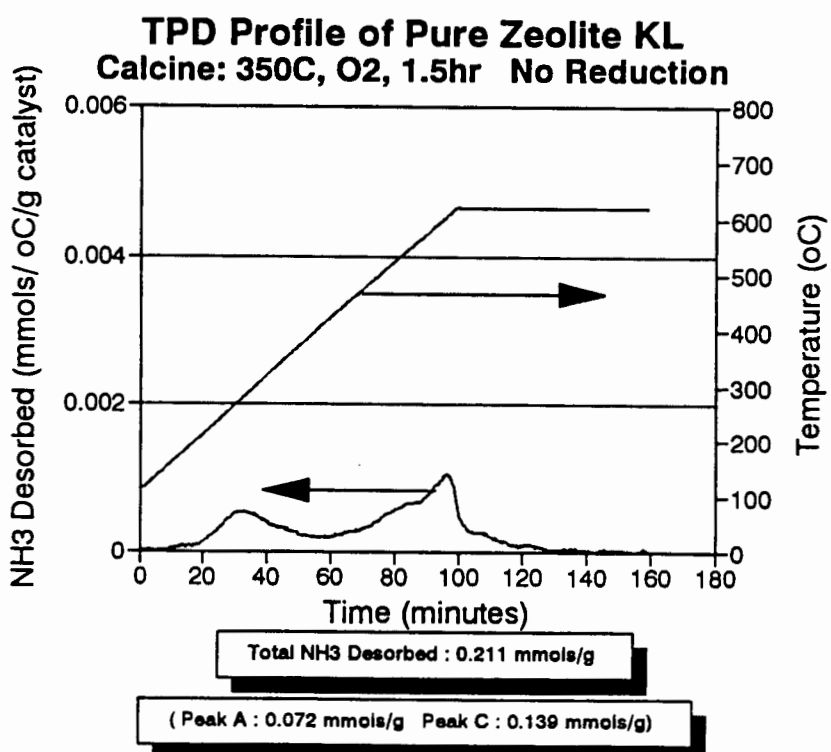


Figure 3.17 showing the TPD profile of zeolite KL calcined : 350°C, O<sub>2</sub>, 1.5 hr. No reduction



In figure 3.18 it can be observed that the first peak is non symmetrical due to a small shoulder appearing after 40 minutes.

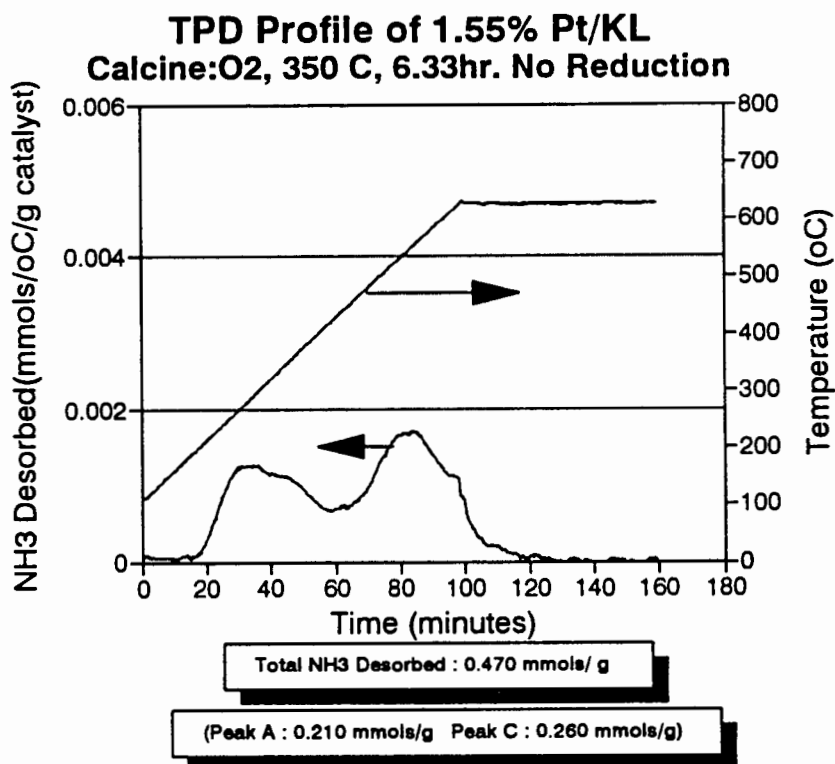


Figure 3.18 showing the TPD profile of 1.55% Pt/KL. Calcined : 350°C, O<sub>2</sub>, 6.33hr. No reduction

Comparing the TPD profile in figure 3.19 to that in figure 3.18 shows that calcination of 1.55% Pt/KL in nitrogen at 350 °C causes the shoulder which starts after 40 minutes to be more pronounced.

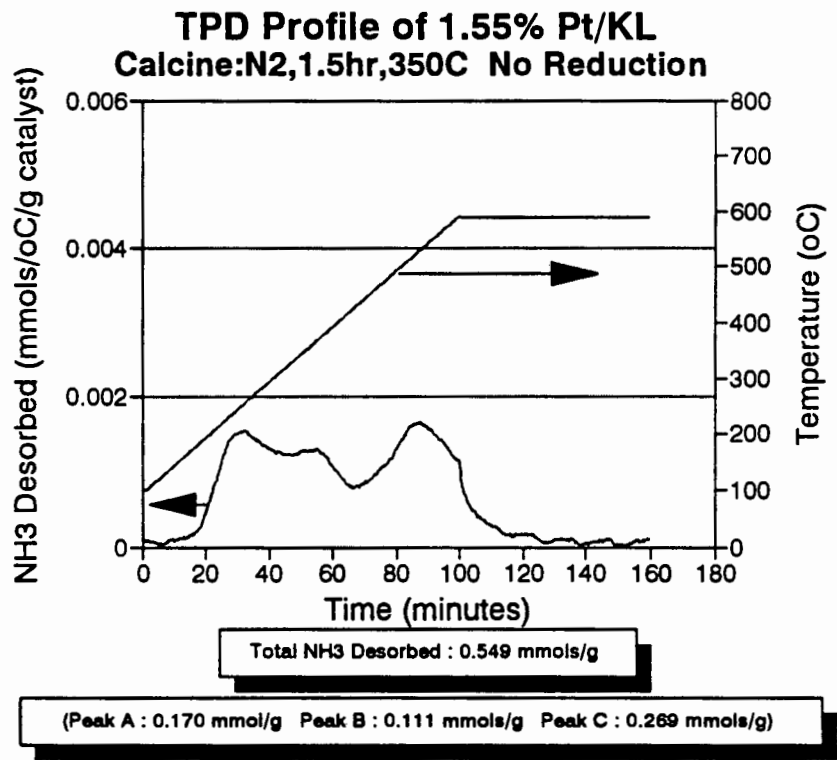


Figure 3.19 showing the TPD profile of 1.55% Pt/KL. Calcined : 350°C, N<sub>2</sub>, 1.5 hr. No reduction.

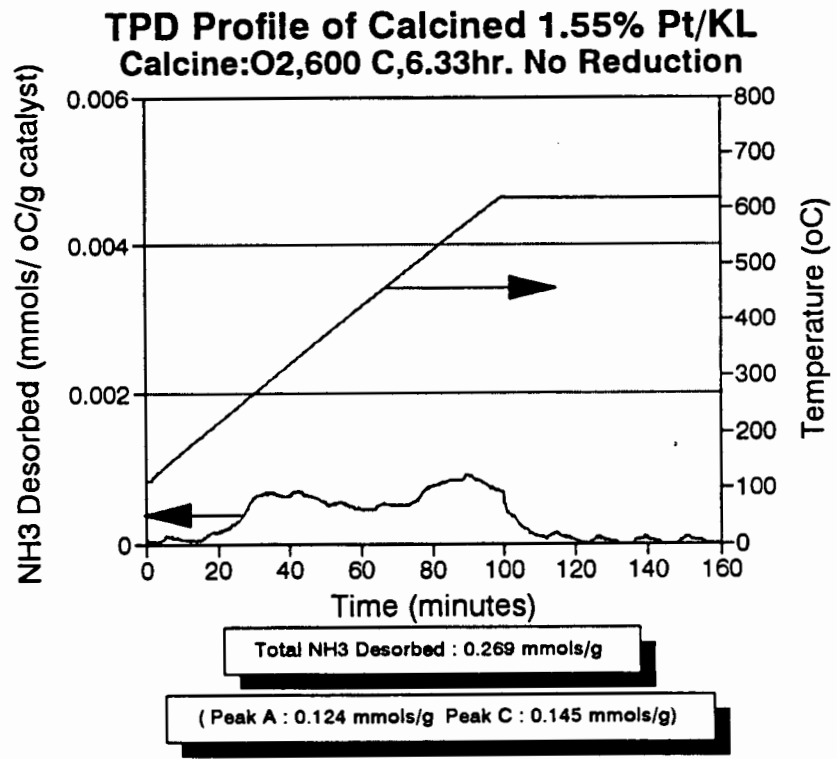


Figure 3.20 showing the TPD profile of 1.55% Pt/KL Calcined : 600°C, O<sub>2</sub>, 6.33hr. No reduction.

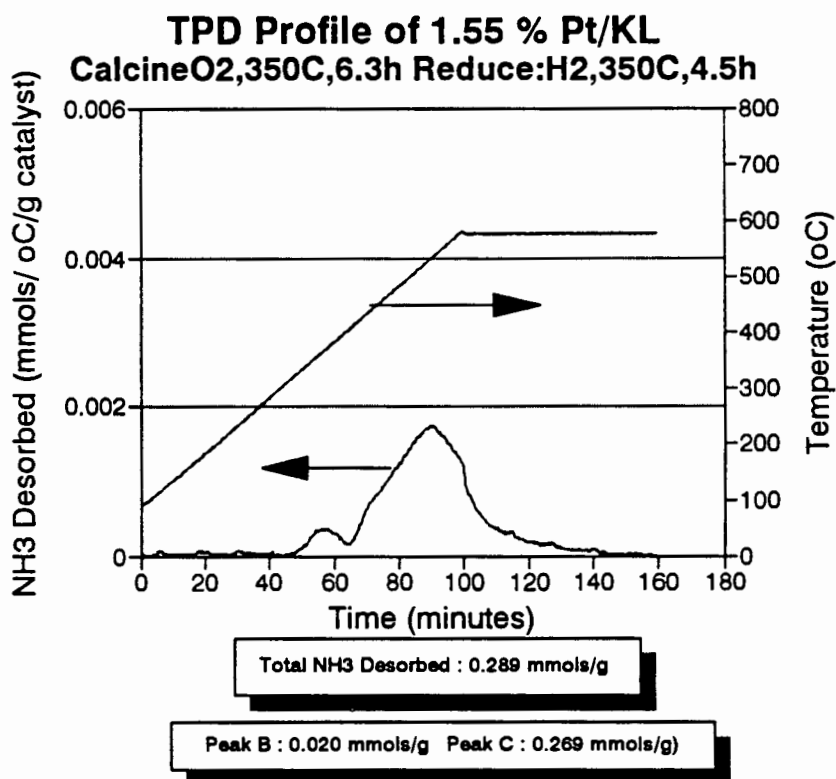


Figure 3.21 showing the TPD profile of 1.55 % Pt/KL. Calcined : 350°C, O<sub>2</sub>, 6.33hr. Reduced : 350°C, H<sub>2</sub>, 4.5hr.

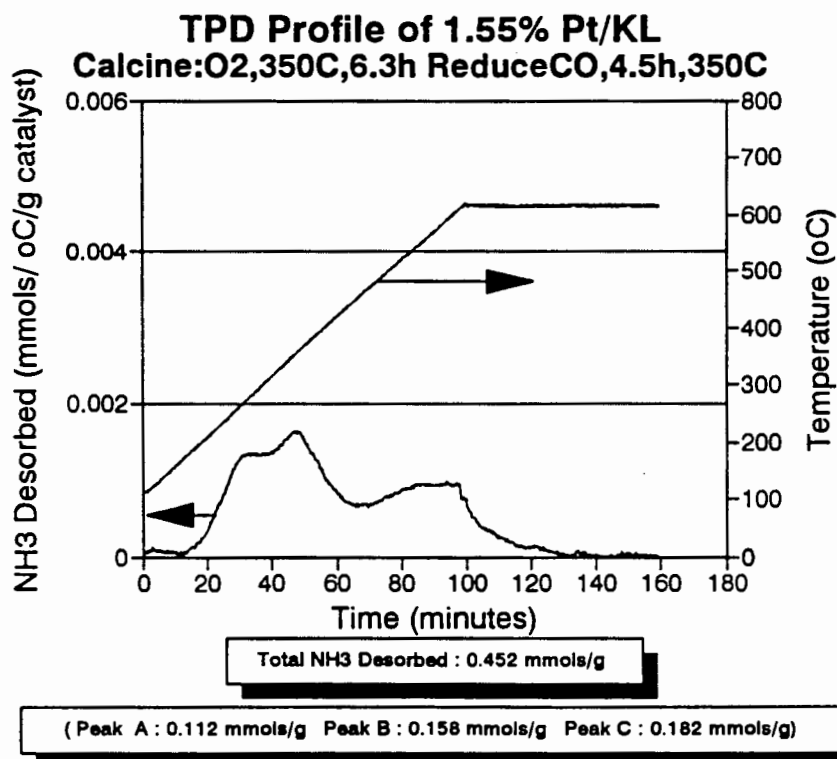
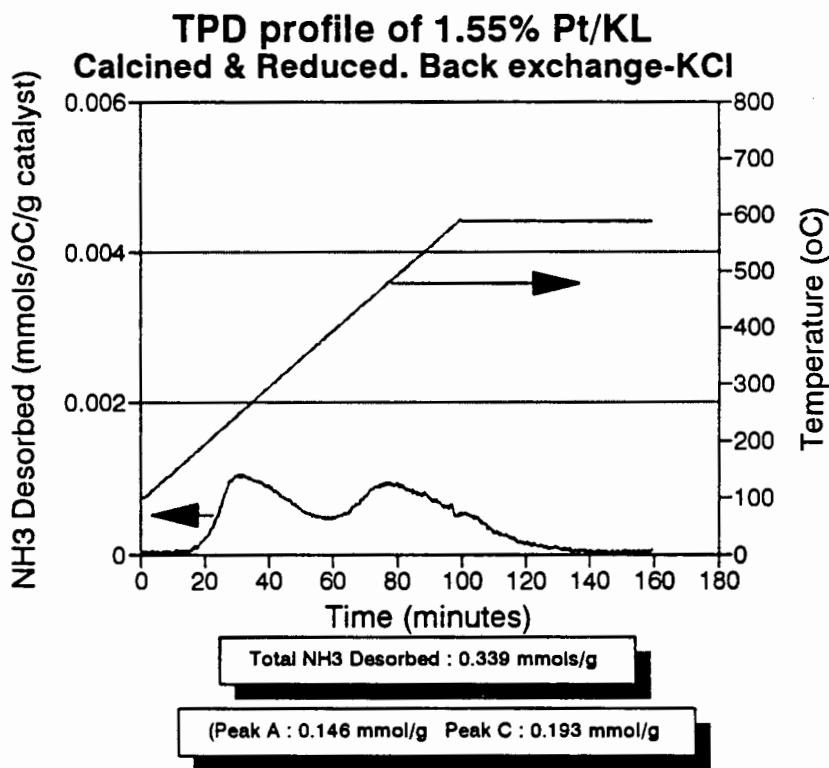


Figure 3.22 showing the TPD profile of 1.55 % Pt/KL Calcined : 350°C, O<sub>2</sub>, 6.33hr. Reduced : 350°C, CO, 4.5hr.

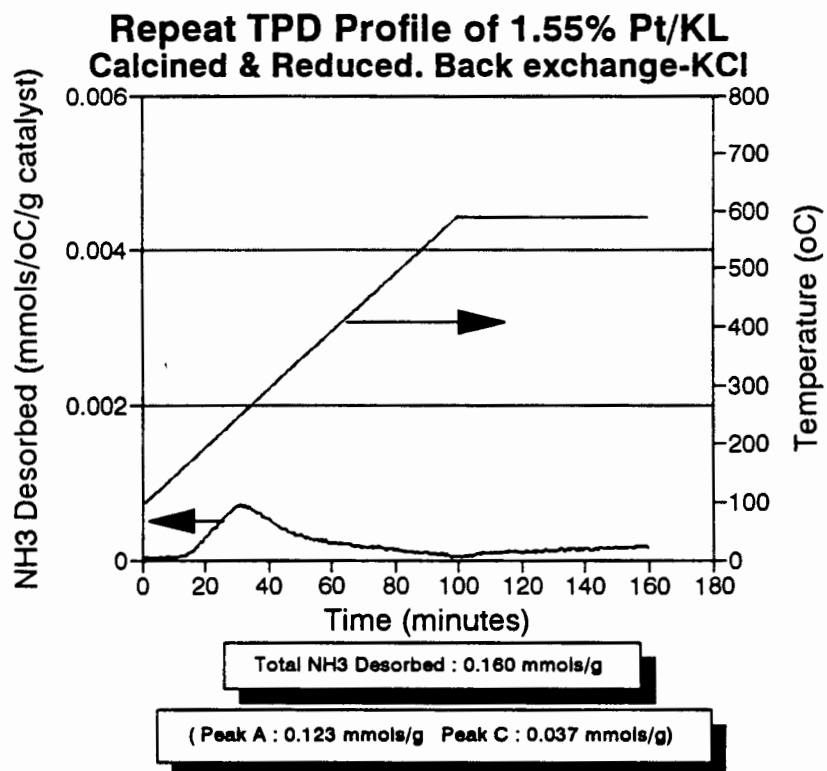
The shoulder starting after 40 minutes in figures 3.18 and 3.19 is even more pronounced in figure 3.22



Calcination conditions : 350 C, O<sub>2</sub>, 1.5 hours Reduction conditions : 350 C, H<sub>2</sub>, 1.5 hours

**Figure 3.23** showing the TPD profile of 1.55% Pt/KL. Back exchanged with K<sup>+</sup> using KCl in O<sub>2</sub> at 350 °C. Prior to back exchange, sample had been calcined in O<sub>2</sub> and reduced in H<sub>2</sub>.

It is possible that the first peak obtained for the Pt/KL zeolites was due to weakly adsorbed ammonia. It is also possible that during the TPD analysis procedure, dehydroxylation was occurring at high temperatures. In order to determine whether these two phenomena were taking place during the TPD analysis, it was decided to perform the TPD of one sample, cool it down to room temperature in an inert atmosphere and then repeat the TPD. This was done for the sample whose TPD profile is presented in figure 3.23. The obtained "repeat" TPD profile is presented in figure 3.24. It is note-worthy that in figure 3.24 all the peaks shown in figure 3.23, except for the first one, disappeared. Unlike other TPD profiles, the ammonia desorption curve increased steadily after 97 minutes (580 °C).



Calcination conditions : 350 C, O<sub>2</sub>, 1.5 hours Reduction conditions : 350 C, H<sub>2</sub>, 1.5 hours

**Figure 3.24** showing a repeat of the TPD profile of 1.55% Pt/KL. Back exchanged K<sup>+</sup> using KCl in O<sub>2</sub> at 350 °C.

A summary of the TPD results for Pt/KL samples is presented in table 3.3

Sample	Acidity (mmols/g)				Desorption Peak Temperatures (°C)
	Peak A <sup>a</sup>	Peak B <sup>b</sup>	Peak C <sup>c</sup>	Total	
Untreated zeolite KL	0.107	-	0.137	0.244	270, - 600
Zeolite KL Calcined :350°C, O <sub>2</sub> , 1.5 hr. No reduction	0.072	-	0.139	0.211	270, - 600
1.55 % Pt/KL Calcined:350°C, O <sub>2</sub> , 6.33hr. No reduction	0.210	-	0.260	0.470	270, - 520
1.55 % Pt/KL Calcined:350°C, N <sub>2</sub> , 1.5hr. No reduction	0.170	0.110	0.269	0.549	250, 350, 520
1.55 % Pt/KL Calcined:600°C, O <sub>2</sub> , 6.33h. No reduction	0.124	-	0.145	0.269	290, - 570
1.55 % Pt/KL Calcined:350°C, O <sub>2</sub> , 6.3h. Reduced:350°C, H <sub>2</sub> , 7h		0.020	0.269	0.289	- 350, 520
1.55 % Pt/KL Calcined:350°C, O <sub>2</sub> , 6.3h Reduced:350°C, CO, 7h	0.112	0.158	0.182	0.452	280, 350, 520
1.55 % Pt/KL Calcined:350°C, O <sub>2</sub> , 1.5h Reduced:350°C, H <sub>2</sub> , 1.5 h. Back exchanged:KCl, 350°C	0.146	-	0.193	0.339	240, - 450
Repeat TPD of back exchanged sample above.	0.123	-	0.037	0.160	240 - -

a : Peak A in range 240 °C - 290 °C

b : Peak B in range 340 °C - 350 °C

c : Peak C in range 520 °C - 600 °C

**Table 3.3** showing a summary of the TPD results for Pt/KL samples.

For 1.55 % Pt/SiO<sub>2</sub> one peak corresponding to 0.556 mmols/g acidity was observed at 470 °C while for Pt/SiO<sub>2</sub> one peak corresponding to 0.526 mmols/g acidity was observed at 480 °C. The surface area of the SiO<sub>2</sub> was 300m<sup>2</sup>/g.

## 3.5 Chemisorption Results

### 3.5.1 Carbon Monoxide Chemisorption

The dispersion of platinum is a measure of the fraction of platinum atoms whose surface area is exposed to the chemisorbing gas. A stoichiometric ratio between the chemisorbing gas and the platinum is assumed in the calculation of dispersion. For carbon monoxide analysis, a stoichiometric ratio of 1 was assumed between the platinum and the carbon monoxide.

Some of the chemisorption results obtained using carbon monoxide gave dispersion values greater than 100 %. Since the atomic absorption analysis of the Pt/KL and Pt/HY samples agreed with the analysis of the ion-exchange solutions, the reason for the dispersion values greater than 100 % could not have been due to an error in platinum content analysis. Carbon monoxide could adsorb onto one platinum atom to give several configurations namely, linear, bridged and a configuration in which more than one carbon monoxide molecule adsorb onto one platinum particle to give surface carbonyls. The linear configuration would give a stoichiometry of one while the surface carbonyl form would give a stoichiometry greater than one. Such differences in adsorption configurations could result in calculated dispersion values greater than 100 %. However, chemisorption analysis data can be used qualitatively in comparing the relative metal dispersion of the different samples as long as the conditions of the chemisorption analysis are kept constant for all the samples.

#### 3.5.1.1 Reproducibility of catalyst preparation procedure and chemisorption technique.

All the Pt/KL samples prepared for chemisorption analysis were ion exchanged at 40 °C for 24 hours except for the ones whose ion exchange temperature and time are specified. Prior to performing any chemisorption analysis, it was imperative to determine whether untreated zeolite KL would chemisorb carbon monoxide. It was found that the zeolite KL would not chemisorb any carbon monoxide.

In order to test the reproducibility of the catalyst preparation procedure, two samples of 1.55 % Pt/KL from the master batch were calcined and reduced separately in the preparation

rigs. Calcination was done in oxygen while increasing the temperature from 25 °C to 350 °C at 108.3 °C/10 minutes and maintaining the temperature at 350 °C for 1.5 hours. The reduction was done in hydrogen while increasing the temperature from 25 °C to 350 °C at a rate of 21.6 °C/10 minutes with the temperature being held at 350 °C for 4.5 hours. The platinum dispersion was then assayed using carbon monoxide chemisorption. The results are shown in table 3.4

Volume CO Chemisorbed (cc/g STP)	Metallic Surface Area (m <sup>2</sup> /g catalyst)	% Dispersion
2.053	4.413	116
1.986	4.269	111

**Table 3.4** showing the reproducibility of the catalyst preparation procedure.

Chemisorption analysis of the sample giving a platinum dispersion of 116% was repeated in order to test the reproducibility of the chemisorption procedure. The obtained metal dispersion was 113% which is within the acceptable error margin of +/- 5% for the apparatus.

### 3.5.1.2 Effect of ion exchange temperature on dispersion.

Two separate batches of zeolite KL were loaded with 1.55 wt % platinum at ion exchange temperatures of 15 °C and 40 °C respectively. A third batch was ion exchanged with 0.78 wt % platinum at 100 °C. A sample from each batch was then taken and calcined in oxygen while ramping the temperature from 25 °C to 350 °C at 12.5 °C/ 10 minutes with subsequent holding of the temperature at 350 °C for 6.66 hours. The samples were then reduced in hydrogen while increasing the temperature from 25 °C to 350 °C at a rate of 21.6 °C/ 10 minutes and holding the temperature at 350 °C for 4.5 hours. The dispersion of the platinum on the samples determined using chemisorption is shown in figure 3.25.



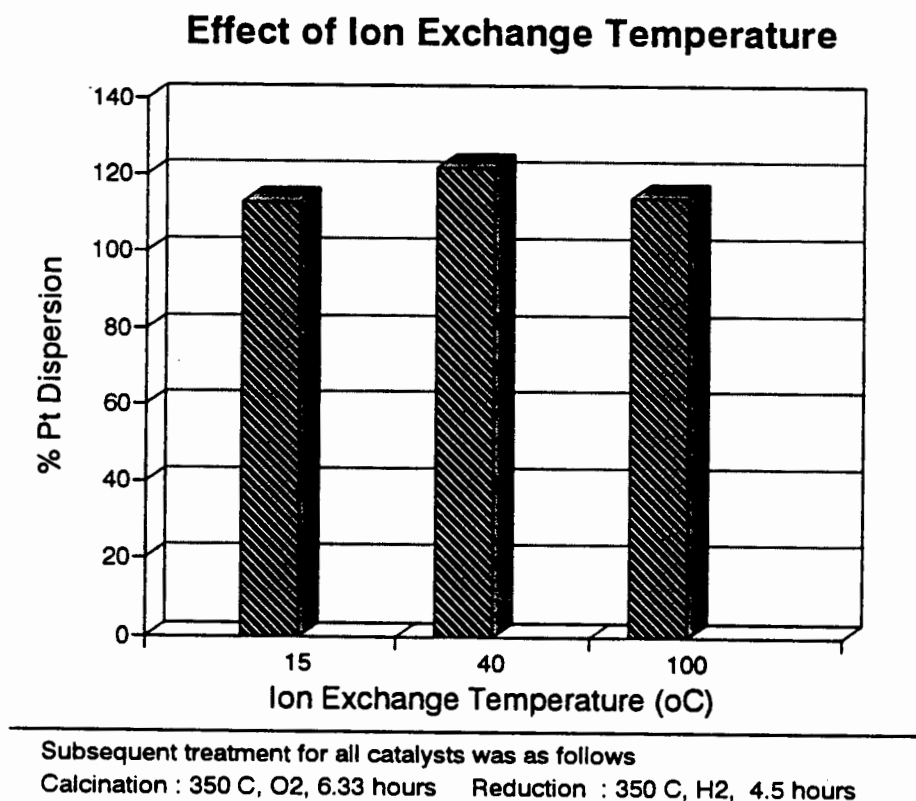


Figure 3.25 showing the effect of ion exchange temperature on dispersion

### 3.5.1.3 Effect of ion exchange time on dispersion.

In addition to ion exchanging zeolite KL with 1.55 wt % platinum at 40 °C for 24 hours, two other ion exchange times were looked at. One sample was ion exchanged at 40 °C for 2 hours while the other was ion exchanged in three cycles of 2 hours each at 40 °C. The final platinum loaded onto the zeolite was 1.55 wt % in each case. These samples were then calcined in oxygen while increasing the temperature from 25 °C to 350 °C at 108.3 °C/ 10 minutes with subsequent holding of the temperature at 350 °C for 1.5 hours. They were then reduced in hydrogen while increasing the temperature at 108.3 °C/ 10 minutes and holding the temperature at this value for 1.5 hours. The metal dispersion results obtained are presented in table 3.5.

Ion Exchange Time at 40°C	Vol. CO Chemisorbed (cc/g STP)	Metallic Surface Area (m <sup>2</sup> /g catalyst)	% Dispersion
24 hr	1.982	4.269	111
2 hr	2.022	4.389	114
3 * 2 hr cycles	1.955	4.204	111

Table 3.5 showing the effect of ion exchange time on dispersion

### 3.5.1.3 Chemisorption results of Factorial Design for calcination

The results of the factorial design for calcination are presented in table 3.6. The calcination conditions for the catalysts are presented in the first column. All the catalysts were reduced in hydrogen while increasing the temperature from 25 °C to 350 °C at a rate of 21.6 °C/ 10 minutes and subsequently holding the temperature at 350 °C for 4.5 hours.

Sample Calcination	Vol. CO Chemisorbed (cc/g STP)	Metallic Surface Area (m <sup>2</sup> /g catalyst)	% Dispersion
N <sub>2</sub> , 350 °C, 2 hr <sup>a</sup>	1.478	3.091	81
O <sub>2</sub> , 350 °C, 2 hr <sup>a</sup>	1.985	4.267	111
N <sub>2</sub> , 600 °C, 2 hr <sup>a</sup>	0.783	1.683	44
O <sub>2</sub> , 600 °C, 2 hr <sup>a</sup>	1.353	2.908	76
N <sub>2</sub> , 350 °C, 11 hr <sup>b</sup>	0.991	2.130	56
O <sub>2</sub> , 350 °C, 11 hr <sup>b</sup>	1.965	4.225	111
N <sub>2</sub> , 600 °C, 11 hr <sup>b</sup>	0.902	1.940	51
O <sub>2</sub> , 600 °C, 11 hr <sup>b</sup>	0.973	2.091	55

a : The temperature was increased from 25 °C to the final value in 1 hour and then held at the final value for another hour.

b : The temperature was increased from 25 °C to the final value in 4.33 hours and then held at the final value for 6.66 hours.

Table 3.6 showing the chemisorption results of Factorial Design for calcination of 1.55% Pt/KL

A summary of the results presented in table 3.6 are shown in table 3.7

Calcination Medium : O <sub>2</sub>			Calcination Medium : N <sub>2</sub>		
	350°C	600°C		350°C	600°C
2 hr	<b><i>111</i></b>	<b><i>76</i></b>	2 hr	<b><i>81</i></b>	<b><i>44</i></b>
11 hr	<b><i>111</i></b>	<b><i>55</i></b>	11 hr	<b><i>56</i></b>	<b><i>51</i></b>

**Table 3.7** showing a summary of the chemisorption results for Factorial Design for calcination (the dispersion values are in bold italics).

#### 3.5.1.4 Additional studies of the effect of calcination time in oxygen on dispersion.

Three samples of 1.55 wt % Pt/KL were calcined respectively in oxygen as follows i.) increase the temperature at 54.2 °C/10 minutes from 25 °C to 350 °C and hold at 350 °C for 1 hour (total time of 2 hours), ii.) increase the temperature at 12.5 °C/10 minutes from 25 °C to 350 °C and hold at 350 °C for 2.17 hours (total time of 6.5 hours), iii) increase the temperature at 12.5 °C/10 minutes from 25 °C to 350 °C and hold at 350 °C for 6.33 hours (total time of 11 hours). The samples were then reduced in hydrogen while increasing the temperature from 25 °C to 350 °C at a rate of 21.6 °C/ 10 minutes and holding the temperature at 350 °C for 4.5 hours. The chemisorption results obtained for these samples are shown in figure 3.26

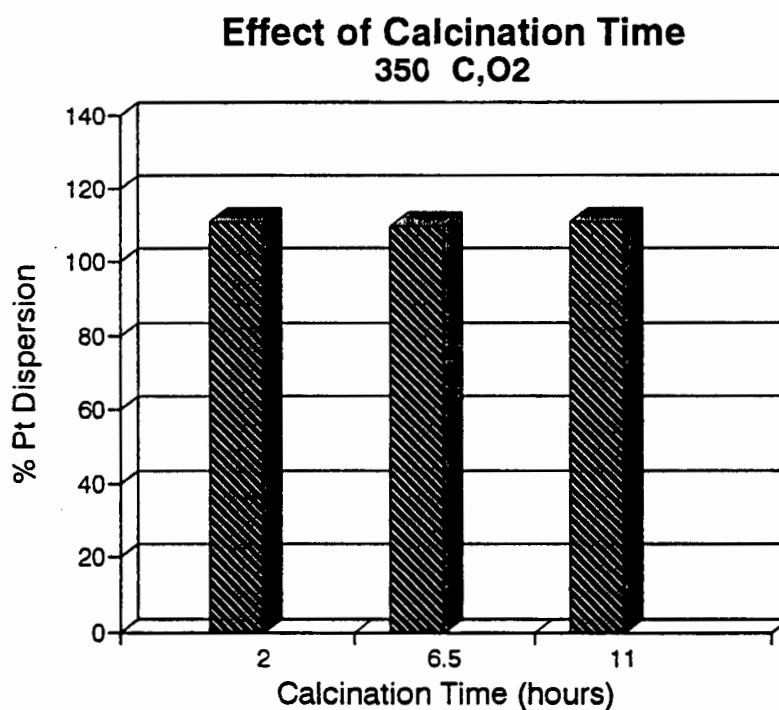


Figure 3.26 showing the effect of calcination time on dispersion

### 3.5.1.5 Effect of rate of temperature increase from 25 °C to 350 °C during calcination.

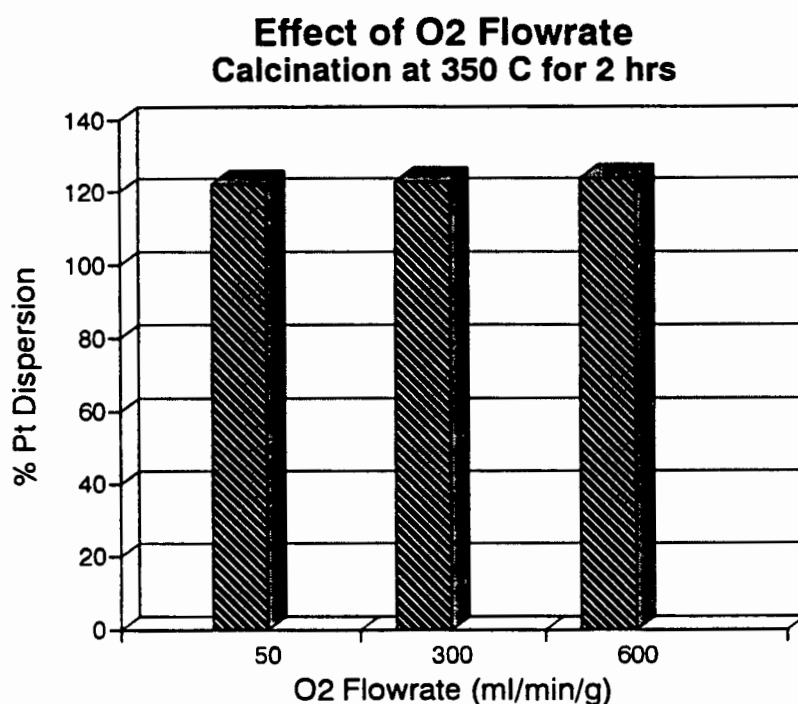
Four samples of 1.55 wt % Pt/KL were calcined in oxygen at 350 °C while ramping the temperature from 25 °C to 350 °C at 5 °C/10 minutes, 12.5 °C/ 10 minutes, 54.2 °C /10 minutes and 108.3 °C/ 10 minutes. After reaching 350 °C, the temperature was maintained at this value for 1.5 hours. After cooling the samples in nitrogen they were then reduced in hydrogen while increasing the temperature from 25 °C to 350 °C at a rate of 21.6 °C/ 10 minutes and holding the temperature at 350 °C for 4.5 hours. The chemisorption results obtained for these samples are presented in table 3.8.

Rate of Temperature Increase (°C/10 min)	Vol. CO Chemisorbed (cc/g STP)	Metallic Surface Area (m <sup>2</sup> /g catalyst)	% Dispersion
0.5	2.020	4.343	114
12.5	1.965	4.225	111
54.2	1.985	4.267	111
108.3	2.053	4.413	116

Table 3.8 showing the effect of rate of temperature increase during calcination on dispersion

### 3.5.1.6 Effect of oxygen flowrate during calcination on dispersion.

Three samples of 1.55 wt % Pt/KL were calcined in oxygen while increasing the temperature from 25 °C to 350 °C at a rate of 54.2 °C/10 minutes. The samples were calcined in oxygen flowrates of 50 ml/minute/g catalyst , 300 ml/minute/g catalyst and 600 ml/minute/g catalyst respectively. They were subsequently reduced in hydrogen while increasing the temperature at a rate of 21.6 °C/ 10 minutes from 25 °C to 350 °C. The temperature was maintained at 350 °C for another 4.5 hours. The metal dispersion results obtained for these samples are shown in figure 3.27.



After calcination, samples were reduced in H<sub>2</sub> while increasing the temperature from 25 C to 350 C at 21.6 C/10 min. The temperature was then maintained at 350 C for 4.5 hours

Figure 3.27 showing the effect of oxygen flowrate during calcination on dispersion

### 3.5.1.7 Effect of not reducing the catalyst after calcination in oxygen.

Before investigating the effect of reduction on platinum dispersion, it was important to determine whether the unreduced sample would chemisorb carbon monoxide. Two samples were calcined in oxygen while increasing the temperature from 25 °C to 350 °C at 12.5 °C/ 10 minutes. The platinum dispersion of one sample was immediately determined using

chemisorption while the other sample was reduced in hydrogen while increasing the temperature from 25 °C to 350 °C at 108.3 °C/ 10 minutes and maintaining the temperature at 350 °C for 1.5 hours before performing the chemisorption analysis. The results are shown in table 3.9.

Sample Reduction	Vol. CO Chemisorbed (cc/g STP)	Metallic Surface Area (m <sup>2</sup> /g catalyst)	% Dispersion
No reduction	2.217	4.765	125
H <sub>2</sub> , 350 °C. 2 hr	1.982	4.261	111

Table 3.9 showing the effect of not reducing the 1.55% Pt/KL sample after calcination in oxygen.

### 3.5.1.8 Chemisorption results of Factorial Design for reduction

The results of the factorial design for reduction are presented in table 3.10. All the samples contained 1.55 wt % platinum and were calcined in oxygen while increasing the temperature from 25 °C to 350 °C at 108.3 °C/10 minutes and subsequently holding the temperature at 350 °C for 1.5 hours. The reduction conditions for the catalysts are presented in the first column.

Sample Reduction	Vol. CO Chemisorbed (cc/g STP)	Metallic Surface Area (m <sup>2</sup> /g catalyst)	% Dispersion
H <sub>2</sub> , 150 °C, 2 hr <sup>a</sup>	1.952	4.197	110
CO, 150 °C, 2 hr <sup>a</sup>	0.309	0.665	17
H <sub>2</sub> , 350 °C, 2 hr <sup>a</sup>	2.064	4.436	116
CO, 350 °C, 2 hr <sup>a</sup>	0.205	0.441	12
H <sub>2</sub> , 150 °C, 7 hr <sup>b</sup>	1.899	4.084	107
CO, 150 °C, 7 hr <sup>b</sup>	0.278	0.598	15
H <sub>2</sub> , 350 °C, 7 hr <sup>b</sup>	1.985	4.268	111
CO, 350 °C, 7 hr <sup>b</sup>	0.269	0.579	15

a : The temperature was increased from 25 °C to the final value in 1 hour and then held at the final value for another hour.

b : The temperature was increased from 25 °C to the final value in 2.5 hours and then held at the final value for 4.5 hours.

Table 3.10 showing the chemisorption results of Factorial Design for reduction

Another sample which had been calcined under similar conditions to the samples used in the factorial design for reduction was reduced in hydrogen while ramping the temperature to 600 °C in 2.5 hours and subsequently keeping the temperature at 600 °C for 4.5 hours. The dispersion for this sample was found to be 56 %.

The samples which were reduced in carbon monoxide looked very dark grey compared to the samples which had been reduced in hydrogen. A summary of the results presented in table 3.10 are shown in table 3.11

Reduction Medium : H <sub>2</sub>				Reduction Medium : CO		
	150°C	350°C	600°C		150°C	350°C
2 hr	<b>110</b>	<b>116</b>	-	2 hr	<b>17</b>	<b>12</b>
7 hr	<b>107</b>	<b>111</b>	<b>56</b>	7 hr	<b>15</b>	<b>15</b>

**Table 3.11** showing a summary of the chemisorption results for Factorial Design for reduction (the dispersion values are in bold italics).

### 3.5.1.9 Effect of rate of temperature increase from 25 °C to 350 °C during reduction.

Two samples of 1.55 wt % Pt/KL were calcined in oxygen while ramping the temperature from 25 °C to 350 °C at a rate of 108.3 °C/ 10 minutes and subsequently holding the temperature at 350 °C for 1.5 hours. The samples were then reduced in hydrogen while increasing the temperature from 25 °C to 350 °C at 21.6 °C/ 10 minutes and at 108.3 °C/ 10 minutes respectively. The dispersion of the platinum was then determined using chemisorption.

Rate of Temperature Increase (°C/10 min)	Vol. CO Chemisorbed (cc/g STP)	Metallic Surface Area (m <sup>2</sup> /g catalyst)	% Dispersion
21.6	2.053	4.413	116
108.3	1.982	4.261	111

**Table 3.12** showing the effect on dispersion of rate of temperature increase during reduction in hydrogen

### 3.5.1.10 Comparison between different platinum loading methods employed.

#### Calcination at 350 °C in oxygen

1.55 % Pt/KL samples prepared by liquid ion exchange, and incipient wetness impregnation were calcined in oxygen while increasing the temperature from 25 °C to 350 °C at 108.3 °C/ 10 minutes with subsequent holding of the temperature at 350 °C for 1.5 hours. They were then reduced in hydrogen while increasing the temperature at 108.3 °C/ 10 minutes and holding the temperature at this value for 1.5 hours. Another sample was ion exchanged via solid state ion exchange using  $\text{Pt}(\text{NH}_3)_4\text{Cl}_2$  salt to load the platinum onto the zeolite. The solid state ion exchange was performed in oxygen while increasing the temperature from 25 °C to 350 °C at 108.3 °C/ 10 minutes with subsequent holding of the temperature at 350 °C for 6.5 hours. It was then reduced in hydrogen while increasing the temperature from 25 °C to 350 °C at 108.3 °C/10 minutes maintaining the temperature at this value for 6.5 hours. In solid state ion exchange 48.4 % of the added platinum was loaded onto the zeolite to give 0.75 wt % Pt/KL. This was determined using atomic absorption spectroscopy. The results are shown in tables 3.13.



Loading Method	Wt % Pt Loaded	Vol. CO Chemisorbed (cc/g STP)	Metallic Surface Area (m <sup>2</sup> /g catalyst)	% Dispersion
Liquid ion exchange	1.55	2.053	4.413	116
Impregnation	1.55	1.820	3.913	102
Solid state ion exchange	0.75	1.166	2.506	134

**Table 3.13** showing the comparison between different platinum loading methods for samples calcined in oxygen at 350 °C.

**Calcination at 600 °C in nitrogen**

Two 1.55% Pt/KL samples prepared by liquid ion exchange, and incipient wetness impregnation were calcined in nitrogen while increasing the temperature from 25 °C to 600 °C at 127.8 °C/ 10 minutes with subsequent holding of the temperature at 600 °C for 1.5 hours. They were then reduced in hydrogen while increasing the temperature at 108.3 °C/ 10 minutes to 350 °C and holding the temperature at this value for 1.5 hours. Platinum was loaded onto the third sample via solid state ion exchange in nitrogen while increasing the temperature at 127.8 °C/ 10 minutes from 25 °C to 600 °C and holding the temperature at 600 °C for 6.5 hours. It was subsequently reduced in hydrogen while increasing the temperature from 25 °C to 350 °C at 21.6 °C/ 10 minutes and maintaining the temperature at this value for 1.5 hours. As for the solid state ion exchange at 350 °C, the platinum loaded onto the zeolite gave 0.75 wt % Pt/KL when analysed using atomic absorption spectroscopy. The metal dispersion results are presented in table 3.14.

Loading Method	Wt % Pt Loaded	Vol. CO Chemisorbed (cc/g STP)	Metallic Surface Area (m <sup>2</sup> /g catalyst)	% Dispersion
Liquid ion exchange	1.55	0.783	1.683	44
Impregnation	1.55	0.538	1.158	33
Solid state ion exchange	0.75	0.266	0.573	31

**Table 3.14** showing the comparison between different platinum loading methods for samples calcined in nitrogen at 600 °C.

### 3.5.1.11 Effect of different calcination media on platinum dispersion.

Table 3.15 gives the dispersion obtained for three 1.55 % Pt/KL samples that were calcined in oxygen, nitrogen and hydrogen. All the samples were calcined in their respective medium while increasing the temperature from 25 °C to 350 °C at 108.3 °C/ 10 minutes and holding the temperature at 350 °C for 1.5 hours. The samples calcined in oxygen and nitrogen were subsequently reduced in hydrogen while increasing the temperature at 21.6 °C /10 minutes and maintaining the temperature at 350 °C for 4.5 hours.

Calcination Medium	Vol. CO Chemisorbed (cc/g STP)	Metallic Surface Area (m <sup>2</sup> /g catalyst)	% Dispersion
oxygen	2.053	4.413	116
nitrogen	1.478	3.091	81
hydrogen	1.371	2.946	78

**Table 3.15** showing the effect of different calcination media on dispersion.

### 3.5.1.12 Chemisorption results on 1.43 wt % Pt/HY.

The platinum dispersion on 1.43 % Pt/HY samples was determined in order to compare with the dispersion values obtained for 1.55 wt % Pt/KL. One sample was calcined in oxygen while increasing the temperature at 12.5 °C/10 minutes from 25 °C to 350 °C and maintaining the temperature at 350°C for 6.33 hours. A second sample was calcined in nitrogen while increasing the temperature from 25 °C to 600 °C at 22.1 °C/ 10 minutes and then maintaining the temperature at this value for 6.33 hours. Both samples were then reduced in hydrogen while increasing the temperature at 21.6 °C/ 10 minutes from 25 °C to 350 °C with subsequent holding of the temperature at 350 °C for 4.5 hours. Table 3.16 shows the platinum dispersion of these samples as well as that of 1.55 Pt/KL samples treated under similar conditions.

Sample	Calcination Temp. (°C)	Vol. CO Chemisorbed (cc/g STP)	Metallic Surface Area (m <sup>2</sup> /g catalyst)	% Dispersion
1.43 % Pt/HY	350	1.334	2.867	81
1.55 % Pt/KL	350	1.965	4.225	111
1.43 % Pt/HY	600	0.704	1.541	43
1.55 % Pt/KL	600	0.973	2.091	55

Table 3.16 showing the comparison between dispersion of 1.43 % Pt/HY and 1.55 % Pt/KL samples treated at similar conditions.

## 3.5.2 Hydrogen Chemisorption

### 3.5.2.1 Hydrogen chemisorption test cycles on 0.5 % Pt/Al<sub>2</sub>O<sub>3</sub>

Hydrogen chemisorption was carried out on the standard sample of 0.5 % Pt/Al<sub>2</sub>O<sub>3</sub> provided by suppliers of the chemisorption equipment. A ratio of 1 hydrogen atom per platinum atom

was used to calculate the platinum dispersion. Figure 3.28 shows the effect on the hydrogen uptake of varying the evacuation time while reducing the temperature from 350 °C to 35 °C. According to the suppliers of the chemisorption equipment used, measurement of the platinum dispersion on this sample using carbon monoxide should yield platinum dispersion of 33 %  $\pm$  5 %.

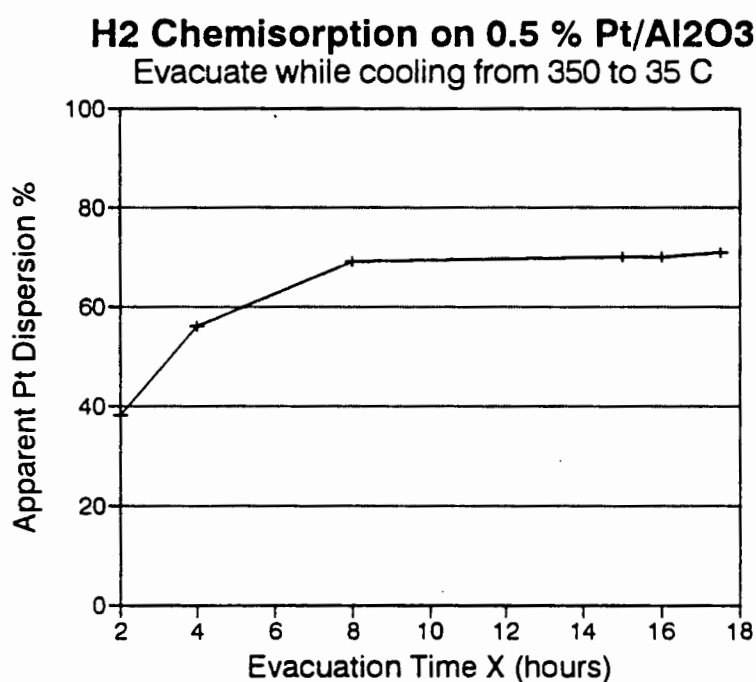


**Figure 3.28** showing the apparent dispersion vs evacuation time for hydrogen chemisorption on 0.5 % Pt/Al<sub>2</sub>O<sub>3</sub>.

### 3.5.2.2 Hydrogen chemisorption test cycles on 0.78 % Pt/KL

A number of hydrogen chemisorption test cycles were performed on 0.78 % Pt/KL. This sample had been calcined in nitrogen at 350 °C for 2 hours. During the chemisorption cycles, the evacuation time at 350 °C was varied. In order to test whether a leak existed in the chemisorption equipment (see section 2.2.3.2), the vacuum at 350 °C was replaced by 106.7 kPa nitrogen flow.

Another set of hydrogen chemisorption test cycles were performed on the same sample. In this set of cycles, the evacuation time was varied while reducing the temperature from 350 °C to 35 °C. For comparison purposes, carbon monoxide chemisorption cycles were also performed on the 0.78 % Pt/KL. The evacuation time was also varied while reducing the temperature from 350 °C to 35 °C. The results are presented in figures 3.29, 3.30 and 3.31.

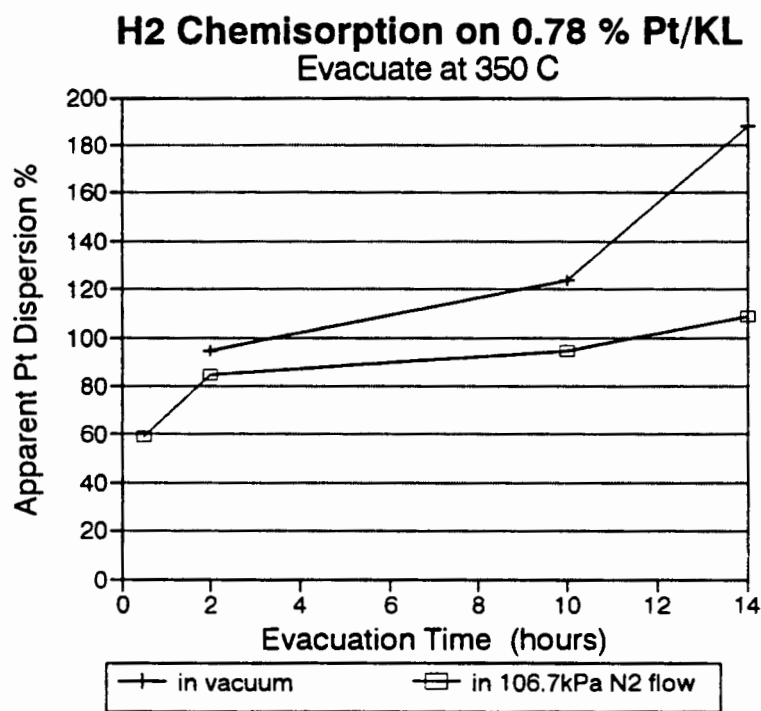


**Figure 3.29** showing the apparent dispersion vs evacuation time for hydrogen chemisorption on 0.78 % Pt/KL. Evacuation time at 350 °C was varied.

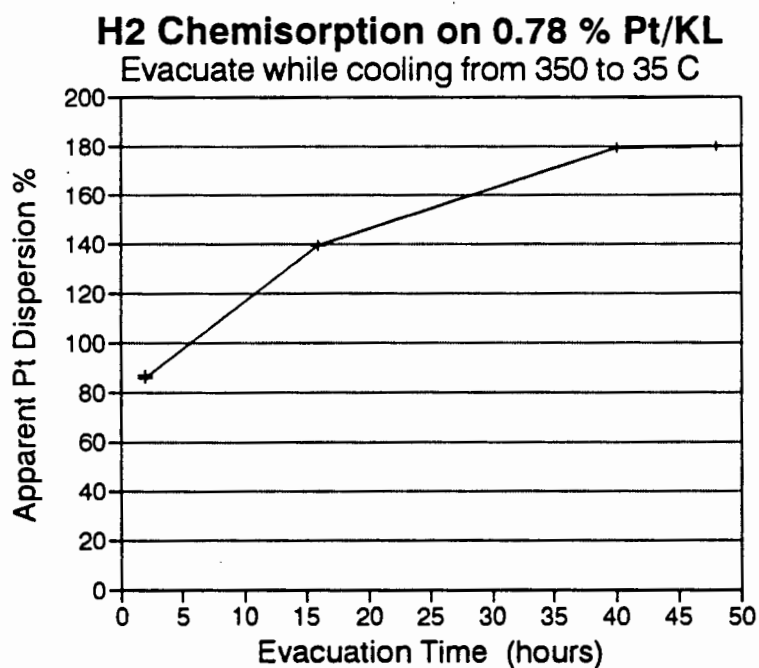


**Figure 3.30** showing the apparent dispersion vs evacuation time for hydrogen chemisorption on 0.78 % Pt/KL. Evacuation time was varied while cooling from 350 °C to 35 °C.

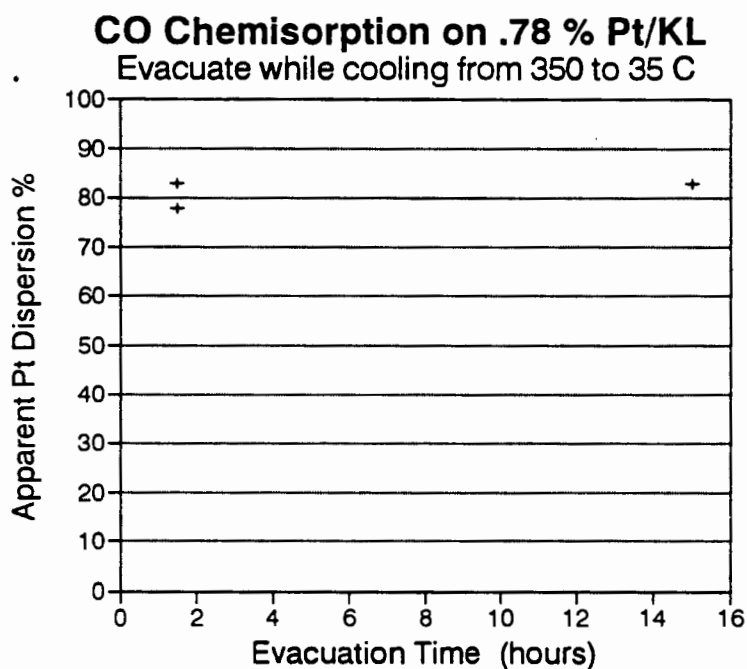


**Figure 3.31** showing the apparent dispersion vs evacuation time for carbon monoxide chemisorption on 0.78 % Pt/KL. Evacuation time was varied while cooling from 350 °C to 35 °C.

### 3.6. Transmission Electron Microscopy (TEM)

In order to verify the carbon monoxide chemisorption results, platinum particle sizes of selected samples were analysed using TEM. Samples which had shown high platinum dispersion for chemisorption had very few visible platinum clusters which had to be looked for carefully. However samples that had shown low platinum dispersion had many large platinum clusters which were easily identified. The magnification on the TEM plates 3.1 to 3.6 is 200 000 times.

Plate 3.1 showing the TEM image of untreated zeolite KL

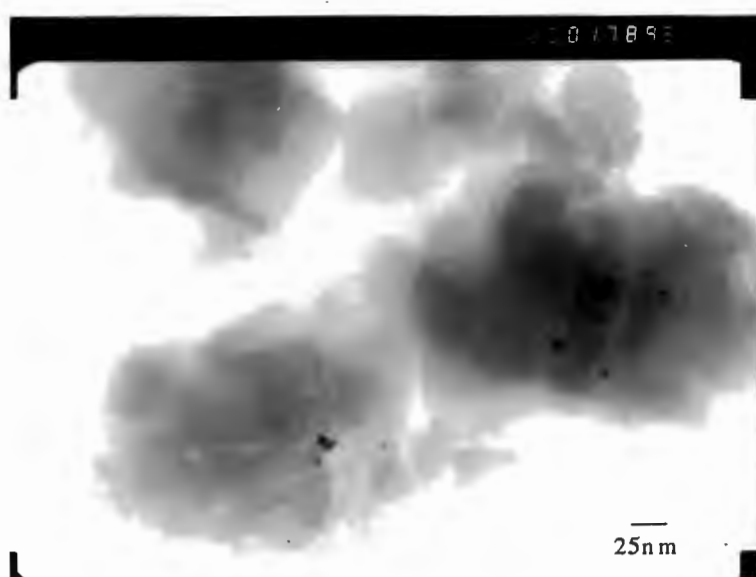
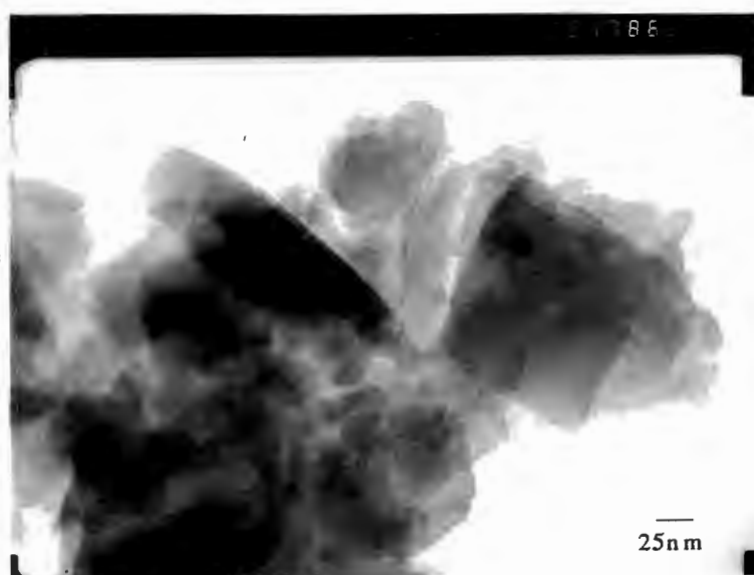
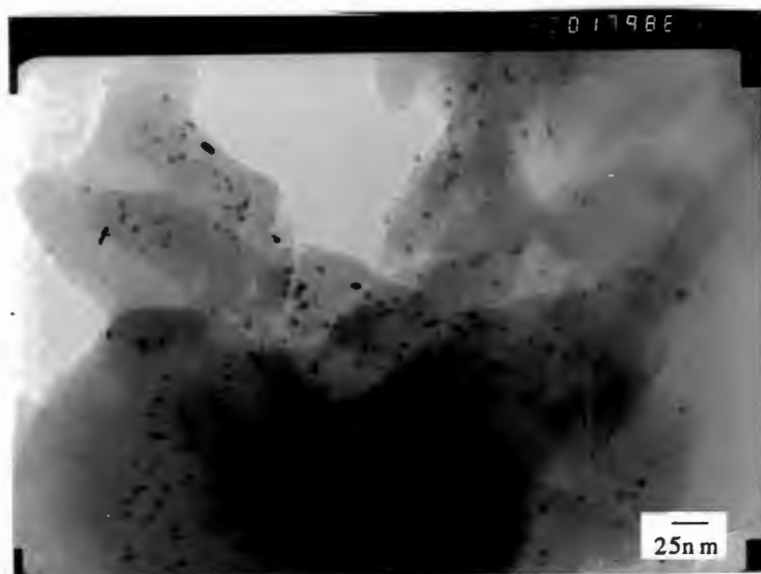


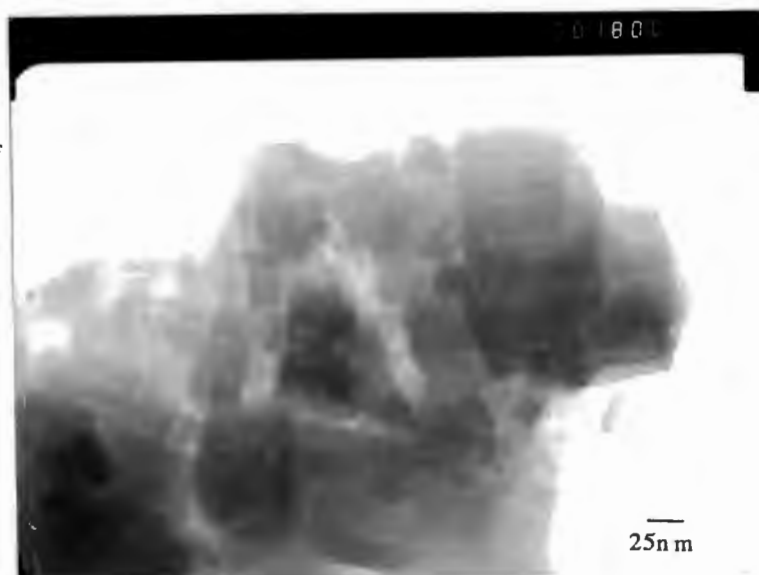
Plate 3.2 showing the TEM image of 1.55% Pt/KL calcined in O<sub>2</sub> at 350 °C for 6.33 hours and reduced in H<sub>2</sub> at 350 °C for 4.5 hours (Based on CO chemisorption platinum dispersion was found to be 111 %)

**Plate 3.3** showing the TEM image of 1.55% Pt/KL calcined in  $N_2$ , at 600 °C for 6.33 hours and reduced in  $H_2$  at 350 °C for 4.5 hours (Based on CO chemisorption platinum dispersion was found to be 44 %)



**Plate 3.4** showing the TEM image of 1.55% Pt/KL calcined in  $O_2$ , at 350 °C for 1.5 hours and reduced in CO at 350 °C for 1.5 hours (Based on CO chemisorption platinum dispersion was found to be 12 %)

**Plate 3.5** showing the TEM image of 0.75% Pt/KL solid state ion exchanged in  $O_2$ , at 350 °C for 6.5 hours and reduced in  $H_2$  at 350 °C for 4.5 hours (Based on CO chemisorption platinum dispersion was found to be 134%)





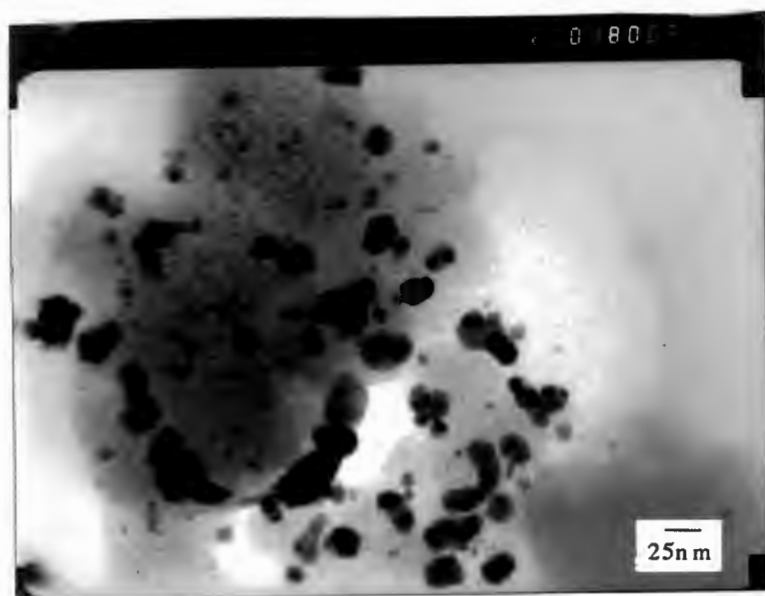


Plate 3.6 showing the TEM image of 0.75 % Pt/KL solid state ion exchanged in  $N_2$ , at 600 °C for 6.5 hours and reduced in  $H_2$  at 350 °C for 4.5 hours (Based on CO chemisorption platinum dispersion was found to be 31%)

### 3.7 Energy Dispersive X-Ray (EDX) Analysis

EDX was used as a means to confirm that the large particles observed by TEM in samples with low platinum dispersion were indeed platinum and not some contamination. It was also necessary to show that although the platinum particles on samples with high dispersion could not be detected by TEM, there was platinum present on these samples.

The 1.55% Pt/KL sample with the platinum dispersion of 44 % had areas with visible platinum clusters when analysed using TEM. These areas were then analysed on EDX. The results obtained are shown in table 3.17. The sample with 111 % platinum dispersion had areas which did not have visible platinum clusters. When these areas were analysed on the EDX facility they gave the results shown in table 3.18. This sample had very few visible platinum clusters. For detailed explanation on the spectra acquisition see section 2.2.7. As expected, the silicon to aluminium ratio for both samples was found to be close to 3. This correlated well with the results from the electron beam micro-analysis.

Element	Spectrum 1 (Atomic %)	Spectrum 2 (Atomic %)	Spectrum 3 (Atomic %)	Ave. value (Atomic %)
Al	21.12	19.01	21.03	20.39
Si	60.34	57.99	54.44	57.59
K	10.27	7.55	13.52	10.45
Pt	8.29	13.65	11.02	10.99

**Table 3.17** showing the results of EDX analysis on areas with visible platinum clusters for a sample with a platinum dispersion of 44%.

Element	Spectrum 1 (Atomic %)	Spectrum 2 (Atomic %)	Spectrum 3 (Atomic %)	Ave. value (Atomic %)
Al	21.13	20.19	23.17	21.53
Si	66.51	66.40	66.13	64.15
K	11.59	12.83	10.00	12.65
Pt	0.77	0.58	0.70	0.68

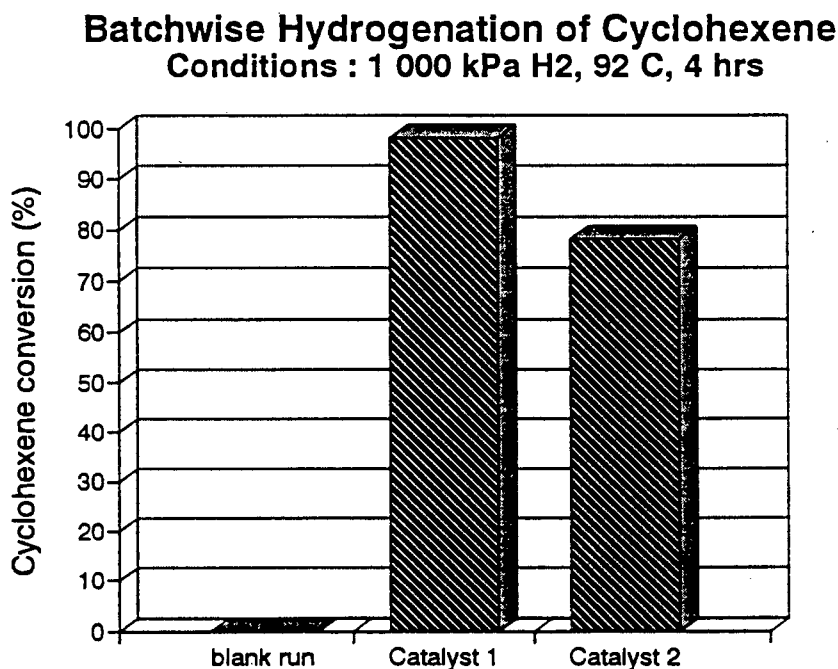
**Table 3.18** showing the results of EDX analysis on areas without visible platinum clusters for a sample with a platinum dispersion of 111%.

## 3.8 Chemical Reactions

### 3.8.1 Hydrogenation Results

#### 3.8.1.1 Hydrogenation of cyclohexene

Figure 3.40 shows the results of batch-wise hydrogenation of cyclohexene to cyclohexane over two catalysts. The reactions took place in an autoclave. In each case studied, the selectivity to cyclohexane was 100 %. The mass balance was within an error margin of 2 %. It is evident from the results that regardless of whether the platinum particles on both of the 1.55 % Pt/KL are in the pores or on the external surface of the zeolite, they are accessible to the cyclohexene.



Blank run : no catalyst in autoclave

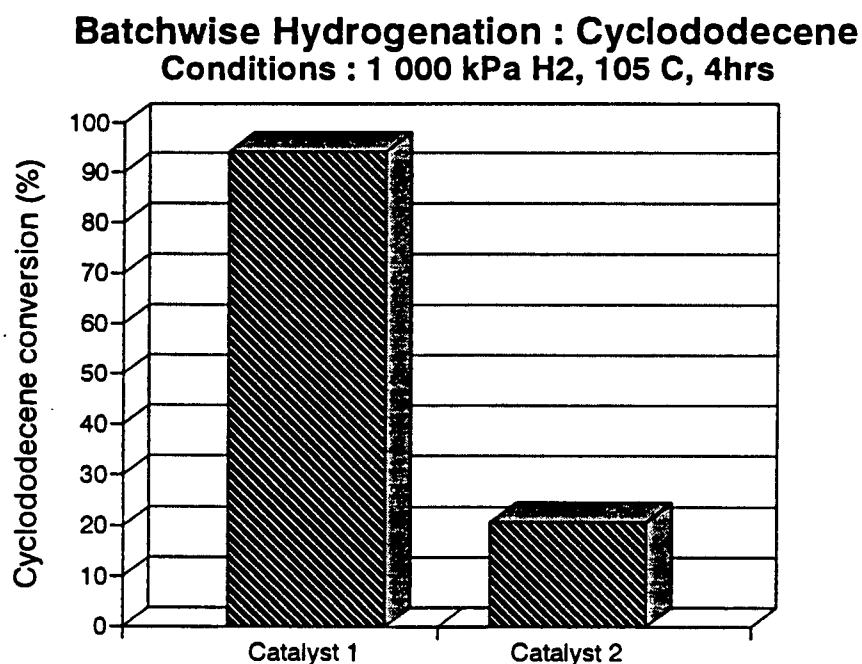
Catalyst 1 : 1.55% Pt/KL calcined in O<sub>2</sub> at 350 C for 6.33 hours. Reduced in H<sub>2</sub> at 350 C for 4.5 hours  
(platinum dispersion : 111 %)

Catalyst 2 : 1.55% Pt/KL calcined in N<sub>2</sub> at 600 C for 6.33 hours. Reduced in H<sub>2</sub> at 350 C for 4.5 hours.  
(platinum dispersion : 44 %)

Figure 3.40 showing the results of batchwise hydrogenation of cyclohexene to cyclohexane

### 3.8.1.2 Hydrogenation of cyclododecene

During the hydrogenation of cyclododecene to cyclododecane, the selectivity to cyclododecane was 100%. The mass balance was within an error margin of 3%. Figure 3.41 shows the results.



Catalyst 1 : 1.55% Pt/KL calcined in O<sub>2</sub> at 350 C for 6.33 hours. Reduced in H<sub>2</sub> at 350 C for 4.5 hours (platinum dispersion : 111%)

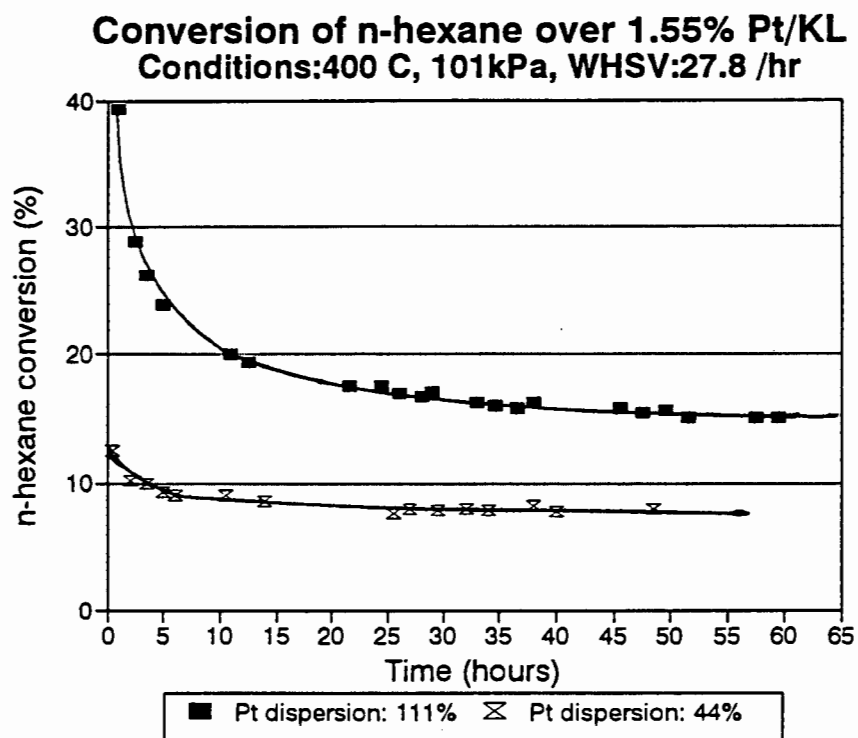
Catalyst 2 : 1.55% Pt/KL calcined in N<sub>2</sub> at 600 C for 6.33 hours. Reduced in H<sub>2</sub> at 350 C for 4.5 hours (platinum dispersion : 44%)

Figure 3.41 showing the results of batchwise hydrogenation of cyclododecene to cyclododecane

### 3.8.1 Aromatisation Of n-hexane Results

Figure 3.42 compares the activity of the two catalysts employed in the conversion of n-hexane. The reaction was carried out at 400 °C in hydrogen flow and a hexane weight hourly space velocity (WHSV) of 27.8 hr<sup>-1</sup>. The hydrogen/n-hexane mole ratio was 3.0. Table 3.19 shows the selectivities of the different products obtained at the specified conversions. The selectivities are based on the mass fractions of the product stream. The conversion over the

two catalysts were not the same at the conditions studied, therefore the selectivities obtained cannot be compared directly.



**Figure 3.42** comparing the activities of the catalysts used in the conversion of n-hexane.

Conversion of n-hexane over 1.55 % Pt/KL catalysts Conditions : 400°C, 101 kPa, WHSV : 27.8 hr <sup>-1</sup>		
Product	Catalyst Pt dispersion : 111 % Conversion : 15.5 %	Catalyst Pt dispersion : 44 % Conversion : 7.6 %
	% Selectivity	% Selectivity
C1	6.7	3.0
C2	5.3	3.8
C3	9.0	3.3
nC4	7.2	4.0
nC5	4.4	0.0
2m-C5	22.3	18.9
3m-C5	18.4	17.7
2m-1-C5=	0.0	2.7
t-2-C6=	0.0	5.2
2m-2-C5=	2.7	12.2
c-2-C6=	1.4	5.8
MCP *	11.5	15.8
B **	11.0	7.5

\* MCP stands for methyl-cyclopentane

\*\* B stands for benzene

**Table 3.19** showing the product selectivities for the conversion of n-hexane over 1.55 % Pt/KL catalysts.

## **CHAPTER 4**

## 4 DISCUSSION

### 4.1 XRD And Elemental Analysis

Comparing the simulated XRD pattern for zeolite KL ( $\text{Na}_3\text{K}_6\text{Si}_{27}\text{O}_{72}\text{H}_2\text{O}$ ) (figure 3.1) and that for the zeolite KL used in this study (figure 3.2) showed that these zeolites have the same crystal structure. The slight deviation from the simulated pattern, such as the absence of the peak at  $2\theta = 9.5$  and the reduced peak height at  $2\theta = 6$  and  $2\theta = 12$  could be due to the absence of sodium in the assayed zeolite KL.

The atomic absorption spectroscopy results gave the platinum content on the zeolite KL and HY as 1.55 wt % and 1.43 wt % respectively. The electron beam micro-analysis results (section 3.2.2) yielded the expected Si/Al ratios of the zeolite KL of 3 which was the same as that reported in literature [Breck, 1974]. Results obtained using Energy Dispersive Analysis (EDX) confirmed the silicon/aluminium ratio obtained using electron beam analysis (section 3.7).

### 4.2. Ion Exchange

#### 4.2.1. Ion Exchange Temperature

Figures 3.3. and 3.4. indicate that for the level of platinum loading studied, the amount of platinum loaded onto the zeolite was independent of the ion exchange temperature. Close to 99% of the platinum in solution was ion exchanged onto the zeolite within 40 minutes. This would suggest that at temperatures as low as 15 °C, the rate of the ion exchange reaction is fast and that the activation energy for this process is low.

Figure 3.25. showing percentage platinum dispersion as a function of ion exchange temperature indicated that the ion exchange temperature would not play a significant role in the dispersion of the platinum in zeolite KL. Although the dispersion of the sample ion exchanged at 40 °C appeared to be slightly higher than that of the samples ion exchanged at



15 °C and 100 °C, this difference was within the allowable error margin of 5% for chemisorption. [Micromeritics, 1993]

#### 4.2.2. Ion Exchange Solution Concentration

If all the potassium ions on zeolite KL were ion exchanged out by the platinum ions, then the total theoretical ion exchange capacity of platinum onto the zeolite KL would be 26 wt %. The solutions used to ion exchange 1.55 wt % platinum onto the zeolite were therefore dilute compared to the ones needed to ion exchange all the potassium out of the zeolite in one cycle. Loading the platinum onto the zeolite using ion exchange cycles with even more dilute solutions did not affect the dispersion of the platinum as shown in table 3.5.

#### 4.2.3. Ion Exchange Time

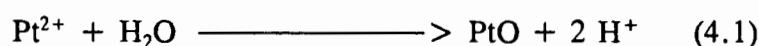
Based on the CO chemisorption results presented in table 3.5, it can be inferred that the ion exchange periods studied at 40°C do not affect the dispersion of the platinum. According to figures 3.3, 3.4 and 3.5 the ion exchange of all the platinum in solution onto the zeolite occurred in less than 40 minutes. This indicated that ion exchanging for long periods as found in literature [Hong *et al*, 1991] and [Gallezot *et al*, 1975] is not necessary for low platinum loadings.

### 4.3. Calcination

#### 4.3.1. Calcination Medium

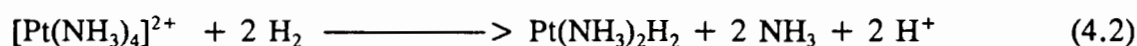
It was found that the calcination medium greatly affected the platinum dispersion on zeolite KL. According to table 3.15, calcination in oxygen gave the highest dispersion, while calcination in nitrogen and hydrogen gave lower but similar platinum dispersion values.

In an oxidising atmosphere, the decomposing ammonia ligands of the  $\text{Pt}(\text{NH}_3)_4^{2+}$  complex would react with the oxygen to give water and nitrogen thus leaving  $\text{Pt}^{2+}$  ions attached to the zeolite wall. [Exner *et al*, 1982] The water would then react with  $\text{Pt}^{2+}$  ions to yield PtO and protons as shown in equation 4.1.[Park *et al*, 1986]



In this scheme very few of the ammonia ligands co-ordinated to the platinum would be able to reduce the  $\text{Pt}^{2+}$  by donating electrons to the platinum ions. However, some degree of reduction of  $\text{Pt}^{2+}$  by the ammonia ligands (auto-reduction) can be expected for calcination in oxygen. [Sachtler, 1992] and [Ostgard, 1992]

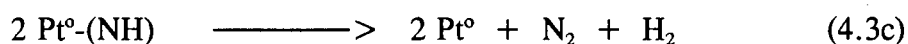
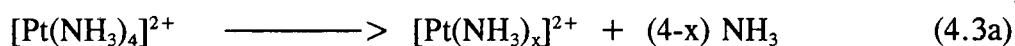
Calcination in hydrogen is likely to cause sintering due to the formation of hydrides. Hydride formation would occur according to the equation:



The hydride  $\text{Pt}(\text{NH}_3)_2\text{H}_2$  is very labile and can lead to platinum sintering. [Alvarez *et al*, 1988] This sintering would account for the lowered platinum dispersion.

If calcination is done in an inert medium like nitrogen, then the ammonia ligands produced would not be decomposed to nitrogen and water as would be the case for calcination in oxygen. In an inert atmosphere, reduction of the platinum ions by the co-ordinated ammonia

ligands would occur to yield neutral platinum particles [Alvarez *et al*, 1986 ]. This process is shown below:



According to Sachtler [1992], auto-reduction would lead to the formation of large metal clusters. This could be one of the reasons why calcination in nitrogen resulted in catalysts with lower platinum dispersion compared to catalysts calcined in oxygen.

If the hydrogen produced in equation 4.3c comes into contact with either the ammonia complex  $[\text{Pt}(\text{NH}_3)_4]^{2+}$  or the partially decomposed complex  $[\text{Pt}(\text{NH}_3)_x]^{2+}$  then it could react to produce hydrides according to equation 4.2. These hydrides would subsequently lead to sintering of the platinum, again resulting in a lowered dispersion.

#### 4.3.2 Effect Of Oxygen Flowrate During Calcination

Figure 3.27 shows that varying the oxygen flowrate during calcination from 50 ml/minute/g catalyst to 600 ml/minute/g catalyst did not affect the platinum dispersion. Theoretically, a very high flowrate of oxygen should enhance the removal of the products of ammonia decomposition from the vicinity of the platinum ions in order to avoid "auto-reduction". However, Ostgard and co-workers found that for oxygen flowrates of 1 000 ml/minute/g some level of reduction of the platinum ions by the ammonia ligands occurred on Pt/KL [Ostgard *et al*, 1992]. From the TPD results it is evident that some acidity was produced during calcination in oxygen at a flowrate of 300 ml/minute/g catalyst (section 4.7). In oxygen, the ammonia ligands could decompose to yield nitrogen and water leaving  $\text{Pt}^{2+}$  ions. The water produced could then react with the  $\text{Pt}^{2+}$  ions resulting in the formation of Bronsted acidity according to equation 4.1.

Bronsted acidity could also have been formed as a result of the reduction of platinum ions by the ammonia ligands according to equation 4.3. This auto-reduction would also cause

sintering of the platinum metal. However in oxygen, the degree of sintering would be reduced [Sachtler, 1992]. Since the dispersion was independent of the flowrates studied (50ml/minute/g - 600 ml/minute/g), it could be inferred that at these flowrates, the extent of auto-reduction of the platinum ions by the ammonia ligands was the same.

If the rate of removal of the products of the decomposition of ammonia from the zeolite pores was diffusion controlled, then for a certain calcination medium, the flowrate in the gas phase would not affect the rate of removal of the ammonia ligands from the zeolite pores. The rate of removal of the ligands would depend on the difference in the concentration of the ammonia ligands between the pores of Pt/KL and the gas phase. At the flowrates studied, the concentration in the gas phase was effectively zero.

#### **4.3.3 Calcination Temperature**

It is important to calcine samples at temperatures at which the ammonia ligands would disintegrate. Calcination at temperatures less than 300 °C would lead to partial decomposition of the platinum complex (section 3.3.1). The partially decomposed platinum complex would then form hydrides during the subsequent hydrogen reduction process according to reaction 4.2.

Calcination at the lower temperature (350 °C) produced high platinum dispersion while calcination at the higher temperature (600 °C) produced low platinum dispersion (table 3.16). This was observed for platinum loaded on KL and HY supports. However for treatment at the same temperature, the dispersion in the Pt/KL samples was higher than for the Pt/HY samples.

In Pt/HY calcination at 350 °C could leave most of the platinum ions in the supercages where they would be readily reduced by hydrogen during the reduction step. Calcination at 600 °C could cause most of the platinum ions to migrate to the sodalite cages and hexagonal prisms where they would be stabilised by the high negative charge density in these sites. After reduction, the platinum particles in the sodalite cages and hexagonal prisms would exit to the supercages. If they encountered other platinum atoms in these supercages, they would

coalesce with them to form platinum particles whose size would be limited by the sizes of the supercages. If they do not encounter other platinum atoms in the supercage, they would then migrate to the external surface of the zeolite where they would then form large clusters (section 1.3.5.1). [Gallezot *et al*, 1975] Agglomeration of the platinum particles could also occur via the formation of  $(\text{PtO})_n$  particles during high temperature calcination in oxygen if water vapour was present [Park *et al*, 1986]. Reduction of the large  $(\text{PtO})_n$  particles would lead to sintering.

In zeolite KL calcination at a high temperature (600 °C) could also cause the platinum particles to migrate to the locked sites. These would be in the 6 and 8 membered ring openings of the zeolite. A similar observation was reported by Hughes *et al* for barium in zeolite KL when calcined at 600 °C [Hughes *et al*, 1986]. As in Pt/HY these particles could exit the locked sites after reduction and migrate to the 12 membered ring openings of the zeolite KL or to the external surface where they would form large platinum clusters.

At a high calcination temperature of 600 °C the decomposition of the ammonia complex would be very rapid providing a momentarily high ammonia concentration around the partially decomposed  $\text{Pt}(\text{NH}_3)_x^{2+}$  complex. This could lead to the formation of mobile hydrides which would then lead to the sintering of the platinum. This provides an additional explanation why the dispersion at 600 °C was lower than at 350 °C.

Sintering due to a thermal effect at 600 °C could provide a further explanation for the low platinum dispersion obtained for samples calcined at 600 °C. At 600 °C, the interaction between the platinum particles and the zeolite wall would be reduced due to an increase in thermal energy of the platinum particles. This could cause the platinum particles to easily agglomerate to form clusters resulting in a lower dispersion.

Zeolite HY and zeolite KL have different compositions, pore sizes and charge stabilising cations. These differences could lead to the formation of larger platinum clusters on zeolite HY than on zeolite KL when the conditions of treatment for these catalysts are the same. Dong *et al* [1994] found that in mono-functional catalysts such as Pt/KL and Pt/SiO<sub>2</sub>, the support pores affected the size and location of the platinum particles. Mielzarski *et al* showed

that zeolite KL had the ability to stabilise small platinum particles. This could have been due to the lack of acidity on zeolite KL causing enhanced interaction between the platinum and the zeolite [Mielkzarski *et al*, 1992]. The basic potassium ions in zeolite KL could donate electrons to the platinum particles thus stabilising them. Zeolite HY is more acidic compared to zeolite KL and it has bigger pores (12.1 Å). Zeolite KL pores are 7.4 Å. Therefore the differences in the acidity and pore sizes between zeolite HY and KL could have contributed to the differences in the dispersion of Pt/HY and Pt/KL catalysts which had been calcined and reduced at similar conditions.

#### 4.3.4 Rate of Temperature Increase

The rate of temperature increase was found not to influence the platinum dispersion as shown in table 3.8. Sachtler advocated that under laboratory conditions, increasing the temperature at a slow rate (0.5 °C/minute) in very high oxygen flowrates (> 1 000 ml/min/g) would limit the reduction of platinum by co-ordinated ammonia ligands (auto-reduction). Auto-reduction would also lead to sintering of the platinum particles [Sachtler, 1992]. Never the less, at the experimental conditions employed, the results obtained did not support Sachtler's concerns about the rate of temperature increase during calcination.

#### 4.3.5 Effect of Calcination Time in Oxygen At 350 °C

The dispersion of the platinum metal was found to be independent of the calcination times studied in oxygen at 350 °C (figure 3.26). For calcination in oxygen at 350 °C there is a minimum time period needed for total decomposition of the ammonia ligands. Apparently, maintaining the sample at 350 °C for time periods beyond this minimum did not affect the platinum dispersion.

## 4.4. Reduction

### 4.4.1 Temperature Programmed Reduction

#### 4.4.1.1 TPR of 1.55 Pt/KL samples

The TPR curve of 1.55 % Pt/KL calcined in oxygen at 350°C (figure 3.8) showed two distinct peaks at 115°C and 350°C as well as a shoulder commencing at 42°C. The shoulder at 42°C could represent the reduction of PtO, however due to limitations of the experimental equipment (section 2.2.4.) the full peak could not be obtained. Ostgard *et al* have also shown that PtO would be reduced at low temperatures (less the 11°C). [1992] The peak at 115°C represented reduction of the Pt<sup>2+</sup> ions situated in the 12 membered ring channels of the zeolite KL while the peak at 350°C represented the reduction of Pt<sup>2+</sup> ions situated in the locked sites of the zeolite KL. The locked sites could be in the 6 and 8 membered ring channels of the zeolite KL. This was in agreement with the work done by Ostgard *et al*. [1992]. The H<sub>2</sub>/Pt ratio of 1.03 obtained for this sample (table 3.2) indicated that the platinum valency was close to 2.

The sample of 1.55 % Pt/KL calcined in N<sub>2</sub> at 350°C exhibited a shoulder starting at about 42 °C as well as a peak at 370°C. The peak at 370°C was non symmetrical owing to the presence of a shoulder starting at 220°C. As before, the shoulder starting at 42°C was attributed to the reduction of PtO. The PtO could have been formed during the calcination step (while increasing the temperature from 25 °C to 350°C) from the reaction between the water in the zeolite pores and the Pt<sup>2+</sup> ions. This could have occurred according to reaction 4.1.

The peak at 115°C, representing the reduction of Pt<sup>2+</sup> ions in the 12 membered ring channels was missing for the sample calcined in nitrogen. This could have been due to the reduction of these Pt<sup>2+</sup> ions by the co-ordinating ammonia ligands in Pt(NH<sub>3</sub>)<sub>4</sub><sup>2+</sup>. This would be expected to occur in an inert calcination medium such as nitrogen [Sachtler 1992], [Alvarez, 1988]. The peak at 370°C would have been due to the reduction of Pt<sup>2+</sup> in locked sites of the zeolites. The H<sub>2</sub>/Pt ratio of 1.14 obtained for the samples indicated that the valency of the

platinum ions was close to 2. However, the value of the  $H_2/Pt$  ratio was expected to be slightly less than 1 since some "auto reduction" of the platinum ions by the ammonia ligands would take place when calcination is done in nitrogen.

When calcined at 600°C in  $O_2$ , the TPR profile of 1.55% Pt/KL did not show a peak at 115 °C assigned to the reduction of platinum species in the main channels of the zeolite KL. It is possible that during calcination at 600 °C, many of the platinum species migrated to the locked sites of the zeolite KL. This could explain the absence of the peak at 115 °C. However, the TPR profile showed a shoulder starting at 43°C and a non symmetrical peak starting at 250°C and peaking at 430°C. The profile had a similar shape to that of the 1.55% Pt/KL calcined at 350°C in nitrogen. However, the peak representing the reduction of  $Pt^{2+}$  ions in locked sites was bigger and it occurred at a higher temperature. It was expected for the peak of the sample calcined at 600 °C to be bigger since more platinum species would be expected to migrate to the locked sites at this high temperature. The locked sites would be the 8 and 6 membered ring channels. The  $Pt^{2+}$  species on these positions would have their charge stabilised by the high negative charge density in these sites. They would require higher temperatures for reduction to occur.

Compared to the eight membered ring channels of zeolite KL, the six membered ring channels are smaller (figure 1.5). Thus the negative charge density in the six membered ring channels could be higher than in the eight membered ring channels. This could result in a stronger charge stabilisation of the platinum ions in the six membered ring channels. The platinum ions in the six membered ring channels could thus be reduced at a higher temperature compared to the platinum ions in the eight membered ring channels. It is possible that during calcination at 600 °C, most of the platinum ions migrated to the six membered ring channels while for calcination at 350 °C, most of the platinum ions migrated to the eight membered ring channels. This could explain why the reduction peak assigned to the reduction of platinum species in locked sites occurred at a higher temperature (430 °C) for the sample calcined at 600 °C while this peak occurred at a lower temperature (370 °C) for the sample calcined at 350 °C.

The  $H_2/Pt$  ratio of 2.64 obtained for the sample calcined at 600 °C indicated that the valency



of the platinum could have been greater than 4. It can be speculated that calcination at 600 °C in oxygen could have resulted in the formation of platinum oxides containing platinum ions with oxidation states higher than two as suggested by Park *et al.* [1986]. One of the platinum oxides could have been PtO<sub>2</sub>. This could explain why the value of the H<sub>2</sub>/Pt ratio obtained for this sample was more than double the value expected for the reduction of Pt<sup>2+</sup> ions.

It is also possible that small amounts of hydrogen spillover occurred on all the Pt/KL samples. Since the pressure of the hydrogen in the H<sub>2</sub>/N<sub>2</sub> stream was low, little spillover could have occurred (section 4.4.1.2). This hydrogen spillover could also have contributed to the high H<sub>2</sub>/Pt ratios obtained for the Pt/KL samples.

#### 4.4.1.2 TPR of 1.43 % Pt/HY samples

TPR profiles of Pt/HY were obtained and compared with those of Pt/KL.

##### 1.43% Pt/HY calcined at 350 °C

The TPR profile of the sample of 1.43 % Pt/HY calcined at 350 °C in oxygen exhibited two peaks (figure 3.11). The shoulder starting at about 42 °C which has been assigned to the reduction of PtO was missing in this sample. It was not clear why this peak was missing. The peak at 120 °C was attributed to the reduction of Pt<sup>2+</sup> ions in the supercages of the HY zeolite while the small peak at 350 °C was attributed to the reduction of Pt<sup>2+</sup> in the locked sites of the zeolite such as in the sodalite cages and the hexagonal prisms. It is evident from figure 3.11 that the peak at 120 °C showed more hydrogen uptake than was required for the reduction of all the platinum ions in the zeolite. The H<sub>2</sub>/Pt ratio of 23.77 was much greater than the theoretically expected value of 1 for the reduction of Pt<sup>2+</sup> ions. This could have been due to hydrogen spillover onto the zeolite HY at 100 °C

##### 1.43% Pt/HY calcined at 600 °C

The TPR profile of the 1.43 % Pt/HY sample calcined in oxygen at 600 °C showed two peaks - one at 60 °C and the other at 120 °C (figure 3.12). The TPR profile of 1.43 % Pt/HY calcined in nitrogen at 600 °C showed two smaller peaks at similar positions to the

sample calcined in oxygen (figure 3.13). Due to the limitations of the TPR equipment, the first peak could not be represented as a full peak. This peak could have represented the reduction of PtO at low temperatures. The peak at 120 °C could have represented the reduction of Pt<sup>2+</sup> ions in the supercages. The two peaks were also associated with hydrogen spillover as can be seen by the very high H<sub>2</sub>/Pt ratios obtained (table 3.2).

The peak appearing at 350 °C in the TPR profile of 1.43 % Pt/HY sample calcined in oxygen at 350 °C was missing for the samples calcined at 600 °C. This peak was attributed to the reduction of platinum ions in the locked sodalite cages and hexagonal prisms of the zeolite. Its absence in the TPR profiles of samples calcined at 600 °C could indicate that very few platinum ions were present in the sodalite cages and hexagonal prisms for these samples. Since the samples calcined at 600 °C had low platinum dispersion (table 3.16), this could suggest that for the samples calcined in oxygen at 600 °C, the agglomeration of the particles occurred via the formation of (PtO)<sub>n</sub> agglomerates as suggested by Park *et al.* [1986] These agglomerates would form in the supercages of the zeolite HY. The sample calcined in nitrogen could have formed agglomerates as a result of reduction by the ammonia ligands during calcination leaving few unreduced platinum ions. The peaks observed on this sample could have largely been due to hydrogen spillover onto the zeolite HY.

## Hydrogen Spillover

Roland and co-workers have reported H<sub>2</sub>/Pt ratios greater than 10 for Pt/HNaY samples. They have attributed this to spillover which is a phenomenon involving the formation of an active species on one surface phase and the migration of this species onto another phase which is not able to form this species itself. In some metal supported systems, H<sub>2</sub>/metal ratios greater than 100 have been observed. [Roland *et al.*, 1994] According to these researchers, the adsorption rate of hydrogen onto the platinum metal can be described by the Langmuir isotherm and is characterised by an initial period with a high adsorption rate and a subsequent period with a lower and constant adsorption rate. They found the adsorption rate to be a maximum at 100 °C. [Roland *et al.*, 1994]. The thermally activated diffusion from the platinum onto the support can be assumed to be proportional to  $\exp[-E_B/kT]$  where  $E_B$  is the activation energy for diffusion,  $k$  the Boltzman constant and  $T$  the temperature.

Thus an increase in temperature would lead to an increased flux onto the support. However according to Langmuir's isotherm, desorption from the metal phase would occur at high temperatures. Thus increasing the temperature would lead to opposite influences on the equilibrium of adsorption. [Roland *et al*, 1994]. This phenomenon would explain why at lower temperatures (less than 130 °C) high hydrogen uptake was observed for Pt/HY samples while at higher temperatures, virtually no hydrogen uptake was observed.

Hydrogen spillover could explain why  $H_2$ /Pt ratios higher than theoretically possible were observed for the Pt/HY samples. Hydrogen spillover was observed to occur at temperatures assigned to the reduction of PtO and  $Pt^{2+}$  in the supercages. This would be in agreement with the theory that neutral metal particles are needed for the spillover to occur. [Roland *et al*, 1994].

Hydrogen spillover could also explain why in Pt/KL the  $H_2$ /Pt obtained for some of the samples was slightly higher than 1. Sharma *et al* [1994] have reported hydrogen spillover onto Pt/KL catalysts. It is also possible that in Pt/KL samples, hydrogen spillover is dependent on hydrogen pressure as observed by Kramer *et al* [1979] for Pt/ $Al_2O_3$ . This could explain why in TPR studies where only 5 vol %  $H_2$  in  $N_2$  was used, little hydrogen spillover was observed. On the other hand, in hydrogen chemisorption studies where the pressure of the hydrogen used was close to 101 kPa, much hydrogen spillover was observed (section 3.5.2.2).

#### 4.4.2. Reduction Temperature

Table 3.11 shows a summary of the chemisorption results for Factorial Design for reduction. It is evident from these results that reduction at either 150°C or 350°C does not greatly affect dispersion of the metal. Based on the TPR results for 1.55% Pt/KL it would be expected that some of the Pt species would be unreduced at 150°C. However, the unreduced Pt species would still chemisorb CO as proved by the results shown in table 3.9. Therefore, for catalytic purposes in which the platinum in its reduced state is needed, it would be advantageous to reduce the Pt/KL samples at 350°C instead of 150°C.

The reason why samples that were not reduced in hydrogen exhibited higher platinum dispersion than those that had been reduced in hydrogen (table 3.9), could have been due to the fact that electrostatic requirements for the bonding of  $\text{Pt}^{2+}$  to the zeolite framework stops platinum ions from migrating along the zeolite channels. However, after reduction, platinum atoms formed would easily migrate along the walls of the zeolite to coalesce with other atoms thus forming slightly larger particles.

Reducing samples at 600°C in hydrogen resulted in a low platinum dispersion. This is because at high temperatures, the platinum particles agglomerate and sinter into large particles.

#### 4.4.2.1. Rate of temperature increase from 25°C to 350°C during reduction

The rate of temperature increase during reduction was shown to have negligible effect on the platinum dispersion as shown in table 3.12. This agreed with the work of Sachtler [1992] who reported that the rate of temperature increase could be important during calcination and not during reduction. Sachtler claimed that slow heating rates of 0.5°C/min during calcination in oxygen would minimise the reduction of the Pt by the co-ordinating ligands.

#### 4.4.3 Reduction Medium

Table 3.11 clearly showed that reduction in hydrogen would lead to catalyst samples with better platinum dispersion compared to samples that had been reduced in carbon monoxide. The poor dispersion obtained for the samples reduced in carbon monoxide could be explained by the formation of platinum carbonyls as well as the deposition of carbon formed via the Boudouard reaction. The carbon could block the zeolite pores making platinum particles inaccessible to the chemisorbing carbon monoxide gas.

##### 4.4.3.1 Formation of platinum carbonyls

Chang *et al* have reported the formation of  $[\text{Pt}_6(\text{CO})_{18}]^{2-}$  clusters on zeolite Y which had been rendered basic by the addition of caesium. They showed that after treatment above 120 °C

in a vacuum, de-carbonylation occurred to yield platinum metal clusters. [Chang *et al*, 1993]. They also showed that  $[\text{Pt}_{15}(\text{CO})_{30}]^{2-}$  formed on the surface of MgO could be de-carbonylated by evacuation at 120 °C to yield  $\text{Pt}_{15}$  clusters. Re-carbonylation of the clusters led to further agglomeration of the platinum.

Reduction of the 1.55% Pt/KL in carbon monoxide was done at 150 °C and 350 °C. Before applying carbon monoxide chemisorption, the samples were evacuated at the respective temperatures. It was possible that formation of carbonyl clusters with subsequent de-carbonylation occurred during this treatment. If the observation by Chang and co-workers for  $[\text{Pt}_{15}(\text{CO})_{30}]^{2-}$  clusters on MgO was applicable for Pt/KL samples then it could explain the very low dispersion values obtained for the 1.55 % Pt/KL samples which were reduced in carbon monoxide.

There are two classes of platinum clusters namely columnar species  $[\text{Pt}_3(\text{CO})_6]^{2-n}_n$  and large platinum carbonyl anions such as  $[\text{Pt}_{19}(\text{CO})_{22}]^{4-}$ . The structures of these platinum clusters are shown in figures 4.1 and 4.2. In the presence of a hydrogen species, the platinum carbonyl structure such as  $[\text{Pt}_{38}(\text{CO})_{44}\text{Hx}]^{2-}$  could be formed. This structure is described by Cotton and Wilkinson [1988]

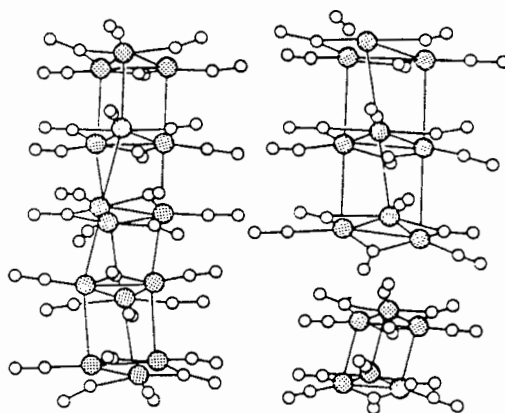


**Figure 4.1** showing the structure of  $[\text{Pt}_3(\text{CO})_6]^{2-n}_n$  ions with  $n = 2, 3$  and  $5$  [from Cotton and Wilkinson, 1988]

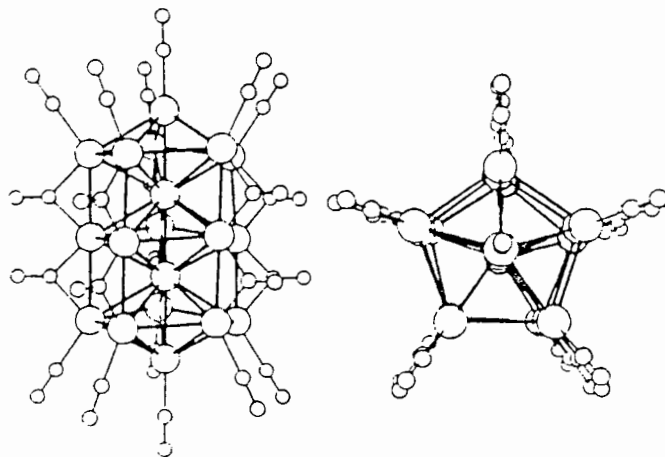
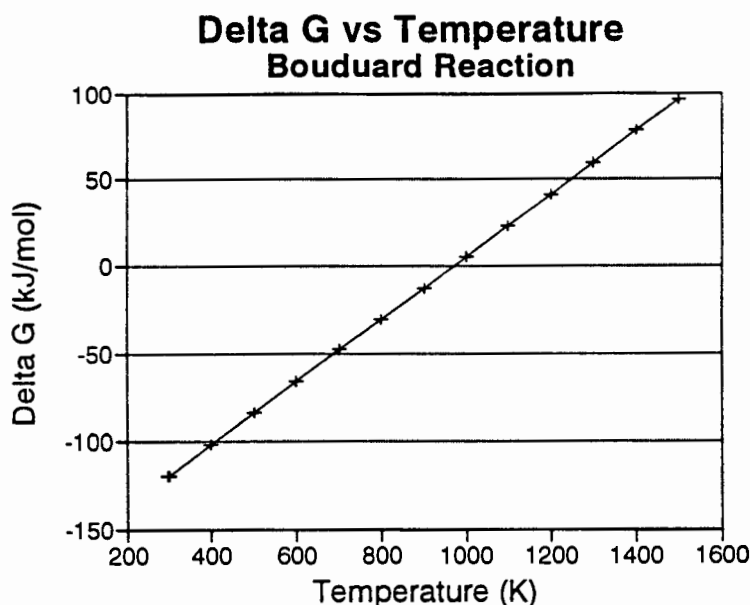


Figure 4.2 showing two views of the  $[\text{Pt}_{19}(\text{CO})_{22}]^+$  ion structure [from Cotton and Wilkinson, 1988]

If any platinum carbonyl clusters were formed during carbon monoxide reduction, they could have yielded platinum clusters as evidenced by plate 3.4 showing the TEM image of a sample that had been reduced in carbon monoxide. The formation of platinum carbonyls would occur at temperatures well above 35 °C since the carbon monoxide chemisorption analysis at 35 °C of a calcined and un-reduced 1.55 Pt/KL sample showed a high dispersion (table 3.9).

#### 4.4.3.2 Boudouard reaction

Figure 4.3 shows the relationship between the Gibbs free energy ( $\Delta G$ ) and temperature for the Boudouard reaction :  $2 \text{CO}_{(g)} \rightarrow \text{CO}_{2(g)} + \text{C}_{(s)}$ .



**Figure 4.3** showing the  $\Delta G$  vs  $T$  relationship for the Bouduard reaction. (Data used for  $\Delta G$  calculations was obtained from Holland and Anthony, 1979)

The curve in figure 4.3 shows that the reaction is feasible at low temperatures. However, it is possible that the reaction is only kinetically feasible at higher temperatures. At the temperatures of reduction used (150 °C, 350 °C), the Bouduard reaction could possibly take place resulting in the deposition of carbon in the zeolite pores. If much carbon had been deposited on the samples studied, they would have turned black. The samples did not turn black after carbon monoxide reduction but they exhibited a much darker shade of grey compared to the samples reduced in hydrogen. This could have indicated the deposition of small quantities of carbon. The dark grey colour could also have been due to the formation large platinum particles formed from platinum carbonyl clusters as described in section 4.4.3.1. Plate 3.4 of the TEM results showed that the sample reduced in carbon monoxide had many dark particles. The dark particles could not have been due to carbon deposited on the samples since at the conditions of the TEM instrument operation, carbon particles would not give dark images.

Comparing the TEM images of the sample reduced in carbon monoxide (plate 3.4) with those of other samples which yielded low dispersion (plates 3.3 and 3.6), it was evident that the platinum particles in the sample reduced in carbon monoxide were smaller. The platinum dispersion of the samples reduced in carbon monoxide (12 %) was much lower than the

platinum dispersion of samples with TEM images shown in plates 3.3 and 3.6 (44 % and 31 %). This observation further supported the speculation that small amounts of carbon were deposited on the zeolite samples during carbon monoxide reduction. The carbon could have blocked the pores of the zeolite rendering the platinum in the pores inaccessible to the carbon monoxide during chemisorption analysis. The carbon could also have covered the platinum particles thus making the platinum surface unavailable for chemisorption.

#### 4.4.3.2 Strong adsorption of carbon monoxide during reduction

It had been speculated that another factor which could contribute to the low dispersion of platinum for samples reduced in carbon monoxide could be the strong adsorption of carbon monoxide onto the platinum species during the reduction process. It had been feared that the evacuation procedure of the samples after carbon monoxide reduction and before determining the metal dispersion would not be able to remove all the carbon monoxide strongly adsorbed during the reduction step. Since carbon monoxide chemisorption was used to determine the platinum dispersion, it had been speculated that this could have resulted in erroneously low platinum dispersion values.

After re-reduction at 150 °C in carbon monoxide and before the chemisorption step, samples were evacuated at 150 °C,  $5 \cdot 10^{-3}$  mm Hg for 6 hours. Samples re-reduced in carbon monoxide at 350 °C were evacuated at 350 °C,  $5 \cdot 10^{-3}$  mm Hg for 4 hours (section 2.2.3.1). This treatment would have ensured the complete removal of any strongly adsorbed carbon monoxide from the sample. Figure 3.31 shows the results of carbon monoxide chemisorption cycles on a Pt/KL sample whose evacuation time was varied while cooling down from 350 °C to 35 °C. In between the chemisorption cycles, the sample was evacuated at  $5 \cdot 10^{-3}$  mm Hg, 35 °C for 1 hour. If carbon monoxide strongly adsorbed onto the sample was not removed during the evacuation, then the dispersion values obtained would have become less with each cycle. As shown in figure 3.31 the dispersion was constant at about 80 %. Thus the speculation that the inability to remove strongly adsorbed carbon monoxide would result in erroneously low platinum dispersion values was incorrect.



#### **4.4.4. Reduction Time**

Table 3.11 shows that the periods of reduction investigated did not significantly affect the metal dispersion. This was expected. At a certain temperature, it is important that the contact time between the reducing agent and the sample is long enough to ensure that all the platinum species reducible at this temperature are reduced. If all the reducible platinum species at a certain temperature are reduced, then maintaining the sample at this temperature for longer periods should not affect the platinum dispersion.

### **4.5. Comparison Between Liquid Ion Exchange, Impregnation And Solid State Ion Exchange As Methods of Incorporating The Platinum Onto Zeolite KL.**

#### **4.5.1 Treatment In Oxygen, At 350°C**

For samples heated to 350°C in oxygen and subsequently reduced in H<sub>2</sub> at 350°C, the solid state ion exchange procedure gave the highest metal dispersion. This is evidenced by the results in table 3.13 as well as the TEM results. Plate 3.5 showing the TEM image of the sample treated at 350 °C under solid state ion exchange shows that the platinum particles were well dispersed and too small to be detected at the TEM conditions used. Plate 3.2 shows the TEM image of the sample prepared via liquid ion exchange with subsequent calcination in oxygen at 350 °C. This plate indicates that although the platinum was well dispersed, it formed a few clusters which could be detected at the TEM conditions employed unlike the sample treated in oxygen at 350 °C under solid state ion exchange. In solid state ion exchange, the amount of Pt loaded onto the zeolite (0.75 %) was less than that incorporated via liquid ion exchange and impregnation (1.55%). At present, little is known about the mechanisms of solid state ion exchange. [Beyer and Karge, 1988] The exchange of bivalent cations such as Pt<sup>2+</sup> into the zeolite by solid state ion exchange is more difficult compared to monovalent cations. [Karge, 1992] For a required metal loading, salt/zeolite mixtures containing an excess of ingoing cations may need to be used.

In solid state ion exchange, the platinum salt and the zeolite KL were well mixed before heating in O<sub>2</sub> (section 2.1.4). During calcination, the ammonia ligands could have been decomposed while the Pt(NH<sub>3</sub>)<sub>4</sub><sup>2+</sup> was still outside the zeolite pores to yield Pt<sup>2+</sup> ions. The Pt<sup>2+</sup> ions have a Van der Waals ionic radius of 0.8Å and they can easily migrate into the pores of the zeolite (diameter of 7.1Å to 7.4Å) to ion exchange out the potassium. After ion exchanging out the potassium, they would leave enough space in the pores to allow other Pt<sup>2+</sup> ions to migrate further down the pores in order to ion exchange out the potassium ions along the channels.

In liquid ion exchange, the whole Pt(NH<sub>3</sub>)<sub>4</sub><sup>2+</sup> ion whose Van der Waals diameter is about 5Å would be ion exchanged onto the zeolite. Since the zeolite pore diameter is about 7.4 Å the space left between the ion exchanged complexes and the wall might not be large enough to allow many more Pt(NH<sub>3</sub>)<sub>4</sub><sup>2+</sup> complexes to migrate further along the pores. This could result in the ion exchange of the Pt(NH<sub>3</sub>)<sub>4</sub><sup>2+</sup> taking place close to the mouths of the zeolite pores. During calcination in oxygen, some "auto reduction" of the Pt<sup>2+</sup> by the ligands could occur in the sample prepared by liquid ion exchange. Since the ion exchanged platinum species could be closer together towards the pore mouth of the zeolite, the measure of coalescence would be greater than that in samples prepared by solid state ion exchange.

In the presence of oxygen, the ammonia ligands could decompose to yield nitrogen and water leaving Pt<sup>2+</sup> ions. The water could then react with the platinum ions to yield hydrogen ions according to equation 4.1. The hydrogen ions produced could react with chloride ions present during the solid state ion exchange, resulting in the formation of HCl<sub>(g)</sub>. [Ostgard *et al.*, 1992] The acidity of the sample prepared by solid state ion exchange would thus be expected to be lower than the acidity for the sample prepared via liquid ion exchange in which the chloride ions were removed by washing (section 2.1.1). The presence of chloride ions in the samples prepared by solid state ion exchange could also lead to the formation of Pt<sup>iv</sup> which would in turn enhance the dispersion of the platinum. [Forger and Jaeger, 1989]

In impregnation, the Pt(NH<sub>3</sub>)<sub>4</sub><sup>2+</sup> complex would be attached onto the zeolite primarily by an adsorption process. Thus impregnation does not necessarily involve stoichiometric ratio between the K<sup>+</sup> ions in zeolite KL and the incoming platinum ions. However, if chloride ions

were present (as is the case with impregnated samples), they could enhance the dispersion of the platinum via the formation of  $\text{Pt}^{\text{IV}}$ . [Forger and Jaeger, 1989]

#### 4.5.2 Treatment At 600 °C In Nitrogen

For samples calcined in nitrogen at 600 °C, the platinum dispersion was higher for the sample prepared via liquid ion exchange while for samples prepared via impregnation and solid state ion exchange the dispersion values were similar and low (table 3.14). It is possible that for the samples prepared by liquid ion exchange and impregnation, calcination in nitrogen at 600 °C resulted in the auto-reduction of the platinum ions by the ammonia ligands. In an inert medium and at a high temperature, the semi-instantaneous decomposition of the ammonia ligands would provide a momentarily high ammonia concentration around the platinum ions. This could result in the formation of mobile hydride species which could subsequently lead to sintering of the platinum particles.[Reagan *et al*, 1981]. The degree of sintering could be greater in samples prepared by impregnation because unlike in liquid ion exchange involving stoichiometric exchange of the potassium by the platinum, the platinum would be attached onto the zeolite by adsorption. The platinum complexes loaded via impregnation could be closer together compared to those loaded via liquid ion exchange and this could enhance the sintering of platinum in samples prepared by impregnation.

During the performance of solid state ion exchange at 600 °C in nitrogen, the "auto-reduction" of the platinum ions as well as the formation of hydrides could have occurred while the platinum species was still outside the zeolite pores. Since there would be no interaction between the platinum species and the zeolite wall, the platinum would easily sinter to form large particles on the external surface of the zeolite. For the samples prepared by liquid ion exchange, there would be ionic interaction between the platinum and the zeolite wall. This interaction would limit the formation of large platinum clusters.

## 4.6 Hydrogen Chemisorption

Results of hydrogen chemisorption on 0.5 wt % Pt/Al<sub>2</sub>O<sub>3</sub> showed a platinum dispersion level of 70 % which was more than double the value expected from carbon monoxide chemisorption (33% +/- 5%). Other workers when using hydrogen chemisorption to measure dispersion found values which were 1.6 to 4 times greater than the expected values. [Adler, 1960], [Kip *et al.*, 1986] These workers attributed their findings to multiple adsorption of hydrogen onto the platinum particles. However, Kramer and Andre [1979] attributed the high H/Pt atom ratio obtained to a spillover effect. They reported that the rate of hydrogen spillover was dependent on the hydrogen pressure.

In the chemisorption treatment, the samples were re-reduced in hydrogen at 350 °C for 2 hours before cooling down under vacuum to 35 °C. Cooling down the sample from 350 °C to 35 °C took less than an hour. Therefore the greater part of the evacuation time X (figure 3.28) consisted of the time taken to maintain the catalyst under vacuum at 35 °C. If hydrogen had been spilled over onto the support it would be desorbed slowly at this low temperature. [Roland *et al.*, 1994]. The desorption process could have been the reverse of the spillover process i.e the hydrogen atoms would migrate along the alumina support to the platinum particles where they would reform hydrogen molecules. The hydrogen molecules would then be removed from the sample at the pressure of  $5 \cdot 10^{-3}$  mm Hg employed. For the Pt/Al<sub>2</sub>O<sub>3</sub> removal of the spilled over hydrogen at 35 °C could have reached an equilibrium after 8 hours as shown in figure 3.28. For a sample evacuated at 35 °C for longer than 8 hours, repeating the chemisorption cycle would result in further hydrogen spillover. The spilled over hydrogen would replace the hydrogen removed during the evacuation at 35°C. This could explain why a constant dispersion value of 70 % was obtained for the 0.5 % Pt/Al<sub>2</sub>O<sub>3</sub> sample for an evacuation time X greater than 8 hours (figure 3.28).

The spillover effect could also be used to explain the results obtained for the 0.78 % Pt/KL shown in figures 3.29 and 3.30. Other researchers such as Vaarkamp *et al* [1990] have observed this effect on Pt/KL. In figure 3.29, longer evacuation times than those studied would be needed for the removal of hydrogen to reach an equilibrium. The amount of

hydrogen removed from the sample in nitrogen flow at 350 °C was less than that removed in a vacuum at 350 °C. Thus in a nitrogen flow, an even longer time would be required for the removal of hydrogen from the sample before it reaches an equilibrium.

In figure 3.29 nitrogen flow was used in place of a vacuum at 350 °C in order to test whether a leak existed in the chemisorption equipment. If a leak existed, it would allow some air to enter the system and possibly oxidise the platinum to platinum oxide. The platinum oxide would then have required hydrogen for reduction in addition to the hydrogen needed for chemisorption. However, figure 3.29 showed that even after treatment in nitrogen flow at 350 °C, the amount of hydrogen taken up by the sample resulted in an apparent dispersion value greater than 100 %. This indicated that a leak was not present in the system.

Figure 3.31 showed that for carbon monoxide chemisorption test cycles, the obtained platinum dispersion obtained was independent of the evacuation time period while cooling the sample from 350 °C to 35 °C under vacuum. Based on these results, it was decided to employ carbon monoxide chemisorption in place of hydrogen chemisorption to determine the dispersion of the metal surface area.

## 4.7 Acidity

In the preparation of Pt/KL samples for use in aromatisation reactions, it was important to keep the acidity of the samples to a minimum since a high catalyst acidity would result in a high selectivity to cracked products. [Mielzarski *et al*, 1992] The acidity of platinum samples was determined using ammonia TPD analysis.

Before accurate analysis of TPD data obtained for Pt/KL samples could be made, it was important to determine whether reduced platinum metal would strongly adsorb ammonia. This was done by performing TPD analysis of platinum loaded onto a supposedly inert carrier such as silica ( $\text{SiO}_2$ ) without any acid sites. The amount of ammonia desorbed from the Pt/ $\text{SiO}_2$  was compared with the amount of ammonia desorbed from  $\text{SiO}_2$  only. Figure 3.14 and 3.15 showed that the silica did contain some acidity. However, the difference in the acidity of the Pt/ $\text{SiO}_2$  and of the pure  $\text{SiO}_2$  showed that the platinum did not strongly adsorb ammonia. Unlike the Pt/KL zeolites, Pt/ $\text{SiO}_2$  samples did not exhibit a peak in the temperature range 240 °C-290 °C. This peak has been assigned to the desorption of weakly adsorbed ammonia. This peak could have been absent from the Pt/ $\text{SiO}_2$  samples because the silica used (Davisil grade 646 supplied by Aldrich Chemical Company) had a surface area of 300m<sup>2</sup>/g compared to zeolite KL (Union Carbide) with a much higher surface area. Zeolite KL also has narrower pores which could have retarded the complete removal of the weakly adsorbed ammonia when the sample was flushed with helium at 100 °C (section 2.2.5).

### 4.7.1 Acidity Of Zeolite KL Without Any Platinum

TPD profiles of nearly all the Pt/KL samples showed peaks representing ammonia desorption at three sets of temperature ranges. These were designated as peak A : 240 °C - 290 °C; peak B : 340 °C - 350 °C and peak C : 520 °C - 600 °C.

Untreated zeolite KL and zeolite KL calcined in oxygen at 350 °C had similar TPD profiles (figures 3.16 and 3.17). Two peaks were obtained as shown in table 3.3. The first peak (at 270 °C) could have been due to weakly adsorbed ammonia while the second peak (at 600 °C)

could have been due to ammonia desorption from strong Bronsted acidity. It is possible that the zeolite KL used contained some acid sites left over from the synthesis of the zeolite. If strong Bronsted acid sites existed in the zeolite structure, they could be removed at high temperature via de-hydroxylation to yield Lewis acid sites. The water given off during de-hydroxylation would then be detected by the TCD and the signal obtained interpreted as an ammonia signal. This would make the peak appearing in the 520 °C to 600 °C range (peak C) appear larger than it would be were it to represent ammonia desorption only. Molecular sieves could not be used to trap the water produced during de-hydroxylation since ammonia and water have similar molecular sizes. The peak at 600 °C representing strong acidity has also been reported in literature for untreated zeolite KL. [Mielczarski *et al*, 1992]

#### **4.7.2 Acidity Of Calcined 1.55 wt % Pt/KL samples**

##### **4.7.2.1 1.55% Pt/KL calcined at 350 °C in O<sub>2</sub> for 6.33 hours without subsequent reduction**

The sample of 1.55 % Pt/KL calcined in oxygen at 350 °C for 6.33 hours without subsequent reduction gave larger peaks compared to those of the sample without platinum (compare figure 3.17 and figure 3.18). Even though calcination was done in oxygen, some reduction of the platinum ions by the co-ordinating ammonia ligands would be inevitable [Sachtler, 1992]. This auto-reduction process would result in the formation of H<sup>+</sup> ions according to equation 4.3b. These ions would then attach onto the zeolite framework to yield both weak and strong Bronsted acidity. The decomposition of ammonia ligands in oxygen could also yield nitrogen and water. The water could then react with the platinum ions to yield hydrogen ions (equation 4.1) which would in turn attach onto the zeolite wall to give Bronsted acid sites. Strong Bronsted acidity occurs if the interaction between the zeolite and the H<sup>+</sup> ions is weak while weak Bronsted acidity occurs if this interaction is strong.

In figure 3.18, the shoulder appearing on the first peak after 40 minutes (300 °C) could have indicated the onset of the peak appearing in the temperature range 340 °C to 350 °C. This shoulder could have been due to the presence of weak Bronsted acid sites on the zeolite. The acidity could have been formed as a result of the auto-reduction of the Pt<sup>2+</sup> by the co-ordinating ammonia ligands or as a result of the reaction between platinum ions and the water

formed during the decomposition of ammonia ligands in oxygen. Thus the first peak in the TPD profile in figure 3.18 could have been due to both weakly adsorbed ammonia and ammonia adsorbed onto weak Bronsted acid sites. The peak in the temperature range 520 °C - 600 °C was also larger compared to a similar peak of the untreated zeolite KL. This could have been due to some strong Bronsted acidity also resulting from the auto-reduction of the platinum by the ammonia ligands. Compared to the zeolite KL sample without platinum, this sample would exhibit more de-hydroxylation since it contained more H<sup>+</sup> ions attached to the zeolite walls. If de-hydroxylation was occurring, this could make the second peak representing ammonia desorption at high temperatures appear bigger than the the second peak for the sample without platinum.

#### **4.7.2.2 1.55% Pt/KL calcined at 350 °C in N<sub>2</sub> for 6.33 hours without subsequent reduction**

Compared to the 1.55 % Pt/KL sample calcined in oxygen at 350 °C, the sample calcined in nitrogen showed a bigger shoulder which peaked in the temperature range 340 °C to 350 °C (figure 3.19) This shoulder could have been due to weak Bronsted acidity formed as a result of reduction of platinum ions by ammonia ligands. The acidity of the sample calcined in nitrogen would be expected to be more than that of the sample calcined in oxygen since the degree of auto-reduction of the platinum by the ammonia ligands would be expected to be more in an inert calcination medium. [Alvarez *et al.*, 1988] The amount of ammonia desorbed at the high temperature peak (520 °C - 600 °C range) for the sample calcined in nitrogen was the same as that for the sample calcined in oxygen (table 3.3). This could have indicated that the strong acidity was not increased by heating the sample in an inert medium.

#### **4.7.2.3 1.55% Pt/KL calcined at 600 °C in O<sub>2</sub> for 6.33 hours without subsequent reduction**

Figure 3.20 shows the TPD profile of the sample that had been calcined in oxygen at 600 °C without subsequent reduction. Compared to the sample calcined in oxygen at 350 °C, the two peaks obtained for this sample were obtained in similar temperature ranges namely 240 °C - 290 °C and 520 °C - 600 °C. However, the peaks for the sample calcined at 600 °C were smaller indicating that during calcination at 600 °C, the hydroxyl groups on the zeolite could have been removed via de-hydroxylation to form Lewis acid sites. These hydroxyl



groups could have been formed as a result of either auto-reduction of the platinum by the ammonia ligands or as a result of the reaction between platinum ions and the water formed during the decomposition of ammonia ligands in oxygen. It is also possible that some Bronsted acidity could have been present in the zeolite after synthesis. De-hydroxylation would result in reduced Bronsted acidity of the sample.

It should be borne in mind that after calcination at 600 °C, the sample was exposed to the atmosphere before performing the TPD analysis (section 2.2.5). If all the Bronsted acid sites had been removed via de-hydroxylation during calcination, then the Lewis acid sites formed could have interacted with water vapour in the atmosphere resulting in the restoration of some of the Bronsted acid sites.

#### **4.7.3 Acidity Of Calcined And Reduced 1.55 wt % Pt/KL samples**

##### **4.7.3.1 1.55% Pt/KL calcined at 350 °C in O<sub>2</sub> for 6.33 hours and reduced in H<sub>2</sub> at 350 °C for 4.5 hours**

The sample calcined in oxygen at 350 °C and reduced in hydrogen at 350 °C (figure 3.21) did not show a peak in the temperature region 240 °C - 290 °C (peak A) unlike in the TPD profiles of all the other samples. It was not clear why this sample did not exhibit a peak in the temperature range 240 °C - 290 °C assigned to the desorption of weakly adsorbed ammonia. However, this sample exhibited a peak at 350 °C (peak B) which could have been due to the desorption of ammonia chemisorbed onto weak Bronsted acid sites as in the sample which was calcined in nitrogen without subsequent reduction.

The total Bronsted acidity of the sample reduced in hydrogen should have been greater than for samples which were not reduced in hydrogen. This is because reduction in hydrogen would generate 2 H<sup>+</sup> ions for every Pt<sup>2+</sup> reduced. The 520 °C - 600 °C peak for the sample calcined in oxygen and reduced in hydrogen represented the same amount of acidity (0.27 mmols/g) as the sample that had been calcined at 350 °C without subsequent reduction (table 3.3, also compare figures 3.18 and 3.21). The acidity of the samples in which all the platinum ions had been reduced by the co-ordinating ammonia ligands would be expected to be similar to the acidity of the sample reduced in hydrogen. If all the platinum ions were

auto-reduced by calcination in nitrogen, then the amount of acid sites produced during auto-reduction in nitrogen would be similar to those obtained after reduction in hydrogen. The total acidity of the sample calcined in nitrogen without subsequent reduction (0.549 mmols/g) was larger than the acidity of the sample calcined in oxygen and followed by reduction in hydrogen (0.289). The difference could have been due to the absence in the sample reduced in hydrogen of the peak representing the desorption of weakly adsorbed ammonia in the temperature range 240 °C - 290 °C (table 3.3).

Since the sample reduced in hydrogen should have at least the same amount of Bronsted acid sites as the sample calcined in nitrogen, it should have exhibited peaks in similar temperature ranges to those exhibited by the sample calcined in nitrogen.

#### **4.7.3.2 1.55% Pt/KL calcined at 350 °C in O<sub>2</sub> for 6.33 hours and reduced in CO at 350 °C for 4.5 hours**

Comparing the shoulder appearing after 40 minutes (300 °C) for the sample calcined in oxygen and reduced in carbon monoxide (figure 3.22) with the shoulder in the TPD profiles of samples calcined in oxygen and nitrogen (figures 3.18 and 3.19) showed that this shoulder appeared as a distinct peak in the range 340 °C - 350 °C after reduction in carbon monoxide. This peak was attributed to the desorption of ammonia ligands attached to weak Bronsted acid sites.

The total acidity of a sample calcined in oxygen without subsequent reduction should be the same as the total acidity of the sample calcined in oxygen with subsequent reduction in carbon monoxide. As shown in table 3.3 the total acidity values for these two samples were similar. Comparison of the total acidity values in figures 3.18 and 3.22 also shows this.

For the peak in the temperature range 340 °C - 350 °C (peak B), a mere shoulder in the sample calcined in oxygen without subsequent reduction was obtained (figure 3.18). In the sample reduced in carbon monoxide, a distinct peak was obtained in the temperature range 340 °C - 350 °C. The peak representing the desorption from strong Bronsted acidity (range 520 °C - 600 °C) was smaller for the sample reduced in carbon monoxide when compared

to the TPD profile of the sample calcined in oxygen without subsequent reduction.

These observations suggested the possibility that carbon monoxide was interacting with strong Bronsted acid sites to render them as weak Bronsted acid sites. Strong Bronsted acidity is obtained if the interaction between the Bronsted acid site and the zeolite wall is weak. Weak Bronsted acidity is obtained if the converse of this is true. The weakening of the strong Bronsted acid sites by the carbon monoxide interaction could occur via the formation of large platinum carbonyls such as  $[\text{Pt}_{38}(\text{CO})_{44}\text{Hx}]^{2-}$  whose structure is described by Cotton and Wilkinson [1988].

#### 4.7.4 Acidity Of Calcined, Reduced And Back Exchanged 1.55 wt % Pt/KL samples

##### First TPD Analysis

Figure 3.23 shows the TPD profile of 1.55 % Pt/KL which had been calcined and reduced followed by back exchanging the  $\text{H}^+$  ions with  $\text{K}^+$  ions. The  $\text{H}^+$  ions would have been produced during the reduction of  $\text{Pt}^{2+}$  ions with hydrogen. Comparing the TPD profile of this sample with those presented in figures 3.18, 3.19 and 3.22, it was evident that the shoulder appearing after 40 minutes (300 °C) and peaking at about 350 °C (peak B) was significantly reduced indicating the removal of some weak Bronsted acidity. Peak C (temperature range 520 °C - 600 °C) which was assigned to the desorption of ammonia chemisorbed onto strong Bronsted acid sites, was reduced by about 29 % when compared to the TPD profiles of figures 3.18 and 3.19 (table 3.3). This could have indicated the removal of strong acid sites by back exchanging them with  $\text{K}^+$ . As in the case of other samples, de-hydroxylation could have occurred causing the second peak to increase beyond the size representing the true amount of ammonia desorbed from strong acid sites. Peak C which was assigned to the desorption of ammonia from strong Bronsted acid sites appeared at a lower temperature of 450 °C compared to the high temperature desorption peak of other samples which was observed in the temperature range 520 °C - 600 °C. It was not clear why this peak occurred at a lower temperature for this sample.

Back exchanging of the  $\text{H}^+$  ions by  $\text{K}^+$  was done via solid state ion exchange using twice the

amount of potassium ions needed to completely remove all the  $H^+$  ions. More studies would be needed to determine the optimum conditions for the removal of  $H^+$  ions by the  $K^+$  using solid state ion exchange.

### Second TPD Analysis

After obtaining the first TPD profile of the calcined, reduced and back exchanged sample, the sample was cooled in helium and a repeat TPD profile obtained. The repeat TPD profile presented in figure 3.24 confirmed two speculations namely i) The first peak in the temperature range  $240\text{ }^{\circ}\text{C}$  -  $290\text{ }^{\circ}\text{C}$  (peak A) could have been due to the desorption of weakly adsorbed ammonia and ii) de-hydroxylation could have occurred at high temperatures removing Bronsted acid sites from the zeolites. Lewis acid sites would be formed after de-hydroxylation. [Ward, 1967]

During the first TPD analysis some de-hydroxylation could have occurred. This de-hydroxylation could have removed most of the weak and strong Bronsted acid sites. If in the TPD profiles of other 1.55 % Pt/KL samples, the first peak (temperature range  $240\text{ }^{\circ}\text{C}$  -  $290\text{ }^{\circ}\text{C}$ ) had been due to ammonia desorption from weak Bronsted acid sites only, then this peak would not have been exhibited in the repeat TPD analysis. Therefore the presence of the peak in the temperature range  $240\text{ }^{\circ}\text{C}$  -  $290\text{ }^{\circ}\text{C}$  in the repeat TPD analysis indicated that this peak could have been due to the desorption of weakly adsorbed ammonia. Compared to the first TPD profile, the peak in the temperature range  $240\text{ }^{\circ}\text{C}$  -  $290\text{ }^{\circ}\text{C}$  for the repeat TPD analysis was smaller. This could have indicated that in the first TPD analysis profile, desorption of ammonia from weak Bronsted acid sites could have contributed to the size of peak A (range  $240\text{ }^{\circ}\text{C}$  -  $290\text{ }^{\circ}\text{C}$ ). After de-hydroxylation during the first TPD analysis, the weak Bronsted acid sites would have been removed from the zeolite. The contribution of ammonia desorbed from these sites would be absent in the repeat TPD analysis resulting in a smaller peak in the temperature range  $240\text{ }^{\circ}\text{C}$  -  $290\text{ }^{\circ}\text{C}$ .

The peak observed at  $450\text{ }^{\circ}\text{C}$  in the first TPD profile was not observed in the repeat TPD profile. This could have indicated that de-hydroxylation of the strong Bronsted acid sites had occurred during the first TPD analysis. The steady increase in the ammonia desorption after

97 minutes (580 °C) could have been due to ammonia being desorbed from Lewis acid sites. These are known to be stronger than Brønsted acid sites. [Mielczarski *et al.*, 1992]. The slow desorption of the ammonia could have occurred because the temperature had been kept constant at 600 °C. If de-hydroxylation to form Lewis acid sites occurred as a result of sample treatment at 600 °C, then the slow desorption of ammonia assigned to desorption from Lewis acid sites should have been observed in figure 3.20 showing the TPD profile of 1.55 % Pt/KL calcined at 600 °C in oxygen. After calcination, the sample whose TPD profile is shown in figure 3.20 was exposed to the atmosphere before carrying out the TPD analysis (section 2.2.5). The Lewis acid sites could have reacted with water vapour in the atmosphere to restore some Brønsted acidity. This could explain why some Brønsted acidity and no Lewis acidity was observed on the sample which had been calcined at 600 °C in oxygen.

## 4.8 TEM And EDX Analysis

Transmission Electron Microscopy (TEM) confirmed the results obtained via carbon monoxide chemisorption as well as via the conversion of n-hexane. Catalyst samples with high metal dispersion values had TEM images showing very few visible small platinum clusters (plates 3.2 and 3.5). One of these samples with a platinum dispersion of 111 % showed a high performance in the hydrogenation reactions (figures 3.40 and 3.41) and in the conversion of n-hexane (figure 3.42). Samples with low metal dispersion values had TEM images with many large and clearly visible platinum clusters (plates 3.3 and 3.6). As expected, one of these samples showed a low performance for the aromatisation of n-hexane (figure 3.42).

Energy Dispersive X-ray analysis (EDX) confirmed that the large clusters seen on TEM images were platinum particles and not contamination of the samples. The platinum content obtained for the samples which did not have visible clusters under TEM provided evidence that the platinum was present within the interior of the imaged Pt/KL crystallites. Since this platinum could not be imaged by the electron microscope (for example plate 3.5), it could be inferred that the platinum particles were very small and well dispersed in the zeolite.

## 4.9 Reactions

### 4.9.1 Hydrogenation Reactions

#### 4.9.1.1 Hydrogenation of cyclohexene

Hydrogenation is a metal catalysed reaction. The performance for the catalyst with the high platinum dispersion (111 %) in the hydrogenation of cyclohexene to cyclohexane was higher than the performance of the catalyst with low platinum dispersion (44 %) as shown in figure 3.40. In a highly dispersed Pt/KL sample, most of the platinum would be in the pores of the zeolite while in a poorly dispersed catalyst, most of the platinum would be on the external surface of the zeolite. This could be verified by the TEM image presented in plate 3.3 which showed large platinum clusters of up to 250 Å. Since the zeolite pores are 7.4 Å in diameter, these large platinum clusters would be on the external surface of the zeolite.

Since cyclohexene is a small molecule, it would be expected to adsorb onto the platinum particles located either in the zeolite pores or on the external surface of the zeolite. Thus platinum particles in the zeolite pores or on the external surface of the zeolite would be accessible to the cyclohexene. However, the catalyst with a higher platinum dispersion would have more platinum sites accessible to the cyclohexene compared to the catalyst with low platinum dispersion. This could explain why 98 % conversion of cyclohexene to cyclohexane was observed for the catalyst with 111 % platinum dispersion while 78 % conversion of cyclohexene to cyclohexane was observed for the catalyst with 44 % platinum dispersion (figure 4.40).

#### 4.9.1.2 Hydrogenation of cyclododecene

It had been initially assumed that cyclododecene would be too large to enter into the pores of zeolite KL. Therefore it was hydrogenated over a sample in which a larger fraction of the platinum particles could be on the zeolite surface (44 % dispersion) as well as over a Pt/KL sample whose platinum would be predominantly in the zeolite pores (111 % dispersion). It was believed that the latter catalyst would show low activity for the hydrogenation of a bulky molecule while the catalyst with platinum particles outside the pores of the zeolite would

show a higher activity for the same reaction.

Using the molecular size simulation package BIOSYM, the minimum molecular size of the cyclododecene was determined to be 6.2 Å. Thus this molecule would be able to enter the pores of the zeolite KL which have a diameter of 7.4 Å. This therefore meant that the hydrogenation of cyclododecene over Pt/KL samples was similar to the hydrogenation of cyclohexene over the same catalyst samples. Therefore similar results were obtained. The sample with well dispersed platinum (111 % dispersion) showed 94 % conversion of cyclododecene to cyclododecane while the sample with low dispersion (44 % platinum dispersion) showed 21 % conversion of cyclododecene to cyclododecane (figure 4.41). As for the hydrogenation of cyclohexene, the reason for the difference in catalyst performance would be due to the fact that the catalyst with a higher platinum dispersion would have more platinum sites accessible to the cyclododecene compared to the catalyst with low platinum dispersion.

#### 4.9.2 Conversion Of N-hexane

Figure 3.42 shows the comparison between the performance of 1.55 % Pt/KL with a high platinum dispersion value (111 %) and the Pt/KL sample with a low dispersion value (44 %). As expected, the conversion of n-hexane over a well dispersed Pt/KL sample was higher than the conversion of n-hexane over a poorly dispersed Pt/KL. At steady state the conversion over a sample with 111 % dispersion was nearly double the conversion over a sample with 44 % dispersion. At the conditions of operation, the selectivity to benzene was not very high for both catalysts (table 3.19). At a higher temperature of 450 °C and a lower WHSV of about 1 hr<sup>-1</sup>, the selectivity to benzene could be increased.

These results correlated well with the results from carbon monoxide chemisorption, TEM and EDX studies. The results indicated that Pt/KL samples that have been treated under conditions that yield well dispersed platinum would have higher catalytic activity compared to Pt/KL samples with poorly dispersed platinum.

## **CHAPTER 5**



## **5 CONCLUDING REMARKS AND RECOMMENDATION**

### **5.1 Platinum Loading Procedure**

In liquid state ion exchange, it was established that for the levels of platinum ion exchange studied (1.55 wt %), the temperature of ion exchange, time of ion exchange and ion exchange solution concentration did not have an effect on the final distribution of the platinum. For the preparation of commercial catalysts with about 1.55 % platinum, liquid ion exchange could be performed at 25 °C for about 1 hour. This would save energy and time. Impregnation was found to result in a somewhat lower platinum dispersion compared to samples that had been loaded with platinum via liquid state ion exchange.

Solid state ion exchange resulted in the platinum being well dispersed on the zeolite KL. For samples activated in oxygen at 350 °C, and reduced in hydrogen at 350 °C solid state ion exchange yielded the highest platinum dispersion compared to liquid state ion exchange and impregnation methods. This observation was confirmed by carbon monoxide chemisorption results as well as transmission electron microscopy (TEM) results. However about 50% of the platinum added to the zeolite was ion exchanged at the conditions studied. It would be advantageous to perform further solid state ion exchange experiments in order to determine the optimum conditions that would enable most of the added platinum to be ion exchanged onto the zeolite.

### **5.2 Catalyst Activation**

#### **5.2.1 Calcination Medium.**

Of the three calcination media studied at 350 °C, oxygen gave the best metal dispersion (111%) while nitrogen and hydrogen gave similar but lower metal dispersion values (81% and 78% respectively). Calcination in oxygen would result in the decomposition of ammonia ligands to yield nitrogen and water thus limiting the degree of auto-reduction of

platinum ions by co-ordinating ammonia ligands. Calcination in hydrogen and nitrogen at 350°C resulted in the formation of larger platinum particles compared to samples that had been calcined in oxygen. The reasons for the formation of larger particles could have been the reduction of the platinum ions by ammonia ligands with subsequent formation of mobile hydrides. The mobile hydride would coalesce to form large particles. It was also observed that for calcination at 350°C the range of oxygen flowrate studied (50 - 600 ml/minute/g) did not influence the dispersion of the platinum.

### 5.2.2 Calcination Temperature

Of the two calcination temperatures studied (350°C and 600°C), it was established that calcining at 350°C would yield better dispersion compared to calcination at 600°C. Calcination at temperatures lower than 350 °C could result in partial decomposition of the ammonia ligands. The partially decomposed platinum complex could easily form hydrides when reduced in hydrogen. This would lead to sintering of the platinum.

The rate of temperature increase from room temperature (25 °C) to 350 °C had no effect on the dispersion of the platinum in zeolite KL. The literature reviewed advocated a slow temperature increase rate of 0.5°C/minute and an oxygen flowrate of 1 000 ml/ minute/ g in order to limit the reduction of platinum ions by the co-ordinating ammonia ligands. At the flowrates employed (50 - 600 ml/minute/g) the rate of temperature increase was found to have a negligible effect on the platinum dispersion.

### 5.2.3 Calcination Time in Oxygen.

It was established that calcining in oxygen for short periods (2 hours) or for long periods (11 hours) did not affect dispersion of the platinum.

## 5.3 Catalyst Reduction

### 5.3.1 Temperature Programme Reduction (TPR) Studies

TPR studies showed that platinum species in zeolite KL were reduced at three temperature ranges namely : below 42 °C, 110 °C - 120 °C and 350 °C - 420 °C. The reduction "shoulder" observed at temperatures less than 42°C was attributed to the reduction of PtO while the reduction peak observed in the range 110 °C - 120 °C was attributed to the reduction of Pt<sup>2+</sup> ions situated in the channels of zeolite KL. The reduction peak observed in the temperature range 350 °C - 420 °C was attributed to the reduction of Pt<sup>2+</sup> ions in the locked sites of the zeolite KL. Calcination of Pt/KL at 600 °C in oxygen caused most of the platinum ions to migrate to the locked sites where they required higher temperatures for reduction in hydrogen.

### 5.3.2. Reduction Temperatures

It was established that of the reduction temperatures looked at in hydrogen (150°C, 350°C and 600 °C), 350 °C would yield the most dispersed as well as the most catalytically active Pt/ KL catalyst. Reduction at 150 °C would leave some of the Pt<sup>2+</sup> ions situated in the locked sites unreduced thus rendering them inactive for catalytic purposes. Reduction in hydrogen at 600 °C would result in the sintering of the platinum particles.

The rate of temperature increase during reduction had a negligible effect on the dispersion of the platinum. This was in agreement with some of the reviewed literature.

### 5.3.3 Reduction Medium

Hydrogen was found to be a better reduction medium than carbon monoxide. It is possible that during reduction in carbon monoxide, platinum carbonyls were formed resulting in the agglomeration of platinum particles. In order to confirm the presence of platinum carbonyls after reduction in carbon monoxide, Fourier Transform Infra Red (FTIR) analysis could be

performed on the sample. If the platinum carbonyls were present, then a broad band at  $2\,000\text{ cm}^{-1}$  characterising the Pt-CO band would be observed. [Besoukhanova *et al*, 1981] During reduction in carbon monoxide the Boudouard reaction could have taken place resulting in the formation of small amounts of carbon which could have been deposited onto the zeolite KL causing blockage of the pores thus making platinum particles in the pores inaccessible to incoming molecules. The carbon could also have been deposited on the platinum particles thus making them unavailable for carbon monoxide chemisorption. This could have resulted in the low platinum dispersion values obtained. Pt/KL catalysts with blocked pores would have a low performance in catalytic reactions. Reduction in carbon monoxide did not alter the total acidity of the sample that had been calcined in oxygen. However, the ratio of weak Bronsted acidity to strong Bronsted acidity was increased by reduction in carbon monoxide.

#### **5.3.4 Reduction Time**

The reduction times looked at (2 hours and 7 hours) did not significantly affect the distribution of the platinum in zeolite KL.

### **5.4 Comparison Between The Pt/ KL And Pt/ HY Catalysts**

Under similar ion exchange conditions, slightly less platinum was ion exchanged onto zeolite HY (1,43%) compared to the platinum loaded onto zeolite KL (1,55%). The dispersion of platinum in Pt/ HY samples was less than that obtained in Pt/KL samples calcined and reduced under similar conditions. This difference in dispersion was attributed to the ability of non acidic zeolite KL to stabilise small platinum particles by enhancing the interaction between the platinum and the zeolite. Potassium which is basic could interact strongly with the small platinum particles to increase the charge density on these platinum particles.

### **5.5 Hydrogen Spillover.**

High mole ratios of  $\text{H}_2/\text{Pt}$  obtained during TPR studies of Pt/HY were attributed to hydrogen spillover onto the HY support. The temperature at which the hydrogen spill over was observed ( $110\text{ }^\circ\text{C}$ ), corresponded with the temperatures reported in the literature for

maximum hydrogen spill over onto Pt/ Na HY catalyst.

The Pt/KL samples could not be assayed for platinum dispersion using hydrogen chemisorption. This was because at the conditions of chemisorption analysis, hydrogen spill over was occurring. Recent work by Sharma *et al*, [1994] has shown that under certain conditions, hydrogen spill over can occur onto Pt/KL catalysts.

## 5.6 Acidity

TPD profiles of Pt/ KL samples showed peaks representing ammonia desorption at three sets of temperature ranges namely 240°C - 290 °C; 340°C - 350°C and 520°C - 600 °C. The first peak range was attributed to the desorption of weakly adsorbed ammonia while the ranges of the second and the third peaks were attributed to the desorption of ammonia from weak Bronsted acidity and from strong Bronsted acidity respectively.

It was also established that at temperatures around 600°C de-hydroxylation of hydroxyl groups was occurring resulting in the removal of Bronsted acid sites.

Untreated zeolite KL exhibited two peaks : one in the range 240°C - 290 °C and the second in the range 520 °C - 600 °C. The first peak could have represented the desorption of weakly adsorbed ammonia while the second peak could have represented the desorption of ammonia from strong Bronsted acid sites. This indicated that the untreated zeolite KL contained some acidity possibly due to charge stabilising cations or due to the Bronsted acidity left over from the synthesis of the zeolite.

Calcination of Pt/KL samples without subsequent reduction was found to increase the Bronsted acidity of the catalysts. The acidity increase was greater for samples calcined in nitrogen than for samples calcined in oxygen. This indicated that auto-reduction of Platinum by ammonia ligands was occurring in these samples during calcination.

Calcination at 600 °C resulted in the removal of Bronsted acid sites via de-hydroxylation.

Reduction in carbon monoxide did not increase the total acidity of the sample that had been calcined in oxygen. However, reduction in carbon monoxide increased the ratio of strong Bronsted acidity to weak Bronsted acidity without altering the total acidity of the sample. It was suggested that the increase in the ratio occurred as a result of an interaction between the carbon monoxide and the strong Bronsted acidity.

Using KCl, it was possible to remove some acidity via solid state ion exchange from Pt/KL samples that had been reduced in hydrogen. However, less than half of the added  $K^+$  ions were exchanged onto the zeolite in place of the  $H^+$  ions. In order to establish the optimum conditions for replacing the  $H^+$  with  $K^+$  ions via solid state ion exchange, more experiments would be necessary.

It would be advantageous to perform TPD analysis on Pt/KL samples prepared via impregnation and via solid state ion exchange. Performing solid state ion exchange as well as calcination of impregnated samples in oxygen would be expected to decompose the ammonia ligands resulting in the formation of nitrogen and water. The water would then react with the  $Pt^{2+}$  ions to yield  $PtO$  and  $H^+$  ions. The  $H^+$  ions could then react with the chloride ions present during solid state ion exchange to yield hydrochloric acid vapour. This would reduce the amount of Bronsted sites on the zeolite.

## 5.7 Chemical Reactions

### 5.7.1. Hydrogenation Reactions

The performances of a poorly dispersed and a well dispersed Pt/ KL catalysts in the hydrogenation of cyclohexene showed 78 % conversion and 98 % conversion respectively. This was expected because cyclohexene was readily accessible to the platinum in both catalysts. However the well dispersed catalyst had more exposed active sites than the poorly dispersed catalyst. A similar trend was observed for the hydrogenation of cyclododecene over a well dispersed and a poorly dispersed Pt/ KL (94 % conversion and 21 % conversion respectively). Both cyclohexene and cyclododecene could easily enter in to the pores of the zeolite KL.

It would be advantageous to confirm that catalysts exhibiting low platinum dispersion have large platinum particles predominantly on the external surface of zeolite KL while those with high platinum dispersion have well dispersed platinum particles predominantly in the pores of the zeolite. This could be done by studying the hydrogenation of a molecule more bulky than cyclododecene such as 3,5-di-*t*-butyl phenyl ether. For the hydrogenation of this compound, the performance of a poorly dispersed catalyst should be high while the performance of a well dispersed catalyst should be low.

#### **5.7.1. Aromatisation of n-hexane**

The Pt/ KL sample with well dispersed platinum (111%) had a high performance for the conversion of n-hexane when compared to the catalyst with poor platinum dispersion (44%). This therefore meant that it was very important to carefully produce industrial catalysts with well dispersed platinum for the aromatisation of n-hexane.

**LIST OF REFERENCES**

- Adler S, Kearney J. *The Physical Nature Of Supported Platinum* in **Journal of Physical Chemistry** vol 64 ,1960, pp 208-212.
- Alvarez F; Giannetto G; Montes A; Ribeiro F; Peot G; Guisnet M *Catalytic Properties of PtH Zeolites: Effect of Activation Conditions And of Coke Deposition.* in **Studies in Surface Science And Catalysis " Innovations in Zeolite Technology"**, Grobe *et al* (Eds),Elsevier, Amsterdam, vol 37, 1988, pp 479-486.
- Beaumont P; Pichat I; Barthomeuf D; Trambouze Y; *Infrared Study of Ultrastable Faujasite Type Zeolites* in **Proceedings of The 5th International Conference on Catalysis**, 1992.
- Becker E.R; Nuttall T.A *Controlled Catalyst Distribution on Supports by Co-impregnation* Symposium on " Scientific Basis For The Preparation of Heterogenous Catalysts ", 2nd International Symposium - September 1978 Louvain La Neuve, Belgium, pp 1-9.
- Beran S; Wichterlova B; Karge H *Solid State Incorporation of Manganese (2+) Ions in H-ZSM-5* in **Journal of Chemical Society Faraday Transactions 2** vol 86, 1990, pp 3033 - 3034.
- Besoukhanova C; Guidot J; Barthomeuf D *Platinum Zeolite Interactions In Alkaline L Zeolites - Correlations Between Catalytic Activity And Platinum State* **Journal of Chemical Society. Faraday Transactions 1** vol 77, 1981, pp 1595-1604.
- Besoukharoun E. in **Proceedings of The 7th International Congress on Catalysis**, 1980, p 1420.
- Beyer H; Karge H.G; *Solid State Ion Exchange in Zeolites : Part 1 Alkaline Chlorides/ZSM-5* in **Zeolites** vol 8, 1988, pp 79-81.
- Bong Hong S; Mielczarski E; Davis M.E *Aromatisation of n-Hexane by Platinum-Containing Molecular Sieves* in **Journal of Catalysis** vol 134 1991, pp 349-358
- Breck D.W ; **Zeolites And Molecular Sieves** John Wiley And Sons 1974.



- Chang J.R; Xu Z; Purnell S.K; Gates B.C *Synthesis And Decarbonylation of Platinum Carbonyl Cluster Anions in Zeolite NaY Made Basic By Treatment With CsOH* in **Journal of Molecular Catalysis**, vol 80, 1993, pp 49-58
- Chmelka B.F; Ryoo S; Liu B; Mernaval L.C; Radke C.J; Petersen E. E and Pine A *Probing Metal Cluster Formation in NaY Zeolite by  $^{129}\text{Xe}$  NMR* in **Journal Of American Chemical Society** vol 110, 1988 pp 4465-4467
- Chmelka B.F; Rosin R.R; Went G; Bell A; Radke C; Petersen E *Chemistry of Pt-NaY Zeolite Preparation* in **Studies in Surface Science And Catalysis "Zeolites Facts, Figures Future"** Jacobs *et al* (Eds), Elsevier, Amsterdam, vol 49B, 1991, pp 995-1004
- Cotton F.A; Wilkinson G; **Advanced Inorganic Chemistry** Fifth Ed. John Wiley And Sons, 1988
- Davies M.C and Suib S.L **Selectivity In Catalysis** American Chemical Society Symposium Series 517, American Chemical Society Washington, D.C 1993
- Delafosse D *Formation and Catalytic Properties of Nickel Metal Particles Supported on Zeolites* in **Studies in Surface Science And Catalysis "Catalysis by Zeolites"** Imelik *et al* (Eds) Elsevier, Amsterdam, vol 5, 1980, pp 235-243.
- Delafosse D *Dispersed Metal Particles In Zeolite Carriers* in **Journal de Chemie Physique** vol 83, 1986 pp 791-799.
- Derouane E. G; Vanderveken D J; *Structural Recognition And Preorganisation in Zeolite Catalysis: Direct Aromatisation of n - Hexane on Zeolite L-based Catalyst* in **Applied Catalysis** vol 45, 1988 pp L15-L21
- Dessau D; *Shape Selective Platinum / ZSM-5 Catalysts* in **Journal Of Catalysis** vol 89, 1984, pp 520-527.
- Dong J.L; Zhu J.H; Xu Q.H *Influence of Structure And Acidity-Basicity of Zeolites on Platinum Supported Catalysts For n-C<sub>6</sub> Aromatisation* in **Applied Catalysis A : General**, vol 112, 1994, pp 105-115.

- Dyer A **An Introduction To Zeolite Molecular Sieves** John Wiley And Sons, Chichester, 1988.
- Engelen C.W; Wolthuizen J.; Van Hoof J.H and Zandergen H. W; *Preparation of Bifunctional Pt/H-ZSM5 Catalysts And Their Application For Propane Conversion* in **Studies in Surface Science And Catalysis "New Developments in Zeolite Science And Technology"** Elsevier , Amsterdam, vol 28, 1986, pp 709-716.
- Exner D; Jaeger N; Moller K; Schultz-Ekloff G *Thermal Analysis of The Decomposition Mechanism of Platinum And Palladium Tetrammine Faujasite X* in **Journal of Chemical Society Faraday Transactions I** vol 78, 1982, pp 3537-3544
- Forger K and Jaeger H *Re-dispersion of Pt-Zeolite Catalysts With Chlorine* in **Applied Catalysis** vol 56, 1989, pp 137-147.
- Gallezot P; Alarcon-Diaz J; Daemon A; Renouprez A; Imelik B *Location and Dispersion of Platinum in PtY Zeolites* in **Journal of Catalysis** vol 39, 1975, pp 334-349.
- Gallezot P *The State And Catalytic Properties of Platinum And Palladium Faujasite Type Zeolites* in **Catal. Rev. Sci. Eng.** vol 20(1), 1979, pp 121-154.
- Heise M.S; Schwarz J.A; *Preparation of Metal Distributions Within Catalyst Supports* in **Studies in Surface Science And Catalysis "Preparation of Catalysts IV"** Elsevier, Amsterdam, vol 31, 1987, pp 1-14.
- Hicks R.F; Han W.J; Kooh A.B *Effect of The Alkali Cation on Heptane Aromatization in L Zeolite* in **Proceedings of the 10th International Congress on Catalysis**, 1992 Budapest, Hungary. Guzzi L *et al* (Eds), "New Frontiers in Catalysis". Elsevier 1993, pp 1043-1052.
- Holland C.D; Anthony R. G **Fundamentals Of Chemical Reaction Engineering** Prentice-Hall International Series In The Physical And Chemical Engineering Series, 1979
- Homeyer S.T; and Sachtler W.M.H *Design of Metal Clusters in NaY Zeolites* in **Studies in Surface Science And Catalysis "Zeolite Facts, Figures, Future"** Jacobs *et al* (Eds), Elsevier, Amsterdam, vol 49B, 1991, pp 975-984.

- Hong S. B; Mielczarski E; Davis M.E *Aromatisation of n-Hexane by Platinum-Containing Molecular Sieves* in **Journal of Catalysis** vol 134 1991, pp 349-358
- Hughes J.R; Buss W.C; Tamm P.W; Jacobson R.L; *Aromatisation Of Hydrocarbons Over Platinum Alkaline Earth Zeolites* in **Studies in Surface Science And Catalysis** Gates B.C *et al* (eds), vol 28, 1986, pp 725-732.
- Ihee H; Becue T; Ryoo R; Potvin C; Manoli J-M; Djega Mariadassou G; *Clustering of Platinum Atoms In Zeolite EMT Supercage: Comprehensive Physicochemical Characterisation* in **Studies in Surface Science And Catalysis** "Zeolites And Related Microporous Materials: State of The Art 1994" Weitkamp *et al* (Eds) Elsevier Science B.V., Amsterdam, vol 84, 1994, pp 765-772.
- Jacobs P.A *Zeolites as Bifunctional Catalysts* in **Carboniogenic Activity of Zeolites**, Elsevier, Amsterdam, 1977, pp 183-227.
- Jacobs P.A *Metal Clusters and Zeolites* in **Studies in Surface Science And Catalysis** "Metal Clusters in Catalysis" Gates B.C *et al* (Eds), Elsevier, Amsterdam, vol 29, 1986, pp 357-414.
- Kampers F.W.H; Engelen C.W.R; van Hooff J.H.C; and Koningsberger D.C *Influence of Preparation Method on The Metal Cluster Size of Pt/ZSM-5 Catalysts As Studied With Extended X-ray Absorption Fine Structure Spectroscopy* in **Journal of Physical Chemistry**, vol 94, 1990, pp 8574-8578.
- Karge H.G; Beyer K.H; Borberly G *Solid State Ion Exchange in Zeolites* in **Catalysis Today** vol 3, 1988, pp 41-52.
- Karge H.G; Beyer K.H; *Introduction of Cations Into Zeolites by Solid State Ion Exchange Reactions* in **Studies in Surface Science And Catalysis** " Zeolite Chemistry and Catalysis" Jacobs *et al* (Eds), Elsevier, Amsterdam, vol 69, 1991, pp 43-64.
- Karge H.G *Modifications of Zeolites And New Routes to Ion Exchange* in **Zeolite Microporous Solids : Synthesis, Structure And Reactivity**. E. Derouane *et al* (Eds). Nato ASI Series C : Mathematical And Physical Sciences. Kluwer Academic Publishers, Dordrecht, vol 352, 1992, pp 273-290.

- Kerr , G.T Proceedings 3rd International Conference on Molecular Sieves Advances in **Chemical Series**, No 121 American Chemical Society; Washington D.C. 1973
- Khouw and Davies *Shape Selectivity With Zeolites And Molecular Sieves* pp 208-221 in **Selectivity In Catalysis**, Davies and Suib as (Eds), American Chemical Society Symposium Series 517, American Chemical Society Washington, D.C 1993.
- Kip B. J; Duivenvoorden F.B.B; Koningsberger D.C; Purs R *Determination of Metal Particle Size of Highly Dispersed Rh, Ir, and Pt Catalysts by Hydrogen Chemisorption And EXAFS* in **Journal of Catalysis**, vol 105, 1987, pp 26-38.
- Kouwenhoven H.W; Kroes B; *Preparation Of Zeolitic Catalysts* pp 497-529 in **Studies in Surface Science And Catalysis "Introduction To Zeolite Science And Technology"** Van Bekkum *et al* (Eds), Elsevier, Amsterdam, vol 58, 1991, pp 497-529.
- Kramer R; Andre M; *Adsorption of Atomic Hydrogen on Alumina by Hydrogen Spillover* in **Journal of Catalysis** vol 58, 1979 pp 287-295
- Kustov L. M; Ostgard D; Sachtler W.M.H; *I.R. Spectroscopic Study of Pt/KL Zeolites Using Adsorption Of CO As A Molecular Probe* in **Catalysis Letters** vol 9, 1991, pp 121-126.
- Larsen G; Haller G. C *On The Deactivation of Pt/L Zeolite Catalysts* in **Catalysis Letters**, vol 17, 1993, pp 127-137.
- Lemaitre J.L; Menon P.G; Delannay F *The Measurement Of Catalyst Dispersion in Characterization Of Heterogeneous Catalysts*, Delannay F (Ed) Marcel Dekker (1984)
- Micromeritics Manual, ASAP 2000 Chemi System Operator's Manual V3.00, Part No. 200-42808-01, April 1993.
- Mielczarski E; Bong Hong S; Davis R.J; Davis M.E *Aromatisation of n - Hexane By Platinum - Containing Molecular Sieves* in **Journal of Catalysis** vol 134, 1992, pp 349-358.

- Ostgard D.J; Kustov L; Poepelmeier K.R; Sachtler W.M.H; *Comparison of Pt/KL Catalysts Prepared by Ion Exchange or Incipient Wetness Impregnation* in **Journal Of Catalysis**, vol 133, 1992, pp 342-357.
- Park S.H; Tzou M.S; Sachtler W.M.H; *Temperature Programmed Reduction And Re-Oxidation of Platinum in Y-Zeolites* in **Applied Catalysis**, vol 24, 1986, pp 85-98
- Persaud L; Bard A; Campion A; Fox M; Mallouk T; Webber S; White J A *New Method For Depositing Platinum Exclusively On The Internal Surface of Zeolite L* in **Journal of Inorganic Chemistry**, vol 26, 1987, pp 3825 - 3827.
- Reagan W; Chester A and Kerr G.T *Studies of The Thermal Decomposition And Catalytic Properties Of Some Platinum, Palladium Ammine Zeolites* in **Journal Of Catalysis**, vol 69, 1981, pp 80-100.
- Roland U; Karge H.G; Winkler H *Hydrogen And Deuterium Adsorption On Zeolite Supported Platinum Evidence For Hydrogen And Deuterium Spillover* in **Studies in Surface Science And Catalysis "Zeolites And Related Microporous Materials: State of The Art 1994"** Weitkamp *et al* (Eds), Elsevier Science B.V., Amsterdam, vol 84, 1994, pp 1239-1245.
- Sachtler W.M.H *Zeolite-Transition Metal Catalysis by Design* in **Catalysis Today** vol 15, 1992, pp 419-429
- Scholten J.J.F *Metal Surface Area And Metal Dispersion In Catalysts* in **Studies in Surface Science And Catalysis "Preparation Of Catalysts II"** Delmon B *et al* (Eds), Elsevier Science B.V., Amsterdam, vol 3, 1978, pp 685-714.
- Schoonheid R,A; Vandame L. J; Jacobs P.A and Uytterhoeven J.B *Chemical Surface And Catalytic Properties Of Stoichiometrically Exchanged Zeolites* in **Journal Of Catalysis** vol 43, 1976, pp 292-303.
- Sharma S.B; Miller J.T; Dumesic J.A; *Microcalorimetric Study of Silica-and Zeolite-Supported Platinum Catalysts* in **Journal Of Catalysis** vol 148, 1994, pp 198-204

- Shapiro E.S; Joyner R.W; Minachev K.M and Pudney P.D.A *Structural Studies of Platinum/ZSM-5 Catalysts* in **Journal of Catalysis** vol 127, 1991, pp 366-376.
- Skouge and Leary **Principles Of Instrumental Analysis** 4th Ed. Saunders College 1992
- Spenadel and M. Boudart, *Dispersion of Platinum on Supported Catalysts* in **Journal of Physical Chemistry**, vol 64, 1960, pp 204-207.
- Spurr A.R *A low viscosity epoxy resin embedding medium for electron microscopy* in **Journal of Ultrastructure Res.** , volume 26, 1996, pp 31-42.
- Sugimoto M, Murakawa T, Hirano T and Ohashi H *Novel Regeneration Method Of Pt/KL Zeolite Catalyst For Light Naphtha Refining* in **Applied Catalysis A: General** vol 95, 1993, pp 257-268.
- Sugimoto M; Katsuno H and Murakawa T *Improvement of Platinum Supported Zeolite Catalyst For n-Hexane Aromatisation By Halocarbon Treatment And Alkaline Soaking* in **Applied Catalysis A: General** vol 96, 1993, pp 201-216.
- Szostak R **Molecular Sieves -: Principles Of Synthesis And Identification** Van Nostrand Reinhold, 1989.
- Tauster and Steger *Molecular Die Catalysis: Hexane Aromatisation Over Pt/KL* in **Journal of Catalysis**, vol 125, 1990, pp 387-389.
- Tzou M.S; Jiang H.J; Sachtler W.M.H; *Chemical Anchoring of Platinum in Zeolites* in **Applied Catalysis**, vol 20, 1986, pp 231-238.
- Tzou M.S; Jiang H.J; Sachtler W.M.H *Genesis And Catalysis Of Metal Particles In Zeolites* in **React. Kinet. Catal. Lett.** vol 35, Nos 1-2, 1987, pp 207-217.
- Tzou M.S; Teo B,K; Sachtler W.M.H *Formation Of Pt Particles In Y Type Zeolites* in **Journal Of Catalysis**, vol 113, 1988, pp 220-235.
- Varian **Handbook on Analytical Methods For Flame Spectroscopy** - Publication No 85-100009-00 July 1979 Varian Techtron Pty, Ltd, Springvale, Australia.

- Vaarkamp M; Van Grondelle J; Van Santen R.A; Miller J.T; Meyers B.L; Modica F.S; Lane G.S and Koningsberger D.C *Influence Of Hydrogen Pretreatment On Structural And Catalytic Properties Of A Pt/K-LTL Catalyst* from the **Proceedings of the Ninth International Zeolite Conference Montreal**, R. von Ballmoos *et al* (eds.), 1993, pp 433-440.
- von Ballmoos R; Higgins J.B **Zeolite - Collection of Simulated XRD Powder Diffraction Patterns For Zeolites** vol 10, No. 5, Butterworth - Heinemann, 1990
- Ward J.W The Nature Of Active Sites In Zeolites : i. The Decationated Y Zeolite in **Journal of Catalysis**, vol 9, 1967, pp 225-236
- Wilson G.R and Hall W.K *Studies of The Hydrogen Held by Solids XVIII. Hydrogen And Oxygen Chemisorption on Alumina And Zeolite Supported Platinum* in **Journal Of Catalysis** vol 47, 1970, pp 190-206.
- Whyte T.E *Metal Particle Size Determination Of Supported Metal Catalysts* in **Journal of Catalysis**, vol 81, 1973, pp 117-134.
- Zheng J; Dong J-L; Xu Q-H; *Study of Autoreduction And Dispersion of Platinum in  $\beta$  Zeolite* **Studies in Surface Science And Catalysis "Zeolites And Related Microporous Materials: State of The Art 1994"** Weitkamp *et al* (Eds), Elsevier Science B.V., Amsterdam, vol 84, 1994, pp 1641-1647.

## **APPENDIX A : ELEMENTAL ANALYSIS DURING LIQUID STATE ION EXCHANGE**

### **Data From Monitoring Of Liquid Ion Exchange**

Typical results obtained from the ion exchange of Pt onto zeolite KL

Volume of solution mixed with salt (ml)	:	450.0
Volume of solution mixed with zeolite ml	:	50.0
Dry Mass of zeolite (g)	:	4.4
Amount of platinum (g)	:	0.0682
Amount of platinum salt (g)	:	0.1245
Expected platinum mass % on zeolite	:	1.55
Ion exchange temperature (°C)	:	40.0
Ion exchange time (hours)	:	24

### **Atomic Absorption**

#### **Making Platinum Standard Solutions For Use In Atomic Absorption Studies**

For assaying the liquid samples, it was assumed that most of the platinum would be ion exchanged onto the zeolite leaving at the most, 20 % of the original platinum in the ion exchange solution (ie 12.5 ppm). The platinum concentration of the standard solution containing the highest platinum content was therefore higher than that containing 20 % of the platinum in the original ion exchange solution. The concentrations of the standard solutions chosen were 5, 15, 25 and 40 ppm. Platinum constituted 54.78 molar % of the salt utilised ( $\text{Pt}(\text{NH}_3)_4\text{Cl}_2 \cdot \text{H}_2\text{O}$ ). This meant that 100 ml of 5, 15, 25 and 40 ppm Pt contained 0.00091 g, 0.00274 g, 0.00456 g and 0.00730 g respectively of  $\text{Pt}(\text{NH}_3)_4\text{Cl}_2 \cdot \text{H}_2\text{O}$ . The platinum solution used had to contain 10 000 ppm of lanthanum which was the ionisation suppressant.



**Monitoring the ion exchange of platinum onto zeolite KL via AAS**

Ion exchange temperature : 100 °C

Dilution of solution : 1/10

**Typical Atomic Absorption Spectrum Analysis Results For Platinum**

Assay of platinum standard solutions

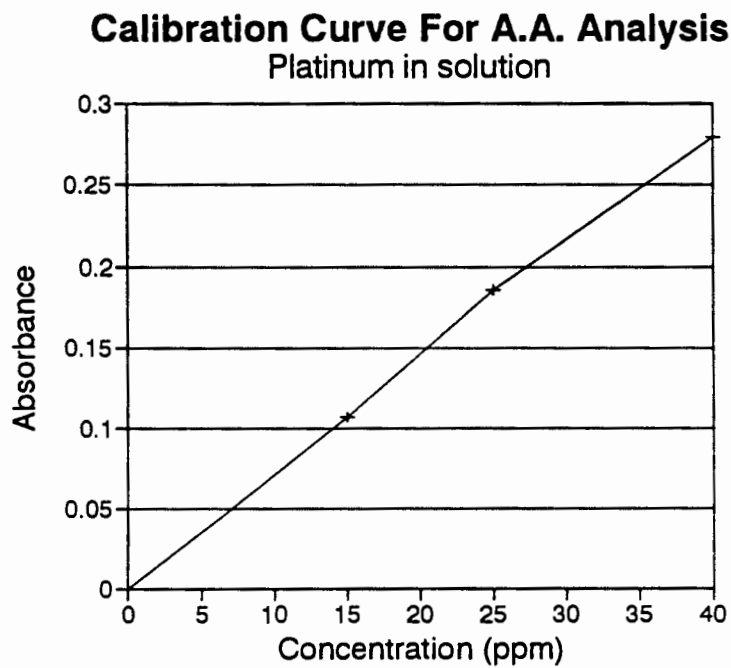


**Figure A1** showing the calibration curve obtained for platinum analysis

**AAS Results from 2 ml solutions periodically taken from ion exchange flask**

Sample Number	Ion Exchange Time (hrs)	ABSORBANCE				Concentration in AAS sample (ppm)
		A	B	C	D	
1	0.66	0.004	0.004	0.004	0.004	0.55
2	1	0.002	0.002	0.002	0.001	0.23
3	1.5	0.001	0.001	0.001	0.001	0.15
4	2	0.001	0.001	0.001	0.001	0.12
5	2.5	0.003	0.003	0.003	0.004	0.46
6	3	0.01	0	0	0.001	0.09
7	4	0.001	0.001	0.001	0.001	0.13
8	5	0.002	0.001	0.002	0.002	0.23
9	7	0.001	0.001	0.002	0.002	0.2
10	8.5	0.001	0.001	0.001	0.001	0.18
11	23.5	0.002	0.002	0.003	0.002	0.33
12	24.5	0.005	0.005	0.004	0.005	0.65
13	25.5	0.002	0.003	0.002	0.002	0.32

**Table A1** showing the results of the Atomic Absorption Spectroscopy (AAS) analysis for 2 ml solutions periodically taken from ion exchange flask.

**Determination of the solution concentration.**

Zeolite KL ion exchanged with platinum at 15 °C

Date 16/02/94		K/L, 0.069 g Pt, Ion exchange temperature : 15 °C						
		Dry Zeolite mass (g): 4.4						
Dilution for Pt : 10				Vol Of Liquid (ml) : 500				
Time (hrs)		Conc Pt in soln (ppm)	Mass Pt in soln mg	Mass Pt (g)	Moles Pt in soln	Moles Pt loaded	Mass Pt loaded	Mass % Pt loaded
0		13.80	69.00	0.069	0.0003	0.0000	0.0000	0.000
0.66		0.40	2.00	0.002	0.0000	0.0003	0.0670	1.523
1		0.91	4.55	0.005	0.0000	0.0003	0.0645	1.465
1.5		0.09	0.45	0.005	0.0000	0.0003	0.0686	1.558
2		0.52	2.60	0.003	0.0000	0.0003	0.0664	1.509
2.5		0.19	0.95	0.001	0.0000	0.0003	0.0681	1.547
3		0.11	0.55	0.001	0.0000	0.0003	0.0685	1.556
4		0.08	0.40	0.000	0.0000	0.0003	0.0686	1.559
5		0.14	0.70	0.001	0.0000	0.0003	0.0683	1.552
7		0.1	0.50	0.001	0.0000	0.0003	0.0685	1.557
8.5		0.16	0.80	0.001	0.0000	0.0003	0.0682	1.550
23.5		0.16	0.80	0.001	0.0000	0.0003	0.0682	1.550
24.5		1.02	5.10	0.005	0.0000	0.0003	0.0639	1.452
25.5		0.28	1.40	0.001	0.0000	0.0003	0.0676	1.536

**Table A2** showing the ion exchange results (liquid samples) for the incorporation of Pt onto zeolite KL at 15 °C.

## Zeolite KL ion exchanged with platinum at 100 °C

Date 16/02/94		Zeolite K/L, 0.069 g Pt, Ion Exchange Temp : 100 °C						
		Dry Zeolite mass (g): 4.4						
Dilution of Solutions : 1/10				Vol. of Ion Exchange Liquid : 500 ml				
Time (hrs)		Conc Pt (ppm)	Mass Pt in soln mg	Mass Pt (g)	Moles Pt in soln	Moles Pt loaded	Mass Pt loaded	Mass % Pt loaded
0.00		13.80	69.00	0.069	0.0004	0.0000	0.0000	0.000
0.66		0.55	2.75	0.003	0.0000	0.0003	0.0663	1.506
1		0.23	1.15	0.001	0.0000	0.0004	0.0679	1.542
1.5		0.15	0.75	0.001	0.0000	0.0004	0.0683	1.551
2		0.12	0.60	0.001	0.0000	0.0003	0.0684	1.555
2.5		0.46	2.30	0.002	0.0000	0.0004	0.0667	1.516
3		0.09	0.45	0.000	0.0000	0.0004	0.0686	1.558
4		0.13	0.65	0.001	0.0000	0.0003	0.0684	1.553
5		0.23	1.15	0.001	0.0000	0.0003	0.0679	1.542
7		0.20	1.00	0.001	0.0000	0.0003	0.0680	1.546
8.5		0.18	0.90	0.001	0.0000	0.0003	0.0681	1.548
23.5		0.33	1.65	0.002	0.0000	0.0003	0.0674	1.531
24.5		0.65	3.25	0.003	0.0000	0.0003	0.0658	1.494
25.5		0.32	1.60	0.001	0.0000	0.0003	0.0674	1.532

Table A3 showing the ion exchange results (liquid samples) for the incorporation of Pt onto zeolite KL at 100 °C.

### Atomic absorption of digested zeolites

Atomic absorption was used to determine the concentration of Pt, Na and K in the zeolite before and after the incorporation process. The method followed in the digestion of the zeolites is as follows

- i) Weigh about 0.3 grams of the zeolite into a par bomb.
- ii) Add 5ml of 40 % hydrofluoric acid into par bomb.
- iii) Close par bomb and insert it and its contents into safety metallic casing and place into an oven maintained at a temperature between 70 °C and 100 °C. Keep in oven for 40 minutes
- iv) Remove from oven and allow to cool to room temperature (25 °C). Open par bomb and check if all of the zeolite has dissolved.
- v) If some of the zeolite is undissolved then add 5 ml of 40 % hydrochloric acid and repeat steps iii) and iv).
- vi) Add 50 ml of boric acid ( 55 g boric acid crystals dissolved in 1000 ml) and transfer par bomb contents into a plastic volumetric flask. Make up the volume to 500 ml.
- vii) In the AAS assay, a certain volume of the solution in vi) was taken and noted. This was then made up to 10 ml containing 10 000 ppm of the ionisation suppressant (Lanthanum).

The standard solutions used to obtain the calibration curve contained the same proportions of hydrofluoric, hydrochloric and boric acids as in the samples to be analysed. As in assaying the liquid samples, the concentrations of the samples assayed for platinum had to be within the concentration range of the standard solutions. The concentration of the standard solution with the highest platinum content was higher than that obtained if all the platinum in the ion exchange solution had been loaded onto the zeolite. The calibration curves obtained for platinum is shown in figure A2.

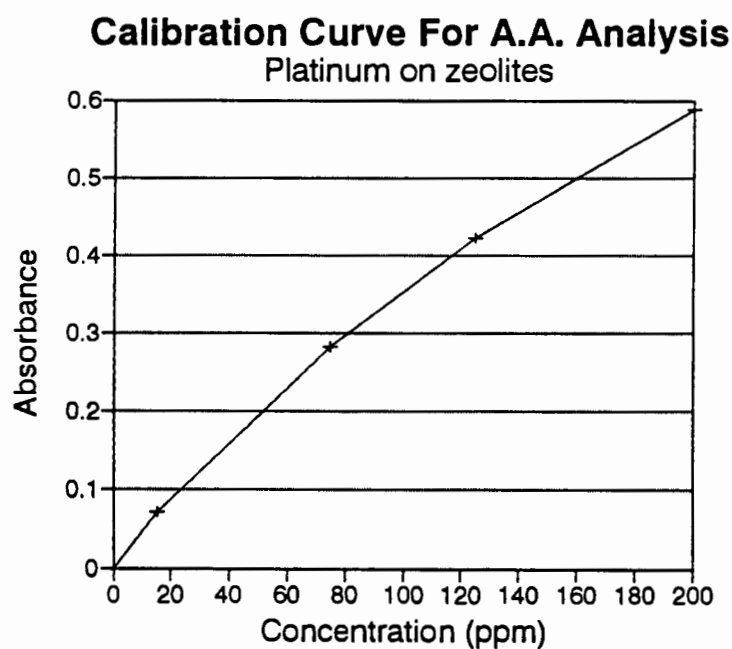


**Figure A2** showing the AAS calibration curve obtained for analysis of platinum in zeolites

#### Detailed Results of AAS For Digested Samples

Element Assayed	Sample Digested *	Dilution (ml digested solution in 10 ml used in AAS assay)	AAS value (ppm)	Conc. on Zeolite dry wt%
Pt	1.55 % Pt/KL	9	9.1	1.55
Pt	untreated KL	9	0.6	0.0
K	1.55 % Pt/KL	9	60.0	12.5
K	untreated KL	9	63.0	13.2

**Table A4** showing the ion exchange results obtained for digested zeolite samples

A typical calculation of how the above results were obtained is shown in example A

**Example A1 : calculating the amount of platinum on the 1.55 % Pt/KL using results in table A4**

Concentration of Pt in 10 ml of solution : 9.1 ppm (i.e 91 $\mu$ g/10ml)

Volume of digested solution in assayed solution : 9 ml

Therefore 9 ml of digested solution contained : 91  $\mu$ g Pt

500 ml of digested solution contained  $500/9 \times 91 = 5000 \mu\text{g Pt} = 5 \text{ mg Pt}$ .

Mass of un-dried zeolite digested : 0.3666 g

Taking the water content in the zeolite to be

12 % (as found experimentally), dried mass of zeolite : 0.3226 g

Therefore amount of Pt in the zeolite is given by  $0.005/0.3226 \times 100 = 1.55 \%$

## APPENDIX B : CHEMISORPTION

### Presentation Of Typical Chemisorption Results

Sample I.D.: 1.55% Pt/KL Calcined at 350°C in O<sub>2</sub> for 2 hours. Reduced in H<sub>2</sub> at 350 °C for 2 hours

### ANALYSIS LOG

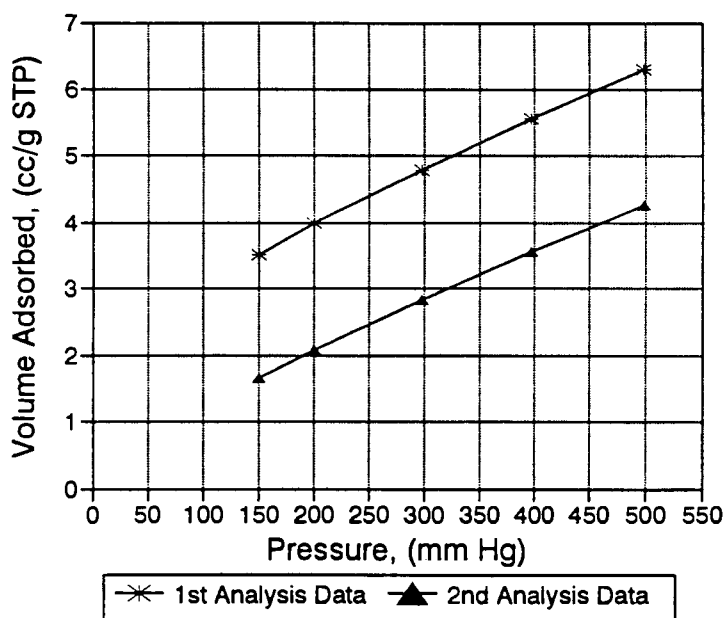
#### Analysis Data

Pressure (mm Hg)	Vol Adsorbed (cc/g STP)	Time Elapsed (HR:MN)
149.9708	3.5072	0:14
200.7032	3.9890	0:20
297.6689	4.7851	0:26
397.5305	5.5596	0:32
497.9197	6.2968	0:38

#### Repeat Analysis Data

Pressure (mmHg)	Vol Adsorbed (cc/g STP)	Elapsed Time (HR:MN)
153.3883	1.6772	1:36
201.5302	2.0726	1:42
298.6511	2.8180	1:48
397.7008	3.5466	1:54
497.9296	4.2533	2:00

### Isortherm Plot





**DIFFERENCE RESULTS**

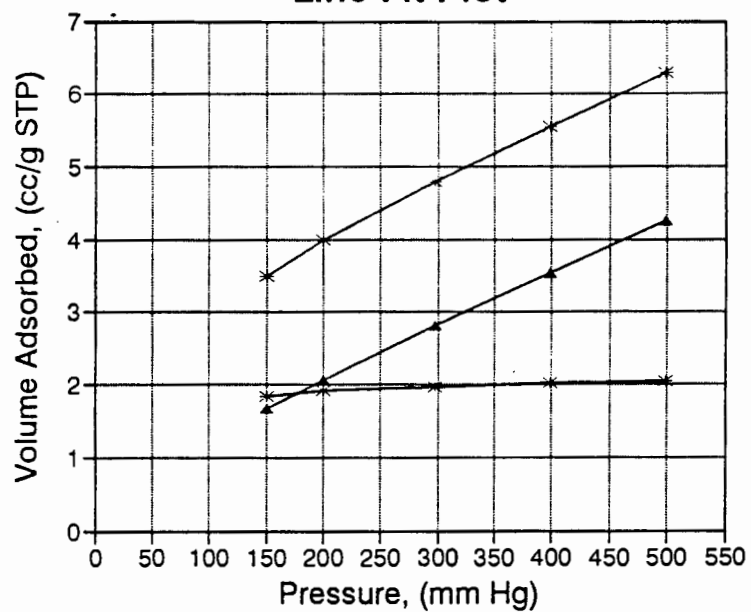
Metal Dispersion : 111.1005 %  
 Metallic Surface Area : 4.2027 m<sup>2</sup>/g  
 Difference Volume Average  
 (Vol 1st - Vol Repeat) : 1.955 cc/g STP

**ANALYSIS REPORT**

Analysis Isotherm		Repeat Analysis Isotherm			Volume Difference
Pressure (mmHg)	Vol Adsorbed (cc/g STP)	Pressure (mmHg)	Vol Adsorbed (cc/g STP)	Elapsed Time (HR:MN)	Vol 1st - Vol repeat (cc/g STP)
149.9708	3.5072	153.3883	1.6772	1:36	1.8350
200.7032	3.9890	201.5302*	2.0726*	1:42*	1.9164*
297.6689	4.7851	298.6511*	2.8180*	1:48*	1.9671*
397.5305	5.5596	397.7008*	3.5466*	1:54*	2.0130*
497.9197	6.2968	497.9296*	4.2533*	2:00*	2.0434*

\* included in the line fit and difference data.

## Line Fit Plot



—\*— 1st Analysis Data    —▲— 2nd Analysis Data    —\*— Vol Difference Data

## APPENDIX C : REACTIONS

### Hydrogenation Reactions

#### Hydrogenation Of Cyclododecene

##### Cyclododecene hydrogenation over a well dispersed Pt/KL sample

Hydrogenation of Cyclododecene over 1.55 % Pt/KL calcined at 350°C, O<sub>2</sub>, 6.33 hr, Reduced at 350, H<sub>2</sub>, 4.5 hr

Dispersion of metal using CO chemisorption (%) : 111

Reaction Conditions : Temperature = 105°C H<sub>2</sub> pressure = 10 bar

Internal standard : n-heptane

GC temperature programme : isothermal at 140 °C

Basis : 100 g total feed							
Compound	RMM	Mass Feed	Mols Feed	Retntn time (mins)	Mass% Prod	Mols Prod	Conversion %
n-heptane	100	49.5	0.495	7.92	50.240	0.502	
cyclododecane	168	1.57	0.009	43.71	47.000	0.280	
cyclododecene isomer 1	166	34.23	0.206	41.06	2.760	0.017	
cyclododecene isomer 2	166	14.7	0.089	43.71	0.000	0.000	94.359*
Total			0.799			0.799	

\* The conversion was based on both cyclododecene isomers.

**Table C1** showing the results obtained for the hydrogenation of cyclododecene over a well dispersed Pt/KL catalyst.

### Cyclododecene hydrogenation over a poorly dispersed Pt/KL sample

Hydrogenation of Cyclododecene over 1.55 % Pt/KL calcined at 600°C, N<sub>2</sub>, 6.33 hr, Reduced at 350, H<sub>2</sub>, 4.5 hr

Dispersion of metal using CO chemisorption (%) : 44

Reaction Conditions : Temperature = 105°C H<sub>2</sub> pressure = 10 bar

Internal standard : n-heptane

GC temperature programme : isothermal at 140 °C

Basis : 100 g total feed							
Compound	RMM	Mass Feed	Mols Feed	Retntn time (mins)	Mass% Prod	Mols Prod	Conversion %
n-heptane	100	50.39	0.504	7.92	50.240	0.502	
cyclododecane	168	1.54	0.009	43.71	8.411	0.050	
cyclododecene isomer 1	166	33.63	0.203	41.06	26.422	0.159	
cyclododecene isomer 2	166	14.44	0.087	43.71	11.600	0.070	20.903*
Total			0.803			0.782	

\* The conversion was based on both cyclododecene isomers.

Mass balance error =  $((0.803 - 0.782) / 0.803) * 100 = 2.61\%$

**Table C2** showing the results obtained for the hydrogenation of cyclododecene over a poorly dispersed Pt/KL catalyst.

## Hydrogenation Of Cyclohexene

### Cyclohexene hydrogenation over a well dispersed Pt/KL sample

Hydrogenation of Cyclohexene over 1.55 % Pt/KL calcined at 350°C, O<sub>2</sub>, 6.33 hr, Reduced at 350 °C, H<sub>2</sub>, 4.5 hr

Dispersion of metal using CO chemisorption (%) : 111

Reaction Conditions : Temperature = 92°C H<sub>2</sub> pressure = 10 bar

Internal standard : n-hexane

GC temperature programme : isothermal at 100 °C

Basis : 100 g total feed							
Compound	RMM	Mass Feed	Mols Feed	Retntn time (mins)	Mass% Prod	Mols Prod	Conversion %
n-hexane	86	33.33	0.387	7.10	31.76	0.369	
cyclohexane	84	0.00	0.000	8.05	66.85	0.796	
cyclohexene	82	66.66	0.813	8.28	1.33	0.016	98.005
Total			1.200			1.181	

$$\text{Mass balance error} = ((1.200 - 1.181) / 1.200) * 100 = 1.6\%$$

**Table C3** showing the results obtained for the hydrogenation of cyclohexene over a well dispersed Pt/KL catalyst.

### Cyclohexene hydrogenation over a poorly dispersed Pt/KL sample

Hydrogenation of Cyclohexene over 1.55 % Pt/KL calcined at 600°C, N<sub>2</sub>, 6.33 hr, Reduced at 350 °C, H<sub>2</sub>, 4.5 hr

Dispersion of metal using CO chemisorption (%) : 44

Reaction Conditions : Temperature = 92°C H<sub>2</sub> pressure = 10 bar

Internal standard : n-hexane

GC temperature programme : isothermal at 100 °C

Basis : 100 g total feed							
Compound	RMM	Mass Feed	Mols Feed	Retntn time (mins)	Mass% Prod	Mols Prod	Conversion %
n-hexane	86	33.33	0.387	7.10	31.71	0.364	
cyclohexane	84	0.00	0.000	8.05	54.04	0.643	
cyclohexene	82	66.66	0.813	8.28	14.55	0.177	78.180
Total			1.200			1.185	

$$\text{Mass balance error} = ((1.200 - 1.185) / 1.200) * 100 = 1.3\%$$

**Table C4** showing the results obtained for the hydrogenation of cyclohexene over a poorly dispersed Pt/KL catalyst.

**Aromatisation Reaction**

Typical GC trace for  
n-hexane conversion

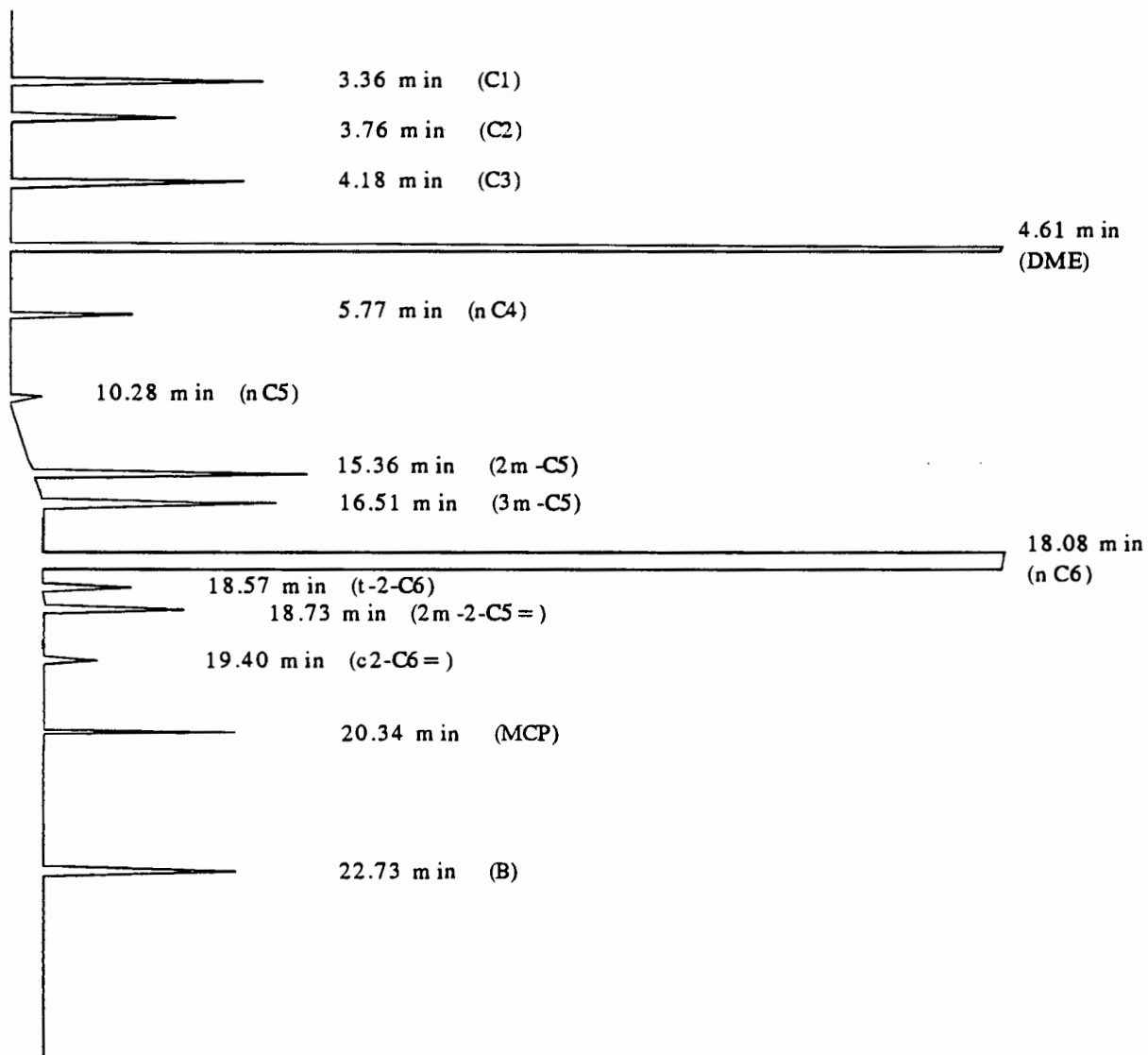


Figure C1 showing the GC trace representing the analysed products of the aromatisation reaction.

**Aromatisation of n-hexane over a well dispersed Pt/KL sample**

Catalyst : 0.1 g of 1.55 % Pt/KL sample calcined at 350 °C, O<sub>2</sub>, 6.33 hours. Reduced at 350 °C, H<sub>2</sub>, 4.5 hours.

Dispersion of metal using CO chemisorption (%) : 111

Reaction Conditions : Temperature = 400 °C, pressure = 101 kPa,

WHSV = 27.8 hr<sup>-1</sup>

Carrier gas : Hydrogen

GC temperature programme: -5 °C for 5 minutes, increase at 3 °C/minute to 30 °C and maintain at 30 °C for 10 minutes. Increase at 15 °C/minute to 270 °C.

Internal Standard : DME (di-methyl-ether)

Analysis taken after 33 hours from the start of the run

Basis : 100 g total feed

Compound	RMM	Mass Feed	Mols Feed	Retn Time (mins)	Mass % Prod.	Mols Prod.	Conver-sion	Mass % Select
C1	16			3.36	0.97	0.06		6.67
C2	30			3.76	0.78	0.03		5.32
C3	44			4.18	1.31	0.03		8.99
DME	46	2.54	0.06	4.61	3.76	0.08		-
n-C4	58			5.77	1.06	0.02		7.24
n-C5	72			10.28	0.64	0.01		4.38
2,2-dm-C4	86			14.65	0.00	0.00		0.00
2m-C5	86			15.36	3.26	0.04		22.30
3m-C5	86			16.51	2.69	0.03		18.38
2m-1-C5=	84			17.10	0.00	0.00		0.00
n-C6	86	97.56	1.13	18.08	81.64	0.95	16.23	-
t-2-C6=	82			18.57	0.00	0.00		0.00
2m-2-C5=	84			18.73	0.40	0.01		2.74
c-2-C6=	82			19.40	0.21	0.00		1.42
MCP*	84			20.34	1.68	0.02		11.53
B**	78			22.73	1.61	0.02		11.04
Total			1.89		100.01	1.26		100.00

\* MCP stands for Methyl-Cyclo-Pentane

\*\* B stands for Benzene

Table C5 showing the results of the aromatisation of n-hexane over a well dispersed Pt/KL catalyst.



## Aromatisation of n-hexane over a poorly dispersed Pt/KL sample

Catalyst : 0.1 g of 1.55 % Pt/KL sample calcined at 600 °C, N<sub>2</sub>, 6.33 hours. Reduced at 350 °C, H<sub>2</sub>, 4.5 hours.

Dispersion of metal using CO chemisorption (%) : 44

Reaction Conditions : Temperature = 400 °C, pressure = 101 kPa,  
WHSV = 27.8 hr<sup>-1</sup>

Carrier gas : Hydrogen

GC temperature programme: -5 °C for 5 minutes, increase at 3 °C/minute to 30 °C and maintain at 30 °C for 10 minutes. Increase at 15 °C/minute to 270 °C.

Internal Standard : DME (di-methyl-ether)

Analysis taken after 33 hours from the start of the run

Basis : 100 g total feed

Compound	RMM	Mass Feed	Mols Feed	Retn Time (mins)	Mass % Prod.	Mols Prod.	Conver-sion	Mass % Select
C1	16			3.36	0.22	0.01		3.00
C2	30			3.76	0.28	0.01		3.82
C3	44			4.18	0.24	0.01		3.31
DME	46	2.58	0.06	4.61	2.98	0.07		-
n-C4	58			5.77	0.30	0.01		4.02
n-C5	72			10.28	0.00	0.00		0.00
2,2-dm-C4	86			14.65	0.00	0.00		0.00
2m-C5	86			15.36	1.39	0.02		18.89
3m-C5	86			16.51	1.30	0.02		17.69
2m-1-C5=	84			17.10	0.20	0.00		2.67
n-C6	86	97.42	1.13	18.08	89.66	1.04	7.96	-
t-2-C6=	82			18.57	0.39	0.01		5.23
2m-2-C5=	84			18.73	0.90	0.01		12.25
c-2-C6=	82			19.40	0.43	0.01		5.83
MCP*	84			20.34	1.16	0.01		15.82
B **	78			22.73	0.55	0.01		7.47
			1.89		100.01	1.22		100.00

\* MCP stands for Methyl Cyclo Pentane

\*\* B stands for Benzene

Table C6 showing the results of the aromatisation of n-hexane over a poorly dispersed Pt/KL catalyst.

### Calculation of Weight Hourly Space Velocity (WHSV)

The WHSV was calculated from equation C1

$$\text{Area (DME)} / \text{Area(n-hexane)} = \text{RF (DME)} * \text{Flow (DME)} / \text{Flow (n-hexane)} \quad (\text{C1})$$

where Area (i) is the area under the GC peak representing compound i

Flow (i) is the volumetric flowrate (ml/minute) of compound i

RF (i) is the G.C response factor of compound i

Using a DME area of 125 605, an n-hexane area of 4 702 381, a DME flow of 0.28 ml/min and a DME response factor of 1.27, the n-hexane flowrate was found to be equal to 13.31 ml/minute or 790.78 ml/hr.

The n hexane fed to the reactor was in the gas phase. Using the ideal gas equation  $PV=nRT$  with  $P = 101.3 \text{ kPa}$ ,  $T = 302 \text{ K}$ , the number of n-hexane moles was found to be equal to 0.0324 which corresponded to a mass of 2.78 g n-hexane /hr. The mass of catalyst loaded into the reactor was 0.1 g. This thus gave a WHSV of  $27.8 \text{ hr}^{-1}$ .

OF MAKING MANY BOOKS THERE IS NO END, AND MUCH STUDY WEARIES THE  
BODY

- Ecclesiastes 12 : 12